

Methodologies for simultaneous optimization of heat, mass, and power in industrial processes

THÈSE N° 8779 (2018)

PRÉSENTÉE LE 12 OCTOBRE 2018

À LA FACULTÉ DES SCIENCES ET TECHNIQUES DE L'INGÉNIEUR

GROUPE SCI STI FM

PROGRAMME DOCTORAL EN ENERGIE

ÉCOLE POLYTECHNIQUE FÉDÉRALE DE LAUSANNE

POUR L'OBTENTION DU GRADE DE DOCTEUR ÈS SCIENCES

PAR

Maziar KERMANI

acceptée sur proposition du jury:

Dr P. Ott, président du jury
Prof. F. Maréchal, Prof. A. Viana Ensinas, directeurs de thèse
Prof. M. El-Halwagi, rapporteur
Prof. Z. Kravanja, rapporteur
Prof. V. Hatzimanikatis, rapporteur



ÉCOLE POLYTECHNIQUE
FÉDÉRALE DE LAUSANNE

Suisse
2018

“It does not require a
majority to prevail, but
rather an irate, tireless
minority keen to set brush
fires on people’s minds.”

– Attributed to Samuel Adams

“Words ought to be a little wild,
for they are the assault of
thoughts on the unthinking.”

– John Maynard Keynes

Acknowledgements

The completion of this thesis wouldn't have been achieved without the help, perseverance, and grit of several beloved people. Every one of them has contributed whether it be directly, or indirectly. Looking at the path that has led me here, there are many instances that could have changed my life completely, if happened differently (a butterfly effect?!). So why not, thank the officer in the U.S. embassy for not giving me the student visa to enter the U.S. and consequently, opening the path for me to come to Switzerland for my studies?!

I would like to thank my thesis directors, Professor François Maréchal and Professor Adriano Ensinas for giving me the opportunity to pursue my PhD studies under their supervisions. François, thank you for providing such a vivid, dynamic, and friendly environment in the group. Thank you for trusting me and letting me pursue my research. Spending more than 7 years at EPFL, talking to other PhD students and hearing their stories, I must admit that you are, by far, the most admired, the coolest, and the most caring supervisor one can dream of. Of course, working with you had its own challenges: having been constantly bombarded by your authentic and sometimes “extra-terrestrial” ideas; jumping between different software and platforms; and not being easily reachable. Today, they don't look to me as challenges anymore. They have shaped me to be an independent thinker and broaden my knowledge beyond my field. Thank you! Adriano, thank you for your continued support and providing me with insightful ideas.

To my jury members, Professor Kravanja, Professor El-Halwagi, and Professor Hatzi-manikatis. I am very grateful to you for having accepted to be part of my thesis committee and your constructive discussions and comments. Special thanks to Professor Rachidi, for his kindness and trust in me and helping me with many life-related situations in Switzerland.

I would like to thank all the members of IPESE group for making the environment so friendly, collaborative, and constructive. To Sylvie, our secretary, for her ultra-organized schedule and doing everything (literally!) so that we, PhD students, can freely focus on our researches. Special thanks to Ivan for always having time for discussions and correcting all my English grammars (except this part!).

The four years of PhD is not just about doing scientific research but also social research. An old friend of mine once told me “it doesn't matter where you live as long as you are surrounded by true friends”. To Monika, Sina, Dilan, Priscilla, Manuel, Sophia, Houman, and Armin for all the hikes, travels, climbs, white cows (!), and discussions. Thank you!

My sincere and deepest gratitude goes to my parents, Soudabeh and Bahram, and my sister, Golriz. This would not have been possible without their supports, dedications and sacrifices. Thank you my dears!

– Vevey, August 2018



Abstract

Efficient consumption of energy and material resources, including water, is the primary focus for process industries to reduce their environmental impact. The Conference of Parties in Paris (COP21) highlighted the prominent role of industrial energy efficiency in combatting climate change by reducing greenhouse gas (GHG) emissions. Consumption of energy and material resources, especially water, are strongly interconnected; and therefore, must be treated simultaneously using a holistic approach to identify optimal solutions for efficient processing. Such approaches must consider energy and water recovery within a comprehensive process integration framework which includes options such as organic Rankine cycles for electricity generation from low to medium temperature heat.

This thesis addresses the issue of how to efficiently manage energy and water in industrial processes by presenting two systematic methodologies for the simultaneous optimization of heat and mass and combined heat and power production. A novel iterative sequential solution strategy is proposed for optimizing heat-integrated water allocation networks through decomposing the overall problem into three sub-problems using mathematical programming techniques. The approach is capable of proposing a set of potential energy and water reduction opportunities that should be further evaluated for technical, economical, physical, and environmental feasibilities. A novel and comprehensive superstructure optimization methodology is proposed for organic Rankine cycle (ORC) integration in industrial processes including architectural features, such as turbine-bleeding, reheating, and transcritical cycles. Meta-heuristic optimization (via a genetic algorithm) is combined with deterministic techniques to solve the problem: by addressing fluid selection, operating condition determination, and equipment sizing.

This thesis further addresses the importance of holistic approaches by applying the proposed methodologies on a kraft pulp mill. In doing so, freshwater consumption is reduced by more than 60%, while net power output is increased by a factor of six. The results exhibit that interactions among these elements are complex and therefore underline the necessity of such methods to explore their optimal integration with industrial processes. The potential implications of this work are broad, extending from total site integration to industrial symbiosis.

Keywords: heat-integrated water allocation network, combined heat and power, superstructure optimization, process integration, mathematical programming, optimization solution strategy, genetic algorithm, holistic approach, industrial symbiosis, multi-objective optimization. ■



Résumé

L'utilisation efficace de l'énergie et des matières premières est l'un des principaux défis du secteur industriel dans le but de réduire son impact environnemental. En effet, la Conférence des Parties à Paris (COP21) a souligné l'importance de l'efficacité énergétique industrielle comme moyen de lutte contre le changement climatique en réduisant les émissions de gaz à effet de serre (GES). Les consommations d'énergie et des matières premières, en particulier l'eau, sont souvent très fortement liées et, par conséquent, doivent être traitées simultanément en utilisant une approche holistique. De telles approches doivent prendre en compte la récupération de l'énergie et de l'eau ainsi que la conversion optimale de l'énergie et la valorisation de l'énergie résiduelle en considérant l'intégration des procédés et des options telles que les cycles de Rankine à fluide organique pour générer de l'électricité à partir de sources thermiques à basses ou moyennes températures.

Cette thèse aborde la question de savoir comment gérer efficacement l'énergie et l'eau dans les procédés industriels. En particulier, elle présente deux méthodes systématiques pour l'optimisation simultanée masse-énergie ainsi que la production simultanée de la chaleur et de l'électricité. Une nouvelle stratégie séquentielle itérative est proposée afin d'optimiser les réseaux intégrés eau-énergie en décomposant le problème global en trois sous-problèmes par le biais de techniques de programmation mathématique. L'approche permet de proposer un ensemble de solutions potentielles afin de réduire la consommation d'énergie et d'eau qui peuvent ensuite être comparées par des critères techniques, économiques, physiques et environnementaux. Une nouvelle méthode basée sur l'utilisation de techniques d'optimisation est ensuite proposée pour calculer l'intégration d'ORC dans des procédés industriels en intégrant les caractéristiques technologiques telles que la préchauffe, le soutirage et les cycles trans-critiques. L'optimisation méta-heuristique (via un algorithme génétique) est combinée avec des techniques déterministes pour résoudre le problème en adressant notamment la sélection du fluide, la détermination de la condition de fonctionnement et le dimensionnement des équipements.

Cette thèse aborde en outre l'importance des approches holistiques en démontrant les méthodes proposées sur une usine de pâte kraft. Ça permet de réduire la consommation d'eau de plus de 60%, tandis que la production nette d'électricité augmente d'un facteur six. Les résultats démontrent que les interactions entre ces éléments sont complexes et soulignent par conséquent la nécessité de telles méthodes pour explorer leur intégration optimale avec les procédés industriels. Les applications potentielles de ce travail sont vastes, allant de l'intégration de site à la symbiose industrielle.

Mots-clés: réseaux intégrés eau-énergie, production chaleur-force, optimisation de superstructure, intégration de procédé, programmation mathématique, stratégie d'optimisation, algorithme génétique, approche holistique, symbiose industrielle, optimisation multi-objective. ■

List of Figures

1.1	Schematic of water pathways in industrial plants	8
1.2	Alternative implementations of non-isothermal mixing	12
1.3	Visualization of some key indicators of the benchmarking case study	27
2.1	Superstructure of combined water and energy network	33
2.2	Overall schematic of connections, parameters, and variables in water network	35
2.3	Visualization of some key indicators of test case I using parallel coordinates	41
2.4	Visualization of some key indicators of test case II (Table 2.3) using parallel coordinates	42
2.5	Visualization of some key indicators of test case III (Table 2.5) using parallel coordinates	46
2.6	Test case III: Final HIWAN design for ΔT_{min} 1.4°C (a) and 10°C (b)	46
2.7	Comparison between current state of the mill and the proposed optimal network	52
3.1	Schematic of the proposed source and sink hyperstructures for HIWAN	58
3.2	Iterative sequential solution strategy proposed for solving HIWAN synthesis problems	65
3.3	Construction of the HIWAN hyperstructure using an illustrative case	67
3.4	Comparison of two approaches for HEN design in water networks	68
3.5	Visualization of key indicators for test case I using parallel coordinates	71
3.6	Visualization of key indicators for test case II using parallel coordinates	72
3.7	Solutions with the lowest HEN cost (test case II)	73
3.8	HEN cost <i>vs</i> operating cost for selected solutions of test case III	74
3.9	Visualization of key indicators for test case III using parallel coordinates	74
3.10	Visualization of key indicators for the simplified kraft case using parallel coordinates	76
3.11	One of the optimal solutions for the simplified kraft case with improved performance	77
4.1	Different types of working fluids	94
4.2	Different ORC architectures in temperature-entropy diagram	98
5.1	Schematic of the proposed ORC superstructure on temperature-entropy diagram	106
5.2	Comparison of linearization techniques (proposed approach <i>vs</i> segmented approach)	112
5.3	Proposed methodology for ORC integration in industrial processes	116
5.4	Grand composite curve of the case study	118
5.5	Case I: GCC and integrated composite curve	121
5.6	Selected working fluids for the case study (case II)	122
5.7	Pareto frontiers of case II for selected working fluids	123
5.8	Results of solution point "A" (Figure 5.7b) for case II	124
5.9	Results of solution point "A" (Figure 5.7b): HEN for below the pinch point	125
5.10	Selected working fluids for the case study (case III)	126
5.11	Results of case III	127
6.1	Schematic of the proposed mathematical superstructure for combined heat, mass, and power integration in industrial processes	141

LIST OF FIGURES

6.2	Schematic of the case study	142
6.3	GCC of the motivating kraft mill illustrating the waste hot streams with potential working fluids	143
6.4	Integration of ORC with waste thermal streams	144
6.5	Integration of ORC with thermal streams and water unit operations	145
7.1	General schematic of water and energy flows in a kraft mill	148
7.2	Layout of the industrial case study including thermal streams and water unit operations	153
7.3	Hot and cold grand composite curves of considered clusters for kraft case study	155
7.4	Grand composite curves of considered clusters for kraft case study	156
7.5	Pareto frontiers of the kraft case study	159
7.6	Pressure level of the recovery boiler and ORC working fluids of the Pareto frontiers . .	160
7.7	Visualization of key indicators of solutions of the Pareto frontiers	161
7.8	Solutions with minimum and maximum value of the three objectives	162
7.9	Schematic of energy balance in the kraft mill case study	163
7.10	Cooling load <i>vs</i> freshwater consumption <i>vs</i> net power production	164
7.11	Integrated grand composite curves of case I	165
7.12	Heat load distribution of case I	166
7.13	Integrated grand composite curve of case II	167
7.14	Heat load distribution of case II	168
7.15	Integrated grand composite curve of case III	169
7.16	Heat load distribution of case III	170
B.1	a) Error of linearization and b) Example of linearization for Pentane	190

List of Tables

1.1	Highlighted gaps in the literature on water allocation networks and their specificities . . .	9
1.2	Literature review of methodologies on HIWAN	16
1.3	Comparison of articles on HIWAN	22
1.4	Operating data of the benchmarking test case [51]	26
1.5	Benchmarking of several HIWAN methodologies	28
1.6	Summary of identified gap in HIWAN synthesis problem	30
2.1	Economic and operating parameters for all test cases [22]	40
2.2	Operating data for test case II [18]	41
2.3	Benchmarking HIWAN methodologies using test case II [18] ⁽¹⁾	43
2.4	Operating data for test case III [107]	44
2.5	Benchmarking of HIWAN methodologies using test case III [107] ⁽¹⁾	45
2.6	Operating data for the simplified kraft pulp case study	50
2.7	Key performance indicators (KPIs) for the simplified kraft pulp case study	51
3.1	Solver options for the illustrative example	66
3.2	Comparison of two approaches based on key HEN indicators ⁽¹⁾	69
3.3	Comparison of results from problem P2 and problem P3	75
4.1	ORC applications	94
4.2	Main focus of the published reviews on ORC	95
4.3	Available review papers on topics related to ORCs	96
4.4	Summary of proposed methodologies for waste heat recovery in industrial processes using ORC	102
5.2	Main equipment included in the superstructure and their governing equations/constraints	108
5.3	Selected objective functions and indicators in this work	109
5.4	Constants of cost functions [83] (Reference year 2001, reference index CEPCI)	113
5.5	Cost data for the case study	113
5.6	Operating data of the case study [7]	117
5.7	Results of benchmarking using the test case	119
5.8	Decision variables and their optimal values for different cases	120
5.9	Input parameters of JEGA [96, 97]	120
6.1	Operating data for the motivating kraft pulp case study	141
6.2	Results of sequential and simultaneous approaches for the motivating example	146
7.1	Parameters for recovery boiler [12]	151
7.2	Parameters for wet open recirculating cooling systems [13]	152
7.3	Freshwater (20°C) consumers in the kraft mill (under the current operating conditions)	155
7.4	Set of decision variables of the optimization	158

LIST OF TABLES

A.1	Assumption and solver options for test case I (subsection 3.5.1)	184
A.2	Assumption and solver options for test cases II and III (subsection 3.5.2 and 3.5.3) . .	184
A.3	Assumption and solver options for simplified industrial case study (subsection 3.5.4) . .	185
A.4	Assumption and solver options for industrial kraft pulp mill (chapter 7)	186
B.1	Algorithm for finding the boundaries of the linearization	187
C.1	Included fluid properties in parallel coordinate tool	191
D.1	Kraft pulp mill industrial case study: water tanks	193
D.2	Kraft pulp mill industrial case study: thermal streams	194
D.3	Kraft pulp mill industrial case study: thermal streams in water network	195
D.4	Kraft pulp mill industrial case study: water unit processes	196
D.5	Kraft pulp mill industrial case study: waste thermal streams	196
D.6	Kraft pulp mill industrial case study: thermal and mass utilities	196

List of Acronyms

ΔT_{min} heat exchanger minimum approach temperature.

adt air-dried tonnes.

CHP combined heat and power.

GA genetic algorithm.

GBD generalized Benders decomposition.

GCC grand composite curve.

GDP generalized disjunctive programming.

GHG greenhouse gas.

GWP global warming potential.

HEN heat exchanger network.

HIMAN heat-integrated mass allocation network.

HIWAN heat-integrated water allocation network.

HLD heat load distribution.

HRAT heat recovery approach temperature.

ICC integer-cut constraint.

LP linear programming.

MEN mass exchange network.

MER minimum energy requirement.

MILP mixed-integer linear programming.

MINLP mixed-integer nonlinear programming.

MOO multi-objective optimization.

MPEC mathematical programming with equilibrium constraints.

NIM non-isothermal mixing.

NLP nonlinear programming.

ORC organic Rankine cycle.

LIST OF ACRONYMS

SA simulated annealing.

SIC specific investment cost.

TAC total annualized cost.

WHR waste heat recovery.

Contents

Acknowledgements	v
Abstract	vii
Résumé	ix
List of figures	xii
List of tables	xiv
List of acronyms	xvi
Introduction	1
 I The big trilemma: water–energy–waste nexus	 5
 1 Survey of methodologies in heat-integrated water allocation network	 7
1.1 Introduction	7
1.2 Classification and analysis of key features	10
1.2.1 Approaches	10
1.2.2 Interconnectivity of heat and water	10
1.2.3 Water network specificities	11
1.2.4 Heat exchanger network synthesis	12
1.2.5 Wastewater regeneration and treatment	14
1.3 Superstructure generation and solution strategies	18
1.3.1 Decomposition	18
1.3.2 Sequential	18
1.3.3 Simultaneous with or without initialization	19
1.3.4 Meta-heuristics	20
1.3.5 Relaxation/Transformation	20
1.4 Other features	25
1.4.1 Superstructure extension	25
1.4.2 Physical improvements	25
1.4.3 Water–energy nexus	25

1.5	Benchmarking analysis	26
1.6	Concluding remarks and future directions	29
2	Targeting methodology with industrial application	31
2.1	Problem statement	31
2.2	Mathematical formulation	32
2.2.1	Water network	34
2.2.2	Fixed-load <i>vs</i> fixed-flow formulations	36
2.2.3	Heat cascade model	37
2.2.4	Heat load distribution	38
2.3	Validation of the proposed methodology	39
2.3.1	Test case I: single-contaminant problem	39
2.3.2	Test case II: single-contaminant problem	41
2.3.3	Test case III: multi-contaminant problem	44
2.4	Methodology for industrial applications	47
2.5	Simplified industrial case study	49
2.6	Conclusion	53
3	Heat-integrated water allocation network design	55
3.1	Problem statement	55
3.2	Mathematical formulation	55
3.2.1	Objective function	59
3.2.2	Constraints	59
3.3	Solution strategy	62
3.4	Illustrative example	66
3.5	Validation and discussion	69
3.5.1	Test case I: single-contaminant problem	70
3.5.2	Test case II: single-contaminant problem	72
3.5.3	Test case III: multi-contaminant problem	73
3.5.4	Simplified industrial case study	75
3.6	Conclusion	78
	References	79
II	Medium-temperature heat recovery	91
4	Survey of methodologies in organic Rankine cycle modeling and optimization	93
4.1	Introduction	93
4.2	State of the art	95
4.2.1	ORC architectures	97
4.2.2	Fluid selection	99
4.2.3	ORC integration in industrial processes	100
5	Optimal integration of organic Rankine cycles in industrial processes	103

Nomenclature	103
5.1 Problem definition	105
5.2 Methodology	105
5.2.1 Mathematical formulation	105
5.2.2 Piece-wise linear envelopes for thermal streams	110
5.2.3 Economic model	112
5.2.4 Thermodynamic model (heat transfer calculation)	113
5.2.5 Solution strategy	115
5.3 Results and discussion	117
5.3.1 Comparative analysis	118
5.3.2 Optimization	119
5.3.2.1 Case I: single-objective optimization	119
5.3.2.2 Case II: multi-objective optimization	121
5.3.2.3 Case III: multi-objective optimization	125
5.4 Conclusion	128
References	129
 III Towards the grand design	 137
 6 Holistic approaches: background and motivation	 139
6.1 Background	139
6.2 Problem definition and proposed approach	140
6.3 Motivating example	140
6.3.1 Case I - sequential approach	142
6.3.2 Case II - simultaneous approach	144
6.4 Conclusion	146
 7 Industrial application: kraft pulp mill	 147
7.1 Kraft process	147
7.2 Data extraction and problem formulation	149
7.2.1 Data classification	149
7.2.2 Problem formulation	151
7.2.2.1 Recovery boiler	151
7.2.2.2 Steam cycle	152
7.2.2.3 Cooling water system	152
7.2.3 Solution strategy	154
7.3 Preliminary analysis	154
7.3.1 Current operating conditions	154
7.3.2 Thermal heat integration	156
7.3.3 ORC and potential working fluids	157
7.4 Results and discussion	157
7.4.1 Pareto frontiers	157
7.4.2 Analysis	159
7.4.2.1 Visualization of all the solutions by several indicators	160

CONTENTS

7.4.2.2	Extreme points	162
7.4.2.3	Cooling utility, freshwater consumption, and net power output	163
7.4.3	Heat integration and heat load distribution	164
7.4.3.1	Case I - no ORC integration	164
7.4.3.2	Case II - maximum electricity production	167
7.4.3.3	Case III - ORC with Isobutene	169
7.5	Conclusion	169
References		173
Concluding remarks		175
Appendix		181
<hr/>		
A Assumptions and solver options for test cases		183
B Algorithm for outer and inner approximation of thermal streams		187
B.1	Bounds of linearization	187
B.2	Lua code for linearization	188
B.3	Error of linearization	190
C Interactive parallel coordinate visualization tool for fluid selection		191
D Kraft pulp mill data		193
Curriculum vitae		197

Introduction

“The cheapest and cleanest energy choice of all is not to waste it”
The Economist [1]

Efficient consumption of energy and material resources, including water, is the primary focus for process industries to reduce their environmental impact. The Conference of Parties in Paris (COP21) highlighted the prominent role of industrial energy efficiency in combatting climate change by reducing greenhouse gas (GHG) emissions. Among the possible techniques to improve industrial process efficiency and optimize the use of energy, water, and other resources, **process integration** (PI) is a powerful approach used in various industrial processes, such as chemicals, food and beverage, and pulp and paper industries. Process integration is a family of methodologies that emerged in response to the oil crisis in 1970s and was initially aimed at increasing energy efficiency and reducing energy consumption through **heat integration** (HI) and pinch analysis. In their seminal works, Flower and Linnhoff [2] and Linnhoff and Flower [3] presented a method for heat recovery known as the pinch design method. Pinch analysis, a simple process integration technique, applies thermodynamic principles to optimize heat recovery systems in industrial facilities. In conducting pinch analysis, process engineers examine the pathways where heat is being used, where it can be recovered, and how it can best be applied across the process. It comprises a diagnosis phase, during which potential for improvement is determined, followed by an optimization phase, during which heat recovery measures that improve energy efficiency are identified. Another major contribution was made by Dhole and Linnhoff [4], who introduced the concept of “**total site**” heat recovery to maximize energy savings. In their work, they proposed a methodology for site-scale targeting of utility consumption and co-generation potentials to overcome the infeasibility of heat recovery between plant site divisions by using indirect heat recovery via hot oil or water loops or a utility system. This was further improved by Hu and Ahmad [5] and Klemeš et al. [6]. However, these methodologies were limited to heat recovery among industrial processes and neglected electricity production, necessitating the development of methodologies for total site heat and power integration [7].

Over the past few decades, process integration has spread into other fields. The general problem of mass exchange network (MEN) synthesis, i.e., **mass integration**, was first introduced by El-Halwagi and Manousiouthakis [8] to select a cost-effective configuration for transferring specific components (e.g., contaminants) from a set of rich (e.g., contaminated) streams to a set of lean (e.g., non-contaminated) streams addressing single (multi)-component [9], regeneration [10], reactive MEN [11] problems, and heat transfer tasks within MEN [12]. Water allocation network optimization, i.e., **water integration**, was first addressed by Takama et al. [13] through the optimization of a superstructure encompassing all recycling and reuse opportunities for oil refinery applications. Wang and Smith proposed graphical-based methodologies (analogous to the heat cascade problem) to address wastewater minimization in industrial pro-

cesses [14, 15, 16]. Later, Shelley and El-Halwagi [17] introduced the notion of ‘component-less’ mass allocation networks, i.e., **property integration**, by focusing on property-based constraints (e.g., volatile organic compounds, viscosity, and toxicity). The consumption of energy and material resources, especially water, are strongly interconnected; energy is used to heat or cool water for process use, whereas water is used in production support or utility networks as steam or cooling water. Thus, water and energy must be treated simultaneously. The seminal work of Savulescu and Smith [18] addressed this problem by proposing a graphical-based methodology combining mass integration and heat integration for **heat-integrated water allocation network (HIWAN)** synthesis.

The growing desire to improve the resource efficiency and environmental impact of industrial processes is directly linked to the optimal management of heat, mass, and power flows. Industrial process heating demands are mainly satisfied by steam being produced in steam cycles at different pressure levels. Steam cycles are also the primary source of electricity generation in industrial plants. Furthermore, the efficiency of other energy conversion systems has to be considered in parallel to heat recovery; thus, combined heat and power production, and the use of heat pumping should also be addressed. This requires the development of holistic approaches addressing these elements simultaneously. Such approaches must consider energy and water recovery within a comprehensive process integration framework that includes other options, such as an organic Rankine cycle (ORC) for electricity generation from low to medium temperature heat that provides heating for low temperature processes or other uses.

Thesis objectives

This thesis addresses the efficient management of energy and water in industrial processes by presenting two systematic methodologies for the simultaneous optimization of heat and mass and combined heat and power production. In particular, three main topics are addressed:

How can heat and water exchanges be systematically managed within industrial processes? How can industrial specificities be addressed in the solution strategy? What are the main criteria in optimizing such systems? What approach can be used to generate a set of energy and water saving opportunities? ([Part I](#))

Given the ORC as a promising technology to produce electricity from low to medium temperature heat, how can it be optimally integrated within a process for maximizing electricity production? What are the influential elements and how can they be addressed in the modeling and optimization stages? ([Part II](#))

How can heat, mass (water), and power flows be simultaneously considered in planning an industrial site? What type of approach and what steps should be taken in tackling such problems? ([Part III](#))

Outline

This thesis is organized as follows: Part I focuses on HIWAN synthesis problems. Chapter 1 provides a comprehensive literature overview in water-related studies. In chapter 2, a

novel linear superstructure is proposed for targeting HIWAN synthesis problems addressing non-isothermal mixing and multi-contaminant cases. Restricted matches and models of water tanks are incorporated to address a wide range of industrial case studies. In chapter 3, a novel iterative sequential solution strategy is proposed for optimizing heat-integrated water allocation networks through decomposing the overall problem into three sub-problems using mathematical programming techniques: targeting, heat load distribution (HLD), and design. The approach is capable of proposing a set of potential energy and water reduction opportunities that should be further evaluated for technical, economical, physical, and environmental feasibilities. Part II proposes a novel and comprehensive superstructure optimization methodology for ORC integration in industrial processes including architectural features, such as turbine-bleeding, reheating, and transcritical cycles. Additional developments include a novel dynamic linearization technique for supercritical and near-critical streams and integrating heat transfer parameter estimation directly in the problem structure. Meta-heuristic optimization (via a genetic algorithm) is combined with deterministic techniques to solve the mathematical problem by fluid selection, operating condition determination, and equipment sizing. Chapter 4 provides a broad introduction to different ORC architectures, the effects of working fluids on the performance of the cycle, and a review of the literature with a focus on mathematical approaches. Chapter 5 details the proposed methodology. Part III aims at bringing together the two methodologies developed in Part I and Part II to emphasize holistic design by proposing a methodology for the simultaneous consideration of heat, mass (water), and power in industrial processes with applications in total site analysis. Chapter 6 provides the background and motivation. Chapter 7 demonstrates the application of the proposed holistic methodology on a kraft pulp mill. ■

References

- [1] T. Economist, Invisible fuel, *The Economist* ISSN 0013-0613.
- [2] J. R. Flower, B. Linnhoff, Synthesis of Heat Exchanger Networks - 2. Evolutionary Generation of Networks with Various Criteria of Optimality., *AIChE Journal* 24 (4) (1978) 642–654, ISSN 0001-1541.
- [3] B. Linnhoff, J. R. Flower, Synthesis of Heat Exchanger Networks - 1. Systematic Generation of Energy Optimal Networks., *AIChE Journal* 24 (4) (1978) 633–642, ISSN 0001-1541.
- [4] V. R. Dhole, B. Linnhoff, Total site targets for fuel, co-generation, emissions, and cooling, *Computers & Chemical Engineering* 17 (1993) S101–S109, ISSN 0098-1354.
- [5] C. W. Hu, S. Ahmad, Total site heat integration using the utility system, *Computers & Chemical Engineering* 18 (8) (1994) 729–742, ISSN 0098-1354.
- [6] J. Klemeš, V. R. Dhole, K. Raissi, S. J. Perry, L. Puigjaner, Targeting and design methodology for reduction of fuel, power and CO₂ on total sites, *Applied Thermal Engineering* 17 (8) (1997) 993–1003, ISSN 1359-4311.
- [7] P. Y. Liew, W. L. Theo, S. R. Wan Alwi, J. S. Lim, Z. Abdul Manan, J. J. Klemeš, P. S. Varbanov, Total Site Heat Integration planning and design for industrial, urban and renewable systems, *Renewable and Sustainable Energy Reviews* 68, Part 2 (2017) 964–985, ISSN 1364-0321.
- [8] M. M. El-Halwagi, V. Manousiouthakis, Synthesis of mass exchange networks, *AIChE Journal* 35 (8) (1989) 1233–1244, ISSN 1547-5905.

- [9] M. M. El-Halwagi, V. Manousiouthakis, Automatic synthesis of mass-exchange networks with single-component targets, *Chemical Engineering Science* 45 (9) (1990) 2813–2831, ISSN 0009-2509.
- [10] M. M. El-Halwagi, V. Manousiouthakis, Simultaneous synthesis of mass-exchange and regeneration networks, *AIChE Journal* 36 (8) (1990) 1209–1219, ISSN 1547-5905.
- [11] M. M. El-Halwagi, B. K. Srinivas, Synthesis of reactive mass-exchange networks, *Chemical Engineering Science* 47 (8) (1992) 2113–2119, ISSN 0009-2509.
- [12] B. K. Srinivas, M. M. El-Halwagi, Synthesis of combined heat and reactive mass-exchange networks, *Chemical Engineering Science* 49 (13) (1994) 2059–2074, ISSN 0009-2509.
- [13] N. Takama, T. Kuriyama, K. Shiroko, T. Umeda, Optimal water allocation in a petroleum refinery, *Computers & Chemical Engineering* 4 (4) (1980) 251–258, ISSN 0098-1354.
- [14] Y. P. Wang, R. Smith, Wastewater minimisation, *Chemical Engineering Science* 49 (7) (1994) 981–1006, ISSN 0009-2509.
- [15] Y. Wang, R. Smith, Wastewater minimization with flowrate constraints, *Chemical Engineering Research and Design* 73 (A8) (1995) 889–904, ISSN 0263-8762.
- [16] Y. Wang, R. Smith, Time Pinch Analysis, *Chemical Engineering Research & Design* 73 (8) (1995) 905–914.
- [17] M. D. Shelley, M. M. El-Halwagi, Component-less design of recovery and allocation systems: a functionality-based clustering approach, *Computers & Chemical Engineering* 24 (9–10) (2000) 2081–2091, ISSN 0098-1354.
- [18] L. E. Savulescu, R. Smith, Simultaneous energy and water minimisation, in: 1998 AIChE Annual Meeting, Miami Beach, Florida, 13–22, unpublished work, 1998.

PART

I

THE BIG TRILEMMA: WATER—ENERGY—WASTE NEXUS

In their processes, industries consume large quantities of energy and water often considered to be peripheral to the process operation. Energy is used to heat or cool water for process use; water is frequently used in production support or utility networks as steam or cooling water. This underlines the interconnectivity of water and energy and that they must be treated simultaneously to address energy and resource use in industrial processes. In this work, novel mathematical superstructures and a sequential solution strategy are proposed to address the design of heat-integrated water allocation networks. In the first step, i.e., the targeting step, a novel mixed-integer linear programming (MILP) superstructure is proposed that provides minimum utility consumptions (or very tight upper bounds) together with a list of potential thermal streams in the water network for achieving these targets. In the second step, thermal matches are identified by solving the HLD model [1, 2, 3] minimizing the number of heat-exchange matches. Based on these information, a novel nonlinear programming (NLP) hyperstructure is developed in the last step for a total heat-integrated water allocation network design combining the water allocation network with the well-known heat exchanger network (HEN) hyperstructure of Floudas and Ciric [4]. Emphasis is placed on generating a set of promising solutions by addressing different key performance indicators. This is achieved via the implementation of integer cut constraints that are applied on the first two steps to support the decision making for potential configurations.

Keywords: heat-integrated water allocation network, superstructure optimization, process integration, pinch analysis, mathematical programming, industrial application, heat exchanger network design, optimization solution strategy.

Acknowledgements: The author acknowledges the support of Swiss Innovation Agency Innosuisse, Swiss Competence Center for Energy Research SCCER EIP, as well as Swiss National Science Foundation (SNSF) and Swiss Agency for Development and Cooperation for providing financial support within the SCOPES 2013-2016 joint research project (CAPE-EWWR: IZ73Zo_1526221)

CHAPTER 1

Survey of methodologies in heat-integrated water allocation network

Overview

This chapter provides a comprehensive overview of the state of the art in water related studies. A comprehensive review of the proposed methodologies is provided with special focus on HIWANS. Key features addressed in water allocation networks are discussed in section 1.2. This includes a classifications of different approaches, solution strategies, and water and heat related criteria, such as wastewater treatment, contaminant constraint, non-isothermal mixing (NIM), and HEN design, among others. The content of this chapter is published in : *Kermani, M., Kantor, I.D., Maréchal, F., 2018. Synthesis of heat-integrated water allocation networks: a meta-analysis of solution strategies and network features. Energies 11, 1158.* <https://doi.org/10.3390/en11051158>

Industries consume large quantities of energy and water in their processes which are often considered to be peripheral to the process operation. Energy is used to heat or cool water for process use; additionally, water is frequently used in production support or utility networks as steam or cooling water. This enunciates the interconnectedness of water and energy and illustrates the necessity of their simultaneous treatment to improve energy and resource efficiency in industrial processes. Since the seminal work of Savulescu and Smith [5] introducing a graphical approach, many authors have contributed to this field by proposing graphically- or optimization-based methodologies. The latter encourages development of mathematical superstructures encompassing all possible interconnections. While a large body of research has focused on improving the superstructure development, solution strategies to tackle such optimization problems have also received significant attention. The goal of the current chapter is to study the proposed methodologies with special focus on mathematical approaches, their key features and solution strategies. Following the convention of Jeżowski [6], solution strategies are categorized into: decomposition, sequential, simultaneous, meta-heuristics and a more novel strategy of relaxation/transformation. A detailed, feature-based review of all the main contributions has also been provided in two tables. Several gaps have been highlighted as future research directions.

1.1 Introduction

This part addresses heat-integrated water allocation networks. Due to the similarities between water and other mass streams [6], such as hydrogen networks [7], property-based networks [8],

and more generally resource conservation networks, the terminology used in this chapter is based on heat-integrated mass allocation network (HIMAN)s. This is to emphasize the fact that most of the methodologies presented in the literature, and in this chapter, can be easily applied to other resources. In HIMAN problems involving water, integration of cooling water becomes especially important [9] as it should be considered in combination with process water to satisfy industrial demands. An example of this from the pulp and paper industry was presented by Suhr et al. [10]. Figure 1.1 illustrates typical water pathways in industrial pulp and paper plants and the strong interconnectivity among different water users.

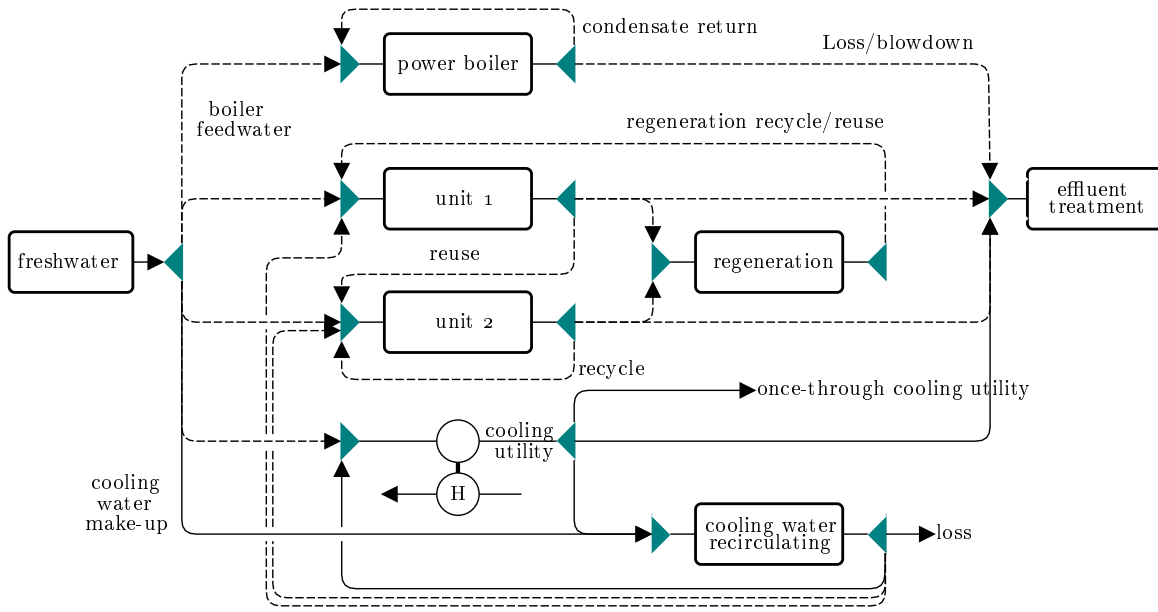


FIGURE 1.1—Schematic of water pathways in industrial plants (dash lines can be subjected to heating or cooling duties)

HIMANs have been extensively studied in the literature since their emergence in 1990 [11, 12, 5] with more than 100 articles covering different aspects and proposing various methodologies. Due to the growing interest in this domain, several review papers have been published that directly or indirectly study different features of HIMAN problems, in particular HEN synthesis, heat-integrated water minimization, and wastewater treatment. Bagajewicz [13] provided an overview of conceptual (i.e., insight-based) and mathematical (i.e., optimization-based) methodologies in water and wastewater minimization [14, 15] with main focus on the authors' main contributions [16, 17, 18]. Later, Foo [19] provided a comprehensive overview of conceptual approaches in water network design (i.e., water pinch analysis) in the 21st century covering single-contaminant fixed flowrate and fixed mass load problems applied to water regeneration, treatment and total water network design. Soon after, Jeżowski [6] published an annotated exhaustive literature review on water networks, analyzing formulations, approaches, and solution strategies from 1980 to 2010. The classification of solution strategies is modified and incorporated in the current work. Use of multi-objective optimization techniques to improve optimization and controllability of the processes together with summary of methodologies related to heat, mass and work exchange networks were provided by Chen and

Wang [20]. Klemeš [21] studied recent advances in water footprinting and life cycle assessment, wastewater minimization, and heat-integrated water allocation networks. More recently, Ahmetović et al. [22] carried out a comprehensive literature review specific to HIMAN and its features covering research published until 2015. The aforementioned review papers span over 20 years of research and development; therefore, some early research directions/gaps that were highlighted could/should have already been addressed. Most of these gaps (Table 1.1) are addressed for mass allocation networks, however they can easily be extended to HIMANs.

TABLE 1.1—Highlighted gaps in the literature on water allocation networks and their specificities

Highlighted Gaps	Remarks/Literature
Fixed concentration problems	As opposed to fixed mass load problems in which outlet concentration is limited (e.g., solubility) and hence mass load becomes variable. (not extensively addressed in the literature)
Multi-contaminant problems	Extensively addressed by mathematical methodologies with use of nonlinear programming techniques [23]
Rigorous modeling	Rigorous water and treatment unit models for retrofit problems in particular (not extensively addressed in the literature)
Batch-wise processes	Seminal work by Wang and Smith [24], and several prominent works covering water allocation network synthesis problem for batch processes [25, 26, 27, 28, 29, 30, 31] (not extensively addressed in the literature of HIMANs)
Non-water processes	In particular hydrogen networks [32]. Topics on “resource conservation network” and “property-based resource conservation networks” are dedicated to address this particularity [33].
Retrofitting	Developing methodologies for plant retrofitting considering technical and geographical constraints to find feasible and practical solutions (not extensively addressed in the literature).
Uncertainty analysis	Uncertainty and operability of water networks due to variations of flow and contamination to find resilient and flexible networks [34, 35, 36, 37, 38, 39]
Multi-period operations	Considering variations of operating condition, e.g., temperature of freshwater, over multiple time horizons (to some extent, this has been addressed by the literature on batch-wise operations).
Heat integration	Extensively studied under HIMAN methodologies and is the main focus of the current article.
Interplant operations	Extensively addressed by Chew et al. [40], Zhou et al. [41], Zhou and Li [42], Ibrić et al. [43], Kermani et al. [44] in HIMAN problems.
Improving solution strategies	Improving deterministic approaches, application of stochastic or hybrid (combined heuristic and mathematics) approaches. Jeżowski [6] highlighted the use of sequential-decomposition techniques or combination of several meta-heuristic (i.e., stochastic, such as genetic algorithm (GA)) approaches as potential directions.
Holistic approaches [45]	Considering synergies among different sections by extending the boundaries to incorporate all aspects in an industrial plant. Several authors aimed at integrating non-water thermal streams [46, 47, 48, 44, 49], cooling utilities [9], and hot utilities (steam cycle) [44] in their methodologies and found that application of holistic approaches can bring economical and environmental benefits to all parties involved. The topic remains under-addressed in the literature.

The remainder of this chapter focuses on major features of HIMAN methodologies which are reviewed with special focus on mathematical approaches proposed after 2015. Table 1.2 at the end of this section provides a comprehensive overview of recent publications following the same approach employed in our previous publication [9]. For a complete review of all the related papers, the reader is referred to the published review papers [13, 19, 6, 20, 21, 22].

1.2 Classification and analysis of key features of heat-integrated water allocation networks

1.2.1 Approaches

There are two main approaches in HIMAN synthesis problems: conceptual and mathematical. Conceptual approaches make use of graphical techniques and expert insight. Several conceptual approaches have been proposed in the past with focus on single-contaminant problems including, but not limited to: two-dimensional grid diagram [5, 50, 51], heat surplus diagram [52], water energy balance diagram [53], superimposed mass and energy curve [54, 55], temperature *vs* concentration diagram [56, 57], and enthalpy difference *vs* flow chart approach [58]. Only two conceptual approaches (concentration order and temperature composite curve [59, 60] and single-temperature-peak design principle [61]) have been proposed to handle multi-contaminant problems.

Mathematical approaches, conversely, are based on superstructure derivation and optimization which take into account many interconnection possibilities in the network design. The mathematical formulation is generally non-convex mixed-integer nonlinear programming (MINLP) and the objective function is mainly defined as minimization of total annualized cost (TAC) of the system, including both operating and investment cost. Solving a rigorous superstructure is very complex and hence requires innovative solution strategies. Mathematical approaches and their solution strategies are analyzed in more detail in section 1.3.

There exists a third approach combining the synergies of conceptual and mathematical approaches. Hybrid methodologies [62, 63, 64, 65, 66, 67, 68, 69] were first highlighted by Bagajewicz [13] as the most effective alternative to their individual applications. Such approaches allow the use of insight-based heuristics in formulating the mathematical models and hence aid mathematical approaches in representing practical and realistic alternatives in their superstructure. Moreover, expert insight can be incorporated in the methodologies to evaluate the solutions at each stage of the solution strategy, similar to the methodology proposed by Kermani et al. [9]. Conceptual approaches can also be used as techniques for initialization of large MINLP superstructures. The research direction is mainly focused on mathematical approaches. From the optimization perspective, mathematical approaches are guaranteed to provide optimal solutions (or near-optimal in non-convex formulations) to the problem, however the feasibility of such solution(s) in practice is not guaranteed. For this reason, hybrid approaches must be the main focus for future research.

1.2.2 Interconnectivity of heat and water

The proposed methodologies (being categorized as conceptual or mathematical approaches) can be categorized into three groups considering the interconnectivity of heat and water as “*separate*”, “*sequential*”, and “*simultaneous*”. In “*separate*” methodologies, fresh water consumption

is minimized in the first step, while the water network is designed without considering temperature constraints of the network. Knowing these two, in the second step, thermal streams will be extracted for heat integration [70, 71, 72, 68]. “*Sequential*” methodologies are similar to “*separate*” methodologies in the fact that fresh water consumption is minimized in the first stage; however, this target is incorporated in the second step, where heat integration and water network design are performed simultaneously [5, 18, 46, 73, 74]. “*Simultaneous*” methodologies, on the other hand, consider all the aforementioned steps simultaneously by taking into account the trade-offs between water consumption and thermal utility consumptions.

1.2.3 Water network specificities

Single vs multiple contaminants: With regard to the constituent of water streams, the problem can be formulated as single-contaminant or multi-contaminant. It should be highlighted that the research focusing on property (e.g., toxicity, viscosity, or acidity) integration in resource conservation approaches can also be categorized under this classification. The mathematical formulations dealing with contaminations are generally nonlinear due to the existence of bilinear terms of type $\dot{\mathbf{m}}_u \mathbf{C}_u$ at the inlet of mixers, where $\dot{\mathbf{m}}_u$ and \mathbf{C}_u are unknown mass flowrate and contamination, respectively. Savelski and Bagajewicz [16] showed that for single-contaminant problems, the contaminant will always reach its highest limit at the outlet of a water unit operation. Therefore, the nonlinear equality constraint at the inlet of a mixer can be formulated as a linear inequality constraint with outlet contamination fixed at its maximum value. Using the necessary condition of optimality proposed by Savelski and Bagajewicz [17] and the maximum driving force [15], Yang and Grossmann [75] formulated a linear model for targeting fresh water consumption in multi-contaminant problems by relaxing the equality constraint of a mixer to an inequality constraint. The direction of relaxation was achieved by applying the KKT (Karush–Kuhn–Tucker) conditions of optimality. They stated that this formulation will result in the exact target under certain conditions and otherwise provides a tight upper bound to the problem.

Fixed-load vs fixed-flow problems: Water minimization problem formulations can be categorized into two groups of fixed-load (FL) problems and fixed-flow (FF) problems [19, 76, 61]. In fixed-load problems, water is essentially a mass transfer medium with the goal of removing a fixed amount of mass load (e.g., contamination) from a process. Cleaning processes are considered as this type of problem. Since water can enter and leave a process u at any level of contamination (\mathbf{C}_u^{in} and \mathbf{C}_u^{out} , respectively), water flowrate (\mathbf{F}_u) through each process varies according to Equation 1.1:

$$\mathbf{F}_u = \frac{L_u}{(\mathbf{C}_u^{out} - \mathbf{C}_u^{in})} \quad \forall u \in \mathbf{WUP} \quad (1.1)$$

where \mathbf{WUP} is the set of water unit processes. This type of problem implies equal flowrates at the inlet and outlet of each water unit processes. Nonetheless, water loss or gain can be modeled as well with additional modifications. The limiting composite curve approach [14] and mass problem table (similar to problem table algorithm in heat cascade) [77] are among the well-known conceptual approaches based on fixed-load problems. For fixed-flow problems, the flowrate through each process is fixed while the water unit process is modeled as two separate units, i.e., source and sink. Conversion of the fixed-load problem into a fixed-flow problem

for single-contaminant processes is completed by fixing the flow to the limiting flowrate using Equation 1.1 (By setting $C_i^{in} = C_i^{in,max}$ and $C_i^{out} = C_i^{out,max}$).

Non-isothermal mixing: There are two types of NIM: homogeneous and heterogeneous. Homogeneous NIM occurs between two cold streams or two hot streams and cannot decrease utility consumption, while heterogeneous NIM takes place between a hot and a cold stream and can decrease, increase, or even have no effect on utility consumption [78]. Heterogeneous NIM potentially reduces the energy consumption as long as it takes place within the pinch interval and between streams with temperatures in the same pinch temperature range. It has the ability of reducing the number of heat exchangers and hence reducing the investment cost. NIM is a non-linear problem, due to the multiplication of mass flowrates and their unknown temperature. There are three main methods for implementing NIM in a water network superstructure, as shown in Figure 1.2:

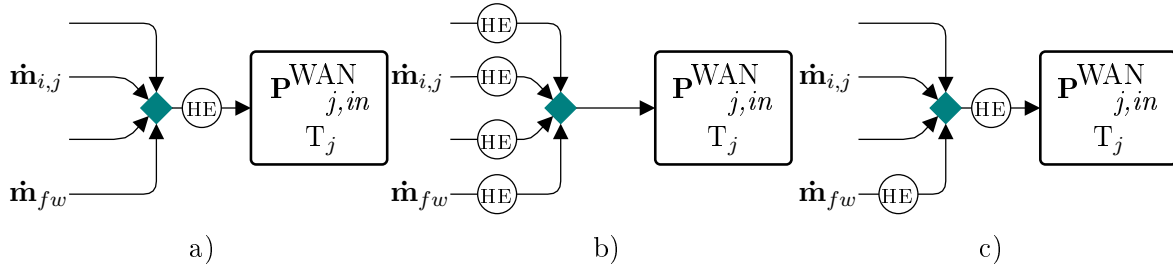


FIGURE 1.2—Alternative implementations of non-isothermal mixing in a mathematical superstructure of HIWAN

In Figure 1.2-a (left), direct heat exchange takes place before an indirect heat exchange: all the streams are mixed non-isothermally and then heated or cooled through a heat exchanger, before entering the water unit. In Figure 1.2-b (middle), indirect heat exchange takes place before a direct heat exchange: the streams from different sources pass through heat exchangers before being mixed non-isothermally. The temperature of mixture and contamination level should meet the requirement of the water unit. This method is non-linear, due to the unknown mass flows and outlet temperatures of each heat exchanger [79]. In Figure 1.2-c (right), the streams are mixed non-isothermally and then pass through a heat exchanger to reach the required temperature. Only water utility streams are allowed to exchange heat indirectly through heat exchangers [80].

1.2.4 Heat exchanger network synthesis

HEN synthesis problem is among the most researched topics in process integration dealing with developing more rigorous superstructures while providing more efficient solution strategies. An early review paper by Gundersen and Naess [81] presents more than 200 publications on this topic while Furman and Sahinidis [82] provides a comprehensive overview of major solution strategies and studies conducted in HEN synthesis until the end of the 20th century. HEN design in HIMAN synthesis problems is different from the classical HEN synthesis problems due to the possibility of stream mixing and splitting within HENs. All conceptual approaches use the classical pinch design method after having maximized the indirect heat exchanges (NIM). To understand the implication of HEN synthesis in HIMAN problems using mathematical

approaches, it is vital to provide a brief summary of HEN synthesis methodologies. The complete HEN superstructure is an MINLP model with nonlinear terms in both the objective function and constraints. Proposed solution strategies are directly affected by the proposed superstructure (modification of the original superstructure by relaxation, linearization, etc.) and can be categorized mainly as sequential *vs* simultaneous solution strategies:

- **Sequential approaches:** The HEN synthesis problem can be broken down into several subproblems which is then solved successively for the minimum total HEN cost. The general approach is a three-step sequential technique. The first step minimizes the utility consumption either through conceptual techniques, such as pinch design method [83] or mathematical techniques by constructing MILP models [1, 84]. Having the utility targets, an MILP model is formulated in the second step to minimize the number of matches between hot and cold streams which is known as the HLD problem [1, 2, 3]. This step can further be divided into subproblems for each pinch interval which effectively minimizes the number of heat exchanger units instead of matches. In the last step, a NLP model [85] can be solved for minimum cost of heat exchanger network subject to results of the two previous steps. Floudas et al. [85] showed that every solution of the second step corresponds to a feasible HEN design in the third step. Floudas and Ciric [4] proposed a decomposition solution strategy for solving the NLP model of HEN synthesis to global optimality using generalized Benders decomposition (GBD) given the HLD matches and the utility targets and a fixed heat recovery approach temperature. Nonetheless, the solutions of the second step will only provide a feasible match with minimum number of matches and cannot guarantee a globally optimum HEN in the third step. Many techniques exist to direct the second step towards better matching results. Implementing integer cut constraints [86] to generate many solutions in the second step with minimum number of matches or using penalty (i.e., ranking) costs for each match in the objective function of the second step are among these techniques. Spaghetti design (i.e., vertical heat transfer model) [87] can also be incorporated into an MILP model (proposed by Gundersen and Grossmann [88] and extended by Gundersen et al. [89]) for targeting and ranking matches which may result in lower capital cost.
- **Simultaneous approaches:** The goal is to design the HEN at once. The two major contributions in this category are the works of Floudas and Ciric [4] and Yee and Grossmann [90] which are based on MINLP modeling. The former is indeed a combination of the MILP model of Papoulias and Grossmann [1] for heat load distribution and the NLP model of Floudas et al. [85] while the latter is based on a stage-wise representation approach [91]. Several assumption are incorporated in the stage-wise approach which results in a linear set of constraints, while the nonlinearity only arises in the objective function due to logarithmic mean temperature difference formulation. However, as is discussed below, this is not the case in HIMAN due to the presence of NIM.

For mathematical approaches, the main difficulty arises in modeling the heat duty of water streams which are not known *a priori*. This is important as the HEN formulation is generally constructed by knowing the set of hot and cold streams in advance. Superstructure-based methodologies are often suggested to solve the problem by incorporating all possible interconnections but the computational burden for a comprehensive superstructure is often cited to be an issue [92]. To address this, a subset of water streams can be integrated with HEN. The survey of the literature shows that fresh water and wastewater streams are dominantly modeled

as a succession of heat exchangers and splitters, and heat exchangers and mixers, respectively. The rest of water streams, i.e., inlet streams, outlet streams, and recycling streams may or may not be included in HEN synthesis superstructure. In mathematical approaches, the dominant HEN superstructures are the modified state-wise superstructure of Yee and Grossmann [90] and the state-space superstructure of Bagajewicz et al. [93]. The former is modified by including stream splitting, stream mixing, and non-isothermal mixing options which consequently makes the problem non-convex with nonlinearities arising in both objective function and constraints. The superstructure formulation of Papoulias and Grossmann [1] has also been used by many authors [62, 9] to generate feasible heat exchange matches while the final HEN design is carried out using pinch design method. The HEN hyperstructure of Floudas and Ciric [4] has also been applied by Leewongtanawit and Kim [94] within a decomposition solution strategy.

1.2.5 Wastewater regeneration and treatment

Water regeneration implies removing impurities using treatment techniques which can later be reused or recycled in the system. Generally, regeneration units are categorized as fixed outlet concentration (provides linear models [6]) or fixed removal ratio approaches. This should not be confused with treatment units which remove impurities in disposed waste due to environmental regulations; though nevertheless, the classification remains the same. Methodologies for optimization of wastewater regeneration and treatment networks can be broadly categorized into conceptual and mathematical approaches. Conceptual approaches for wastewater treatment are limited to non-heat-integrated networks; nevertheless, a short summary of these methodologies is included here as they bring insights into optimal integration of treatment units with processes. Several conceptual techniques have been developed:

- **Fixed-load problems:** Early work on regeneration targeting in this category is based on limiting composite curve approaches [14, 15, 95]. However, as stated by Foo [19], these techniques could not handle all different cases that could arise. In particular, there are cases where implementing the regeneration process changed the pinch point [96] and hence cannot correctly define the minimum fresh water target. Later, several studies proposed using graphical and sequential approaches to overcome this issue, known as revised targeting techniques [97, 98]. They showed that the inlet concentration of a regeneration unit is not always the same as the pinch concentration (assumption that was made in previous work). In each case, a fixed outlet concentration for regeneration units were considered.
- **Fixed-flowrate problems:** Hallale [99] presented a guideline for placement of regeneration units in fixed-flowrate problems. Analogous to the placement of heat pumps in thermal processes, they indicated that in order to reduce the fresh water intake (analogous to reducing hot utility in conventional pinch analysis), a regeneration unit should be placed across the pinch by regenerating water with higher concentration from above the pinch (having excess water, analogous to excess heat below the pinch in conventional pinch analysis) to the lower concentration region below the pinch (water deficit, analogous to heat deficit above the pinch in conventional pinch analysis). The main conceptual methods include ultimate flow targeting, source composite curve, and automated targeting techniques. Nonetheless, separate analysis of wastewater treatment networks and water networks forbids any potential reduction in fresh water consumption.

Mathematical models of wastewater treatment and regeneration are nonlinear in nature due to the existence of bilinear terms and hence resulting in non-convex NLP formulations. Quesada and Grossmann [100] highlighted two formulation approaches in modeling general multi-component problems: considering mass flow and composition components unknown which makes the mass balance constraints of mixers nonlinear, while another approach is to model the individual flows of components which makes the mass balance constraints of splitters nonlinear. The former approach is the dominant one in water allocation networks. Quesada and Grossmann [100] proposed a linearization formulation using McCormick relaxation [101] within a branch and bound procedure to solve the problem to global optimality. Karuppiah and Grossmann [23] were the first to address the advantage of optimization of integrated water networks including wastewater treatment. Similar to Quesada and Grossmann [100] they incorporated the McCormick formulation for convex relaxation of bilinear terms in the original NLP model. They later extended their superstructure to address uncertainty within contamination generation and treatment removal ratio by proposing non-convex MINLP models and solve the problem to optimality. The detailed description of mathematical techniques in solving non-convex NLP and MINLP models are beyond the scope of this review and the readers are encourage to refer to [102, 103, 100, 23, 104, 105, 106].

Dong et al. [107] were the first to address total heat-integrated water allocation networks incorporating wastewater regeneration units and their interconnections within an MINLP superstructure. They showed that the combination of deterministic and stochastic search techniques typically reached the global optimum. Yang and Grossmann [75] have proposed a linear programming (LP) targeting model for water networks involving treatment units using a similar approach to the HEN stage-wise superstructure of Yee and Grossmann [90]. Their proposed model includes as many stages as the number of treatment technologies and one pathway for each unit operation, implying no mixer at the inlet of a treatment unit. The resulting targeting superstructure does not necessarily provide an upper bound, yet does provide approximations of the optimal value of the objective function for the original NLP model. Sharma and Rangaiah [71] applied the same formulation of Bogataj and Bagajewicz [80] for regeneration units while using multi-objective optimization (MOO) through a GA minimizing the total fresh water intake and total regenerated water. Besides two studies [108, 73] that have modeled the treatment units using the fixed outlet contamination approach, others have used the fixed removal ratio approach.

The full list of all the works in HIMANs together with their classifications and key features is presented in Table 1.2.

TABLE 1.2—Literature review of methodologies on HIWAN

	Methodology			Approach		Energy and mass features							
	Conceptual	Mathematical	Combined	Separate	Sequential	Simultaneous	Non-water thermal streams	Mass problem definition	Contaminants	NIM	Storage (water tanks)	Flow/heat loss/gain	Treatment/regeneration
Legends													
S	Single												
M	Multiple												
FL	Fixed load												
FF	Fixed flow												
I/II	Stage 1 or 2 of the methodology												
Srinivas and El-Halwagi [12]		•				•		FL	S				
Papalexandri and Pistikopoulos [11]		•				•		FL	S	•			•
Savulescu and Smith [5]	•				•			FL	S	•			•
Bagajewicz et al. [18]			•		•			FL	S	•			•
Savulescu et al. [109]	•				•			FF	S	•			•
Boondarik Leewongwanawit [110]		•				•		FL	S	•			•
Du et al. [46]		•			•			FL	M				•
Sorin and Savulescu [111]	•				•			FL	S	•			•
Savulescu et al. [50]	•					•		FL	S	•			•
Savulescu et al. [51]	•					•		FL	S	•		•	•
Bogataj and Bagajewicz [112]		•				•		FL	S	•			•
Liao et al. [113]		•			•			FL	S	•			•
Leewongtanawit and Kim [94]		•				•		FF	M	•		•	•
Feng et al. [62]			•			•		FL	M	•			•
Dong et al. [107]		•				•		FL	M	•			•
Bogataj and Bagajewicz [80]		•				•		FL	M	•			•
Xiao et al. [114]		•				•		FL	M	•			•
Manan et al. [52]	•				•			FL/FF	S	•			•
Leewongtanawit and Kim [53]	•				•				S	•			•
Kim et al. [115]		•				•		FL	M				•
Feng et al. [116]		•			•			FL	S	•			
Ataei et al. [63]			•			•		FL	S	•		•	•
Polley et al. [70]	•				•			FL	S				•
Chen et al. [108]		•				•			M	•	•		•
Ataei and Yoo [64]			•			•		FL	M	•		•	•
Wan Alwi et al. [54]	•					•		FL	S	•			•
Martínez-Patiño et al. [56]	•				•			FL	S	•	•		•
Ismail et al. [55]	•					•		FF	S	•			•
Liao et al. [117]		•				•		FL	S	•			•
George et al. [79]		•			•	•		FF	M	•			•
Bandyopadhyay and Sahu [118]	•					•		FL	S				•
Zhou et al. [41]		•				•		FF	M	•			•
Zhou et al. [119]		•				•		FL/FF	M	•			•
Yiqing et al. [78]	•				•			FL	S	•		•	•
Tan et al. [120]		•				•		FF	S	•			•
Sahu and Bandyopadhyay [65]			•		•			FF	M	•		•	•
Renard et al. [47]		•				•	•	FF	S	•			
Martínez-Patiño et al. [57]	•					•		FL	S	•			•
Boix et al. [73]		•			•			FL	S	•			•
Ahmetović and Kravanja [121]		•			I	II		FL	M	•			•
Yang and Grossmann [75]		•				•		FL	M	•			•
Tan et al. [66]			•			•		FL/FF	M	•			•
Rojas-Torres et al. [122]		•				•		FL	M				

1.3 Superstructure generation and solution strategies

In general, the synthesis problem of HIMANs is formulated as an MINLP problem. This is due to the presence of binary variables (existence of heat or mass exchange matches) and continuous variables (operating conditions, e.g., temperature and contamination levels) which are complex to solve. This necessitates the development of robust and efficient solution strategies. Several solution strategies can be applied to HIMAN superstructures depending on the interconnectivity, complexity and completeness of the superstructure. As stated by Jeżowski [6], they can be categorized into linearization, initialization, sequential, decomposition, meta-heuristics and simultaneous techniques. Simultaneous solution strategies for solving MINLP problems may exhibit decomposition or sequential techniques intrinsic to the solver being used. They are, however, categorized under simultaneous strategies. It should also be highlighted that the categorization can overlap to some degree, i.e., several techniques can be combined in a solution strategy. Table 1.3 provides a feature-based representation of all mathematical approaches in HIMAN synthesis problems addressing their objective function(s), mathematical formulation and solution strategy.

1.3.1 Decomposition

Two terminologies of “decomposition” and “sequential” must be clarified here. In both cases, the problem is divided into two or more steps; however, the former consists of a finite number of iterations between the steps given defined termination criteria, while the latter is a uni-directional solution strategy with no iteration. More importantly, in decomposition solution strategies (such as GBD) the results of one step provide inputs for the subsequent steps while in sequential solution strategies, no such interactions exist. Papalexandri and Pistikopoulos [11] proposed an MINLP superstructure for heat and mass exchange networks and solved it using GBD [148] by decomposing the problem into a master MILP model optimizing the network configuration and a primal NLP model optimizing the operating conditions. The MILP model provided a non-decreasing lower bound to the objective function while the NLP model gave a non-increasing upper bound. The stopping criterion was the convergence of the objective functions in the two steps below a predefined threshold. They have allocated the binary and continuous variables to master and primal problems, respectively. Similarly, Leewongtanawit and Kim [94] decomposed their MINLP model into MILP and NLP models and solved them iteratively until no further improvement (beyond a threshold) was observed in the objective function of the NLP model. They decomposed the variables similar to the approach proposed by Floudas and Ciric [4] in HEN synthesis.

1.3.2 Sequential

Several sequential solution strategies have been proposed which commonly optimize water and heat targets within the first or second step using LP [18, 65], MILP [48, 9, 62], or NLP [63, 64] models. Having these targets (with or without the design of water network), an MILP model can be formulated to minimize the number of heat exchange matches [1, 2]. In all cases, the HEN is designed using the pinch design method. Liao et al. [113] proposed a two-step approach for targeting and design by formulating two MINLP models. The first model obtained the water and thermal utility targets with number of stream splits, while the second model minimized the number of heat exchange matches. Dong et al. [107] proposed an iterative

sequential solution strategy by first solving an MINLP model using random initial guesses and later improving the results (solving the MINLP model at each step) by iterative heuristic perturbations in both continuous and binary variables. Liao et al. [117] solved an MILP model minimizing the operating cost together with number of matches (similar to HLD) and used the targets and matches as initialization for the MINLP model of HIMAN. Most recently, Ibric et al. [142] proposed an iterative sequential solution strategy consisting of two steps. An NLP water network model was solved for minimum heat recovery approach temperature (HRAT) to provide a lower bound on the problem. In the second step, an upper bound is assigned to HRAT using a finite number of iterations and a sequence of NLP-MINLP models were solved for each value with the final solution selected as the best among all solutions. Jagannath and Almansoori [141] proposed a sequential solution strategy by introducing three MINLP models: Model A (water network with NIM), Model C (HEN synthesis [90]) and Model B (combined Models A and C). The problem was solved sequentially by solving Model A and a simplified version of Model A to find the water and energy targets. Depending on the results of the two versions, a relaxed version of Model B was solved. At this point, the flow and concentration variables in Model A were fixed and the problem was solved to generate set of solutions using techniques similar to integer cuts. Model C was applied for each solution and the final optimal solution was thus selected as the best of all solutions. The authors mentioned that their sequential approach is computationally exhaustive, yet the solutions are similar to those obtained by simultaneous approaches. More recently, Hong et al. [146] extended their targeting approach [145] by addressing multi-contaminant as well as treatment problems using a sequential solution strategy. An NLP model was formulated to minimize the fresh water consumption in a first step, providing initial values on flow rates and concentrations. An MINLP model was then solved with relaxed/linear TAC in the second step followed by optimization of the original MINLP in the third step.

1.3.3 Simultaneous with or without initialization

For simultaneous approaches, models are mainly formulated as MINLP which are solved using commercial software, such as DICOPT [149], BARON [150, 151], SBB or LINDO [152]. It should be noted that the algorithms underlying these solvers (e.g., outer approximation [153] in DICOPT) are based on decomposition techniques. Nevertheless the original mathematical formulation was not decomposed before solving [112, 115, 120, 143]). Generally, an MINLP model requires good initialization which can be achieved by solving a relaxed instance of the original model either through fixing continuous variables (resulting in an MILP initialization model), fixing binary variables (mainly by excluding the HEN matches, and hence resulting in an NLP model [126, 124, 129, 130, 131, 134]), solving an MINLP model of water network with no heat integration [133], or by generating random values [135, 42]. Boondarik Leewongwanawit [110] used an MILP model for initialization of MINLP superstructure by fixing the contamination loading at the outlet of water units and linearizing the HEN cost formulation. Dong et al. [107] used an NLP formulation of the water network for targeting the utility consumption and further labeling thermal streams (i.e., hot or cold) which was then solved simultaneously.

1.3.4 Meta-heuristics

Over the past years, meta-heuristic techniques have emerged a promising approach for solving problems in process integration. Xiao et al. [114] used evolutionary strategies and manipulations as the last stage of their method for improving water and heat exchanger networks configurations. Du et al. [46] have employed GA combined with simulated annealing (SA) for optimizing water network (MINLP superstructure) and HEN (MINLP superstructure) in an iterative manner. They, however, neglected temperature effects in the water superstructure (first step) and hence construct (i.e., extract) the required thermal streams based on the optimized water network for the second step. Liu et al. [67] proposed a hybrid methodology combining GA-SA with mass pinch and pseudo-T-H-diagram [154]. Other meta-heuristics approaches, such as particle swarm optimization were incorporated in the work of Li [123].

1.3.5 Relaxation/Transformation

Under this classification, the original MINLP model is transformed/simplified/relaxed by re-defining/removing/adding extra constraints. Zhou et al. [135] formulated a HIMAN superstructure using mathematical programming with equilibrium constraints (MPEC) and applied complementarity formulations [155] to model binary variables. They solved the problem by transforming the model into NLP. Liu et al. [137] has applied generalized disjunctive programming (GDP) to formulate discrete and continuous variables of HIMAN by incorporating logical propositions, disjunctions and algebraic constraints. They solved the problem using BARON by transforming the GDP model into MINLP. However their formulation does not address HEN design. Several authors [139, 147] proposed HIMAN superstructures using NLP techniques. Yan et al. [139] adapted the MINLP superstructure of Ahmetović and Kravanja [126] and avoided the use of binary variables by introducing continuous variables in the form of $y = f/(f + \zeta)$ where y indicates the existence of the unit of size f and ζ is a very small parameter ($\sim 10^{-5}f$). Nevertheless, the superstructure *a priori* treated fresh water and wastewater streams as the only cold and hot streams, respectively, involved in heat integration. More recently, Hong et al. [145] proposed a targeting approach using an MILP formulation in which the HEN was designed in a single step. They adapted the HEN transshipment model [1, 90] addressing stream splitting and NIM within the HEN superstructure. One other possibility is by using a discretization approach in which known variables are discretized into a set of known values which will result in an MILP model [66, 156]. Several authors have highlighted the challenges in solving medium and large MINLP problems and proposed a reduction strategy and a reduced superstructure to solve heat-integrated water allocation networks more easily [142, 69]. Wang et al. [69] proposed several heuristics related to contamination monotonicity (only applicable to single-contaminant problems) and pinch principles together with rational NIM in order to simplify the superstructure of Liu et al. [136]. Ibrić et al. [142] also applied several rules to eliminate infeasible and impractical variables and connections from the superstructure. They showed that these simplifications can reduce the computational efforts and hence increase the solving efficiency.

In summary, it was observed that several major superstructures have been used/proposed by previous authors for synthesizing HIMAN problems, addressed specific regions of the solution space and required specific solution strategies. One approach was the HEN hyperstructure formulation of Floudas and Ciric [4] combined with the water allocation network problem such

as in Leewongtanawit and Kim [94], which was solved via a decomposition strategy. Alternatively, Papalexandri and Pistikopoulos [11] proposed a hyperstructure for heat and mass allocation networks by integrating the HEN hyperstructure [4] and an analogous mass exchange hyperstructure [157] to construct the HIMAN hyperstructure. This approach encompassed all possible interactions between the two, where each stream could be split and directed to all heat and mass exchangers while bypass streams were also included. This comprehensive model was formulated as an MINLP problem and solved using GBD. The stage-wise HEN superstructure of Yee and Grossmann [90] was the major formulation used in the literature. As discussed in subsection 1.2.4, the major assumption of the original formulation is the isothermal mixing of streams which consequently forbids many promising alternatives in the HIMAN synthesis problem. This was modified by many authors to address non-isothermal mixing and splitting. This superstructure and the one proposed by Floudas and Ciric [4] (“simultaneous match-network optimization”) are categorized under simultaneous approaches. Their usage in HIMAN synthesis problems requires additional assumptions and simplifications (e.g., not considering all water stream participating in heat exchange) in the hope of alleviating the computational burden of solving the superstructure of all possible opportunities. As an alternative to superstructure representation, the state-space representation of Bagajewicz et al. [93] was addressed in synthesizing HIMANs by several authors [107, 114, 41, 119, 42]. The state-space representation contains the superstructure representation of HIMAN as a special case. Nonetheless, as stated by Bagajewicz et al. [93], this representation can alleviate some of the difficulties arising in superstructure optimization. The representation is based on the definition of a set of input and output variables (e.g., input and output temperatures of thermal streams) and their relations. A state variable, such as heat exchanger inlet temperature or mass exchanger inlet concentration, is defined as a variable which allows calculation of the output variables by relation with the inputs. The state-space is referred to as the set over which the state variables take their values. To this end, the overall input–output relations can be solved via two operators: one dealing with mixing and splitting, and the other with mass or heat exchange. It was shown that use of a particular operator—the assignment operator—can lead to NLP formulations which are better suited for solving large-scale problems.

TABLE 1.3—Comparison of articles on combined water and energy integration (mathematical approaches)

Legends	Objective function(s)	Mathematical formulations					Overall solution strategy					Solution strategies
		TAC	Operating cost	Mass and energy targeting	Number of HE matches	LP	MILP	NLP	MINLP	DNLP	Linearization	
LB Lower bound UB Upper bound NS Fixed set of iterations → Next step ↔ Iteration ↪ Transformed to I/II/III Stage 1,2 or 3 of the methodology												
Srinivas and El-Halwagi [12]	I	•	•	•	II	II	•	•	I	•	MINLP (linearization, flow rate and temperatures) → MILP	I •
Papalexandri and Pistikopoulos [11]	I	•	•	•	II	II	•	•	•	•	GBD (master MILP (LB) ↔ slave NLP (UB))	• •
Bagajewicz et al. [18]	I	•	•	•	II	I	II	•	•	•	Two LPs (min water target → min energy target) → MILP → stream merging procedure	• •
Boondarik Leewongwanawit [110]	•	•	•	•	•	•	•	•	•	•	MINLP (initialization with MILP, fixing outlet concentration)	• •
Du et al. [46]	I	II	•	•	II	I,II	•	•	•	•	MINLP (water network, SA-GA) ↔ MINLP (HEN, GA-SA)	• •
Bogataj and Bagajewicz [112]	I	•	•	•	II	I,II	•	•	•	•	MINLP (solving subsequent NLP models)	• •
Liao et al. [113]	I	•	•	•	II	•	•	•	•	•	MINLP [NLP (SQP) ↔ MILP] → MINLP	• •
Leewongtanawit and Kim [94]	•	•	•	•	•	•	•	•	•	•	MILP (relaxation) → MINLP (MILP ↔ NLP), similar to GBD but stopping criterion: $ obj_{NLP}^{it} - obj_{NLP}^{it+1} \leq \epsilon$ where ϵ is the iteration counter	• •
Feng et al. [62]	I	II	•	•	II	I,II	•	•	•	•	Two MILPs (min water → min energy) → MILP	• •
Dong et al. [107]	•	•	•	•	•	•	•	•	•	•	MINLP (random initial guess) → MINLP (perturbation of continuous variables) → MINLP (perturbation of binary variables) → identify heat load loops and path	• •
Bogataj and Bagajewicz [80]	I	II	•	•	II	I	II	•	•	•	NLP (targeting, labeling thermal streams) → MINLP	• •
Xiao et al. [114]	I	II	•	•	II	I	II	•	•	•	[NLP (min water) → MINLP (HEN)] → initialization (perturbation) MINLP (HIMAN)	• •
Kim et al. [115]	•	•	•	•	•	•	•	•	•	•	MINLP	•
Feng et al. [116]	•	•	•	•	•	•	•	•	•	•	Targeting → minimum number of temperature valleys	•
Ataei et al. [63]	•	•	•	•	•	•	•	•	•	•	NLP (targeting) → graphical approach → NLP (HEN cost)	•
Chen et al. [108]	I	II	•	•	II	I,II	•	•	•	•	MINLP (min water) → [MINLP (min TAC) MILP (min operating cost)]	•
Ataei and Yoo [64]	•	•	•	•	•	•	•	•	•	•	NLP (targeting) → graphical approach → NLP (HEN cost)	•
Liao et al. [117]	I	II	•	•	I	II	•	•	•	•	MINLP (min operating cost + number of matches) → MINLP	•
George et al. [79]	I,II	III	•	•	I,II	III	•	•	•	•	LP → LP → DNLP → NLP	•
Zhou et al. [41]	•	•	•	•	•	•	•	•	•	•	MINLP	•
Zhou et al. [119]	•	•	•	•	•	•	•	•	•	•	MINLP	•
Tan et al. [120]	•	•	•	•	•	•	•	•	•	•	MINLP	•

TABLE 1.3—Comparison of articles on combined water and energy integration (mathematical approaches) (cont'd)

Legends	Objective function(s)	Mathematical formulations					Overall solution strategy					Solution strategies			
		Mass and energy targeting	Operating cost	TAC	Number of HE matches	LP	MILP	NLP	MINLP	DNLP					
LB Lower bound UB Upper bound NS Fixed set of iterations → Next step ↔ Iteration ↷ Transformed to I/II/III Stage 1,2 or 3 of the methodology															
									</						

TABLE 1.3—Comparison of articles on combined water and energy integration (mathematical approaches) (cont'd)

Legends	Objective function(s)	Mathematical formulations	Overall solution strategy	Solution strategies	
LB Lower bound UB Upper bound NS Fixed set of iterations → Next step ↔ Iteration ↷ Transformed to I/II/III Stage 1,2 or 3 of the methodology	Mass and energy targeting	TAC		Linearization	
		Operating cost		Sequential Initialization	
		Number of HE matches	LP MILP NLP MINLP DNLP	Decomposition	
				Met-a-heuristic	
				Simultaneous	
	Zhou and Li [42]	•	•	Local optimum (MINLP ↔ relaxed-MINLP perturbation) → clustering technique	• • •
	Zhou et al. [135]	•	•	MINLP ↷ MPEC ↷ NLP	•
	Liu et al. [136, 137]	•	•	GDP ↷ MINLP	•
	Ghazouani et al. [138]	•	•	MILP	•
	Yan et al. [139]	•	•	NLP (relaxing integers with fractional continuous variables)	•
	Torkfar and Avami [140]	•	•	MINLP (including pressure drops in water network)	NA
	Liang and Hui [72]	I II,III	•	Reducing repeated heating and cooling [18, 116] Model A (min freshwater) → Model B [Relaxed-MINLP (min TAC) → NS [Model A → Model C]]	• • •
	Jagannath and Almansoori [141]	I	II,III	NLP (HRAT _{min} → LB) → NLP (HRAT _{max} → UB) → NS MINLP (for different values of HRAT)	• • •
	Ibrić et al. [142]	I II	I II	MINLP	• • •
	Hong et al. [143]	•	•	ε-constraint MOO (min freshwater, number of water connections) → pinch analysis (MER) → HENMINLP	•
De-León Almaraz et al. [68]	I II	I,II	MINLP (targeting) → HEN (pinch design method) MILP (targeting + design of water network) → MILP (HLD) → pinch design method	• • •	
Wang et al. [69]	•	I II	NLP (HRAT _{min} → LB) → NS [NLP (HRAT _{max} → UB) → Relaxed-MINLP (find matches) → MINLP]	• • •	
Kermani et al. [9]	I II	I,II	MILP → HEN	• • •	
Ibrić et al. [49]	I II	I II	Same as Ibrić et al. [142] MILP	• • •	
Ghazouani et al. [144]	I II	I II	NLP (min freshwater) → MINLP (min relaxed TAC) → MINLP (min TAC)	• • •	
Ibrić et al. [43]	I II	I II	NLP (relaxing integers with fractional continuous variables)	•	
Hong et al. [145]	•	•		• • •	
Hong et al. [146]	I II,III	I II,III		• • •	
Liu et al. [147]	•	•		•	

1.4 Other features

1.4.1 Superstructure extension

Despite the importance of holistic approaches to capture the trade-offs between heat and water, a limited amount of research has included non-water thermal streams in their methodologies. This potential was first addressed by Renard et al. [47], although no case study was presented. Later, Kermani et al. [48] extended their superstructure and presented a simplified kraft mill process by incorporating non-water thermal streams and showed the large potential in their combination. This has been later applied to a real kraft mill [9, 44], also addressing interplant operations. Zhou et al. [41, 119] developed a multi-scale, stage-wise superstructure addressing interplant operations for fixed-load as well as fixed-flowrate problems using MINLP. Most recently, Ibrić et al. [43] extended their superstructure [142] to address interplant operations by use of additional binary parameters to allow or forbid interplant connections. Heat transfer coefficient calculations have also been considered in the work of Torkfar and Avami [140] as a function of stream velocity. They further included pressure drop calculations in HEN and water network design. Their superstructure was formulated using MINLP which is stated as a modified and improved version of the superstructure by Jiménez-Gutiérrez et al. [128]. Use of live steam was first investigated by Savulescu and Smith [5]. They argued that use of live steam in water networks is doubly beneficial since it can reduce the steam consumption and also eliminate the use of heaters, hence reducing the capital cost. To the best of the authors' knowledge, the methodology presented by De-León Almaraz et al. [68] is the only work considering the use of vapor-state water in the water network. For implementation reasons, they modeled the phase change by only considering the sensible heat in the HEN design, while the latent heat is added to the solution via addition of a corresponding hot utility.

1.4.2 Physical improvements

Importance of NIM and its effects on network performance were extensively highlighted throughout the literature [62, 109, 78, 158]. Recently, Martínez-Patiño et al. [159] analyzed direct and indirect heat exchanges by incorporating an exergy component. They concluded that networks having the same water and energy targets may exhibit different exergy losses (due to NIM) which negatively impact the cost of heat exchanger area.

Features of non-water thermal streams and use of live steam in water networks must be studied further as they represent a more realistic approach for application of HIMAN methodologies in industrial applications.

1.4.3 Water–energy nexus

Heat-integrated water allocation network synthesis problems have been treated as a separate research field over the past decades; however, they should be regarded as a special case in the field research related to the water–energy nexus which, in turn, is part of a broader water–energy–food nexus. The water–energy nexus was first mentioned in an annual review paper by Gleick [160], highlighting the interconnectedness of energy and water. The reasoning followed that water is used in extracting and producing fuels and producing electricity via steam while energy is used to produce, transport, and purify water. In addition to the research

discussed in this chapter, work in water–energy nexus domain encompasses developments in the field of desalination technologies, membrane systems, water use in biorefineries, and in shale gas production. The water–energy–food nexus considers the intertwined nature of water, energy, and food by highlighting that water is used to produce food and varieties of crops which, in turn, can be used to produce biofuels. Garcia and You [161] highlighted several research opportunities related to the water–energy nexus: energy and water use in households, novel water sources such as rainwater or water being produced from extraction of fossil fuels, hydropower plants, climate studies, policy planning, and holistic approaches in design of industrial wastewater treatment networks. For comprehensive review of recent contributions and future directions related to the water–energy nexus, the reader is encouraged to refer to review papers by Garcia and You [161], Martinez-Hernandez and Samsatli [162], Lee et al. [163], Albrecht et al. [164], and Dai et al. [165].

1.5 Benchmarking analysis

Similar to the previous review on HIMANs [22], a benchmarking analysis is carried out to illustrate the main features of different methodologies. A well-known single-contaminant case study (Table 1.4) originally proposed by Savulescu and Smith [5] was selected. Over 35 articles have evaluated their proposed methodologies using this case study. The results are provided in Table 1.5 while selected key features are plotted in Figure 1.3 using parallel coordinates for 33 out of 35 articles (two of them lack data to be visualized).

Several network indicators have been selected for the analysis: Number of thermal streams including thermal utilities (N_s^{th}), number of heat exchangers (N_{HE}), total area of heat exchangers (A_{HEN}^{total}), total number of mixing points (N_{mixer}), number of non-isothermal mixing points (N_{mixer}^{NIM}), and number of mass streams in the water network excluding the thermal ones (N_s^m) are among them. Figure 1.3 shows that the number of non-isothermal mixing points as well as number of mass streams (N_s^m) are inversely proportional to the HEN cost, i.e., increasing either of the two will decrease the HEN cost.

This case study further illustrates the necessity of considering more indicators while optimizing heat-integrated water allocation networks. Among the 33 visualized results in Figure 1.3, 29 results possess between 3–5 heat exchangers (the maximum is 10). This may indicate good compromise in HEN investment costs; however, for the same solutions, the number of mixers, non-isothermal mixers and total heat exchange area vary 3–13, 0–10, and 3,500–6,300 m², respectively. These “neglected” indicators should be somehow addressed in HIMAN synthesis problems which necessitate the application of multi-criteria decision making approaches. In addition, no single solution can possess the optimal value for all indicators, which correspondingly requires the generation of a set of potential solutions that can be analyzed, instead of a single “optimal” solution.

TABLE 1.4—Operating data of the benchmarking test case [51]

Units	Mass load (L_u) (g/s)	$C_u^{in,max}$ (ppm)	$C_u^{out,in}$ (ppm)	T_u (°C)	Limiting flowrate (kg/s)
u_1	2	0	100	40	20
u_2	5	50	100	100	100
u_3	30	50	800	75	40
u_4	4	400	800	50	10

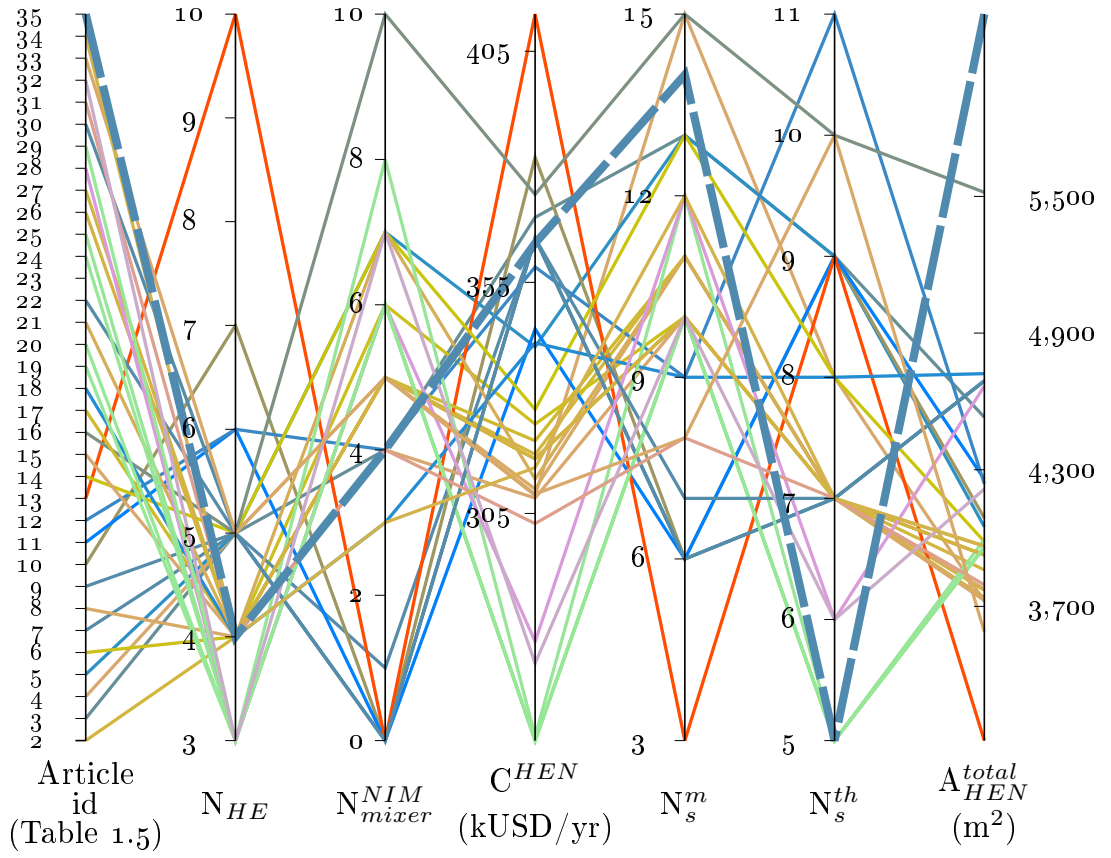


FIGURE 1.3—Visualization of some key indicators of the benchmarking case study (Table 1.5) using parallel coordinates [166]

TABLE 1.5—Benchmarking of several HIMAN methodologies using the four-water-process test case of Savulescu and Smith [5]⁽¹⁾

id	M/C ⁽²⁾	Network indicators ⁽³⁾					Economic indicators ⁽⁴⁾				Comments
		N _s th	N _{HE}	A _{HEN} ^{total} (m ²)	N _{mixer} (N _{NIM} ^{mixer})	N _s ^m	Q _{HEN} ^{total} (kW)	C _{HEN} ^(USD/yr)	C _{TAC} ^(USD/yr)		
1	Savulescu and Smith [5]	C	9	5	NA	10 (6)	15	NA	NA	NA	
2	Bagajewicz et al. [48]	M	7	4	3,860.2	7 (5)	11	22,008	317,798	2,714,858	
3	Savulescu et al. [51]	C	9	5	4,530.9	9 (4)	13	23,585	369,042	3,040,612	
4	Bogataj and Bagajewicz [112]	M	8	5	3,722.1	7 (5)	15	22,006	308,889	2,705,949	Water network identical to Bagajewicz et al. [48].
5	Dong et al. [107]	M	9	5	4,049.6	10 (7)	13	22,680	341,044	2,738,104	
6	Bogataj and Bagajewicz [80]	M	7	4	3,771.1	7 (6)	10	21,943	324,338	2,721,398	
7	Xiao et al. [114]	M	7	5	4,689.7	3 (1)	6	26,040	364,587	2,761,647	
8	Leewongtanawit and Kim [53]	C	7	4	3,775.4	8 (5)	11	22,260	310,283	2,707,343	
9	Polley et al. [70]	option 1	7	5	4,089.6	3 (0)	6	26,040	364,573	2,761,633	
10		option 2	9	7	4,087.8	4 (0)	6	23,100	382,059	2,779,119	
11		option 3	9	6	4,258.4	4 (0)	6	23,940	344,905	2,741,965	
12	Mao et al. [167]	C	11	6	4,238.1	9 (4)	9	24,071	358,328	2,755,388	
13	Wan Alwi et al. [54]	C	9	10	3,111.0	6 (0)	3	26,040	413,022	2,810,682	infeasible HEN (Figure 9 of ref. [54])
14	Martínez-Patiño et al. [56]	C	8	5	3,984.9	9 (7)	13	23,527	327,484	2,954,324	
15	Liao et al. [117]	case a	7	4	3,725.8	7 (4)	10	22,008	308,356	2,705,416	Wastewater streams are merged
16		case b	10	5	5,517.5	13 (10)	15	25,101	374,010	2,771,070	Wastewater streams are treated individually
17	Yiqing et al. [78]	C	7	4	3,964.4	8 (5)	11	22,260	320,716	2,717,776	The best solution among two.
18	Martínez-Patiño et al. [57]	C	8	4	4,721.6	5 (3)	9	26,040	341,915	2,738,975	
19	Ibrić et al. [124]	M	5	3	3,960.1	6 (6)	10	22,344	255,873	2,652,933	Best solution with HRAT = 9°C
20	Ahmetović and Kravanja [126]	M	5	3	3,960.1	6 (6)	10	22,344	255,873	2,652,933	Same as Ibrić et al. [124]
21	Liu et al. [136]	M	7	4	3,739.9	7 (7)	11	22,008	312,440	2,709,500	
22	Hou et al. [59]	C	7	5	4,089.7	3 (0)	6	26,040	364,587	2,761,647	Polley et al. [70], option 1
23	Chen et al. [132]	M	9	12	NA	NA	NA	26,062	NA	NA	
24	Zhou et al. [135]	MPEC	5	3	3,960.8	6 (6)	10	22,344	255,891	2,652,951	Same as Ibrić et al. [124]
25		MINLP	5	3	3,993.1	8 (8)	12	22,362	256,779	2,653,839	
26	Zhao et al. [74]	C	7	4	3,925.7	7 (5)	10	22,260	316,801	2,713,861	
27	Liu et al. [137]	M	7	4	3,925.7	7 (5)	10	22,260	316,801	2,713,861	
28	Liao et al. [58]	C	6	3	4,666.8	8 (6)	12	22,008	277,286	2,674,346	Case 5 - Figure 17-b of ref. [58]
29	Yan et al. [139]	M	5	3	3,960.1	6 (6)	10	22,344	255,873	2,652,933	Same as Ibrić et al. [124]
30	Xie et al. [61]	C	7	5	4,689.7	4 (0)	7	26,040	364,587	2,761,647	
31	Torkfar and Avami [140]	M	7	4	3,734.6	5 (4)	8	22,008	302,830	2,699,890	Wastewater streams are merged
32	Hong et al. [143]	case a	6	3	4,215.3	7 (7)	10	21,000	2,669,640	2,669,640	Wastewater streams are treated individually
33		case b	10	5	3,589.1	6 (5)	8	21,807	309,197	2,706,257	
34	Hou et al. [60]	C	7	4	3,965.6	5 (3)	12	22,260	314,939	2,711,999	
35	Kernani et al. [9]	M	5	4	6,300.0	10 (4)	14	23,012	363,449	2,760,599	Best solution with HRAT = 4°C HEN synthesis using NLP formulation [85]

- (1) All methodologies reached the fresh water target of 90 kg/s. All but two of them reached the thermal utility targets of 3,780 kW of hot utility. Savulescu et al. [51] and Martínez-Patiño et al. [56] have reported 485 and 406 kW of cold utility and 4,265 and 4,186 kW of hot utility, respectively. Where information was not enough to calculate the indicators, ‘NA’ is indicated.
- (2) ‘M’ indicates mathematical approach, while ‘C’ denotes conceptual approach.
- (3) Network indicators are number of thermal streams including thermal utilities (N_s^{th}), number of heat exchangers (N_{HE}), total area of heat exchangers (A_{HEN}^{total}), total number of mixing points (N_{mixer}), number of non-isothermal mixing points (N_{mixer}^{NIM}), number of mass streams in the water network excluding the thermal ones (N_s^m), and total heat load of all the heat exchangers (Q_{HEN}^{total}).
- (4) Economic indicators are HEN cost (C^{HEN}) and total annualized cost (C^{TAC}) which includes operating costs and HEN cost.

1.6 Concluding remarks and future directions

This work presented a meta-analysis of the literature on heat-integrated water allocation networks. Key features of the proposed methodologies have been analyzed with special focus on mathematical programming approaches including HEN synthesis. Developing more rigorous mathematical superstructures necessitates proposing novel solution strategies. The proposed solution strategies have been categorized into decomposition, sequential, simultaneous (with or without initialization), meta-heuristics, and relaxation/transformation strategies. A benchmarking analysis was presented comparing the results of different proposed methodologies from the water and heat exchanger networks perspective. It illustrated how methodologies can produce different results considering other indicators than the typical TAC. Following this review, several gaps have been identified (Table 1.6 summarizes the main gaps):

- ▶ As mentioned previously, despite the importance of addressing synergies among various elements in a typical industrial plant, **holistic approaches** have rarely been addressed in HIMAN synthesis problems. Apart from a limited number of specific publications [47, 48, 9, 44, 49], **non-water thermal streams** have not been combined in HIMAN synthesis. Future research directions should therefore focus on this aspect by proposing more rigorous and efficient superstructures. In addition, use of **live steam** should be investigated using improved formulations.
- ▶ As water is subject to heating and cooling duties, water loops have a role in recovering heat within and between processes. This feature is even more sensible when considering inter-plant operations. Moreover, following the observed gap in holistic approaches, HIMAN synthesis problems should be considered in conjunction with other **heat recovery** technologies including organic Rankine cycles (ORC)s and heat pumps.
- ▶ The literature lacks **multi-period** operations of HIMANs. This is an important feature considering daily and seasonal variations of operating conditions of an industrial plant, including the temperature of freshwater. **Thermal storage tanks** must be combined within HIMAN problems to provide a flexible heat transfer medium over time.
- ▶ **Uncertainty analysis** of HIMANs must be addressed to find resilient networks given the uncertainties in the system including costs and operating conditions.
- ▶ Following the benchmarking analysis, **multi-criteria decision making** approaches must be incorporated in HIMAN synthesis problems to find sets of promising optimal or near-optimal solutions considering diverse economic, environmental, and practical indicators. The application of **stochastic optimization** and **hybrid approaches** should be favored in this direction.
- ▶ Upon the survey of the literature, only one article mentioned large-scale industrial applications [9], yet the methodology is limited to the targeting step. Most of the proposed mathematical methodologies are highly complex and their applications to industrial cases may face computational challenges. Hence, research towards **efficient solution strategies** must be the future trend thus shifting the focus towards reaching practical and good solutions, not necessarily the global optimum.
- ▶ Following the highlighted gaps in Table 1.1, **batch processes** and **retrofitting** remain largely untreated which necessitates further research. ■

TABLE 1.6—Summary of identified gap in HIWAN synthesis problem

Gap	Description/Remarks
<i>Unaddressed gaps</i>	
Fixed concentration problems	Problems with variable mass load
Rigorous modeling	Water and waste treatment models
Multi-period operation	Considering the dynamic nature of systems
Retrofitting	Methods covering partial system retrofit and redesign instead of design
<i>Newly identified gaps</i>	
Better treatment of thermal streams	Considering non-water thermal streams and potential for live steam as part of the problem definition
Utility integration	Considering HIWAN with utility selection and integration concepts
Sensitivity analysis	Generation of multiple or resilient solutions in lieu of global optima
Multi-criteria optimization	Methods which address multiple criteria for decision-making which extend beyond minimization of cost or fresh water consumption, considering an expanded system.
Large-scale problems	Developing approaches to adapt formulations to larger scale problems or reformulation to encourage solution generation for problems on the industrial scale

CHAPTER 2

Targeting methodology with industrial application

Overview

A novel linear superstructure for the optimization of HIWANS is proposed. Non-isothermal mixing is considered using a discretization approach to reduce the number of thermal streams and decrease investment costs by avoiding unnecessary investment on heat exchangers. In addition, restricted matches and models of water tanks are incorporated to address a wide range of industrial cases. The proposed methodology is validated using several test cases from the literature. The results indicate that, in many cases, this approach provides enhanced key indicators when compared with conceptual and nonlinear mathematical optimization approaches. Furthermore, a step-by-step methodology is proposed for industrial applications: 1) plant characterization, 2) quantification of qualitative constraints, 3) modeling, 4) preliminary targeting, 5) optimization, 6) identification and evaluation of reduction opportunities, and 7) projects selection and roadmap implementation. An integer-cut constraint (ICC) technique is applied to systematically generate a set of optimal solutions to support decision-making for cost-effective configurations.

This chapter is an extension of *M. Kermani, Z. Périn-Levasseur, M. Benali, L. Savulescu, F. Maréchal, 2017, A novel MILP approach for simultaneous optimization of water and energy: Application to a Canadian softwood kraft pulping mill, Computers & Chemical Engineering [9]*.

2.1 Problem statement

Two sets of process water unit operations (\mathbf{P}_{out}^{WAN} , \mathbf{P}_{in}^{WAN}) are given. Each unit j in \mathbf{P}_{in}^{WAN} requires water at temperature T_j , with a maximum allowed contamination level of $c_j^{k,max}$ and a flow rate of \mathbf{m}_j . Each unit i in \mathbf{P}_{out}^{WAN} provides water at temperature T_i , with a contamination level of $c_i^{k,max}$ and a flow rate of \mathbf{m}_i . Furthermore, sets of hot and cold non-water process streams (\mathbf{P}^H , \mathbf{P}^C , respectively) are also considered. They are characterized by inlet temperatures ($T_{p,in}^H$, $T_{p,in}^C$), outlet temperatures ($T_{p,out}^H$, $T_{p,out}^C$), and heat loads (Q_p^H , Q_p^C). Thermal hot and cold utilities (\mathbf{U}^H , \mathbf{U}^C , respectively) are also available in case the energy within the system is not sufficient to satisfy energy demands. In addition, multiple freshwater sources and wastewater sinks (\mathbf{U}_{out}^{WAN} , \mathbf{U}_{in}^{WAN}) are given, as multiple water utilities are needed in order to respond to the demand of water having different qualities. Furthermore,

different wastewater sinks accept waste at different contamination levels, according to different wastewater treatment facilities. The objective is to reduce water and energy consumption in the system while satisfying thermal and water demands. In order to better represent the mathematical formulations, certain sets are defined as follows:

$$\mathbf{WAN}_{out} = \mathbf{U}_{out}^{WAN} \cup \mathbf{P}_{out}^{WAN} \quad (2.1)$$

$$\mathbf{WAN}_{in} = \mathbf{U}_{in}^{WAN} \cup \mathbf{P}_{in}^{WAN} \quad (2.2)$$

$$\mathbf{WAN} = \mathbf{WAN}_{in} \cup \mathbf{WAN}_{out} \quad (2.3)$$

$$\mathbf{HS} = \mathbf{U}^H \cup \mathbf{P}^H \bigcup_{u \in \mathbf{WAN}} \mathbf{S}_u^H \quad (2.4)$$

$$\mathbf{CS} = \mathbf{U}^C \cup \mathbf{P}^C \bigcup_{u \in \mathbf{WAN}} \mathbf{S}_u^C \quad (2.5)$$

$$\mathbf{S}_u = \mathbf{S}_u^H \cup \mathbf{S}_u^C \quad \forall u \in \mathbf{WAN} \quad (2.6)$$

where, \mathbf{WAN}_{out} is the set of source water unit operations, \mathbf{WAN}_{in} is the set of sink water unit operations, \mathbf{WAN} is the set of water unit operations, \mathbf{HS} (\mathbf{CS}) is the set of hot (cold) thermal streams in the system including hot water thermal streams, \mathbf{S}_u^H (cold, \mathbf{S}_u^C), and \mathbf{S}_u is the set of thermal streams associated to water unit operation u .

2.2 Mathematical formulation

The proposed superstructure is formulated as a MILP model. It includes a water network, a heat network (using heat cascade model [84]), and connections between the two (i.e., incorporating water thermal streams within the heat cascade model). An innovative linearized formulation of NIM was integrated in the superstructure by fixing temperatures of mixing points at a set of pre-defined values. The primary source of these temperatures is the set of temperatures of water unit operations in the current operating conditions. A variation of these temperatures is possible, but the operational limitations of the process must be considered. Figure 2.1 illustrates a simple superstructure for one wastewater disposal, one freshwater source, and two process water unit operations (one source and one sink). The contamination levels are not shown, for the purpose of simplicity. This simple model contains four (4) temperatures, namely T_i , T_j , T_{fw} , and T_{ww} . All possible interconnections are illustrated.

Objective function The objective function (Equation 2.7) is to minimize the total cost of the system, including operating costs and annualized investment costs. Operating costs consist of freshwater consumption, wastewater production, and hot and cold utility consumption. Annualized investment costs include the investment cost of utilities. Additionally, a ranking (i.e., penalizing) factor is attributed to each thermal stream in the water network. This factor is an estimated investment cost corresponding to a fictitious counter-current heat exchanger in which the thermal stream is passing. The minimum approach temperature is assumed constant for each stream.

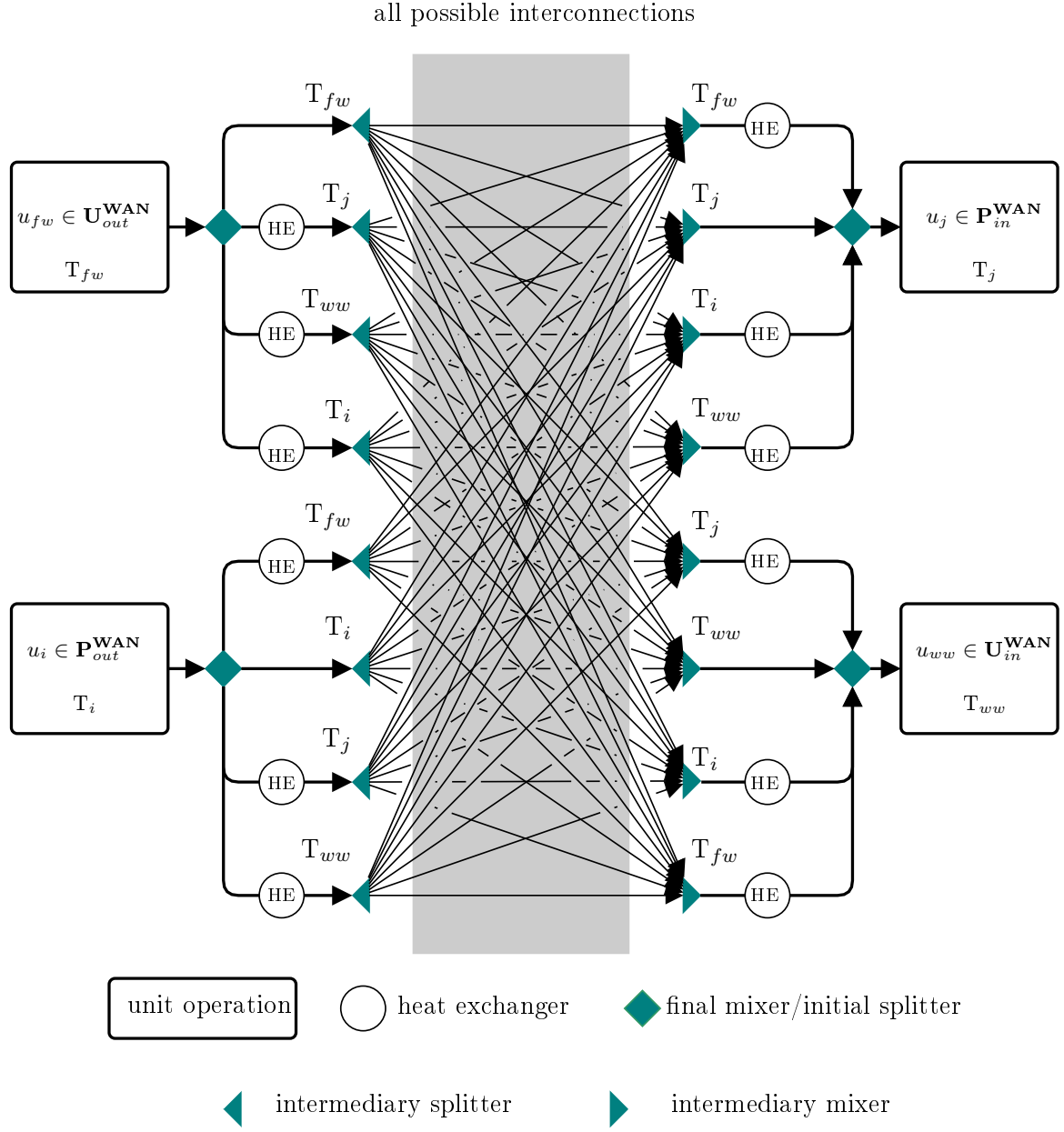


FIGURE 2.1—Superstructure of combined water and energy network

$$\begin{aligned}
 \mathbf{P1} : \min C^{\text{tac}} &= C^{\text{op}} + C^{\text{inv}} \\
 &= \left[\sum_{fw \in \mathbf{U}_{out}^{WAN}} \dot{\mathbf{m}}_{fw} C_{fw} + \sum_{ww \in \mathbf{U}_{in}^{WAN}} \dot{\mathbf{m}}_{ww} C_{ww} \right. \\
 &\quad \left. + \sum_{u \in \mathbf{U}^H} \dot{\mathbf{f}}_u^H q_u^H C_u^H + \sum_{u \in \mathbf{U}^C} \dot{\mathbf{f}}_u^C q_u^C C_u^C \right] \cdot t^{op} \\
 &\quad + \frac{\text{irr}(1 + \text{irr})^{n_{year}}}{(1 + \text{irr})^{n_{year}}} \left[\sum_{u \in \mathbf{U}^H} (\mathbf{y}_u^H I_{f,u}^H + \dot{\mathbf{f}}_u^H I_{p,u}^H) + \sum_{u \in \mathbf{U}^C} (\mathbf{y}_u^C I_{f,u}^C + \dot{\mathbf{f}}_u^C I_{p,u}^C) \right] \\
 &\quad + \frac{\text{irr}(1 + \text{irr})^{n_{year}}}{(1 + \text{irr})^{n_{year}}} \left[\sum_{i \in \mathbf{WAN}} \left(\sum_{T \in \mathbf{T}_i^{WAN}} (\mathbf{y}_{i,T} \cdot I_{f,i,T}^{WAN} + \dot{\mathbf{m}}_{i,T} \cdot I_{p,i,T}^{WAN}) \right) \right]
 \end{aligned} \tag{2.7}$$

where $I_{f,i,T}^{WAN}$ and $I_{p,i,T}^{WAN}$ are the linearized coefficients of the penalizing factor. In a more detailed model, the cost of piping ($C_{i,j}^{pipe}$) (Equation 2.8) can also be added to account for distances between processes ($d_{i,j}$) [40]. However, this would require binary variables ($\mathbf{y}_{i,j}$) to account for the existence of a connection between any two processes.

$$\begin{aligned}
 C_{i,j}^{pipe} &= d_{i,j} \left(\sum_{T \in \mathbf{T}_i^{WAN}} \sum_{T' \in \mathbf{T}_j^{WAN}} (\mathbf{y}_{i,j} \cdot I_f^{pipe} + \dot{\mathbf{m}}_{i,j,T,T'} \cdot I_p^{pipe}) \right) \\
 &\quad \forall i \in \mathbf{WAN}_{out}, \quad j \in \mathbf{WAN}_{in}
 \end{aligned} \tag{2.8}$$

2.2.1 Water network

Figure 2.2 illustrates the parameters, sets, and their associated variables in the water network. The set of temperatures in the water network, \mathbf{T} , is defined as:

$$\mathbf{T} = \{T_j | \forall j \in \mathbf{WAN}_{in}\} \cup \{T_i | \forall i \in \mathbf{WAN}_{out}\} \tag{2.9}$$

The set of temperatures of the source (\mathbf{T}_i^{WAN}) and sink (\mathbf{T}_j^{WAN}) are constructed as:

$$\mathbf{T}_i^{WAN} = \{T \in \mathbf{T} \cup \mathbf{T}_i^{extra} | T \notin \mathbf{T}_i^{forbid}\} \tag{2.10}$$

$$\mathbf{T}_j^{WAN} = \{T \in \mathbf{T} \cup \mathbf{T}_j^{extra} | T \notin \mathbf{T}_j^{forbid}\} \tag{2.11}$$

where \mathbf{T}^{extra} and \mathbf{T}^{forbid} are the set of temperatures that are to be added or forbidden, respectively, for each source or sink to take into account experts' judgements regarding the feasibility of a temperature at which a unit can operate.

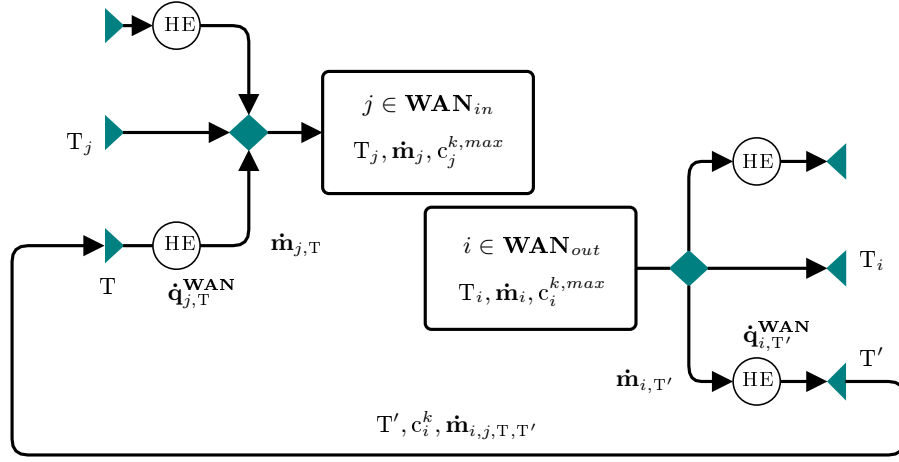


FIGURE 2.2—Overall schematic of connections, parameters, and variables in water network

Initial splitters An overall mass balance (Equation 2.12) and contamination equality (Equation 2.13) holds for each initial splitter:

$$\dot{m}_i = \sum_{T \in \mathbf{T}_i^{WAN}} \dot{m}_{i,T} \quad \forall i \in \mathbf{WAN}_{out} \quad (2.12)$$

$$c_{i,T}^k = c_i^k \quad \forall i \in \mathbf{WAN}_{out}, \quad \forall T \in \mathbf{T}_i^{WAN}, \quad \forall k \in \mathbf{C} \quad (2.13)$$

Intermediary splitters An overall mass balance (Equation 2.14) and contamination equality holds for each intermediary splitter:

$$\dot{m}_{i,T} = \sum_{j \in \mathbf{WAN}_{in}} \sum_{T' \in \mathbf{T}_j^{WAN}} \dot{m}_{i,j,T,T'} \quad \forall i \in \mathbf{WAN}_{out}, \quad \forall T \in \mathbf{T}_i^{WAN} \quad (2.14)$$

Intermediary mixers Intermediary mixers are non-isothermal mixers. Their inlet and outlet temperatures are fixed and given by the corresponding set of temperatures:

$$\sum_{i \in \mathbf{WAN}_{out}} \sum_{T' \in \mathbf{T}_i^{WAN}} \dot{m}_{i,j,T',T} = \dot{m}_{j,T} \quad \forall j \in \mathbf{WAN}_{in}, \quad \forall T \in \mathbf{T}_j^{WAN} \quad (2.15)$$

$$\sum_{i \in \mathbf{WAN}_{out}} \sum_{T' \in \mathbf{T}_i^{WAN}} \dot{m}_{i,j,T',T} \cdot T' = \dot{m}_{j,T} \cdot T \quad \forall j \in \mathbf{WAN}_{in}, \quad \forall T \in \mathbf{T}_j^{WAN} \quad (2.16)$$

Final mixers A multi-contaminant problem has non-linear formulation, due to the multiplication of mass flow and contamination level (Equation 2.18). As shown by Yang and Grossmann [75], fixing the contamination levels at their maximum allowable levels (Equation 2.19), sets the minimum freshwater target to be the same as the optimum predicted by the non-linear equation under specific conditions, i.e., at least one contamination level reaches

its maximum, as well as for all process units with nonzero water reuse streams. Otherwise, it provides a tight upper bound.

$$\sum_{T \in \mathbf{T}_j^{WAN}} \dot{\mathbf{m}}_{j,T} = \dot{\mathbf{m}}_j \quad \forall j \in \mathbf{WAN}_{in} \quad (2.17)$$

$$\sum_{i \in \mathbf{WAN}_{out}} \sum_{T' \in \mathbf{T}_i^{WAN}} \sum_{T \in \mathbf{T}_j^{WAN}} \dot{\mathbf{m}}_{i,j,T',T} \cdot \mathbf{c}_{i,T'}^k = \dot{\mathbf{m}}_j \cdot \mathbf{c}_j^k \quad \forall j \in \mathbf{WAN}_{in} \quad (2.18)$$

$$\sum_{i \in \mathbf{WAN}_{out}} \sum_{T' \in \mathbf{T}_i^{WAN}} \sum_{T \in \mathbf{T}_j^{WAN}} \dot{\mathbf{m}}_{i,j,T',T} \cdot \mathbf{c}_i^{k,max} \leq \dot{\mathbf{m}}_j \cdot \mathbf{c}_j^{k,max} \quad \forall j \in \mathbf{WAN}_{in} \quad (2.19)$$

Overall mass balance

$$\sum_{j \in \mathbf{P}_{in}^{WAN}} \dot{\mathbf{m}}_j + \sum_{ww \in \mathbf{U}_{in}^{WAN}} \dot{\mathbf{m}}_{ww} = \sum_{i \in \mathbf{P}_{out}^{WAN}} \dot{\mathbf{m}}_i + \sum_{fw \in \mathbf{U}_{out}^{WAN}} \dot{\mathbf{m}}_{fw} \quad (2.20)$$

Connections between the water and heat cascade networks

$$\dot{\mathbf{q}}_{i,T}^{WAN} = c_{p,i} \cdot (T - T_i) \quad \forall i \in \mathbf{WAN}_{out}, \quad \forall T \in \mathbf{T}_i^{WAN} \quad (2.21)$$

$$\dot{\mathbf{q}}_{j,T}^{WAN} = c_{p,j} \cdot (T - T_j) \quad \forall j \in \mathbf{WAN}_{in}, \quad \forall T \in \mathbf{T}_j^{WAN} \quad (2.22)$$

Sizing constraints Every unit in the superstructure (including thermal and water streams) is subject to minimum and maximum size constraints. In addition, a binary variable \mathbf{y} is assigned to each unit, indicating its selection.

$$\mathbf{y}_{i,T} \cdot \mathbf{m}_{i,T}^{min} \leq \mathbf{m}_{i,T} \leq \mathbf{y}_{i,T} \cdot \mathbf{m}_{i,T}^{max} \quad \forall i \in \mathbf{P}_{out}^{WAN}, \quad \forall T \in \mathbf{T}_i^{WAN} \quad (2.23)$$

$$\mathbf{y}_{j,T} \cdot \mathbf{m}_{j,T}^{min} \leq \mathbf{m}_{j,T} \leq \mathbf{y}_{j,T} \cdot \mathbf{m}_{j,T}^{max} \quad \forall j \in \mathbf{P}_{in}^{WAN}, \quad \forall T \in \mathbf{T}_j^{WAN} \quad (2.24)$$

$$\mathbf{y}_{fw} \cdot \mathbf{m}_{fw}^{min} \leq \mathbf{m}_{fw} \leq \mathbf{y}_{fw} \cdot \mathbf{m}_{fw}^{max} \quad \forall fw \in \mathbf{U}_{out}^{WAN} \quad (2.25)$$

$$\mathbf{y}_{fw,T} \cdot \mathbf{m}_{fw,T}^{min} \leq \mathbf{m}_{fw,T} \leq \mathbf{y}_{fw,T} \cdot \mathbf{m}_{fw,T}^{max} \quad \forall fw \in \mathbf{U}_{out}^{WAN}, \quad \forall T \in \mathbf{T}_{fw}^{WAN} \quad (2.26)$$

$$\mathbf{y}_{ww} \cdot \mathbf{m}_{ww}^{min} \leq \mathbf{m}_{ww} \leq \mathbf{y}_{ww} \cdot \mathbf{m}_{ww}^{max} \quad \forall ww \in \mathbf{U}_{in}^{WAN} \quad (2.27)$$

$$\mathbf{y}_{ww,T} \cdot \mathbf{m}_{ww,T}^{min} \leq \mathbf{m}_{ww,T} \leq \mathbf{y}_{ww,T} \cdot \mathbf{m}_{ww,T}^{max} \quad \forall ww \in \mathbf{U}_{in}^{WAN}, \quad \forall T \in \mathbf{T}_{ww}^{WAN} \quad (2.28)$$

2.2.2 Fixed-load vs fixed-flow formulations

As discussed in chapter 1, water allocation network problems can be formulated as either fixed-load (FL) or fixed-flow (FF) problems. Fixed-flow formulation is better suited for problems in which water flow through a unit must be kept constant, i.e., water is part of process

demand, whereas fixed-load formulation is better suited for problems in which water is used to remove certain amount of contaminations, i.e., washing units. Equation 2.29 provides the link between water flow through a unit $u \in \mathbf{WAN}$ ($\dot{\mathbf{m}}_u$), the amount of mass load to be removed L_u^k , and its input and output contaminations, $\mathbf{c}_u^{k,in}$ and $\mathbf{c}_u^{k,out}$, respectively, of contaminant $k \in \mathbf{C}$:

$$\dot{\mathbf{m}}_u = \frac{L_u^k}{(\mathbf{c}_u^{k,out} - \mathbf{c}_u^{k,in})} \quad \leftrightarrow \quad \dot{\mathbf{m}}_u \cdot \mathbf{c}_u^{k,in} + L_u^k = \dot{\mathbf{m}}_u \cdot \mathbf{c}_u^{k,out} \quad \forall k \in \mathbf{C} \quad (2.29)$$

For fixed-load problems, flow through the water unit is bounded by Equation 2.30 and Equation 2.31. Transforming a fixed-load problem to a fixed-flow one is carried out by fixing the flow at the maximum value, given by Equation 2.31

$$\dot{m}_u^{min} = \frac{L_u^k}{c_u^{k,out,max}} \quad (2.30)$$

$$\dot{m}_u^{max} = \frac{L_u^k}{(c_u^{k,out,max} - c_u^{k,in,max})} \quad (2.31)$$

Inlet and outlet contaminations are bounded by the maximum allowed level of contamination:

$$\mathbf{c}_u^{k,out} \leq c_u^{k,out,max} \quad \forall u \in \mathbf{WAN}_{out} \quad \forall k \in \mathbf{C} \quad (2.32)$$

$$\mathbf{c}_u^{k,in} \leq c_u^{k,in,max} \quad \forall u \in \mathbf{WAN}_{in} \quad \forall k \in \mathbf{C} \quad (2.33)$$

2.2.3 Heat cascade model

The overall problem is subject to heat cascade constraints [84]. Thermal utilities, non-water process streams, and thermal streams in the water network contribute to heat integration:

$$\begin{aligned} \mathbf{R}_r = \mathbf{R}_{r-1} &+ \sum_{u \in \mathbf{U}^H} \dot{\mathbf{f}}_u^H q_{u,r}^H - \sum_{u \in \mathbf{U}^C} \dot{\mathbf{f}}_u^C q_{u,r}^C && \text{thermal utilities} \\ &+ \sum_{p \in \mathbf{P}^H} q_{p,r}^H - \sum_{p \in \mathbf{P}^C} q_{p,r}^C && \text{non-water process streams} \\ &+ \sum_{i \in \mathbf{WAN}} \sum_{T \in \mathbf{T}_i^{WAN}} \mathbf{m}_{i,T} \cdot q_{i,T,r}^{WAN} && \text{water thermal streams} \\ &&& \forall r \in \{1, \dots, n_r\} \end{aligned} \quad (2.34)$$

$$\mathbf{R}_0 = \mathbf{R}_{n_r} = 0 \quad (2.35)$$

where:

$$\mathbf{y}_u^H \cdot f_u^{H,min} \leq \dot{\mathbf{f}}_u^H \leq \mathbf{y}_u^H \cdot f_u^{H,max} \quad \forall u \in \mathbf{U}^H \quad (2.36)$$

$$\mathbf{y}_u^C \cdot f_u^{C,min} \leq \dot{\mathbf{f}}_u^C \leq \mathbf{y}_u^C \cdot f_u^{C,max} \quad \forall u \in \mathbf{U}^C \quad (2.37)$$

2.2.4 Heat load distribution

Targeting problem **P1** (Equation 2.7) is solved subject to set of constraints (Equations 2.12 to 2.37). The results provide water and energy targets as well as a feasible water network with set of water exchanges and heat loads of all thermal streams. Having solved problem **P1**, the set of all hot (\mathbf{HS}^{hld}) and cold (\mathbf{CS}^{hld}) thermal streams in the network can be listed. In addition, several pinch points will be identified that divide the temperature range into several subnetworks (**SN**). At this stage, HLD will be applied to each subnetwork as a preliminary step, prior to the detailed design of the heat exchanger network. HLD is formulated as an MILP model, based on minimizing the total number of connections among all hot and cold streams [1, 2]. Similar notations introduced by Papoulias and Grossmann [1] are used here for familiarity purposes.

It is important to note that result of HLD is one feasible solution among many possible solutions that exhibits the minimum number of matches. Moreover, in order to keep the targeted thermal utilities intact, no thermal exchange is allowed crossing the pinch point, i.e., matches are limited between thermal streams within each subnetwork. For any subnetwork $l \in \mathbf{SN}$, one can readily define the set of hot and cold thermal streams within each subnetwork ($\mathbf{HS}_l^{hld}, \mathbf{CS}_l^{hld}$, respectively). $\mathbf{HS}_{l,r}^{hld}$ is defined as the set of hot streams within subnetwork l that are present in temperature interval r and above, while $\mathbf{CS}_{l,r}^{hld}$ is defined as the set of cold streams within subnetwork l that are present in temperature interval r . $\mathbf{Q}_{i,j,r} \geq 0$ is defined as the heat exchanged between hot stream i and cold stream j in interval $r \in \mathbf{SN}_l$. Upper and lower bounds can be defined for each match ($Q_{i,j,l}^{min}, Q_{i,j,l}^{max}$) in order to better incorporate practical infeasibilities; to avoid violating thermal utility targets, one should follow the same constraints as in problem **P1**. Heat cascade formulation should be formulated for each hot stream ($\mathbf{R}_{i,r} \geq 0$). By defining binary variables $\mathbf{y}_{i,j,l} \in \{0, 1\}$ to denote the existence of a match between thermal streams within each subnetwork l , the HLD problem will minimize the number of heat exchangers. Ranking factors ($p_{i,j,l}$) can be defined to favor or avoid certain matches:

$$\mathbf{P2} : \min N_{hld} = \sum_{l \in \mathbf{SN}} \sum_{i \in \mathbf{HS}_l^{hld}} \sum_{j \in \mathbf{CS}_l^{hld}} p_{i,j,l} \cdot \mathbf{y}_{i,j,l} \quad (2.38)$$

$$\text{s.t. } (\forall l \in \mathbf{SN})$$

$$\mathbf{R}_{i,r} = \mathbf{R}_{i,r-1} + Q_{i,r} - \sum_{j \in \mathbf{CS}_{l,r}^{hld}} \mathbf{Q}_{i,j,r} \quad \forall i \in \mathbf{HS}_{l,r}^{hld} \quad \forall r \in \mathbf{SN}_l \quad (2.39)$$

$$Q_{j,r} = \sum_{i \in \mathbf{HS}_{l,k}^{hld}} \mathbf{Q}_{i,j,r} \quad \forall j \in \mathbf{CS}_{l,r}^{hld} \quad \forall r \in \mathbf{SN}_l \quad (2.40)$$

$$\sum_{r \in \mathbf{SN}_l} \mathbf{Q}_{i,j,r} \leq Q_{i,j,l}^{max} \cdot \mathbf{y}_{i,j,l} \quad \forall i \in \mathbf{HS}_l^{hld} \quad \forall j \in \mathbf{CS}_l^{hld} \quad (2.41)$$

$$\sum_{r \in \mathbf{SN}_l} \mathbf{Q}_{i,j,r} \geq Q_{i,j,l}^{min} \cdot \mathbf{y}_{i,j,l} \quad \forall i \in \mathbf{HS}_l^{hld} \quad \forall j \in \mathbf{CS}_l^{hld} \quad (2.42)$$

$$Q_{i,j,l}^{max} \leq \min \left\{ \sum_{r \in \mathbf{SN}_l} Q_{i,r}, \sum_{r \in \mathbf{SN}_l} Q_{j,r} \right\}$$

2.3 Validation of the proposed methodology

Although the proposed methodology was designed to tackle large-scale problems, a first validation was conducted using three standard test cases commonly used by the scientific community involved in this area. The first two test cases were single-contaminant threshold problems while the third test case was a multi-contaminant pinched problem. Table 2.1 provides the economic and operating parameters used in these test cases to compare the results and performance of different methodologies. A series of key performance indicators, including energy and water targets, HEN structure, and financial indicators were evaluated for each test case. Network indicators used were the number of thermal streams including thermal utilities (N_s^{th}), number of heat exchangers (N_{HE}), total area of heat exchangers (A_{HEN}^{total}), total number of mixing points (N_{mixer}), number of non-isothermal mixing points (N_{mixer}^{NIM}), number of mass streams in the water network excluding the thermal ones (N_s^m), and total heat load of all heat exchangers (Q_{HEN}^{total}). To provide a logical comparison among different methodologies considering the number of mixing points, it was assumed that a mixing point is required at the intersection of every two flows, e.g., two mixing points are considered for three streams. Financial indicators used were HEN cost (C^{HEN}) and TAC (C^{TAC}).

A priori to HEN design, heat exchange area was estimated following the procedure proposed by Linnhoff and Ahmad [168], in which the process is divided into vertical temperature intervals (**TI**) and the area is calculated for each interval k knowing the logarithmic mean approach temperature (ΔT_{LM}^k), heat loads (q_i^k, q_j^k), and heat transfer coefficients (α_i^k, α_j^k) of all hot (**HS**) and cold (**CS**) thermal streams involved in that interval (Equation 2.43). Knowing the minimum number of heat exchanges, $N^{HE,min}$, (by solving problem **P2**), HEN cost was then estimated by Equation 2.44, in which C^{HEN} is a nonlinear cost correlation given by Equation 2.45 [22]. The parameters are provided in Table 2.1. For all test cases in this section, HEN synthesis was performed for one solution of HLD using the NLP formulation of Floudas and Ciric [4] and hence the total heat exchange area was optimized in order to make better comparison with other methodologies. Problems **P1** and **P2** were solved with CPLEX solver [169]; SNOPT [170] was used to solve the HEN synthesis problem. A full list of solver options for all three test cases are provided in Appendix A.

$$A_{total} [m^2] = \sum_{k \in \mathbf{TI}} \frac{1}{\Delta T_{LM}^k} \left\{ \sum_{i \in \mathbf{HS}} \frac{q_i^k}{\alpha_i^k} + \sum_{j \in \mathbf{CS}} \frac{q_j^k}{\alpha_j^k} \right\} \quad (2.43)$$

$$C^{HEN} = N^{HE,min} C^{HEN} \left(\frac{A_{total}}{N^{HE,min}} \right) \quad (2.44)$$

$$C^{HEN} = Cf^{HEN} + Cp^{HEN} (area)^{\beta^{HEN}} \quad (2.45)$$

2.3.1 Test case I: single-contaminant problem

Test case I was a single-contaminant problem [5] consisting of four isothermal water unit operations (Table 1.4). The comprehensive benchmarking analysis in section 1.5 was car-

TABLE 2.1—Economic and operating parameters for all test cases [22]

Parameters	Units	Values for test cases		
		General (I,II)	III	Simplified kraft section 2.5
Cost of freshwater	USD/t	0.375		0.1525
Cost of cold utility	USD/kWyr	189		18.568
Cost of hot utility (steam, 120°C)	USD/kWyr	377		140.16
Temperatures of cold utility	°C	10 → 20		10 → 35
Heat-transfer coefficient ¹	kW/m ² K	1		
Operating hours	hr/yr	8000		8322
Interest rate	%	8		
Plant lifetime	yr	25		
Temperature of freshwater	°C	20	80	10
Temperature of wastewater	°C	30	60	
Specific heat capacity of water	kJ/kgK	4.2		
Heat exchanger cost coefficients (Equation 2.45) [22]				
	Cf ^{HEN}	USD/yr	8000	
	Cp ^{HEN}	USD/yr/m ^{0.6}	1200	
	β ^{HEN}	-	0.6	

ried out using test case I by analyzing 35 HIWAN methodologies including the proposed targeting methodology (id ‘35’ in Table 1.5 and Figure 2.3). This test case is a threshold problem requiring only hot utility. In general, for cases where the temperatures of freshwater and wastewater are lower than all water unit operations and do not exhibit any losses or gains, thermal utility consumption is proportional to freshwater consumption as given by $Q_{min}^{thermal} = m_{fw}^{min} c_p (T_{ww} - T_{fw})$. For test case I, where the freshwater temperature was lower than wastewater temperature, the formulation provided heat load of the hot utility. The problem was solved for different values of heat exchanger minimum approach temperature (ΔT_{min}); the best solution with the lowest HEN cost is reported here.

Figure 2.3 illustrates some key indicators of test case I using parallel coordinates. Almost all methodologies reached minimum water and energy targets with fresh water consumption of 90 kg/s and hot utility consumption of 3,780 kW. The main deference lay in HEN design, as each methodology used a different approach. Investigating Figure 2.3, the number of heat exchangers varies between three and ten. Results indicate that the greater the number of mixers (in particular, non-isothermal mixers), the lesser the number of heat exchangers and hence, the lower the investment cost. None of the methods found in the literature had included the cost of mixers in their formulation. The heat exchanger area for the proposed methodology was the highest value among all cases, due to the very low ΔT_{min} value of 4°C. Linearization of NIM eliminated potential mixing points and hence increased indirect heat exchange, which can further explain the high heat exchange area. Nonetheless, the new approach favored less thermal streams (five). The proposed approach can give better results compared with conceptual approaches due to two main reasons: (i) a capacity to include more interconnections, and (ii) an ability to simultaneously evaluate the trade-offs between water and energy networks in a systematic manner.

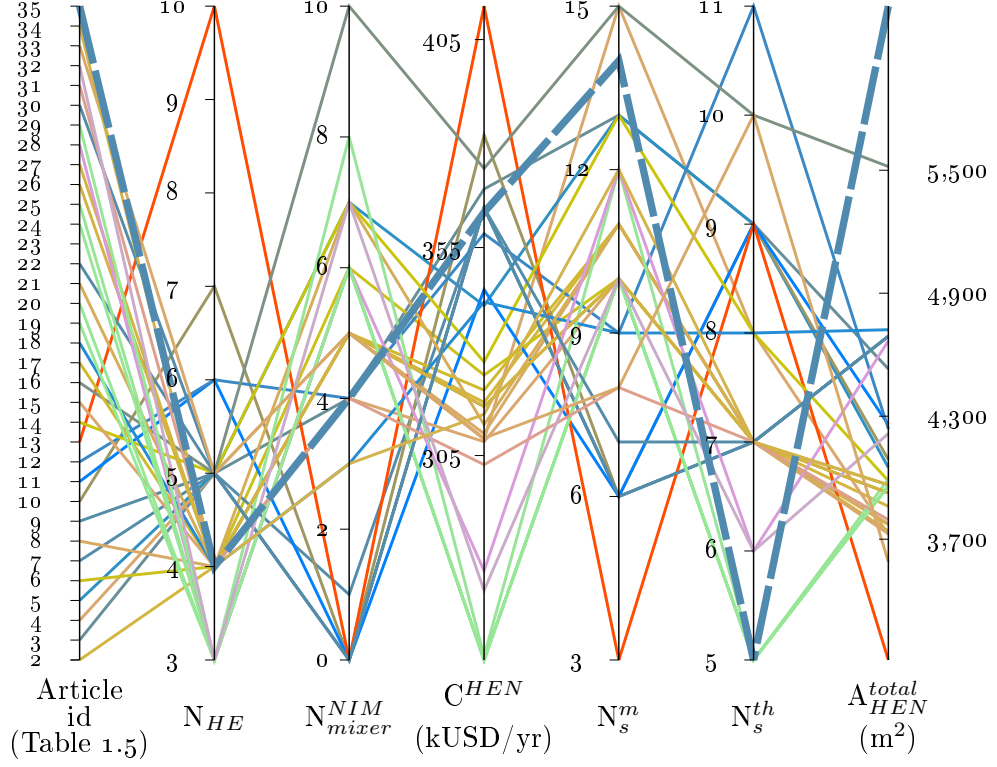


FIGURE 2.3—Visualization of some key indicators of test case I using parallel coordinates

2.3.2 Test case II: single-contaminant problem

Test case II was a single-contaminant problem [18] that consists of eight water unit operations, as presented in Table 2.2. This test case was originally proposed as a fixed-load problem and hence the fixed-load formulation was applied here. This test case is a threshold problem requiring no cold utility; hence the HRAT in problem **P1** has no effect on minimum utility consumption. Nonetheless, this value affects the selection of set of thermal streams in the proposed methodology. The problem was solved for different values of $\Delta T_{min} = \text{HRAT}$; the best solution with the lowest HEN cost is reported here.

TABLE 2.2—Operating data for test case II [18]

Units	(L_u) (g/s)	$c_u^{in,max}$ (ppm)	$c_u^{out,max}$ (ppm)	T_u (°C)	Limiting flowrate (kg/s)
u_1	2.0	25	80	40	36.4
u_2	2.88	25	90	100	44.3
u_3	4.0	25	200	80	22.9
u_4	3.0	50	100	60	60.0
u_5	30.0	50	800	50	40.0
u_6	5.0	400	800	90	12.5
u_7	2.0	400	600	70	10.0
u_8	1.0	0	100	50	10.0

Ten articles have evaluated their methodologies using this test case (Table 2.3 and Figure 2.4). The minimum water consumption found is 125.94 kg/s, corresponding to 5,289.6 kW of hot utility (following the formulation $Q_{min}^H = \dot{m}_{fw}^{min} c_p (T_{ww} - T_{fw})$). Feng et al. [116] have reported a lower value (5,135.8 kW) in which, as discussed by Liang and Hui [72], one thermal stream was neglected. Several methodologies have reported higher freshwater consumption (between 127–128 kg/s) and consequently higher hot utility consumption. Nevertheless, their higher operating costs was compensated by the reduction in HEN cost, so the total cost was reduced. Better incorporation of non-isothermal mixing in the network – as for these cases, higher percentage of mixing points were labeled non-isothermal – resulted in fewer heat exchangers. The number of thermal streams (N_s^{th}) widely varied among the results, ranging from five to sixteen (for approaches considering individual cooling of wastewater streams). Figure 2.4 illustrates the key indicators using parallel coordinates [166]. It can be seen that several indicators are indirectly correlated, i.e., N_{mixer}^{NIM} vs N_{HE} and A_{HEN}^{total} vs N_{mixer} , among others. The proposed methodology in this chapter is highlighted in Figure 2.4 by a dashed-teal line. No single solution in Table 2.3 was better in all indicators, necessitating the application of multi-criteria decision making approaches in HIWAN synthesis problems.

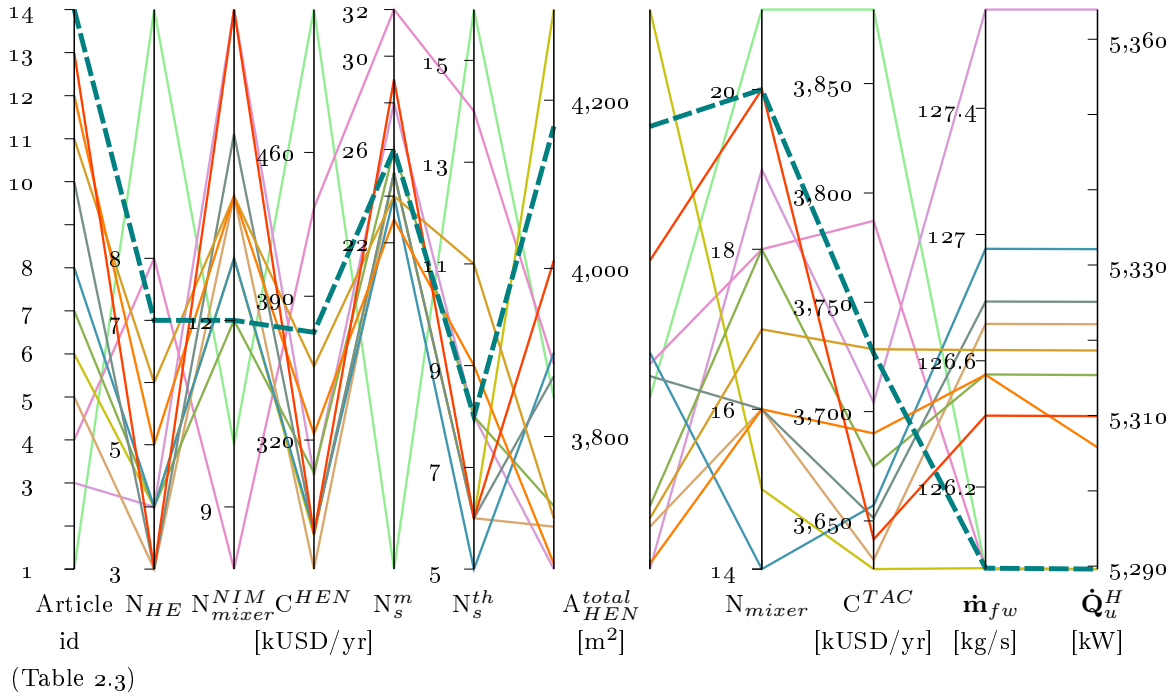


FIGURE 2.4—Visualization of some key indicators of test case II (Table 2.3) using parallel coordinates (dashed-teal-colored line is the proposed targeting approach in this work)

TABLE 2.3—Benchmarking HIWAN methodologies using test case II [18]⁽¹⁾

id	Utility targets				Network indicators					Economic indicators		
	(2)	\dot{m}_{fw} [kg/s]	\dot{Q}_u^H [kW]	N_s^{th}	N_{HE}	A_{HEN}^{total} [m ²]	N_{mixer} (N_{mixer}^{NIM})	N_s^m	Q_{HEN}^{total} [kW]	C_{HEN}^{total} [USD/yr]	C_{HEN}^{TAC} [kUSD/yr]	Comments
1	Bagajewicz et al. [18]	M-C	125.94	5,289.6	16	12	3,846.1	21 (10)	8	23,769	529,534	3,883.8
2	Feng et al. [116]	M	125.94	5,135.8	NA	NA	NA	NA	NA	NA	NA	[72]
3	Liao et al. [117]	case a	127.71	5,363.9	8	4	3,642.3	19 (17)	28	23,475	302,723	3,704.2
4		case b	125.94	5,289.6	14	8	3,886.3	18 (8)	32	24,258	432,939	3,787.3
5	Ibrić et al. [129]	case 1	126.71	5,322.1	6	3	3,692.9	16 (14)	25	22,410	257,155	3,632.1
6		case 2	125.94	5,289.6	6	4	4,307.8	15 (13)	25	24,004	273,612	3,628.0
7	Liu et al. [137]	M	126.56	5,315.4	8	4	3,717.4	18 (12)	26	22,426	304,077	3,674.8
8	Yan et al. [139]	M	126.95	5,332.1	5	4	3,899.7	14 (13)	24	23,290	275,827	3,657.1
9	Liang and Hui [72]	M	125.94	5,289.6	NA	NA	NA	NA	NA	NA	NA	NA
10	Hong et al. [143]	case a	126.79	5,325.1	6	3	3,871.9	16 (15)	25	22,540	274,431	3,651.3
11		case b	126.63	5,318.6	11	6	3,702.7	17 (14)	24	22,762	355,743	3,728.5
12	Wang et al. [69]	M-C	126.56	5,305.8	9	5	3,648.6	16 (14)	23	22,708	322,938	3,690.0
13	Hong et al. [145]	M	126.43	5,309.9	6	3	4,009.3	20 (17)	29	21,871	274,325	3,641.6
14	Kermani et al. [9]	M	125.94	5,289.6	8	7	4,168.8	20 (12)	26	24,155	372,388	3,726.7

- (1) The problem is a threshold problem and all methodologies correctly eliminate the use of cold utility. Where information was not enough to calculate the indicators, 'NA' is indicated.
- (2) 'M' indicates mathematical methodology; 'C' denotes conceptual methodology.
- (3) Wastewater streams are merged and sent to treatment.
- (4) Wastewater streams are treated individually.
- (5) Case 1: heat integration only between freshwater and wastewater streams; case 2: heat integration among all streams.

2.3.3 Test case III: multi-contaminant problem

Test case III was a multi-contaminant problem originally proposed by Dong et al. [107]. The operating data is provided in Table 2.4. It consisted of three water unit operations where three types of contaminants are considered. The results of the proposed targeting methodology

TABLE 2.4—Operating data for test case III [107]

Units	Contaminant	Mass load (L_u) [g/s]	$C_u^{in,max}$ [ppm]	$C_u^{out,in}$ [ppm]	T_u [°C]	Limiting flowrate [kg/s]
u_1	A	3	0	100	100	30
	B	2.4	0	80		
	C	1.8	0	60		
u_2	A	4	50	150	75	40
	B	3	40	115		
	C	3.6	15	105		
u_3	A	1.5	50	125	35	20
	B	0.6	50	80		
	C	2	30	130		

together with benchmarking other approaches are provided in Table 2.5. The problem was a pinch problem in which both hot and cold utilities are required. The minimum water consumption for this test case was 70 kg/s. The minimum hot and cold utility consumptions depend on the values of HRAT. For high values of HRAT (e.g., 10°C for case id 1, 5, 7, and 10 from Table 2.5), hot and cold utility consumptions were 7,140 kW and 1,260 kW, respectively, while for lower values (e.g., 1°C for case id 4, 6, and 11 from Table 2.5) they amounted to 6,053 kW and 173 kW, respectively. For the latter, the operating cost of the overall system was drastically reduced, while the cost of HEN increased due to the lower approach temperature. Nevertheless, the total cost was reduced for lower values of ΔT_{min} . In spite of this total cost reduction, the total heat exchange area increased by a factor of almost five. This could pose problems in real applications where there is not enough space for the installation of such large heat exchangers. Higher values of freshwater consumption (case id 3 and 8 from Table 2.5) exhibit higher levels of non-isothermal mixing, consequently reducing the HEN cost (e.g., 117,252 USD/yr for case id 8). In all cases, the difference between hot and cold utility consumptions followed the formulation $|Q_{min}^H - Q_{min}^C| = m_{fw}^{min} c_p |T_{ww} - T_{fw}|$. Figure 2.6 presents the final HIWAN design of this test case for two values of HRAT. Considering these two designs, thermal connections remained the same with only one additional mass transfer from outlet of one of the coolers of u_1 to the inlet of the cooler of u_3 . In spite of the fact that the total heat exchange area of the two cases were conspicuously different, the retrofit of one solution to another requires no major change in the organization of units except the addition or removal of heat exchange area for different heat exchangers.

TABLE 2.5—Benchmarking of HIWAN methodologies using test case III [107]⁽¹⁾

Utility targets				Network indicators ⁽³⁾					Economic indicators ⁽⁴⁾					
id	(2)	\dot{m}_{fw} [kg/s]	\dot{Q}_u^C [kW]	\dot{Q}_u^H [kW]	N_s^{th} -	N_{HE} -	A_{HEN}^{total} [m ²]	N_{mixer}^{mixer} (N_{NIM}^{NIM})	N_s^m -	Q_{HEN}^{total} [kW]	C_{HEN}^{HEN} [USD/yr]	C^{TAC} [kUSD/yr]		
1	Dong et al. [107]	M-C	70	7,140	1,260	7	6	1,065	4 (2)	5	11,760	200,893	2,781.4	
2	Xiao et al. [114] ⁽³⁾	case 1	M	70	7,608	1,727	10	8	613	4 (3)	2	10,758	185,066	3,030.1
3		case 2	M	78.6	7,863	1,260	7	5	701	3 (3)	4	10,383	150,957	2,961.0
4	Ibrić et al. [124]	EMAT = 1	M	70	6,053	173	6	5	3,718	4 (3)	6	8,573	255,134	2,220.2
5		EMAT = 10 [129, 134]	M	70	7,140	1,260	6	5	659	4 (3)	6	9,660	145,777	2,726.3
6	Yan et al. [139]	M	70	6,052	172	7	5	3,742	4 (4)	7	8,572	256,079	2,220.8	
7	Jagannath and Almansoori [141]	M	70	7,140	1,260	6	5	659	4 (3)	6	9,660	145,777	2,726.3	
8		(4)	M	74.3	8,760	2,520	6	4	522	3 (3)	5	11,280	117,252	3,525.2
9	Kermani et al. [9]	EMAT = 1.4	M	70	6,056	176	7	6	3,312	7 (4)	10	8,576	291,219	2,258.4
10		EMAT = 10	M	70	7,140	1,260	6	6	681.9	8 (5)	11	9,660	164,063	2,744.5
11	Ibrić et al. [142]	EMAT = 1	M	70	6,053	173	6	4	3,724	5 (5)	9	8,573	240,647	2,205.7

- (1) Where information was not enough to calculate the indicators, 'NA' is indicated. In rows 4,6,9, and 11, low thermal utility consumption is due to very low value of ΔT_{min} , resulting in higher heat recovery with higher investment cost. For this reason, the proposed methodology was solved with two values of ΔT_{min} = HRAT to show the potential of the proposed approach.
- (2) 'M' indicates mathematical methodology; 'C' denotes conceptual methodology; 'M-C' represents hybrid methodologies.
- (3) Case 1 represents the result of sequential solution strategy; case 2 corresponds to the result of simultaneous solution strategy.
- (4) The maximum number of piping connections was restricted to seven; the maximum number of heat exchanger units (N_{HE}) was restricted to four.

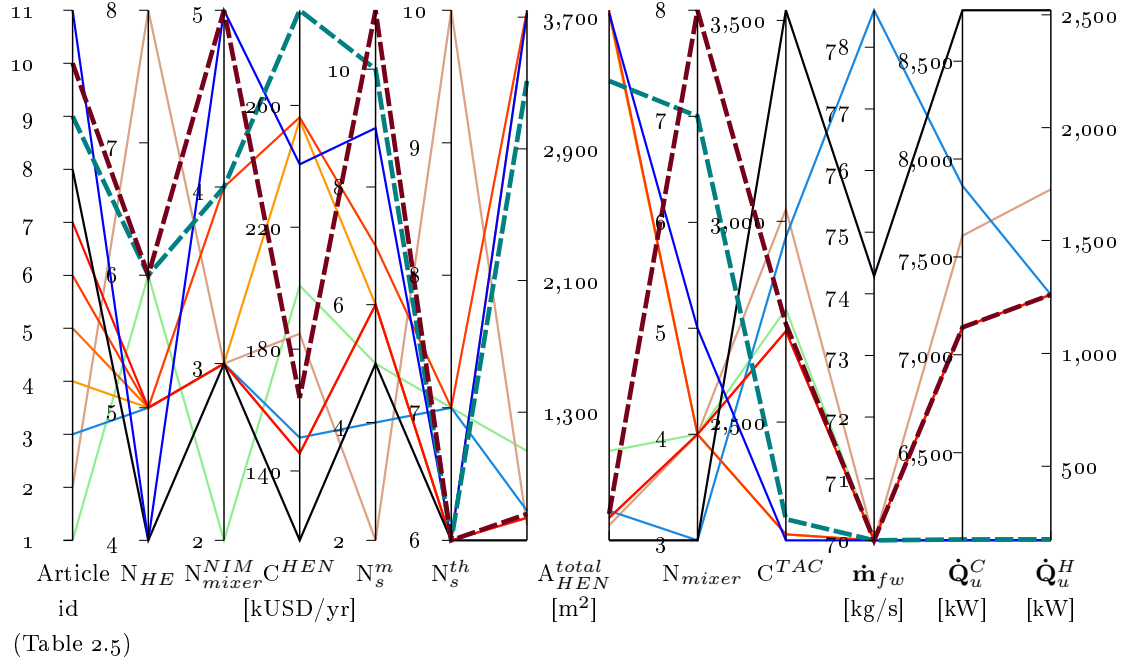


FIGURE 2.5—Visualization of some key indicators of test case III (Table 2.5) using parallel coordinates

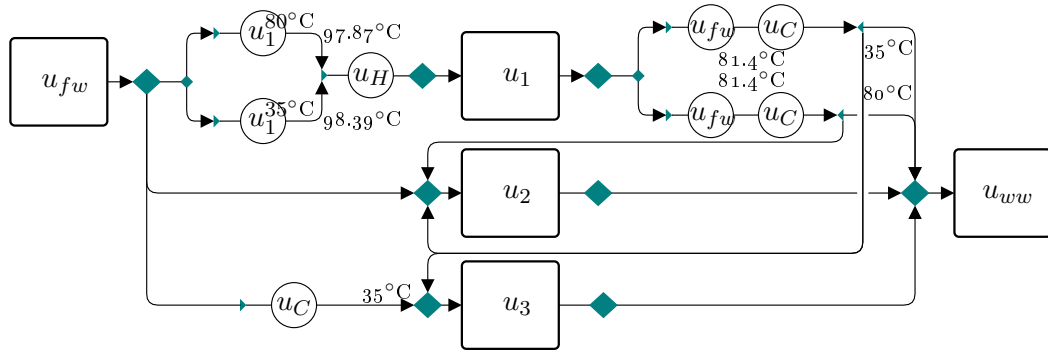
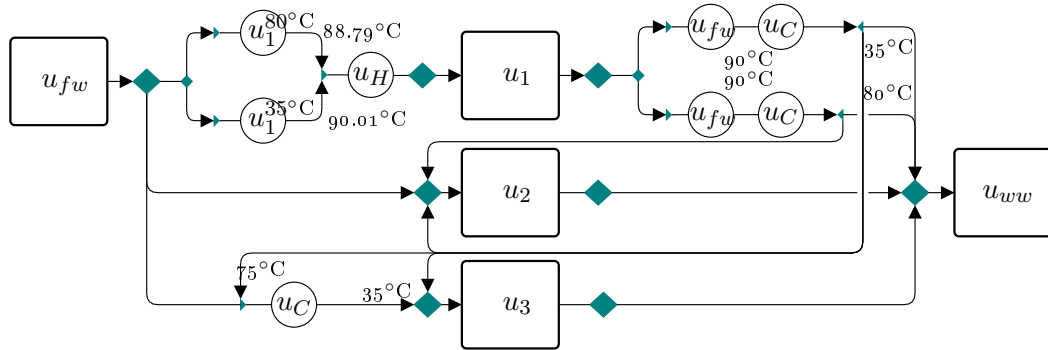

 (a) $\Delta T_{min} = \text{HRAT} = 1.4^\circ\text{C}$

 (b) $\Delta T_{min} = \text{HRAT} = 10^\circ\text{C}$

 FIGURE 2.6—Test case III: Final HIWAN design for ΔT_{min} 1.4°C (a) and 10°C (b)

2.4 Methodology for industrial applications

Available test cases in the literature aim at evaluating the performance of their proposed methodologies on simplified examples for demonstration or proof-of-concept purposes. Existing literature, however, has not considered an industrial case study. Due to highly constrained optimization problems and the complex operational structures of industrial processes, conventional optimization methods are not often directly applicable. This is mainly due to:

- A high number of process streams within the system resulting in network complexities and higher computational time.
- Process topology constraints (i.e., physical locations and restricted exchanges). One major assumption often found in the literature test cases is that any hot stream can exchange heat with any cold stream. This approach, however, becomes difficult in real industrial applications due to geographical and thermodynamic constraints.
- Lack of available and/or reliable data (i.e., having insufficient measurements for mathematical modeling purposes). For example, the contamination levels of the water network involved in the actual industrial production systems need to be taken into account to identify potential practical recovery solutions.

To address the specific configurations of water and heat exchanger networks of industrial processes, two concepts of water tanks and restricted matches are included in the methodology to address the lack of industrial data related to water contamination levels. These concepts were first tested on a simplified pulp and paper process configuration which includes the most important pulping unit operations. A step-wise approach embedding the mathematical formulation above is proposed to tackle large and complex industrial problems:

Step 1 - plant characterization This step consists of characterizing the industrial site and understanding the processes involved, as well as their specificities. This step is crucial, as the subsequent steps rely on a deep understanding of the nature of the processes and their mode of operation. Three elements are important to address at this stage:

- (a) **Establishment of project priorities, mill champion, and study objectives:** Active partnership, constant communication, and participation of mill personnel are key factors of success to produce a quality process integration study at an industrial site, and one that will facilitate the implementation of the energy and water savings opportunities identified using the proposed MILP targeting methodology.
- (b) **Data collection:** This step focuses on collecting necessary and sufficient data from the process. It should be carried out in collaboration with the mill personnel. It involves defining the problem and gathering data in order to build a representative mill model. For water networks, the required data relates to outlet and inlet water streams and their qualities. Recycling, reusing, and regenerating water streams can be excluded, as the superstructure is able to generate these connections and add them to the optimization problem automatically.
- (c) **Mill simulation model:** A simulation model based on mass and energy balances can be an additional tool to facilitate model definition. Access to a reconciled simulated model

of the mill will help in the extraction of a coherent set of data to use in the definition of the mathematical model. Such a model will also help in simulating the energy and water savings opportunities and correctly assessing related impacts on the process.

Step 2 - quantification of qualitative constraints If no data is available on the quality of mass streams (e.g., water contamination), this step aims to introduce recycling and reusing opportunities by applying the concept of restricted matches. Therefore, regular communication with engineering experts on possible and feasible matches is necessary to better incorporate conceptual criteria into the mathematical programming of the proposed methodology. The concept of restricted matches is introduced to account for contamination levels and mill topology constraints. The latter includes economic and process topology limitations (e.g., recycling between two unit operations or a heat exchange between two streams can be beneficial or disadvantageous, depending on economic or physical location limitations). Moreover, the concept of restricted matches does not require the use of contamination levels, which are rarely measured in several industries, in particular, in the pulp and paper processes. This can be implemented by adding upper bound limits, lower bound limits, or strict equality constraints on the total flow between two process unit operations, as given by Equation 2.46:

$$\dot{\mathbf{m}}_{i,j} \begin{cases} = 0, & \text{forbidden match} \\ \leq \mathbf{y}_{i,j} \cdot \mathbf{m}_{i,j}^{max}, & \text{soft restriction, upper bound} \\ \geq \mathbf{y}_{i,j} \cdot \mathbf{m}_{i,j}^{min}, & \text{soft restriction, lower bound} \\ \geq \mathbf{m}_{i,j}^{min}, & \text{hard restriction, lower bound} \\ = \mathbf{m}_{i,j}, & \text{strict equality} \end{cases} \quad (2.46)$$

where $\dot{\mathbf{m}}_{i,j}$ is defined as the total flow between unit i and unit j (Equation 2.47):

$$\dot{\mathbf{m}}_{i,j} = \sum_{\mathbf{T} \in \mathbf{T}_i^{WAN}} \sum_{\mathbf{T}' \in \mathbf{T}_j^{WAN}} \dot{\mathbf{m}}_{i,j,\mathbf{T},\mathbf{T}'} \quad (2.47)$$

$$\forall i \in \mathbf{WAN}_{out}, \quad j \in \mathbf{WAN}_{in}$$

Step 3 - modeling The mathematical model is built using the data collected or extracted from the simulation model of the process. The mathematical modeling uses the MILP formulation described in section 2.2. As in several industries, such as the pulp and paper industry, the contaminant levels are rarely made fully available, the model has been made sufficiently flexible to include contaminant levels if available and uses the concept of restricted matches in the case that contaminant levels are not provided.

Step 4 - preliminary targeting Before any optimization, one can evaluate the preliminary water and energy targets of the whole process. This provides a lower bound for the subsequent step. Due to the inclusion of process constraints, these targets can never be reached in real scenarios.

Step 5 - optimization Solving the optimization problem consists of two sequential MILP formulations:

- i) **Problem P₁ with ICC:** The proposed targeting superstructure is an MILP model consisting of integer variables and continuous variables. It is possible to find alternative optimal solutions to an MILP problem if more than one set of state variables can satisfy the same value of the objective function. These alternatives can be useful, as they allow the decision-maker to find all solutions to a problem. These solutions need to be classified in terms of operating and capital costs. Therefore, an integer cut constraint functionality is used.
- ii) **Problem P₂ - HLD:** The targeting superstructure combined with ICC provides several water networks in the increasing order of the MILP objective function. At this stage, HLD will be applied as a preliminary step, prior to the detailed design of the heat exchanger network, to provide a list of potential heat exchange matches with their corresponding heat load.

Step 6 - identification and evaluation of energy and water reduction opportunities

Several HLD results are available for different optimal water networks. Energy and water reduction opportunities can be extracted at this stage. Recycling and reduction opportunities in the water network and large heat exchanges are targeted to identify opportunities that should be evaluated for economical, physical, and thermodynamic feasibilities. This step should be conducted in collaboration with mill personnel. Any infeasible project can be discarded or added as a constraint if a subsequent iteration is performed.

Step 7 - project selection and implementation road map The most promising projects are selected. The impacts and interactions with other projects are also detailed at this step. A sequence of implementation with short–medium and long-term vision is also proposed. Once again, this step must be completed in close collaboration with mill personnel.

2.5 Simplified industrial case study

A simplified kraft pulp mill case study was chosen to illustrate the potential application of the proposed methodology using the concepts of restricted matches and water tanks. Stream data are provided in Table 2.6, which includes the available hot process streams and process water streams of five (5) main kraft departments (i.e., stock preparation, washing, bleaching, pulp machine, and recausticizing). Given that quantitative contamination levels of water streams were not available, qualitative restrictions were defined and modeled using the concept of restricted matches. The following operational constraints were considered:

- (1) Outlet of recausticizing, washing, and bleaching cannot be recycled.
- (2) Outlet of pulp machine can only be recycled in washing section.
- (3) Outlet of stock preparation can only be recycled in bleaching section.
- (4) No freshwater can be used to dilute wastewater streams.
- (5) No recycling can take place within each tank.
- (6) A connection is possible from warm water tank to hot water tank.

The number of water tanks added to the superstructure corresponded to the number of tanks available in the existing process. However, it was possible to define additional tanks that could be considered as new equipment with associated capital cost. In the present case study, only existing tanks were defined, namely warm and hot water tanks.

TABLE 2.6—Operating data for the simplified kraft pulp case study

	T_{in} [°C]	T_{out} [°C]	\dot{m} [kg/s]		T_{in} [°C]	T_{out} [°C]	Heat load [kW]
Water unit operations				Process thermal streams			
Pulp machine (1)	50	50	10	Surface condenser (1)	65	65	-7,560
Bleaching (2)	70	70	20	Turpentine condenser (2)	95	50	-10,920
Washing (3)	65	65	35	Effluent (3)	75	40	-2,205
Stock preparation (4)	62	62	25	Dryer exhaust (4)	59	30	-1,050
Recausticization (5)	35	35	20	Contaminated condensate (5)	80	65	-630
Water utilities				Thermal utilities			
Fresh water	-	10	-	Hot utility (Steam)	120	120	-
Waste water	30	-	-	Cold utility	10	35	-
Water tanks							
Warm water tank	35	35	-	Hot water tank	62	62	-

In the current operating conditions, 137 kg/s of freshwater was used to meet water demands while cooling process hot streams. Moreover, 3,392 kW of hot utility was used to heat water streams in order to satisfy water demands. Wastewater was disposed at 58.6°C, which should be cooled to 30°C, requiring 136 kg/s of cooling water. The existing water network and heat exchangers are illustrated in Figure 2.7a. Most non-water thermal streams (H_1 to H_4) were being used to heat freshwater streams. However, about 22 kg/s of water from the warm water tank and 5 kg/s of water from the hot water tank were directed to wastewater disposal. This, combined with the fact that there were no recycling options, increased the freshwater intake, and consequently, the hot utility consumption. Total cost amounts to 1,341.9 kUSD/yr, corresponding to an operating cost of utility consumptions (assuming that heat exchangers were already in place).

Following the procedure explained in section 2.4 (step 5), problem **P2** was solved given the results of problem **P1** to generate potential thermal matches. In order to compare results with other methodologies in the literature, similar to test cases I to III, NLP formulation of Floudas and Ciric [4] was solved as the third step. In addition to the application of ICC on **P1** to generate a set of solutions exhibiting different combinations of water thermal streams, ICC can also be applied to problem **P2** to generate a set of potential thermal matches. The simplified test case was solved by applying 20 integer cuts to problem **P1** ($N_{icc}^{P1} = 20$) and 100 integer cuts to problem **P2** ($N_{icc}^{P2} = 100$). The best solution exhibiting minimum HEN cost is presented here. HRAT and ΔT_{min} were assumed to be 10°C.

Several key performance indicators were calculated and are presented in Table 2.7. Compared with current operating conditions, the proposed methodology exhibited a highly integrated water network with maximum water recycling, resulting in 80 kg/s of freshwater consumption. It should be noted that minimum freshwater consumption with no water reuse/recycling is 110 kg/s; however, due to the imposed constraints, all water at the outlet from the pulp machine unit (u_1) could be recycled in the washing unit (u_3 , 10 kg/s) and all of bleaching unit demand (u_2 , 20 kg/s) could be met by the outlet of the stock preparation unit (u_4)

(Figure 2.7b). This brought a 41.6% reduction in freshwater consumption compared with current operating conditions. Due to this decrease, the heat load of the process thermal streams (22,365 kW) was more than what the water network required, resulting in the complete elimination of hot utility consumption. Overall, the operating cost reduced by more than 50%. The corresponding HEN design is shown in Figure 2.7b. The number of heat exchangers, mixers, and mass streams increased, exhibiting a more complicated heat-integrated water allocation network, as illustrated in Figure 2.7b.

TABLE 2.7—Key performance indicators (KPIs) for the simplified kraft pulp case study

		Reference	Case a [49] ³	Case b [49] ³	Current work ⁴
Utility indicators					
Freshwater	kg/s	137	89.904	89.904	80
Hot utility	kW	3,392	0	0	0
Cold utility ¹	kW	14,270	14,813	14,813	15,645
	kg/s	135.8	141.1	141.1	149.0
Total water consumption ²	kg/s	272.8	231.0	231.0	229.0
Waste outlet temperature	°C	54.8	30	30	30
Network indicators					
	N_s^{th}	-	15	9	11
	N_{HE}	-	8	6	10
	A_{HEN}^{total}	m ²	2,977.9	2,891.8	2,444.9
N_{mixer}	(N_{mixer}^{NIM})	-	9 (7)	11 (11)	9 (8)
	N_s^m	-	5	17	16
Financial indicators					
	C^{op}	kUSD/yr	1,366.1	685.8	685.8
	C^{HEN}	kUSD/yr	0	301.1	285.6
	C^{TAC}	kUSD/yr	1,341.9	986.9	971.4

1 - For reference case, cold utility is required to cool waste streams to 30°C (The cold utility was assumed as freshwater from 10°C to 35°C). A counter-current heat exchanger was assumed.

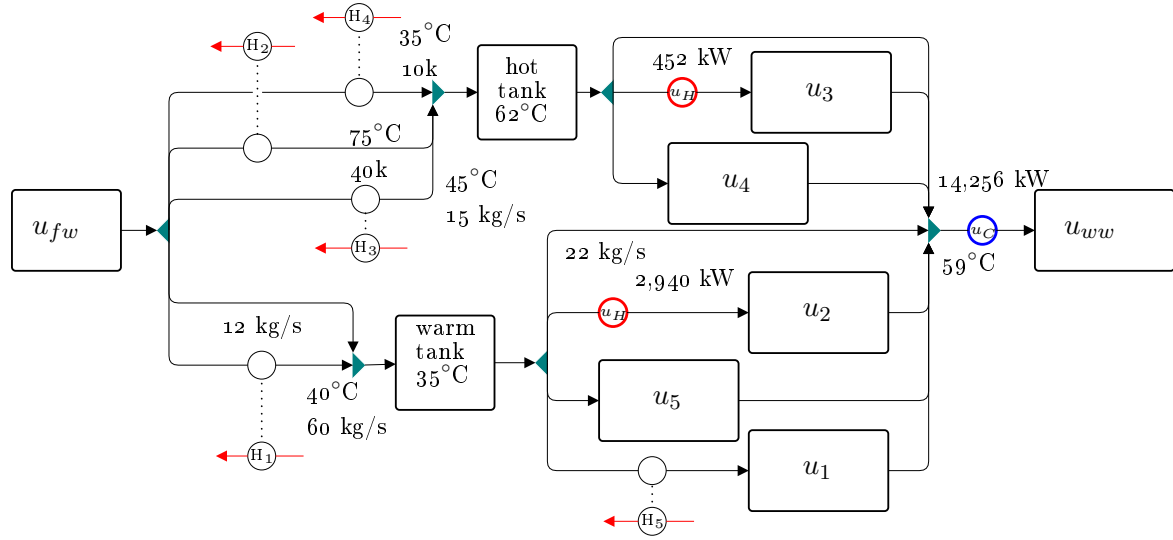
2 - Sum of freshwater and cooling water.

3 - Ibrić et al. [49]: Case a is solved by fixing the temperatures of tanks at current values. Case b was solved by optimizing these temperatures: warm water tank at 50°C and hot water tank at 78.15°C.

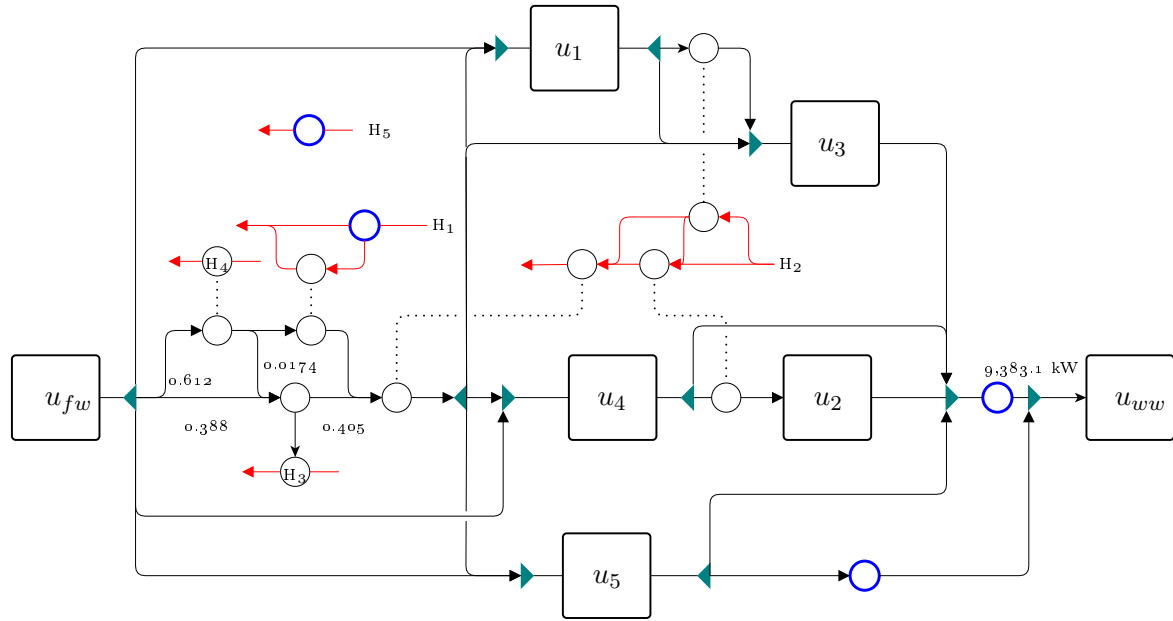
4 - The solution with lowest C^{HEN} is presented here ($n_{icc}^{P_1} = 1$, $n_{icc}^{P_2} = 41$)

Ibrić et al. [49] have also solved this problem (case a in Table 2.7). The freshwater consumption was reported to be 89.904 kg/s. The increased freshwater consumption exhibited a higher heat recovery from the process thermal streams and consequently reduced the cooling duty of cooling water (14,813 kW compared with 15,645 kW). As a result, the operating cost was 4.5% higher than the proposed solution in the current work. Nevertheless, due to their nonlinear formulation of HIWAN, the reported HEN design exhibited a lower cost (301.1 kUSD/yr). The proposed methodology provides fewer possibilities of mixing temperatures due to its linear formulations, which explains the higher number of mixers than in the work of Ibrić et al. [49]. The reported total cost by Ibrić et al. [49] was only 2.7% lower than the one proposed in this work.

Up to this point, temperatures of water tanks were fixed at their given values in Table 2.6. Savulescu and Alva-Argaez [171] argue that temperatures of water tanks must be optimized



(a) Current operating conditions



(b) Selected solution of the proposed methodology

FIGURE 2.7—Comparison between current state of the mill and the proposed optimal network

according to the water network specifications of the plant. This has been addressed by Ibrić et al. [49] where they optimized these temperatures (case b in Table 2.7). The result exhibited the same operating costs (same freshwater and cooling utility consumptions). The optimized temperatures of water tanks contributed to a higher degree of non-isothermal mixing which in turn reduced the heat exchanger area and consequently the HEN cost.

2.6 Conclusion

This chapter presented a novel MILP superstructure for targeting HIWAN problems addressing non-isothermal mixing and multi-contaminant problems. A step-by-step algorithm has also been proposed for finding a set of solutions for industrial applications combining HLD and ICC. Several test cases from the literature were selected for benchmarking analysis. Results of test cases I to III illustrated that the proposed methodology can reach minimum water and thermal utility consumptions; however, the final HEN design may or may not exhibit KPI improvements. This is because the linearized targeting model cannot fully explore the entire feasible region due to discretization of temperatures in water networks and hence limits possibilities in exploiting non-isothermal mixing opportunities. This drawback was also apparent in the simplified kraft pulp mill case study presented in section 2.5.

The sequential nature of the proposed methodology puts more emphasis on minimizing the operating costs in problem **P1** when the HEN is optimized using the sequential procedure proposed by Floudas and Ciric [4]. This was observed for the simplified kraft mill case study for which the proposed methodology reached lower operating costs than Ibrić et al. [49] (more than 4%). One drawback to this approach is that the final HIWAN design may exhibit a higher total cost that, considering financial policies, is not favored. However, from another perspective which is common for industrial applications, investment decisions are here-and-now decisions, whereas operating costs are variable and influenced by the price of resources. In the current political and environmental conditions, reducing resource consumption may therefore be a better decision, hence favoring the sequential approach by emphasizing the reduction of operating costs.

Chapter 3 will aim at proposing a mathematical superstructure and a novel solution strategy to address final HIWAN design that exhibits a higher degree of non-isothermal mixing and lower investment costs. Following the discussion from this section, the sequential approach will be maintained and trade-offs between operating and HEN costs will be addressed in the next chapter. ■

CHAPTER 3

Heat-integrated water allocation network design

Overview

In this chapter, a novel hyperstructure is proposed to address the design of HIWANs and is solved using an iterative sequential solution strategy. The overall HIWAN problem is decomposed into three sub-models. The first two models were introduced in the previous chapter, namely: targeting (problem **P1**) and HLD models (problem **P2**) [1, 2, 3]. Problem **P1** provides minimum targets in thermal utilities and freshwater consumption together with potential water thermal streams and their states (i.e., hot or cold). Problem **P2** provides a feasible set of heat exchange matches among these thermal streams. This chapter adapts the NLP model of HEN design [4] by including a water network model to solve the total HIWAN synthesis problem. This model is formulated as an NLP and the governing equations are described in this chapter. The methodology is validated by literature case studies introduced in the previous chapter. Results exhibit that despite having a sequential solution strategy, better performance can be reached.

3.1 Problem statement

Following the problem definition given in section 2.1, two sets of water unit operations (\mathbf{P}_{in}^{WAN} , \mathbf{P}_{out}^{WAN}) are given. Each unit j in \mathbf{P}_{in}^{WAN} needs water at temperature T_j , with a maximum allowed contamination level of $c_j^{k,max}$. Each unit i in \mathbf{P}_{out}^{WAN} provides water at temperature T_i , with maximum allowed contamination level of $c_i^{k,max}$. In addition, For mass-transfer water unit operations, a mass load of L_u must be removed from the process. Furthermore, sets of hot and cold non-water process streams ($\mathbf{P}^H, \mathbf{P}^C$, respectively) are also considered. Thermal hot and cold utilities ($\mathbf{U}^H, \mathbf{U}^C$, respectively) are also available in the event that the energy available within the system is not sufficient to satisfy energy demands. In addition, multiple freshwater sources and wastewater sinks ($\mathbf{U}_{out}^{WAN}, \mathbf{U}_{in}^{WAN}$) are given. The objective is to design a heat-integrated water allocation network (HIWAN) that exhibits minimum TAC.

3.2 Mathematical formulation

The overall HIWAN synthesis problem comprises binary variables and nonlinear (including bilinear) constraints and hence is a non-convex MINLP problem. The method in this chapter

proposes decomposing the problem into three sub-models. The first two models were introduced in the previous chapter, namely: targeting (MILP) and HLD (MILP) models [1, 2, 3]. The mathematical formulation of the third model is presented in this section. This model is formulated using NLP with the objective of minimizing the annualized capital investment subject to utility targets (results of problem **P1**, set as upper bound) and heat exchange matches (results of problem **P2**).

As discussed in chapter 1, the main issues in modeling HIWANs are the choice of water thermal streams (i.e., interconnections between water allocation network and HEN) and their states (hot or cold). This is important as the HEN formulation is generally constructed by knowing the set of hot and cold streams in advance. To address this, a subset of water streams can be integrated with HEN. This subset mainly comprises freshwater and wastewater streams while other types (i.e., inlets, outlets, and recycling streams) may or may not be subjected to thermal duties. Freshwater and wastewater streams are dominantly modeled as a succession of heat exchangers and splitters, and heat exchangers and mixers, respectively. Throughout the literature, freshwater streams are modeled as cold streams while wastewater streams are modeled as hot streams. The main assumption is that freshwater and wastewater units have the lowest temperatures among all process unit operations. For other types of streams, this procedure is carried out by defining two thermal streams and assigning binary variables and constraints to ensure the activation of only one state.

The proposed NLP hyperstructure of HIWAN in this work addresses these two issues using a different approach. In problem **P1**, a discretization technique is applied in which any water stream can be heated or cooled from its initial temperature to reach any other temperature in the water network. By assigning binary variables to the existence of each thermal stream, problem **P1** minimizes the operating cost of the network by selecting potential thermal streams within the water network. This allows cold and hot streams to be selected for both source and sink units. Problem **P2** minimizes the number of thermal matches among this set of streams. The HIWAN hyperstructure proposed for the third step (Figure 3.1), and the focus of this chapter, is based on the NLP hyperstructure of Floudas and Ciric [4] (Figure 3.1-a) and has been adapted to the HIWAN problem by applying the following modifications:

- ▶ Final mixers are removed from superstructures of streams associated with source water units. Hence, the modified superstructure allows for stream splitting from any heat exchanger outlet of source water units. (Figure 3.1-b)
- ▶ Initial splitters are removed from superstructures of streams associated with sink water units. Hence, the modified superstructure allows for stream mixing at any heat exchanger inlet for sink water units. (Figure 3.1-c)
- ▶ By-pass streams are added between different superstructures associated to one source or one sink (shown as dashed arrows in Figure 3.1-b and Figure 3.1-c). This mimics $\mathbf{f}_{l,l'}^{B,k}$ in the HEN hyperstructure (Figure 3.1-a), which characterizes the flow from the splitter following the match between k and l' to the mixer preceding the match between k and l within superstructure of stream k .
- ▶ As opposed to the HEN hyperstructure for which heat loads of each match (\dot{Q}_l^k) are fixed at their optimal values from the HLD model, the proposed HIWAN hyperstructure relaxes this constraint; hence, \dot{Q}_l^k can become zero indicating that the match is no longer necessary. For non-water thermal streams (cold or hot), the sum over hot or cold streams, respectively, is fixed to the stream heat load. In essence, \dot{Q}_l^k for non-water

thermal stream is allowed to deviate from its optimal value determined by the HLD model.

- A main assumption in the proposed hyperstructure is the value of HRAT for which problem **P1** and problem **P2** are solved. This value affects the targeting values of thermal utilities as well as the set of potential thermal streams and their matches. As a result, the model should be solved iteratively for several values of HRAT. The NLP hyperstructure is then solved for ΔT_{min} values equal to HRAT.
- Solving the HEN hyperstructure model provides good initialization for the HIWAN problem.

These modifications produce the following novelties:

- Freshwater and wastewater streams can have hot or cold thermal duties. This addition treats situations in which freshwater cooling or wastewater heating is required.
- In most of the proposed superstructures in the literature, only one thermal stream is assigned to the outlet of a source water unit operation. As a result, no water stream can be split at the outlet of a heat exchanger for mixing with other streams. This issue is handled in the proposed HIWAN hyperstructure by removing the final mixers of source units. This issue is also treated for sink units by addressing their initial mixers.

In order to present the constraints in a coherent way, similar set definitions of Floudas and Ciric [4] have been adapted to represent stream superstructures and matches:

- 1) Set **MA** is the set of thermal matches (k, l) :

$$\mathbf{MA} = \left\{ (k, l) \mid k \in \mathbf{HS} \text{ and } l \in \mathbf{CS} \text{ and } \mathbf{y}_{k,l}^{\text{hld}} = 1 \right\} \quad (3.1)$$

- 2) Set **HCS** is the set of all thermal streams:

$$\mathbf{HCS} = \mathbf{HS} \cup \mathbf{CS} \quad (3.2)$$

- 3) Set **SM_k** is the set of streams matching with stream $k \in \mathbf{HCS}$ [4]:

$$\mathbf{SM}_k = \left\{ k' \mid (k \in \mathbf{HS} \wedge k' \in \mathbf{CS} \wedge (k, k') \in \mathbf{MA}) \vee \right. \\ \left. (k \in \mathbf{CS} \wedge k' \in \mathbf{HS} \wedge (k', k) \in \mathbf{MA}) \right\} \quad (3.3)$$

- 4) Set **SM_{i,k}** is the set of streams matching with stream $k \in \mathbf{S}_i$ of water unit $i \in \mathbf{WAN}$

$$\mathbf{SM}_{i,k} = \left\{ k' \mid i \in \mathbf{WAN} \wedge k \in \mathbf{S}_i \wedge k' \in \mathbf{SM}_k \right\} \quad (3.4)$$

Moreover, in massflow variables, superscripts *O*, *I*, and *B* denote heat exchanger inlet, outlet, and by-pass stream, respectively.

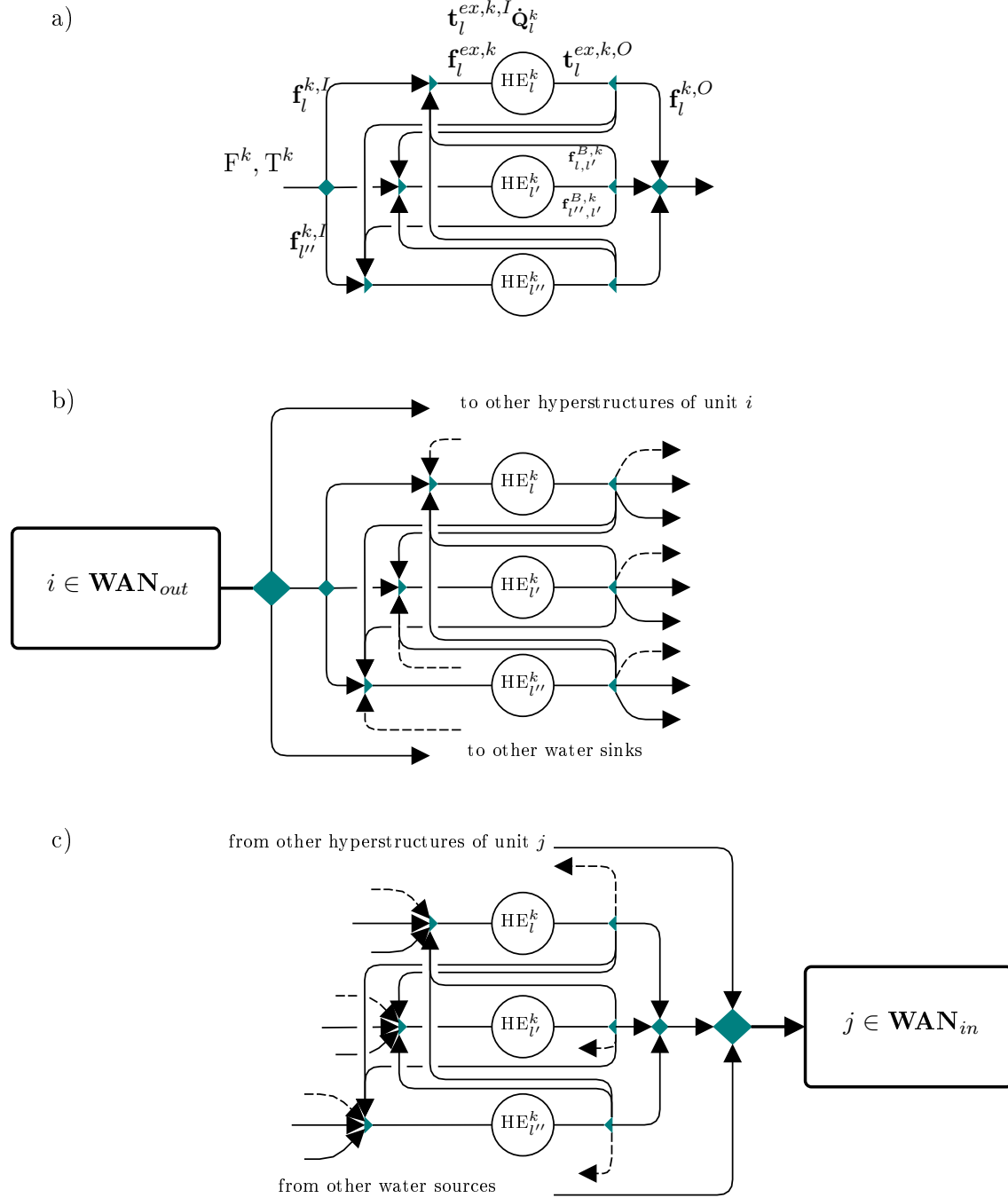


FIGURE 3.1—Schematic of the proposed source and sink hyperstructures based on HEN hyperstructure [4] (dashed arrows indicate flows among hyperstructures of the same source or the same sink similar to the definition of $\mathbf{f}_{l,l'}^{B,k}$ and $\mathbf{f}_{l'',l'}^{B,k}$)

3.2.1 Objective function

The objective function is the total network investment cost, which is the sum of investment costs over all heat exchangers:

$$\mathbf{P}_3 : \min C^{inv} = \sum_{(i,j) \in \mathbf{MA}} \alpha \left(\frac{\mathbf{Q}_{i,j}}{\mathbf{U}_{i,j} \mathbf{LMTD}_{i,j}} \right)^\beta = \sum_{(i,j) \in \mathbf{MA}} \alpha \left(\mathbf{A}_{i,j} \right)^\beta \quad (3.5)$$

where, $\mathbf{Q}_{i,j}$ is the heat load of match (i, j) which, as stated before, is not fixed at its optimal value from problem \mathbf{P}_2 but rather defined as a variable. This makes the objective function non-convex. $\mathbf{LMTD}_{i,j}$ is the logarithmic mean temperature difference of match (i, j) defined as:

$$\mathbf{LMTD}_{i,j} = \frac{\Delta \mathbf{T}_{1,i,j} - \Delta \mathbf{T}_{2,i,j}}{\ln \frac{\Delta \mathbf{T}_{1,i,j}}{\Delta \mathbf{T}_{2,i,j}}} \quad (3.6)$$

Equation 3.6 is simplified using Chen's approximation [172]:

$$\mathbf{LMTD}_{i,j} = \left(\Delta \mathbf{T}_{1,i,j} \cdot \Delta \mathbf{T}_{2,i,j} \cdot \frac{\Delta \mathbf{T}_{1,i,j} + \Delta \mathbf{T}_{2,i,j}}{2} \right)^{1/3} \quad (3.7)$$

3.2.2 Constraints

Figure 3.1 illustrates the basics of the proposed hyperstructure for a water source, a water sink, and a non-water thermal stream.

Mass and energy balances in water network

- 1) Mass balance at the initial splitter of source unit $i \in \mathbf{WAN}_{out}$:

$$\dot{\mathbf{m}}_i = \sum_{k \in \mathbf{S}_i} \sum_{l \in \mathbf{SM}_{i,k}} \dot{\mathbf{m}}_{i,l}^{k,I} + \sum_{j \in \mathbf{WAN}_{in}} \left(\dot{\mathbf{m}}_{i,j} + \sum_{k \in \mathbf{S}_j} \sum_{l \in \mathbf{SM}_{j,k}} \dot{\mathbf{m}}_{i,j,l}^{k,I} \right) \quad (3.8)$$

where, $\dot{\mathbf{m}}_i$ is the flowrate of source unit i , $\dot{\mathbf{m}}_{i,l}^{k,I}$ is the flowrate from source unit i towards the inlet of heat match (k, l) in superstructure of stream k , $\dot{\mathbf{m}}_{i,j}$ is the flow rate between source unit i and sink unit j , and $\dot{\mathbf{m}}_{i,j,l}^{k,I}$ is the flowrate from source unit i towards the inlet of heat match (k, l) in superstructure of stream k of sink unit j .

- 2) Mass balance at the splitter following a match of source unit $i \in \mathbf{WAN}_{out}$ ($k \in \mathbf{S}_i$, $l \in \mathbf{SM}_{i,k}$):

$$\dot{\mathbf{m}}_{i,l}^{ex,k} = \sum_{k' \in \mathbf{S}_i} \sum_{\substack{l' \in \mathbf{SM}_{i,k'} \\ k \neq k' \vee l \neq l'}} \dot{\mathbf{m}}_{i,l',l}^{B,k',k} + \sum_{j \in \mathbf{WAN}_{in}} \left(\dot{\mathbf{m}}_{i,l,j}^{k,O} + \sum_{k' \in \mathbf{S}_j} \sum_{l' \in \mathbf{SM}_{j,k'}} \dot{\mathbf{m}}_{i,l,j,l'}^{k,O,k',I} \right) \quad (3.9)$$

where, $\dot{\mathbf{m}}_{i,l}^{ex,k}$ is the flowrate through heat exchanger of match (k, l) in superstructure of stream k of source unit i , $\dot{\mathbf{m}}_{i,l',l}^{B,k',k}$ is the flowrate from the outlet of heat exchanger of

match (k, l) in superstructure of stream k towards the inlet of heat exchanger of match (k', l') in superstructure of stream k' where both heat exchangers belong to source unit i , $\dot{\mathbf{m}}_{i,l,j}^{k,O}$ is the flowrate towards sink unit j , and $\dot{\mathbf{m}}_{i,l,j,l'}^{k,O,k',I}$ is the flowrate towards the inlet of heat exchanger of match (k', l') in superstructure of sink unit j .

- 3) Mass balance at the mixer preceding a match of source unit $i \in \mathbf{WAN}_{out}$ ($k \in \mathbf{S}_i$, $l \in \mathbf{SM}_{i,k}$):

$$\dot{\mathbf{m}}_{i,l}^{ex,k} = \sum_{k' \in \mathbf{S}_i} \sum_{\substack{l' \in \mathbf{SM}_{i,k'} \\ k \neq k' \vee l \neq l'}} \dot{\mathbf{m}}_{i,l,l'}^{B,k,k'} + \dot{\mathbf{m}}_{i,l}^{k,I} \quad (3.10)$$

- 4) Energy balance at the mixer preceding a match of source unit $i \in \mathbf{WAN}_{out}$ ($k \in \mathbf{S}_i$, $l \in \mathbf{SM}_{i,k}$):

$$\dot{\mathbf{m}}_{i,l}^{ex,k} \cdot \mathbf{t}_{i,l}^{ex,k,I} = \sum_{k' \in \mathbf{S}_i} \sum_{\substack{l' \in \mathbf{SM}_{i,k'} \\ k \neq k' \vee l \neq l'}} \dot{\mathbf{m}}_{i,l,l'}^{B,k,k'} \cdot \mathbf{t}_{i,l'}^{ex,k',O} + \dot{\mathbf{m}}_{i,l}^{k,I} \cdot T_i \quad (3.11)$$

where $\mathbf{t}_{i,l}^{ex,k,I}$ ($\mathbf{t}_{i,l'}^{ex,k',O}$) is the temperature at the outlet (inlet) of heat exchanger of match (k, l) ((k', l')) in superstructure of stream i , and T_i is the temperature of source unit i .

- 5) Mass balance at the final mixer of sink unit $j \in \mathbf{WAN}_{in}$:

$$\dot{\mathbf{m}}_j = \sum_{k \in \mathbf{S}_j} \sum_{l \in \mathbf{SM}_{j,k}} \dot{\mathbf{m}}_{j,l}^{k,O} + \sum_{i \in \mathbf{WAN}_{out}} \left(\dot{\mathbf{m}}_{i,j} + \sum_{k \in \mathbf{S}_i} \sum_{l \in \mathbf{SM}_{i,k}} \dot{\mathbf{m}}_{i,l,j}^{k,O} \right) \quad (3.12)$$

- 6) Mass balance at the splitter following a match of sink unit $j \in \mathbf{WAN}_{out}$ ($k \in \mathbf{S}_j$, $l \in \mathbf{SM}_{j,k}$):

$$\dot{\mathbf{m}}_{j,l}^{ex,k} = \sum_{k' \in \mathbf{S}_j} \sum_{\substack{l' \in \mathbf{SM}_{j,k'} \\ k \neq k' \vee l \neq l'}} \dot{\mathbf{m}}_{j,l',l}^{B,k',k} + \dot{\mathbf{m}}_{j,l}^{k,O} \quad (3.13)$$

- 7) Mass balance at the mixer preceding a match of sink unit $j \in \mathbf{WAN}_{out}$ ($k \in \mathbf{S}_j$, $l \in \mathbf{SM}_{j,k}$):

$$\dot{\mathbf{m}}_{j,l}^{ex,k} = \sum_{k' \in \mathbf{S}_j} \sum_{\substack{l' \in \mathbf{SM}_{j,k'} \\ k \neq k' \vee l \neq l'}} \dot{\mathbf{m}}_{j,l,l'}^{B,k,k'} + \sum_{i \in \mathbf{WAN}_{out}} \left(\dot{\mathbf{m}}_{i,j,l}^{k,I} + \sum_{k' \in \mathbf{S}_i} \sum_{l' \in \mathbf{SM}_{i,k'}} \dot{\mathbf{m}}_{i,l',j,l}^{k',O,k,I} \right) \quad (3.14)$$

- 8) Energy balance at the mixer preceding a match of sink unit $j \in \mathbf{WAN}_{out}$ ($k \in \mathbf{S}_j$, $l \in \mathbf{SM}_{j,k}$):

$$\begin{aligned} \dot{\mathbf{m}}_{j,l}^{ex,k} \cdot \mathbf{t}_{i,l}^{ex,k,I} &= \sum_{k' \in \mathbf{S}_j} \sum_{\substack{l' \in \mathbf{SM}_{j,k'} \\ k \neq k' \vee l \neq l'}} \dot{\mathbf{m}}_{j,l,l'}^{B,k,k'} \cdot \mathbf{t}_{j,l'}^{ex,k',O} \\ &+ \sum_{i \in \mathbf{WAN}_{out}} \left(\dot{\mathbf{m}}_{i,j,l}^{k,I} \cdot T_i + \sum_{k' \in \mathbf{S}_i} \sum_{l' \in \mathbf{SM}_{i,k'}} \dot{\mathbf{m}}_{i,l',j,l}^{k',O,k,I} \cdot \mathbf{t}_{i,l'}^{ex,k',O} \right) \end{aligned} \quad (3.15)$$

- 9) Energy balance in matches of stream $k \in \mathbf{S}_u$ of water unit $u \in \mathbf{WAN}$:

$$\mathbf{Q}_{k,l} = \dot{\mathbf{m}}_{i,l}^{ex,k} c_p |\mathbf{t}_{i,l}^{ex,k,O} - \mathbf{t}_{i,l}^{ex,k,I}| \quad (3.16)$$

Contamination constraints

- 10) Contamination equality constraint at the final mixer of sink unit $j \in \mathbf{WAN}_{in}$ for contaminant $k \in \mathbf{C}$:

$$\begin{aligned} \dot{\mathbf{m}}_j \cdot \mathbf{c}_j^{k,in} = & \sum_{i \in \mathbf{WAN}_{out}} \left(\dot{\mathbf{m}}_{i,j} + \sum_{k \in \mathbf{S}_i} \sum_{l \in \mathbf{SM}_{i,k}} \dot{\mathbf{m}}_{i,l,j}^{k,O} \right. \\ & \left. + \sum_{k' \in \mathbf{S}_j} \sum_{l' \in \mathbf{SM}_{j,k'}} \left(\dot{\mathbf{m}}_{i,j,l'}^{k',I} + \sum_{k \in \mathbf{S}_i} \sum_{l \in \mathbf{SM}_{i,k}} \dot{\mathbf{m}}_{i,l,j,l'}^{k,O,k',I} \right) \right) \cdot \mathbf{c}_i^{k,out} \end{aligned} \quad (3.17)$$

where $\mathbf{c}_j^{k,in}$ is the contamination level of contaminant k at the inlet of sink unit j , and $\mathbf{c}_i^{k,out}$ is the contamination level of contaminant k at the outlet of source unit i .

- 11) Contamination at the inlet of unit $j \in \mathbf{WAN}_{in}$ should be less than a maximum allowed value:

$$\mathbf{c}_j^{k,in} - \mathbf{c}_j^{k,in,max} \leq 0 \quad (3.18)$$

- 12) Mass transfer equality constraint for mass transfer unit $u \in \mathbf{WAN}$:

$$\sum_{j \in \mathbf{WAN}_{u,in}} \dot{\mathbf{m}}_j \cdot \mathbf{c}_j^{k,in} + L_u - \sum_{i \in \mathbf{WAN}_{u,out}} \dot{\mathbf{m}}_i \cdot \mathbf{c}_i^{k,out} = 0 \quad (3.19)$$

where $\dot{\mathbf{m}}_j = \dot{\mathbf{m}}_i$ and $\mathbf{WAN}_{u,in}$ ($\mathbf{WAN}_{u,out}$) is the set of sinks (sources) associated to mass transfer unit u

- 13) Outlet contamination of unit $i \in \mathbf{WAN}_{out}$ should be less than a maximum allowed value:

$$\mathbf{c}_i^{k,out} - \mathbf{c}_i^{k,out,max} \leq 0 \quad (3.20)$$

Mass and energy balances in non-water streams superstructure The mass and energy balances of non-water thermal streams follow the same constraints of the HEN synthesis problem of Floudas and Ciric [4]:

- 14) Mass balance at the initial splitter of stream $k \in \mathbf{HCS}$:

$$F^k - \sum_{l \in \mathbf{SM}_k} \mathbf{f}_l^{k,I} = 0 \quad (3.21)$$

where, F^k is the heat capacity flowrate of stream k and $\mathbf{f}_l^{k,I}$ is the heat capacity flowrate of stream k towards inlet of heat exchanger of match $(k,l)/(l,k)$ in the superstructure of stream k .

- 15) Mass balance at the mixer preceding a heat exchanger of stream $k \in \mathbf{HCS}$:

$$\mathbf{f}_l^{ex,k} - \mathbf{f}_l^{k,I} - \sum_{l' \in \mathbf{SM}_k, l' \neq l} \mathbf{f}_{l,l'}^{B,k} = 0 \quad \forall l \in \mathbf{SM}_k \quad (3.22)$$

16) Mass balance at the splitter following a heat exchange match of stream $k \in \mathbf{HCS}$:

$$\mathbf{f}_l^{ex,k} - \mathbf{f}_l^{k,O} - \sum_{l' \in \mathbf{SM}_k, l' \neq l} \mathbf{f}_{l',l}^{B,k} = 0 \quad \forall l \in \mathbf{SM}_k \quad (3.23)$$

17) Energy balance at the mixer preceding a heat exchange match of stream $k \in \mathbf{HCS}$:

$$\mathbf{f}_l^{ex,k} \cdot \mathbf{t}_l^{ex,k,I} - \mathbf{f}_l^{k,I} \cdot T_k - \sum_{l' \in \mathbf{SM}_k, l' \neq l} \mathbf{f}_{l,l'}^{B,k} \cdot \mathbf{t}_{l'}^{ex,k,O} = 0 \quad \forall l \in \mathbf{SM}_k \quad (3.24)$$

18) Energy balance of heat exchange match $(k, l) \in \mathbf{MA}$ (as mentioned previously, heat load is defined as a variable in the HIWAN model):

$$\begin{aligned} Q_{k,l} &= \mathbf{f}_l^{ex,k} \cdot (\mathbf{t}_l^{ex,k,I} - \mathbf{t}_l^{ex,k,O}) \\ Q_{k,l} &= \mathbf{f}_k^{ex,l} \cdot (\mathbf{t}_k^{ex,l,O} - \mathbf{t}_k^{ex,l,I}) \end{aligned} \quad (3.25)$$

19) Energy balance of hot and cold non-water thermal streams:

$$Q_k = \sum_{l \in \mathbf{SM}_k} Q_{k,l} \quad \forall k \in \mathbf{HCS} | k \notin \bigcup_{u \in \mathbf{WAN}} \mathbf{S}_u \quad (3.26)$$

This constraint holds for all thermal streams $k \in \mathbf{HCS}$ that do not belong to any water unit operation. Q_k is the heat load of non-water thermal stream k .

Temperature difference constraints

20) Temperature difference at the two ends of heat exchanger $(k, l) \in \mathbf{MA}$:

$$\Delta \mathbf{T1}_{k,l} = \mathbf{t}_l^{ex,k,I} - \mathbf{t}_k^{ex,l,O} \quad \Delta \mathbf{T2}_{k,l} = \mathbf{t}_l^{ex,k,O} - \mathbf{t}_k^{ex,l,I} \quad (3.27)$$

21) Minimum approach temperature difference:

$$\Delta \mathbf{T1}_{k,l} \geq \Delta T_{min} = HRAT \quad \Delta \mathbf{T2}_{k,l} \geq \Delta T_{min} = HRAT \quad (3.28)$$

3.3 Solution strategy

As discussed in section 3.2, the HIWAN synthesis problem is decomposed into three steps:

Step 1: Targeting model (problem **P1-MILP**) is solved. At this step, a value of HRAT is assumed for water thermal streams. For non-water thermal streams, this value depends on the nature of the stream and problem requirements or can be assigned based on general assumptions. A solution of this model provides the utility targets of HIWAN synthesis problem and a list of water thermal streams with their corresponding heat loads. Moreover, a water allocation network will be generated satisfying the temperature and contamination constraints (section 2.2-Equation 2.7).

Step 2: Heat load distribution model (problem **P2-MILP**) is solved. The input of this model is the list of thermal streams with their corresponding heat loads from step 1. A solution of this model provides a set of potential thermal matches with their corresponding heat loads which exhibits the minimum number of heat exchangers. Several solutions may exist with the minimum number of heat exchangers. This is addressed in the proposed solution strategy by applying ICC. The water allocation network is fixed at its solution from step 1 (section 2.2-Equation 2.38) for this stage.

Step 3: HIWAN hyperstructure model (model **P3-NLP**) is solved. The model takes the water data and utility targets from step 1, while the thermal matches and their heat loads are provided from step 2. Since the water allocation network superstructure is embedded in this model, the water allocation network from step 1 can be changed but provides an initial, feasible solution. Additionally, heat loads of thermal matches are relaxed at this step, hence heat exchanger flows can reach zero, indicating that the optimized water network flows and temperatures do not require the existence of this exchanger. The variables of this problem, i.e., flows, temperatures, and heat loads of all heat exchangers, are initialized by solving the HEN hyperstructure of Floudas and Ciric [4] (model **P3^{init}-NLP**). It should be highlighted that a solution to **P3^{init}-NLP** is a feasible solution to HIWAN synthesis problem.

Solving the above-mentioned steps in sequence provides at most, two solutions to the HIWAN synthesis problem, i.e., solutions of **P3^{init}-NLP** and **P3-NLP**. Compared with simultaneous approaches, sequential approaches are solved more easily due to reduced problem size at each step. Nevertheless, similar drawbacks observed for sequential solution strategies that are applied in HEN synthesis problems [4] are also valid in this case:

- a) The trade-off between operating cost and investment cost (i.e., number of matches and area) cannot be fully captured in sequential solution strategies.
- b) The nature of HIWAN synthesis problem is non-convex and hence global optimality cannot be guaranteed.
- c) The solution of problem **P2-MILP** is only one feasible solution providing the minimum number of heat exchangers. Therefore, sequentially minimizing the number of heat exchangers followed by HEN synthesis, does not guarantee a HIWAN exhibiting the lowest total cost.

To address these drawbacks, an iterative sequential solution strategy is proposed by applying an integer cut constraint on problems **P1** and **P2**. In addition, the problem is solved for different values of HRAT to address the pinch point decomposition of temperature intervals and to get different utility targets with the goal of achieving lower investment costs. Applying an integer cut constraint at steps 1 and 2 provides two-fold benefits:

- By assuming the overall synthesis problem encompassing all water thermal streams and states (hot and cold), problems **P1** and **P2** limit the search space to a specific region, i.e., a specific set of potential thermal streams with their corresponding states and a specific set of thermal matches. This allows for a smaller problem size at step 3 and hence provides guidance towards a good solution. Applying an integer cut constraint generates several “reduced-size” problems and increases the opportunities for identifying good solutions.

- By applying, for example, $N_{icc}^{\mathbf{P1}}$ and $N_{icc}^{\mathbf{P2}}$ integer cuts at steps 1 and 2, respectively, $(N_{icc}^{\mathbf{P1}} + 1)(N_{icc}^{\mathbf{P2}} + 1)$ solutions to the HIWAN synthesis problem can be generated. These solutions can be ranked based on different key performance indicators and thus guide the decision-making process towards finding a “*good*” solution.

Figure 3.2 illustrates the proposed solution strategy. One must take into account that, similar to other methodologies, the choice of solver and its options affects the path which the solution strategy takes.

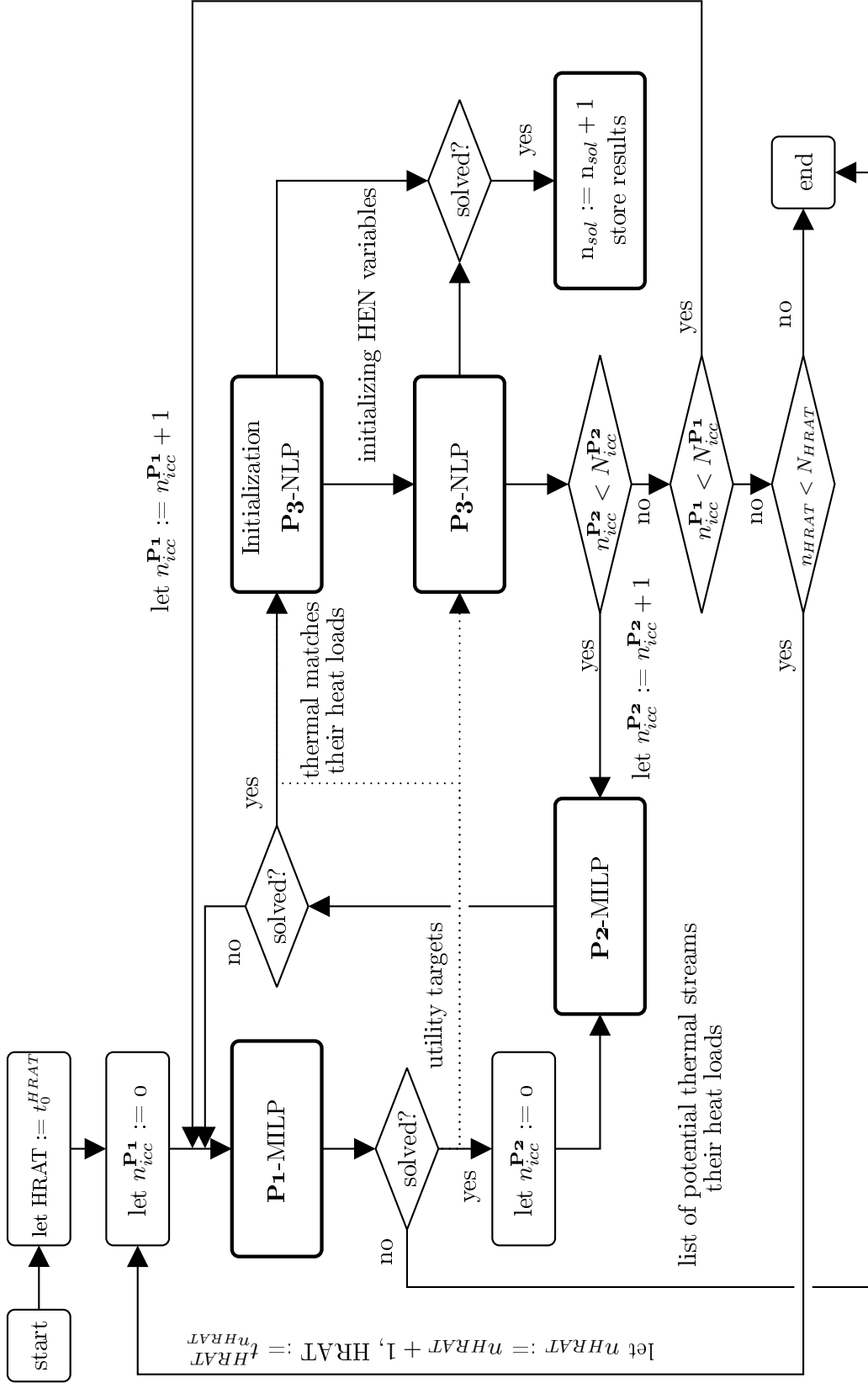


FIGURE 3.2—Iterative sequential solution strategy proposed for solving HIWAN synthesis problems

3.4 Illustrative example

Test case I (subsection 2.3.1) [5] was selected to demonstrate the generation of the proposed HIWAN hyperstructure. First, problem **P1** is solved providing minimum freshwater, hot and cold utility consumptions of 90 kg/s, 3,780 kW, and 0 kW, respectively. Problem **P1** also provides a feasible water allocation scheme. Given the list of thermal streams, problem **P2** is solved which results in seven matches (Figure 3.3-a). There are several solutions to problem **P2** with an objective function value of seven. For the sake of illustration, the fourth solution (by applying three integer cuts) is shown in Figure 3.3-a and will be discussed hereafter. CPLEX solver [169] is used for both MILP problems (Table 3.1). Figure 3.3-b presents the HIWAN hyperstructure constructed based on the results provided in Figure 3.3-a. The HIWAN hyperstructure generation follows the same approach as HEN hyperstructure [4], as shown in Figure 3.3-a. The inlet of unit u_2 has one cold thermal stream which has one match with hot utility u_H , one match with wastewater unit u_{ww} and one match with its outlet; hence, one superstructure with three matches is defined for this stream. Wastewater unit u_{ww} has two cold streams with one and three matches. This results in a hyperstructure consisting of two stream superstructures as illustrated in Figure 3.3-b. As presented in Figure 3.1 for the proposed hyperstructure, mass flows can be split from source unit heat exchanger outlets and mixed at sink unit heat exchanger inlets. This has been illustrated in Figure 3.3-b with thicker, colored arrows.

HIWAN synthesis is solved for problem **P3** as well as for HEN model of Floudas and Ciric [4]. SNOPT solver [170] is used to solve both models (Table 3.1). Its algorithm is based on sequential quadratic programming (SQP) approach and its solutions are locally optimum. It has to be pointed out that problem **P3** is non-convex and hence the global optimality of the solutions cannot be guaranteed. The solution of the NLP hyperstructure of Floudas and Ciric [4] is shown in Figure 3.4a. Since this solution is based on the results of HLD, all seven heat exchangers are active. The area of heat exchangers 3 (55.4 m²) and 7 (196.4 m²) are relatively small compared to the others (Table 3.2). This approach, however, does not account for the possibility of stream mixing and splitting. HIWAN hyperstructure addresses these possibilities by embedding the water allocation network within the HEN hyperstructure. Figure 3.4b-b presents the results of the proposed hyperstructure. Through increased possibilities for stream mixing and splitting, hence increased possibility of non-isothermal mixing, three out of the seven targeted heat exchangers are not required. The flows in bold illustrate the new possibilities embedded in the proposed HIWAN hyperstructure. Consequently the HEN cost is reduced by 22.47 % (290,799 compared to 375,089 kSUD/yr). Table 3.2 provides the temperatures, flows and heat loads associated to heat exchangers in both cases.

TABLE 3.1—Solver options for the illustrative example

stage	options	value	description
AMPL [173]	<i>presolve_eps</i>	10^{-5}	maximum difference between lower and upper bounds in constraint violations
P1 -MILP	<i>mipgap</i>	10^{-4}	relative improvement in integer solution below which optimization is terminated
	<i>integrality</i>	10^{-10}	a variable is considered to have an integral value if it lies within that of an integer
P2 -MILP	<i>mipgap</i>	10^{-4}	
	<i>integrality</i>	10^{-4}	
P3 -HEN-NLP [4]	<i>feas_tol</i>	10^{-5}	satisfying upper and lower bounds of variables and linear constraints
P3 -NLP	<i>feas_tol</i>	10^{-4}	

3.4 ILLUSTRATIVE EXAMPLE

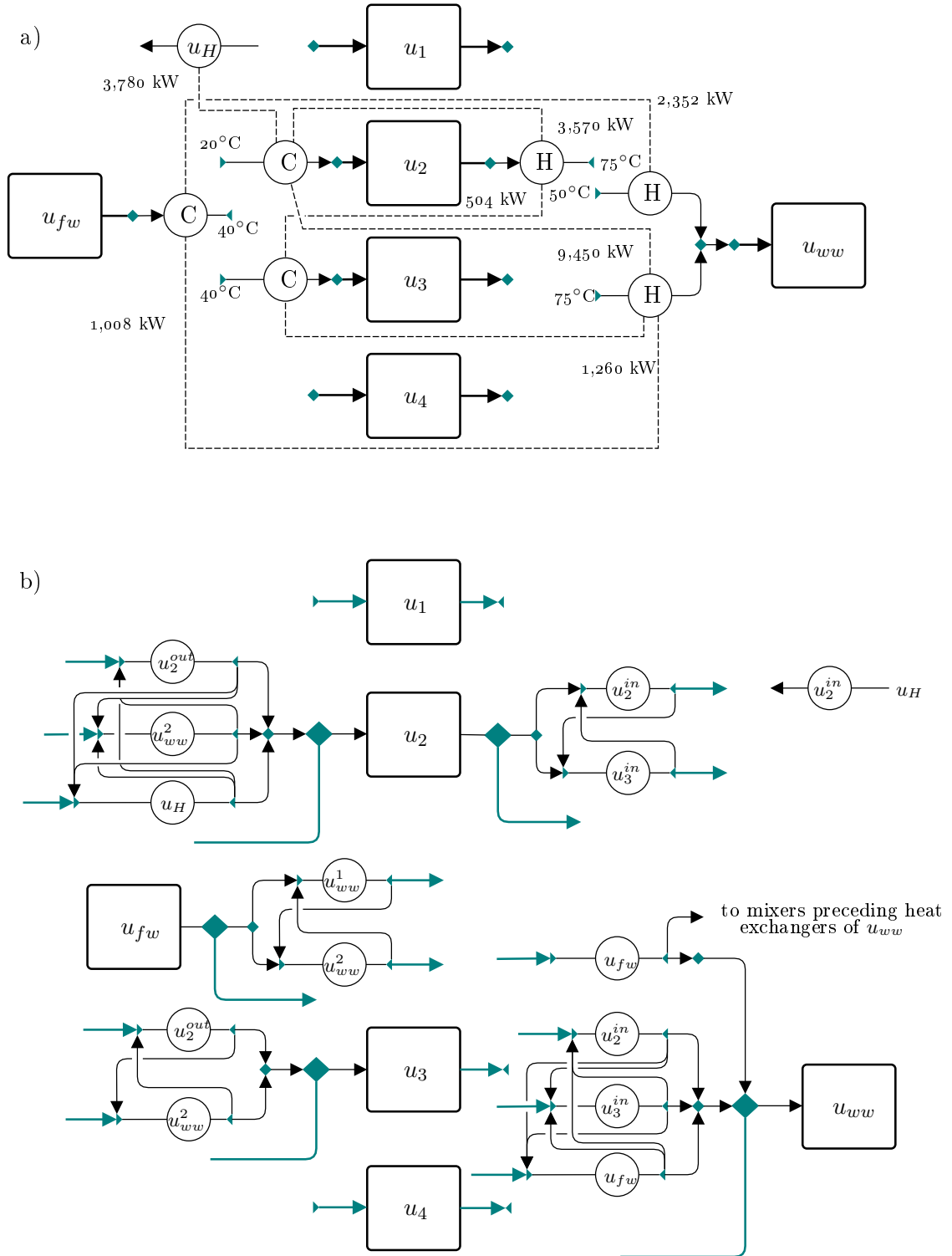


FIGURE 3.3—Illustrative case: a) results of problem **P1** and **P2**, b) construction of HIWAN hyper-structure



FIGURE 3.4—Comparison of two approaches for HEN design in water networks (dashed lines are unselected options of the related hyperstructure)

TABLE 3.2—Comparison of two approaches based on key HEN indicators⁽¹⁾

	$y_{i,j}$	$t_j^{ex,i,I}[^{\circ}\text{C}]$	$t_j^{ex,i,O}[^{\circ}\text{C}]$	$t_i^{ex,j,I}[^{\circ}\text{C}]$	$t_i^{ex,j,O}[^{\circ}\text{C}]$	$\text{LMTD}_{i,j}[^{\circ}\text{C}]$	$Q_{i,j}[\text{kW}]$	$A_{i,j}[\text{m}^2]$	$C_{i,j}^{inv}[\text{USD}/\text{yr}]$
1	$u_H-u_2^{in(2)}$	120.00	120.00	81.96	99.96	28.1	3780.0	269.2	42,453
2	$u_2^{out}-u_2^{in}$	100.00 (-)	74.61 (-)	64.62 (-)	81.62 (-)	13.8 (-)	3,570.0 (-)	518.9 (-)	59,078 (-)
3	$u_2^{out}-u_3^{in}$	100.00 (-)	77.70 (-)	64.96 (-)	74.96 (-)	18.2 (-)	504.0 (-)	55.4 (-)	21,342 (-)
4	$u_{ww}^1-u_{fw}$	50.00 (50.24)	30.00 (30.00)	20.00 (20.00)	40.00 (40.03)	10.0 (10.1)	2,352.0 (3,371.4)	470.4 (667.3)	56,157 (67,398)
5	$u_{ww}^2-u_2^{in}$	75.00 (91.92)	30.00 (30.00)	20.00 (20.00)	65.00 (81.93)	10.0 (10.0)	9,450.0 (13,004.7)	1,890.0 (2,602.2)	118,932 (142,397)
6	$u_{ww}^2-u_3^{in}$	75.00 (75.01)	50.52 (55.24)	40.00 (40.00)	65.00 (57.86)	10.3 (16.2)	1,260.0 (1,782.5)	245.7 (220.3)	40,613 (38,550)
7	$u_{ww}^2-u_{fw}$	50.20 (-)	30.20 (-)	20.00 (-)	39.87 (-)	10.3 (-)	1,008.0 (-)	196.4 (-)	36,514 (-)
Total								3,645.9 (3,759.0)	375,089 (290,799)

(1) i and j represent hot and cold streams, respectively. Values in parentheses are results of HIWAN hyperstructure.

(2) Same values in both cases.

3.5 Validation and discussion

Several test cases from the literature (introduced in section 2.3) were selected to validate the mathematical formulation and the proposed iterative sequential solution strategy. The cost data were presented in Table 2.1. The maximum number of integer cuts was limited to 50, though one sub-problem (**P1** or **P2**) may become infeasible before reaching its respective limit, at which point the algorithm terminates the corresponding integer cut loop. In combination with application of the integer cut constraint, small minimum sizes were introduced for all units in problem **P1** (Equation 2.23 to Equation 2.28). Similarly, for problem **P2**, minimum allowed heat exchange between hot stream i and cold stream j in pinch interval l is set at a small positive number ($Q_{i,j,l}^{min} > 0$ Equation 2.42). These two additions prevent generation of multiple identical solutions. Furthermore, to investigate the trade-off between investment cost and operating cost, the HRAT in problem **P1** was varied between 1°C and 10°C with step of 1°C ($N_{HRAT} = 10$). These values are passed to problem **P3** for ΔT_{min} . As discussed in section 2.3, test cases I and II are threshold problems and hence the value of HRAT does not affect the utility consumptions. This, however, becomes a decisive factor for test case III [107] where both hot utility and cooling utility are required. In this section, only solutions of HIWAN hyperstructure are presented. Parallel coordinate visualization tool is used to illustrate all solutions and selected key performance indicators. These key performance indicators (KPI)s were previously introduced in section 2.3 and are listed here for the sake of completeness:

- Resource indicators: freshwater and thermal utility consumptions, \dot{m}_{fw} , \dot{Q}_u^H , \dot{Q}_u^C ;
- Network indicators: N_s^{th} (number of thermal streams), N_{HE} (number of heat exchangers), A_{HEN}^{total} (total area of heat exchangers), N_{mixer} (number of mixing points), N_{mixer}^{NIM} (number of non-isothermal mixing points), N_s^m (number of mass streams in the water network), and Q_{HEN}^{total} (total heat load of all heat exchangers);
- Economic indicators: C^{HEN} (HEN cost) and C^{TAC} (total annualized cost).

It should be noted that test cases I to III were intentionally designed by the scientific community to validate their mathematical formulations and solution strategies. Due to complexity of

solving non-convex MINLP problems that arise in HIWAN synthesis, and tendency towards local optimality in such problems, it can be argued that these test cases are not easily solved but with multiple manipulations of solvers and their intrinsic options to reach *one good* single solution. Thus main goal and contribution of the proposed solution strategy in this work is to solve the HIWAN problem by first reducing the search space, then generating many solutions to the problem. To this end, many solutions can be generated for problem **P3** which can be seen as approaching an optimal point from different starting points (solutions of problems **P1** and **P2**).

3.5.1 Test case I: single-contaminant problem

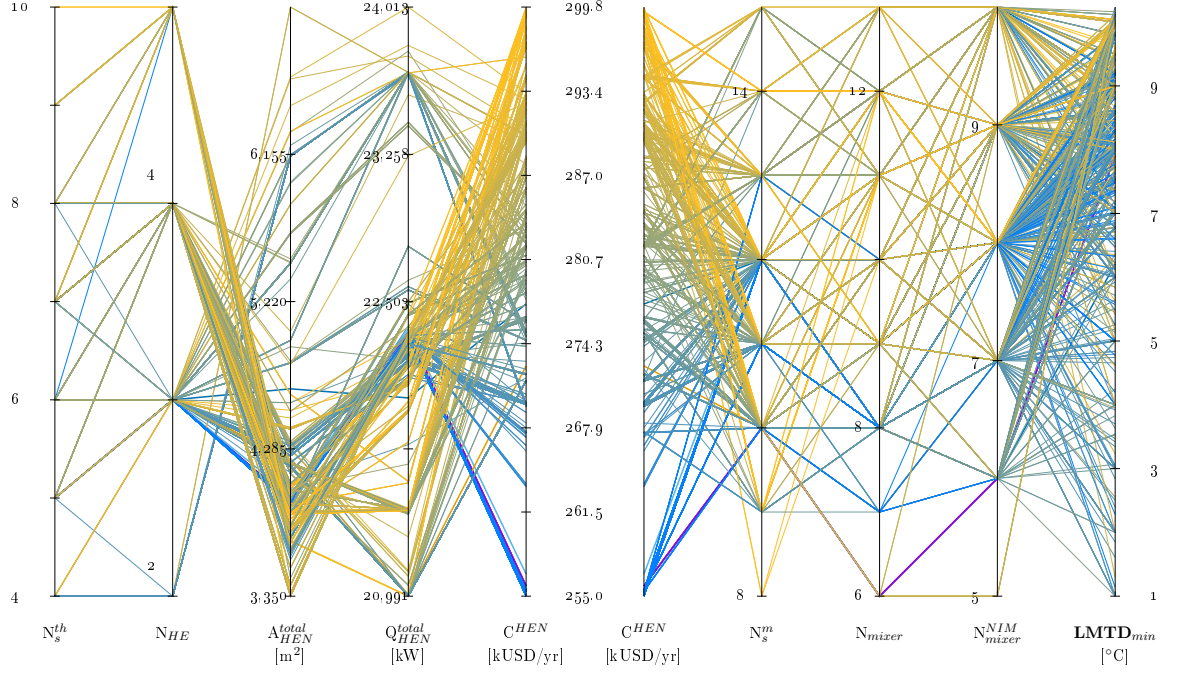
As presented in subsection 2.3.1, this test case exhibits 90 kg/s of freshwater consumption and 3,780 kW of hot utility consumption (minimum targets, 2,397.0 kUSD/yr in operating cost). Table A.1 provides the assumptions and solver options for this test case. Out of 26,010 potential solutions, 6,462 solutions exist to problem **P2** – in fact, problem **P1** converged for all integer cuts, while problem **P2** was found to be infeasible for low HRAT values after few integer cuts. 3,611 solutions exist to problem **P3**. They exhibit a wide spectrum of solutions with HEN cost (the objective function in problem **P3**) ranging from 255.1 kUSD/yr (the minimum value within the literature) to 660.9 kUSD/yr. Among these, 3,506 solutions exhibit HEN cost in the range reported in the literature (referring to Table 1.5, the maximum observed cost is 413.0 kUSD/yr). To visualize this set of solutions, several filters were imposed to further reduce the number of solutions:

- $C^{HEN} \leq 300$ kUSD/yr;
- $N_s^m \leq 15$, maximum value reported in the literature for this test case in (Table 1.5);
- $N_{mixer} \leq 13$, maximum value reported in the literature for this test case in (Table 1.5);
- $N_{mixer}^{NIM} \leq 10$, maximum value reported in the literature for this test case in (Table 1.5);

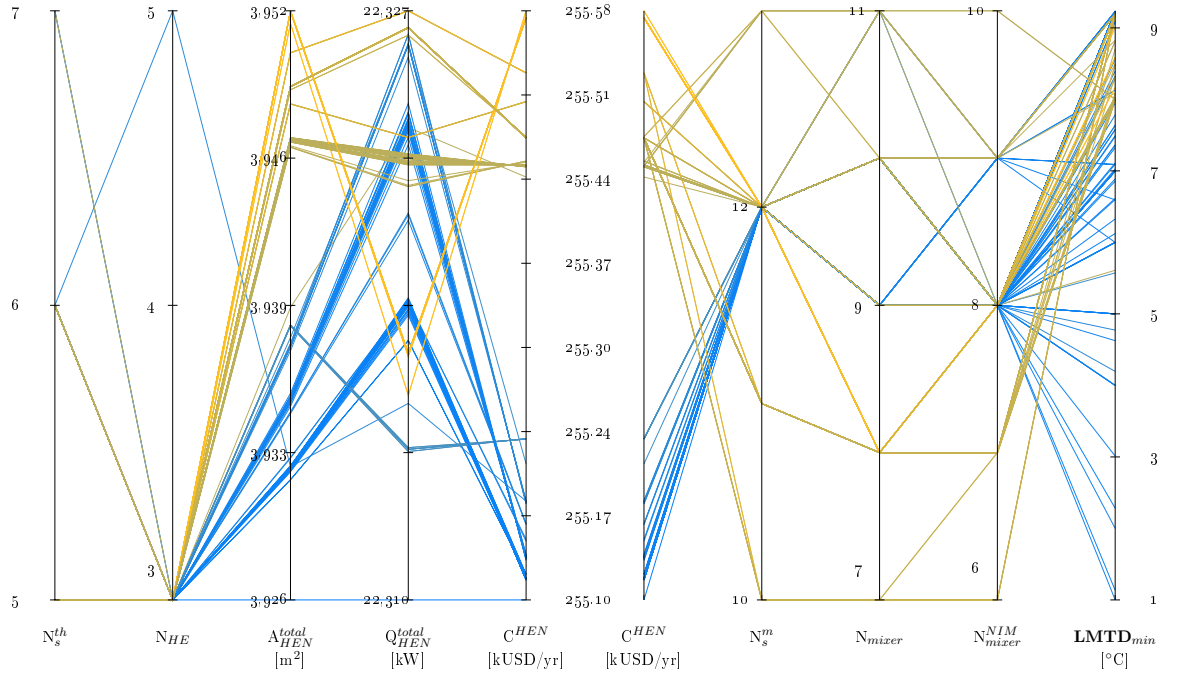
Figure 3.5a presents 2,247 solutions which remain after filtering. Selected results from the literature (from Table 1.5 with HEN cost lower than 300 kUSD/yr) are also plotted in this figure in bold. The number of heat exchangers (N_{HE}) varies between two and five, where two is the lowest number of heat exchangers reported for this test case by the proposed solution strategy. Figure 3.5a illustrates an inverse correlation between the number of heat exchangers and their total area. The total area (A_{HEN}^{total}) varies between 3,350 m² and 7,090.7 m². The total area of heat exchangers reported in the literature varies between 3,111 m² (Wan Alwi et al. [54]) and 6,300 m². However, it should be noted that the HEN design reported by Wan Alwi et al. [54] is infeasible due to a violation of ΔT_{min} .

Figure 3.5b presents the solutions exhibiting the lowest HEN cost in the range of 255 kUSD/yr. This figure illustrates the vast possibility of solutions with the same minimum HEN cost (375 solutions in this case). Almost all solutions in the literature are present in the list of solutions generated by the sequential solution strategy. It should also be noted that many solutions exist for problem **P3** which have the same key performance indicators and hence are overlapping in Figure 3.5a and Figure 3.5b. Given the fact that the solutions of problems **P1** and **P2** differ for each (due to inclusion of integer cut constraints), it is important to notice that simply optimizing the temperatures and flows within a water network (i.e., solving problem **P3**) for a given set of thermal streams (i.e., solving problem **P1**) and a given set of heat exchangers (i.e., solving problem **P2**) can yield the same solutions.

3.5 VALIDATION AND DISCUSSION



(a) All 2,447 solutions (test case I)



(b) Solutions with the lowest HEN cost (test case I)

FIGURE 3.5—Visualization of key indicators for test case I using parallel coordinates

3.5.2 Test case II: single-contaminant problem

As presented in subsection 2.3.2, this test case exhibits 125.94 kg/s of freshwater consumption and 5,289.6 kW of hot utility consumption with 3,354.4 kUSD/yr in operating cost (i.e., the minimum utility targets). Table A.2 provides all the assumptions and solver options for this test case. Out of 26,010 possible solutions, 5,260 solutions exist to problem **P2**. The objective value of problem **P2** varies between 6 and 15. From this set of solutions, 565 solutions converged for problem **P3**, among which, HEN cost varies between 272.1 kUSD/yr and 529.3 kUSD/yr for 554 solutions. The minimum HEN cost reported by the literature is 257.2 kUSD/yr (Ibrić et al. [129]), however, the freshwater and utility consumptions were reported to be 126.717 kg/s and 5,322.1 kW, respectively. As with test case I, several filters were applied to further reduce the number of solutions to aid in visualization:

- $N_s^m \leq 32$, maximum value reported in the literature for this test case in Table 2.3;
- $N_{mixer} \leq 21$, maximum value reported in the literature for this test case in Table 2.3;
- $N_{mixer}^{NIM} \leq 17$, maximum value reported in the literature for this test case in Table 2.3;

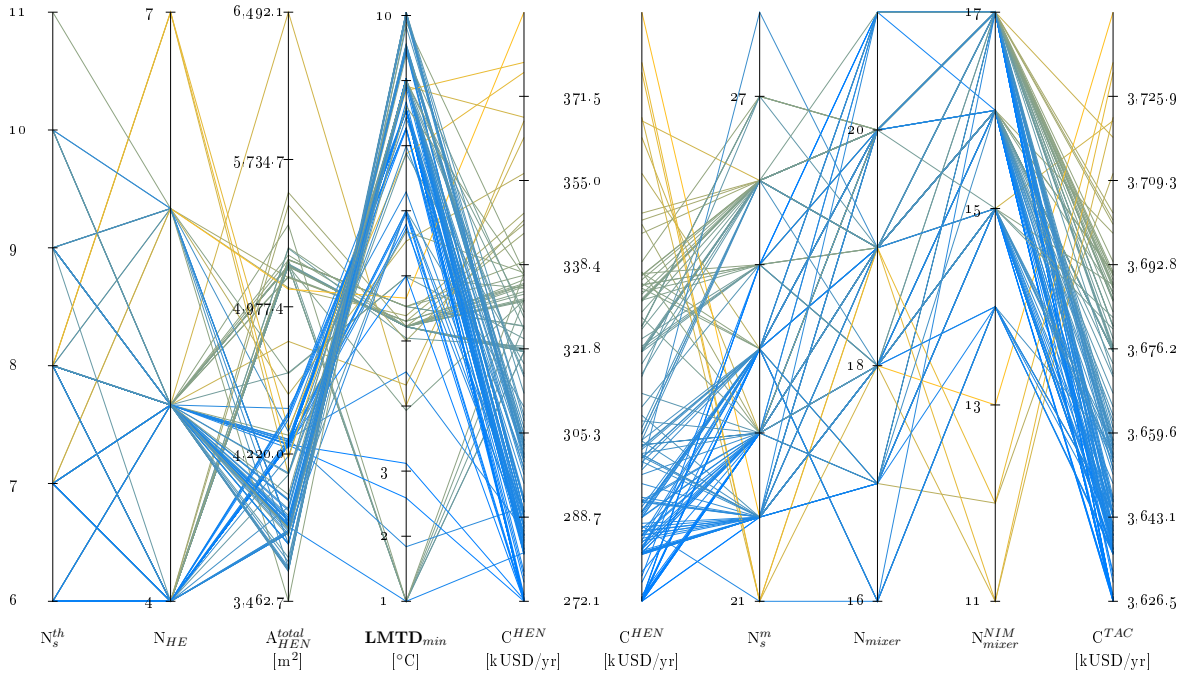


FIGURE 3.6—Visualization of key indicators for test case II using parallel coordinates (155 solutions are shown here)

After applying these filters, Figure 3.6 presents the remaining 155 solutions. Figure 3.7 illustrates 22 solutions exhibiting the lowest HEN cost within the generated set of solutions. Considering total annualized cost as the main objective in this case study, the proposed set of solutions encompass the design with lowest cost of 3,626.5 kUSD/yr. Comparing this solution with the minimum reported in the literature (3,628 kUSD/yr), one can observe that the proposed sequential solution strategy can reach the minimum while also proposing a set of solutions in the vicinity which differ in other KPIs as illustrated in Figure 3.7. The advantage

of such approach is being able to select from a set of solutions which are similar in one KPI (or the objective) while potentially having “hidden” benefits in another one (i.e., unaddressed KPI in the objective function). For instance, from Figure 3.7, among all solutions with the lowest HEN cost, the solution with the lowest number of mixers and mass streams exhibits a simpler network design while its HEN cost is increased by less than 0.1% compared with the minimum value.

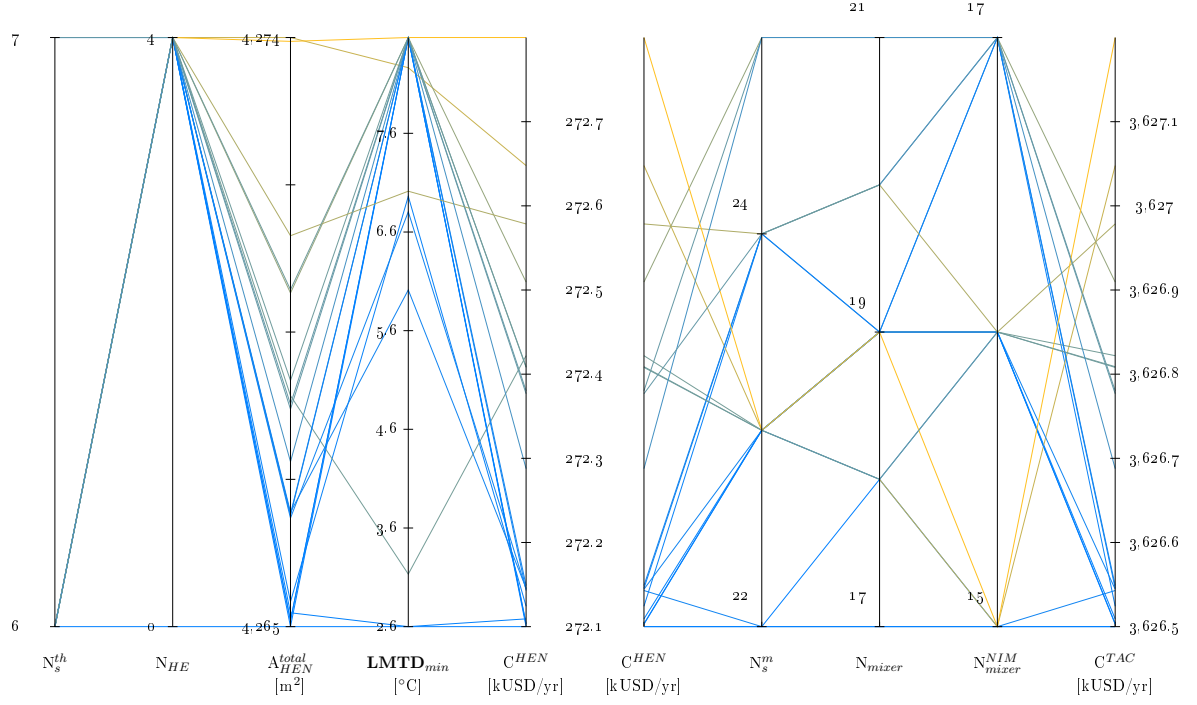


FIGURE 3.7—Solutions with the lowest HEN cost (test case II)

3.5.3 Test case III: multi-contaminant problem

As presented in subsection 2.3.3, this test case is a pinch problem with minimum freshwater consumption of 70 kg/s. The value of HRAT affects the thermal utility consumptions (Figure 3.8). Furthermore, higher hot utility consumption means more thermal matches among water thermal streams and hot utility (for this test case at 120°C) and hence higher approach temperature in heat exchangers which consequently reduces the HEN cost. This was illustrated in the solution of Jagannath and Almansoori [141] where the authors constrained the number of heat exchangers and mass exchanges to four and seven, respectively, and reached 74.3 kg/s of freshwater consumption, 8,760 kW of hot utility and 2,520 kW of cold utility (minimum approach temperature is 20°C). Although they reported the lowest HEN cost, their solution exhibits the highest total cost and the highest thermal utility consumption among the reported values in the literature.

Table A.2 provides all the assumptions and solver options for this test case. Out of 26,010 possible solutions, 982 solutions exist to problem **P2**. For any solution of problem **P1**, problem **P2** became infeasible after six integer cuts. The objective value of problem **P2** varies between six and nine. Among these solutions, 299 converged for problem **P3** with minimum and maximum HEN costs of 146.3 kUSD/yr and 353.8 kUSD/yr, respectively. Figure 3.8 illustrates

HEN and operating costs of these solutions for different values of ΔT_{min} . Figure 3.9 illustrates the key performance indicators of these 299 solutions.

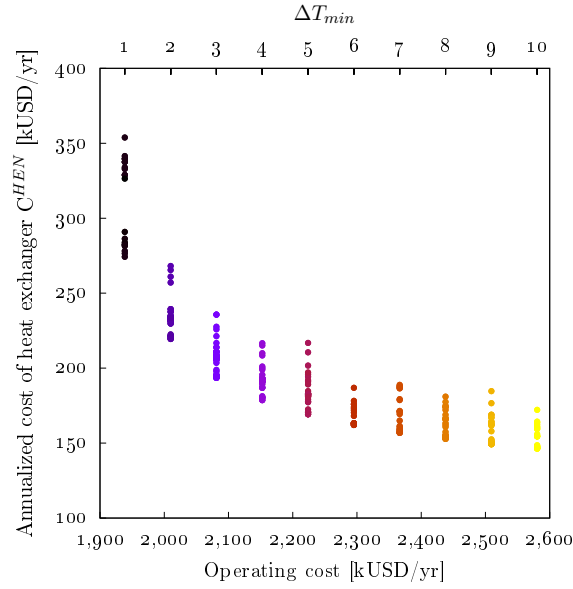


FIGURE 3.8—HEN cost *vs* operating cost for selected solutions of test case III

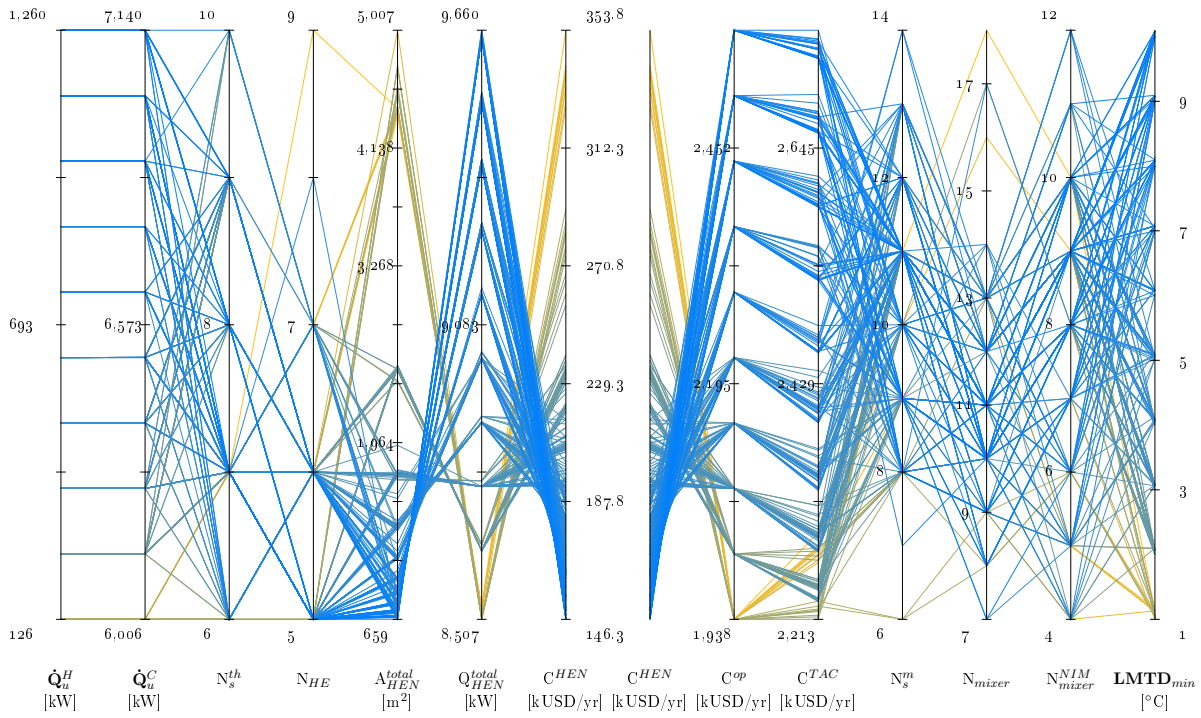


FIGURE 3.9—Visualization of key indicators for test case III using parallel coordinates (299 solutions are shown here)

3.5.4 Simplified industrial case study

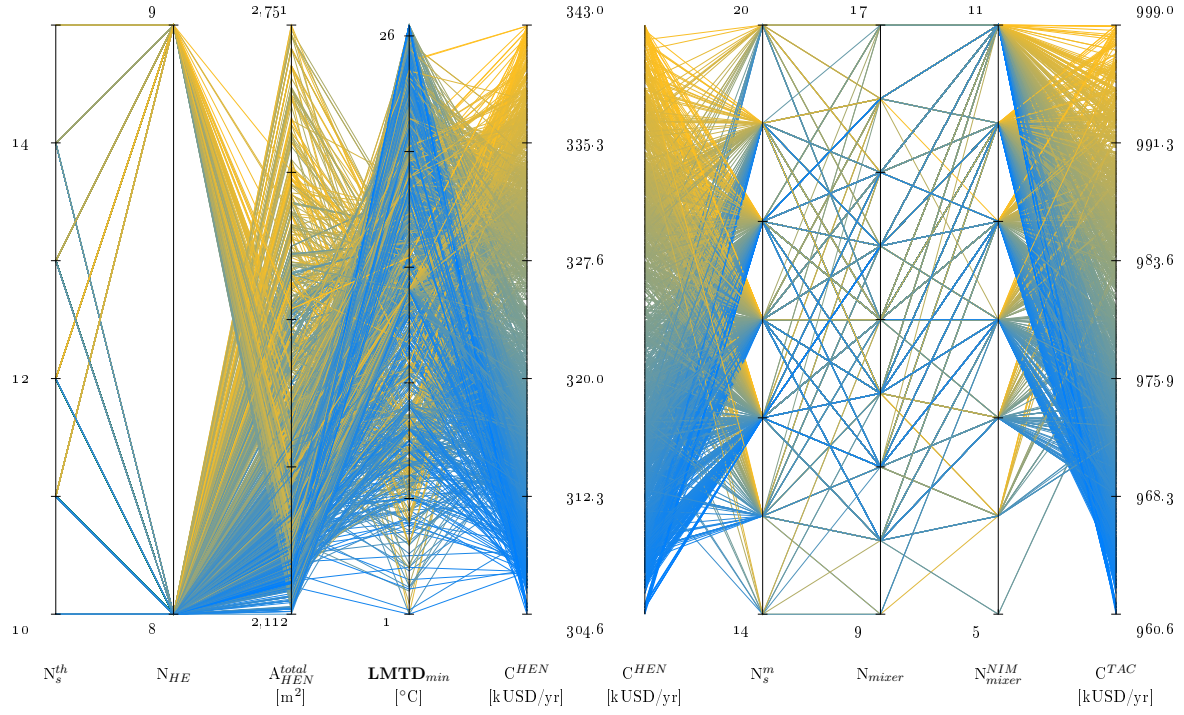
The simplified industrial case study introduced in section 2.5 is revisited here. Similar to previous case studies problems **P1** and **P2** are solved for 50 integer cuts. Table A.3 provides all the assumptions and solver options for this test case. 3,588 solutions exist for problem **P3**. All solutions reach 80 kg/s of freshwater consumption with 15,645 kW of cold utility. To visualize this set of solutions, several filters are imposed to further reduce the number of solutions:

- $C^{HEN} \leq 343$ kUSD/yr (Table 2.7);
- $N_s^m \leq 20$;
- $N_{mixer} \leq 17$ (Table 2.7);
- $N_{mixer}^{NIM} \leq 11$ (Table 2.7);

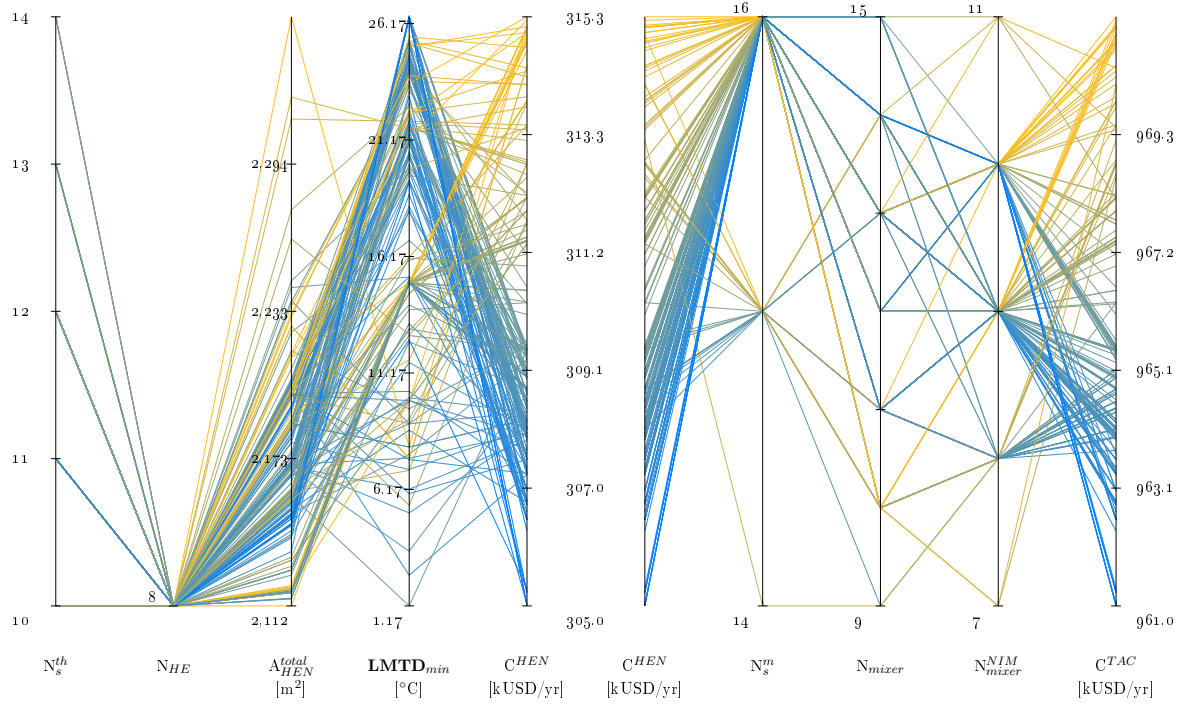
Overall, 2,053 solutions satisfy the above criteria which are visualized in Figure 3.10a. Number of heat exchangers are limited to 8 and 9, while the area varies between 2,100 and 2,750 m². It can be observed from this figure that, for a given number of mixers and mass streams, the HEN cost varies over the entire range which enunciates the fact that minimization of HEN cost and providing a single solution would not satisfy other important criteria. The lowest total cost reached by the proposed solution strategy is 960.6 kUSD/yr which is less than the lowest reported in the literature (971.4 kUSD/yr [49]). It should also be highlighted that the solution proposed by Ibrić et al. [49] considered the optimization of tank temperatures, while these temperatures are fixed for the analysis presented herein. Moreover, all proposed solutions in this work exhibit 11% lower freshwater consumption than the solution reported in the literature. Figure 3.10b illustrates all of the solutions (240) proposed by the sequential solution strategy which exhibit lower total cost than 971.4 kUSD/yr. Figure 3.10b shows that for a given number of heat exchangers (8 for these solutions), increasing the number of non-isothermal mixing points lowers the total cost. Figure 3.11 presents one of the optimal HIWAN designs. Table 3.3 provides a comparison between problems **P2** and **P3** in terms of thermal matches and their heat loads.

TABLE 3.3—Comparison of results from the HLD solution (problem **P2**) and HIWAN hyperstructure (problem **P3**) based on thermal matches and their heat loads for the optimal solution shown in Figure 3.11

Thermal match	$Q_{i,j}$ (problem P2) [kW]	$Q_{i,j}$ (problem P3) [kW]
surface condenser $\rightarrow u_C$	5,418.1	5,436.8
surface condenser $\rightarrow u_{fw}^{70^\circ\text{C}}$	2,141.9	2,123.2
turpentine condenser $\rightarrow u_{2,in}^{62^\circ\text{C}}$	671.9	666.9
turpentine condenser $\rightarrow u_{fw}^{70^\circ\text{C}}$	10,248.1	10,253.1
contaminated condensate $\rightarrow u_C$	630.0	630.0
effluent $\rightarrow u_{1,out}^{62^\circ\text{C}}$	105.0	0
effluent $\rightarrow u_{fw}^{70^\circ\text{C}}$	2,100.0	2,205.0
dryer exhaust $\rightarrow u_{fw}^{70^\circ\text{C}}$	1,050.0	1,050.0
$u_{5,in}^{30^\circ\text{C}} \rightarrow u_C$	213.9	0
$u_{ww}^{62^\circ\text{C}} \rightarrow u_C$	9,383.1	9,578.3



(a) All 2053 solutions



(b) Solutions with lower TAC cost than the value reported in the literature (240 solutions)

FIGURE 3.10—Visualization of key indicators for the simplified kraft case using parallel coordinates

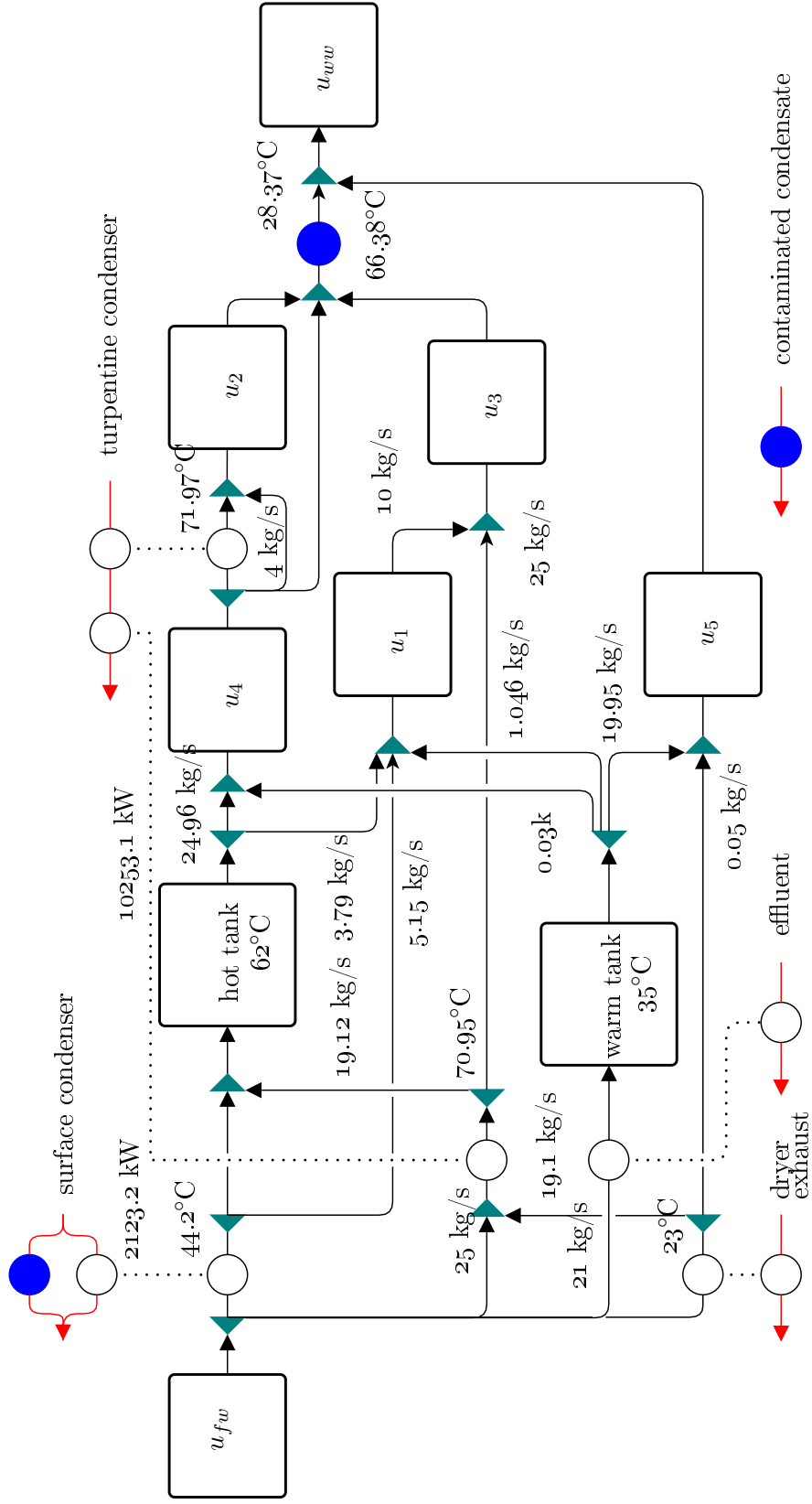


FIGURE 3.11—One of the optimal solutions for the simplified kraft test case exhibiting improved performance: $\dot{m}_{fw} = 80$ kg/s, $\dot{Q}_u^C = 15,645$ kW, $N_{HE} = 8$, $A_{HEN}^{total} = 2147.9$ m², $LMTD_{min} = 26.46^\circ\text{C}$, $C^{HEN} = 306.78$ kUSD/yr, $C^{TAC} = 656.0$ kUSD/yr, $C^{TAC} = 962.8$ kUSD/yr, $N_s^m = 16$, $N_{mixer} = 11$, $N_{mixer}^m = 9$.

3.6 Conclusion

Two main complexities have been observed within the HIWAN methodologies in the literature. One difficulty is selecting the state of water thermal streams in the HEN design as this choice affects the overall mathematical formulation in MINLP models. This, in turn, introduces the second difficulty of selecting thermal matches with undefined states of the water thermal streams; thus, resulting in a complex MINLP formulation. These two complexities have been addressed by solving problems **P1** (targeting model) and **P2** (HLD) in sequence prior to the final HIWAN design which identify the states and potential thermal matches, respectively. A novel HIWAN hyperstructure with NLP formulation has been proposed in this chapter for final design of HIWANs which exhibits higher degrees of non-isothermal mixing and lower investment costs. In addition, an iterative sequential solution strategy is proposed in this work by solving the sub-problems with integer cut constraints applied both on problem **P1** and problem **P2**. As discussed, this approach can be viewed as a technique of reducing the search space at each iteration to a set of potential water thermal streams and a set of potential matches and then solving HIWAN synthesis problem for the reduced space. Applying the proposed methodology on several test cases from the literature illustrated the fact that the methodology is not only able to reach minimum total cost of the system (the only objective function used in the literature), but also generates a set of alternative “good” solutions exhibiting various results with respect to other key performance indicators.

The choice of HEN cost as the main objective in the literature cases should not be the sole measure of optimality as these basic functions for heat exchanger cost reflect an average, observed correlation for overall networks and hence should not be used as the decisive factor in proposing a final design. The proposed approach in this work overcomes this limitation by generating and analyzing a set of solutions and applying multi-objective optimization to propose competing solutions exhibiting multiple decision criteria.

This part of the thesis proposed a methodology for simultaneous optimization of resource consumption and thermal process requirements. Water is regarded as a heat transfer medium, recovering heat among and between processes, while also appearing as a process requirement for water-consuming units that require different temperatures and qualities. For low temperature heat, technologies such as ORCs combined with thermal storage can compete with water loops as they exploit the exergy in hot thermal streams for electricity production and provide heat at a lower temperature (in the condenser) to the process or for other uses. Part II of this report focuses on analyzing ORC architectures and proposes a methodology for their optimal integration in industrial processes. ■

References

- [1] S. A. Papoulias, I. E. Grossmann, A structural optimization approach in process synthesis—II: Heat recovery networks, *Computers & Chemical Engineering* 7 (6) (1983) 707–721, ISSN 0098-1354.
- [2] F. Marechal, I. Boursier, B. Kalitventzeff, Synep1 : A methodology for energy integration and optimal heat exchanger network synthesis, *Computers & Chemical Engineering* 13 (4–5) (1989) 603–610, ISSN 0098-1354.
- [3] J. Cerda, A. W. Westerburg, Synthesizing heat exchanger networks having restricted stream/stream matches using transportation problem formulations, *Chemical Engineering Science* 38 (10) (1983) 1723–1740, ISSN 0009-2509.
- [4] C. A. Floudas, A. R. Ciric, Strategies for overcoming uncertainties in heat exchanger network synthesis, *Computers & Chemical Engineering* 13 (10) (1989) 1133–1152, ISSN 0098-1354.
- [5] L. E. Savulescu, R. Smith, Simultaneous energy and water minimisation, in: 1998 AIChE Annual Meeting, Miami Beach, Florida, 13–22, unpublished work, 1998.
- [6] J. Jeżowski, Review of Water Network Design Methods with Literature Annotations, *Industrial & Engineering Chemistry Research* 49 (10) (2010) 4475–4516, ISSN 0888-5885.
- [7] G. P. Towler, R. Mann, A. J. Serriere, C. M. D. Gabaude, Refinery Hydrogen Management –Cost Analysis of Chemically Integrated Facilities, *Industrial & Engineering Chemistry Research* 35 (7) (1996) 2378–2388, ISSN 0888-5885.
- [8] M. D. Shelley, M. M. El-Halwagi, Component-less design of recovery and allocation systems: a functionality-based clustering approach, *Computers & Chemical Engineering* 24 (9–10) (2000) 2081–2091, ISSN 0098-1354.
- [9] M. Kermani, Z. Périn-Levasseur, M. Benali, L. Savulescu, F. Maréchal, A novel MILP approach for simultaneous optimization of water and energy: Application to a Canadian softwood Kraft pulping mill, *Computers & Chemical Engineering* ISSN 0098-1354.
- [10] M. Suhr, G. Klein, I. Kourti, M. R. Gonzalo, G. G. Santonja, S. Roudier, L. D. Sancho, Best available techniques (BAT) reference document for the production of pulp, paper and board, JRC science and policy reports, Industrial Emissions Directive 2010/75/EU Integrated Pollution Prevention and control -, URL <http://eippcb.jrc.ec.europa.eu/reference/pp.html>, 2015.
- [11] K. P. Papalexandri, E. N. Pistikopoulos, A multiperiod MINLP model for the synthesis of flexible heat and mass exchange networks, *Computers & Chemical Engineering* 18 (11–12) (1994) 1125–1139, ISSN 0098-1354.
- [12] B. K. Srinivas, M. M. El-Halwagi, Synthesis of combined heat and reactive mass-exchange networks, *Chemical Engineering Science* 49 (13) (1994) 2059–2074, ISSN 0009-2509.
- [13] M. Bagajewicz, A review of recent design procedures for water networks in refineries and process plants, *Comput. Chem. Eng* (2000) 24.
- [14] Y. P. Wang, R. Smith, Wastewater minimisation, *Chemical Engineering Science* 49 (7) (1994) 981–1006, ISSN 0009-2509.

-
- [15] Y. Wang, R. Smith, Wastewater minimization with flowrate constraints, *Chemical Engineering Research and Design* 73 (A8) (1995) 889–904, ISSN 0263-8762.
- [16] M. J. Savelski, M. J. Bagajewicz, On the optimality conditions of water utilization systems in process plants with single contaminants, *Chemical Engineering Science* 55 (21) (2000) 5035–5048, ISSN 0009-2509.
- [17] M. Savelski, M. Bagajewicz, On the necessary conditions of optimality of water utilization systems in process plants with multiple contaminants, *Chemical Engineering Science* 58 (23–24) (2003) 5349–5362, ISSN 0009-2509.
- [18] M. Bagajewicz, H. Rodera, M. Savelski, Energy efficient water utilization systems in process plants, *Computers & Chemical Engineering* 26 (1) (2002) 59–79, ISSN 0098-1354.
- [19] D. C. Y. Foo, State-of-the-Art Review of Pinch Analysis Techniques for Water Network Synthesis, *Industrial & Engineering Chemistry Research* 48 (11) (2009) 5125–5159, ISSN 0888-5885.
- [20] Z. Chen, J. Wang, Heat, mass, and work exchange networks, *Frontiers of Chemical Science and Engineering* 6 (4) (2012) 484–502, ISSN 2095-0179, 2095-0187.
- [21] J. J. Klemeš, Industrial water recycle/reuse, *Current Opinion in Chemical Engineering* 1 (3) (2012) 238–245, ISSN 2211-3398.
- [22] E. Ahmetović, N. Ibrić, Z. Kravanja, I. E. Grossmann, Water and energy integration: A comprehensive literature review of non-isothermal water network synthesis, *Computers & Chemical Engineering* 82 (2015) 144–171, ISSN 0098-1354.
- [23] R. Karuppiah, I. E. Grossmann, Global optimization for the synthesis of integrated water systems in chemical processes, *Computers & Chemical Engineering* 30 (4) (2006) 650–673, ISSN 0098-1354.
- [24] Y. Wang, R. Smith, Time Pinch Analysis, *Chemical Engineering Research & Design* 73 (8) (1995) 905–914.
- [25] J. K. Kim, R. Smith, Automated Design of Discontinuous Water Systems, *Process Safety and Environmental Protection* 82 (3) (2004) 238–248, ISSN 0957-5820.
- [26] D. C. Y. Foo, Z. A. Manan, Y. L. Tan, Synthesis of maximum water recovery network for batch process systems, *Journal of Cleaner Production* 13 (15) (2005) 1381–1394, ISSN 0959-6526.
- [27] T. Majoz, Wastewater minimisation using central reusable water storage in batch plants, *Computers & Chemical Engineering* 29 (7) (2005) 1631–1646, ISSN 0098-1354.
- [28] K.-F. Cheng, C.-T. Chang, Integrated Water Network Designs for Batch Processes, *Industrial & Engineering Chemistry Research* 46 (4) (2007) 1241–1253, ISSN 0888-5885.
- [29] L.-J. Li, R.-J. Zhou, H.-G. Dong, State-Time-Space Superstructure-Based MINLP Formulation for Batch Water-Allocation Network Design, *Industrial & Engineering Chemistry Research* 49 (1) (2010) 236–251, ISSN 0888-5885.
- [30] R.-J. Zhou, L.-J. Li, W. Xiao, H.-G. Dong, Simultaneous optimization of batch process schedules and water-allocation network, *Computers & Chemical Engineering* 33 (6) (2009) 1153–1168, ISSN 0098-1354.
- [31] N. D. Chaturvedi, S. Bandyopadhyay, Optimization of Multiple Freshwater Resources in a Flexible-Schedule Batch Water Network, *Industrial & Engineering Chemistry Research* 53 (14) (2014) 5996–6005, ISSN 0888-5885.
- [32] G. Liu, H. Li, X. Feng, C. Deng, Novel method for targeting the optimal purification feed flow rate of hydrogen network with purification reuse/recycle, *AIChE Journal* 59 (6) (2013) 1964–1980, ISSN 1547-5905.
- [33] M. M. El-Halwagi, 13 - Conserving Material Resources through Process Integration: Material

- Conservation Networks A2 - Klemeš, Jiří J., in: Handbook of Process Integration (PI), Woodhead Publishing Series in Energy, Woodhead Publishing, ISBN 978-0-85709-593-0, 422–439, URL <http://www.sciencedirect.com/science/article/pii/B9780857095930500137>, 2013.
- [34] E. N. Pistikopoulos, Uncertainty in process design and operations, *Computers & Chemical Engineering* 19, Supplement 1 (1995) 553–563, ISSN 0098-1354.
- [35] D. A. Straub, I. E. Grossmann, Design optimization of stochastic flexibility, *Computers & Chemical Engineering* 17 (4) (1993) 339–354, ISSN 0098-1354.
- [36] T.-Y. L. Min-Ho Suh, Robust Optimal Design of Wastewater Reuse Network of Plating Process, *Journal of Chemical Engineering of Japan - J CHEM ENG JPN* 35 (9) (2002) 863–873.
- [37] A. P. R. Koppol, M. J. Bagajewicz, Financial Risk Management in the Design of Water Utilization Systems in Process Plants, *Industrial & Engineering Chemistry Research* 42 (21) (2003) 5249–5255, ISSN 0888-5885.
- [38] R. R. Tan, D. E. Cruz, Synthesis of robust water reuse networks for single-component retrofit problems using symmetric fuzzy linear programming, *Computers & Chemical Engineering* 28 (12) (2004) 2547–2551, ISSN 0098-1354.
- [39] R. Karupiah, I. E. Grossmann, Global optimization of multiscenario mixed integer nonlinear programming models arising in the synthesis of integrated water networks under uncertainty, *Computers & Chemical Engineering* (2008) 145–160.
- [40] I. M. L. Chew, R. Tan, D. K. S. Ng, D. C. Y. Foo, T. Majozi, J. Gouws, Synthesis of Direct and Indirect Interplant Water Network, *Industrial & Engineering Chemistry Research* 47 (23) (2008) 9485–9496, ISSN 0888-5885.
- [41] R.-J. Zhou, L.-J. Li, H.-G. Dong, I. E. Grossmann, Synthesis of Interplant Water-Allocation and Heat-Exchange Networks. Part 1: Fixed Flow Rate Processes, *Industrial & Engineering Chemistry Research* 51 (11) (2012) 4299–4312, ISSN 0888-5885.
- [42] R.-J. Zhou, L.-J. Li, Simultaneous Optimization of Property-Based Water-Allocation and Heat-Exchange Networks with State-Space Superstructure, *Industrial & Engineering Chemistry Research* ISSN 0888-5885.
- [43] N. Ibrić, E. Ahmetović, Z. Kravanja, F. Maréchal, M. Kermani, Synthesis of single and interplant non-isothermal water networks, *Journal of Environmental Management* 203 (Part 3) (2017) 1095–1117, ISSN 0301-4797.
- [44] M. Kermani, A. S. Wallerand, I. D. Kantor, F. Maréchal, A Hybrid Methodology for Combined Interplant Heat, Water, and Power Integration, in: A. Espuña, M. Graells, L. Puigjaner (Eds.), *Computer Aided Chemical Engineering*, vol. 40 of *27 European Symposium on Computer Aided Process Engineering*, Elsevier, 1969–1974, doi: \bibinfo{doi}{10.1016/B978-0-444-63965-3.50330-5}, URL <http://www.sciencedirect.com/science/article/pii/B9780444639653503305>, 2017.
- [45] P. Y. Liew, W. L. Theo, S. R. Wan Alwi, J. S. Lim, Z. Abdul Manan, J. J. Klemeš, P. S. Varbanov, Total Site Heat Integration planning and design for industrial, urban and renewable systems, *Renewable and Sustainable Energy Reviews* 68, Part 2 (2017) 964–985, ISSN 1364-0321.
- [46] J. Du, X. Meng, H. Du, H. Yu, X. Fan, P. Yao, Optimal Design of Water Utilization Network with Energy Integration in Process Industries, *Chinese Journal of Chemical Engineering* 12 (2) (2004) 247–255.
- [47] L. Renard, Z. Périn-Levasseur, L. Salgueiro, L. E. Savulescu, F. Maréchal, M. Benali, Combined heat and mass integration: A benchmarking case study, in: I. D. Lockhart Bogle, M. Fairweather (Eds.), *Proceeding of 22nd European Symposium on Computer Aided Process Engineering*, 22nd European Symposium on Computer Aided Process Engineering, Elsevier, 2012.

-
- [48] M. Kermani, Z. Périn-Levasseur, M. Benali, L. Savulescu, F. Maréchal, An Improved Linear Programming Approach for Simultaneous Optimization of Water and Energy, in: P. S. V. a. P. Y. L. Jiří Jaromír Klemeš (Ed.), *Computer Aided Chemical Engineering*, vol. 33 of *24th European Symposium on Computer Aided Process Engineering*, Elsevier, 1561–1566, URL <http://www.sciencedirect.com/science/article/pii/B9780444634559500957>, 2014.
- [49] N. Ibrić, E. Ahmetović, Z. Kravanja, F. Maréchal, M. Kermani, Simultaneous synthesis of non-isothermal water networks integrated with process streams, *Energy* ISSN 0360-5442.
- [50] L. Savulescu, J.-K. Kim, R. Smith, Studies on simultaneous energy and water minimisation—Part I: Systems with no water re-use, *Chemical Engineering Science* 60 (12) (2005) 3279–3290, ISSN 0009-2509.
- [51] L. Savulescu, J.-K. Kim, R. Smith, Studies on simultaneous energy and water minimisation—Part II: Systems with maximum re-use of water, *Chemical Engineering Science* 60 (12) (2005) 3291–3308, ISSN 0009-2509.
- [52] Z. A. Manan, S. Y. Tea, S. R. W. Alwi, A new technique for simultaneous water and energy minimisation in process plant, *Chemical Engineering Research and Design* 87 (11) (2009) 1509–1519, ISSN 0263-8762.
- [53] B. Leewongtanawit, J.-K. Kim, Improving energy recovery for water minimisation, *Energy* 34 (7) (2009) 880–893, ISSN 0360-5442.
- [54] S. R. Wan Alwi, A. Ismail, Z. A. Manan, Z. B. Handani, A new graphical approach for simultaneous mass and energy minimisation, *Applied Thermal Engineering* 31 (6–7) (2011) 1021–1030, ISSN 1359-4311.
- [55] A. Ismail, S. Alwi, Z. Manan, Simultaneous targeting and design for non-mass transfer based water and energy reduction, in: 2011 4th International Conference on Modeling, Simulation and Applied Optimization (ICMSAO), 1–8, doi: \bibinfo{doi}{10.1109/ICMSAO.2011.5775563}, 2011.
- [56] J. Martínez-Patiño, M. Picón-Núñez, L. M. Serra, V. Verda, Design of water and energy networks using temperature–concentration diagrams, *Energy* 36 (6) (2011) 3888–3896, ISSN 0360-5442.
- [57] J. Martínez-Patiño, M. Picón-Núñez, L. M. Serra, V. Verda, Systematic approach for the synthesis of water and energy networks, *Applied Thermal Engineering* 48 (2012) 458–464, ISSN 1359-4311.
- [58] Z. Liao, X. Hong, B. Jiang, J. Wang, Y. Yang, Novel graphical tool for the design of the heat integrated water allocation networks, *AIChE Journal* (2015) n/a–n/aISSN 1547-5905.
- [59] Y. Hou, J. Wang, Z. Chen, X. Li, J. Zhang, Simultaneous integration of water and energy on conceptual methodology for both single- and multi-contaminant problems, *Chemical Engineering Science* 117 (2014) 436–444, ISSN 0009-2509.
- [60] Y. Hou, W. Xie, Z. Duan, J. Wang, A conceptual methodology for simultaneous optimization of water and heat with non-isothermal mixing, *Frontiers of Chemical Science and Engineering* 11 (2) (2017) 154–165, ISSN 2095-0179, 2095-0187.
- [61] W. Xie, Y. Hou, Y. Wang, J. Wang, A heuristic approach based on a single-temperature-peak design principle for simultaneous optimization of water and energy in fixed flowrate systems, *Chemical Engineering Science* 152 (2016) 323–342, ISSN 0009-2509.
- [62] X. Feng, Y. LI, X. YU, Improving Energy Performance of Water Allocation Networks Through Appropriate Stream Merging, *Chinese Journal of Chemical Engineering* 16 (3) (2008) 480–484, ISSN 1004-9541.
- [63] A. Ataei, M. Panjeshahi, S. Karbassian, Simultaneous Energy and Water Minimization-Approach for Systems with Optimum Regeneration of Wastewater, *Research Journal of Environmental Sciences* 3 (6) (2009) 604–618, ISSN 18193412.

-
- [64] A. Ataei, C. K. Yoo, Simultaneous Energy and Water Optimization in Multiple- Contaminant Systems with Flowrate Changes Consideration, *International Journal of Environmental Research* 4 (1) (2010) 11–26, ISSN 1735-6865.
- [65] G. C. Sahu, S. Bandyopadhyay, Energy optimization in heat integrated water allocation networks, *Chemical Engineering Science* 69 (1) (2012) 352–364, ISSN 0009-2509.
- [66] Y. L. Tan, D. K. S. Ng, M. M. El-Halwagi, D. C. Y. Foo, Y. Samyudia, Synthesis of Heat Integrated Resource Conservation Networks with Varying Operating Parameters, *Industrial & Engineering Chemistry Research* 52 (22) (2013) 7196–7210, ISSN 0888-5885.
- [67] L. Liu, J. Du, M. M. El-Halwagi, J. M. Ponce-Ortega, P. Yao, A systematic approach for synthesizing combined mass and heat exchange networks, *Computers & Chemical Engineering* 53 (2013) 1–13, ISSN 0098-1354.
- [68] S. De-León Almaraz, M. Boix, L. Montastruc, C. Azzaro-Pantel, Z. Liao, S. Domenech, Design of a water allocation and energy network for multi-contaminant problems using multi-objective optimization, *Process Safety and Environmental Protection* ISSN 0957-5820.
- [69] Y. Wang, R. Li, X. Feng, Rule-based optimization strategy for energy efficient water networks, *Applied Thermal Engineering* 110 (2017) 730–736, ISSN 1359-4311.
- [70] G. T. Polley, M. Picón-Núñez, J. d. J. López-Macié, Design of water and heat recovery networks for the simultaneous minimisation of water and energy consumption, *Applied Thermal Engineering* 30 (16) (2010) 2290–2299, ISSN 1359-4311.
- [71] S. Sharma, G. P. Rangaiah, Multi-objective Optimization of Heat Integrated Water Networks in Petroleum Refineries, in: P. S. V. a. P. Y. L. Jiří Jaromír Klemeš (Ed.), *Computer Aided Chemical Engineering*, vol. 33 of *24th European Symposium on Computer Aided Process Engineering*, Elsevier, 1531–1536, URL <http://www.sciencedirect.com/science/article/pii/B9780444634559500908>, 2014.
- [72] Y. Liang, C.-W. Hui, A shortcut model for energy efficient water network synthesis, *Applied Thermal Engineering* 96 (2016) 88–91, ISSN 1359-4311.
- [73] M. Boix, L. Pibouleau, L. Montastruc, C. Azzaro-Pantel, S. Domenech, Minimizing water and energy consumptions in water and heat exchange networks, *Applied Thermal Engineering* 36 (2012) 442–455, ISSN 1359-4311.
- [74] H.-P. Zhao, T.-C. Chan, Z.-Y. Liu, Design of water and heat networks with single contaminant, *Asia-Pacific Journal of Chemical Engineering* 10 (2) (2015) 219–227, ISSN 1932-2143.
- [75] L. Yang, I. E. Grossmann, Water Targeting Models for Simultaneous Flowsheet Optimization, *Industrial & Engineering Chemistry Research* 52 (9) (2013) 3209–3224, ISSN 0888-5885.
- [76] J. P. Teles, P. M. Castro, A. Q. Novais, MILP-based initialization strategies for the optimal design of water-using networks, *Chemical Engineering Science* 64 (17) (2009) 3736–3752, ISSN 0009-2509.
- [77] P. M. Castro, H. A. Matos, A. Q. Novais, An efficient heuristic procedure for the optimal design of wastewater treatment systems, *Resources, Conservation and Recycling* 50 (2) (2007) 158–185, ISSN 0921-3449.
- [78] L. Yiqing, M. Tingbi, L. Sucai, Y. Xigang, Studies on the effect of non-isothermal mixing on water-using network’s energy performance, *Computers & Chemical Engineering* 36 (2012) 140–148, ISSN 0098-1354.
- [79] J. George, G. C. Sahu, S. Bandyopadhyay, Heat Integration in Process Water Networks, *Industrial & Engineering Chemistry Research* 50 (7) (2011) 3695–3704, ISSN 0888-5885.
- [80] M. Bogataj, M. J. Bagajewicz, Synthesis of non-isothermal heat integrated water networks in chemical processes, *Computers & Chemical Engineering* 32 (12) (2008) 3130–3142, ISSN

- 0098-1354.
- [81] T. Gundersen, L. Naess, The synthesis of cost optimal heat exchanger networks: An industrial review of the state of the art, *Computers & Chemical Engineering* 12 (6) (1988) 503–530, ISSN 0098-1354.
 - [82] K. C. Furman, N. V. Sahinidis, A Critical Review and Annotated Bibliography for Heat Exchanger Network Synthesis in the 20th Century, *Industrial & Engineering Chemistry Research* 41 (10) (2002) 2335–2370, ISSN 0888-5885.
 - [83] B. Linnhoff, E. Hindmarsh, The pinch design method for heat exchanger networks, *Chemical Engineering Science* 38 (5) (1983) 745–763, ISSN 0009-2509.
 - [84] F. Maréchal, B. Kalitventzeff, Process integration: Selection of the optimal utility system, *Computers & Chemical Engineering* 22, Supplement 1 (1998) S149–S156, ISSN 0098-1354.
 - [85] C. A. Floudas, A. R. Ciric, I. E. Grossmann, Automatic synthesis of optimum heat exchanger network configurations, *AIChE Journal* 32 (2) (1986) 276–290.
 - [86] E. Balas, R. Jeroslow, Canonical Cuts on the Unit Hypercube, *SIAM Journal on Applied Mathematics* 23 (1) (1972) 61–69, ISSN 0036-1399.
 - [87] S. Ahmad, Heat exchanger networks: cost trade-offs in energy and capital., PhD Thesis, University of Manchester, Institute of Science and Technology, UK, 1985.
 - [88] T. Gundersen, I. E. Grossmann, Improved optimization strategies for automated heat exchanger network synthesis through physical insights, *Computers & Chemical Engineering* 14 (9) (1990) 925–944, ISSN 0098-1354.
 - [89] T. Gundersen, S. Duvold, A. Hashemi-Ahmady, An extended vertical MILP model for Heat Exchanger Network Synthesis, *Computers & Chemical Engineering* 20 (Supplement 1) (1996) S97–S102, ISSN 0098-1354.
 - [90] T. F. Yee, I. E. Grossmann, Simultaneous optimization models for heat integration—II. Heat exchanger network synthesis, *Computers & Chemical Engineering* 14 (10) (1990) 1165–1184, ISSN 0098-1354.
 - [91] T. F. Yee, I. E. Grossmann, Z. Kravanja, Simultaneous optimization models for heat integration—I. Area and energy targeting and modeling of multi-stream exchangers, *Computers & Chemical Engineering* 14 (10) (1990) 1151–1164, ISSN 0098-1354.
 - [92] D. Yue, G. Guillén-Gosálbez, F. You, Global optimization of large-scale mixed-integer linear fractional programming problems: A reformulation-linearization method and process scheduling applications, *AIChE Journal* 59 (11) (2013) 4255–4272, ISSN 1547-5905.
 - [93] M. J. Bagajewicz, R. Pham, V. Manousiouthakis, On the state space approach to mass/heat exchanger network design, *Chemical Engineering Science* 53 (14) (1998) 2595–2621, ISSN 0009-2509.
 - [94] B. Leewongtanawit, J.-K. Kim, Synthesis and optimisation of heat-integrated multiple-contaminant water systems, *Chemical Engineering and Processing: Process Intensification* 47 (4) (2008) 670–694, ISSN 0255-2701.
 - [95] W. C. J. Kuo, R. Smith, Design of Water-Using Systems Involving Regeneration, *Process Safety and Environmental Protection* 76 (2) (1998) 94–114, ISSN 0957-5820.
 - [96] W. C. J. Kuo, R. Smith, Designing for the Interactions Between Water-Use and Effluent Treatment, *Chemical Engineering Research and Design* 76 (3) (1998) 287–301, ISSN 0263-8762.
 - [97] J. Bai, X. Feng, C. Deng, Graphically Based Optimization of Single-Contaminant Regeneration Reuse Water Systems, *Chemical Engineering Research and Design* 85 (8) (2007) 1178–1187, ISSN 0263-8762.

-
- [98] X. Feng, J. Bai, X. Zheng, On the use of graphical method to determine the targets of single-contaminant regeneration recycling water systems, *Chemical Engineering Science* 62 (2007) 2127–2138.
- [99] N. Hallale, A new graphical targeting method for water minimisation, *Advances in Environmental Research* 6 (3) (2002) 377–390, ISSN 1093-0191.
- [100] I. Quesada, I. E. Grossmann, Global optimization of bilinear process networks with multicomponent flows, *Computers & Chemical Engineering* 19 (12) (1995) 1219–1242, ISSN 0098-1354.
- [101] G. P. McCormick, Computability of global solutions to factorable nonconvex programs: Part I — Convex underestimating problems, *Mathematical Programming* 10 (1) (1976) 147–175, ISSN 0025-5610, 1436-4646.
- [102] C. A. Floudas, A. Aggarwal, A. R. Ciric, Global optimum search for nonconvex NLP and MINLP problems, *Computers & Chemical Engineering* 13 (10) (1989) 1117–1132, ISSN 0098-1354.
- [103] C. A. Floudas, V. Visweswaran, A global optimization algorithm (GOP) for certain classes of nonconvex NLPs—I. Theory, *Computers & Chemical Engineering* 14 (12) (1990) 1397–1417, ISSN 0098-1354.
- [104] E. Ahmetović, I. E. Grossmann, Global superstructure optimization for the design of integrated process water networks, *AIChE Journal* 57 (2) (2011) 434–457, ISSN 1547-5905.
- [105] D. C. Faria, M. J. Bagajewicz, Global Optimization of Water Management Problems Using Linear Relaxation and Bound Contraction Methods, *Industrial & Engineering Chemistry Research* 50 (7) (2011) 3738–3753, ISSN 0888-5885.
- [106] D. C. Faria, M. J. Bagajewicz, A new approach for global optimization of a class of MINLP problems with applications to water management and pooling problems, *AIChE Journal* 58 (8) (2012) 2320–2335, ISSN 1547-5905.
- [107] H.-G. Dong, C.-Y. Lin, C.-T. Chang, Simultaneous optimization approach for integrated water-allocation and heat-exchange networks, *Chemical Engineering Science - CHEM ENG SCI* 63 (14) (2008) 3664–3678, ISSN 0009-2509.
- [108] C.-L. Chen, H.-L. Liao, X.-P. Jia, Y.-J. Ciou, J.-Y. Lee, Synthesis of heat-integrated water-using networks in process plants, *Journal of the Taiwan Institute of Chemical Engineers* 41 (4) (2010) 512–521, ISSN 1876-1070.
- [109] L. E. Savulescu, M. Sorin, R. Smith, Direct and indirect heat transfer in water network systems, *Applied Thermal Engineering* 22 (8) (2002) 981–988, ISSN 1359-4311.
- [110] J.-K. K. Boondarik Leewongwanawit, Design and optimisation of combined water and energy systems .
- [111] M. Sorin, L. E. Savulescu, On Minimization of the Number of Heat Exchangers in Water Networks, *Heat Transfer Engineering* 25 (5) (2004) 30–38, ISSN 0145-7632.
- [112] M. Bogataj, M. J. Bagajewicz, Design of non-isothermal process water networks, in: V. P. a. P. e. Agachi (Ed.), *Computer Aided Chemical Engineering*, vol. 24 of *17th European Symposium on Computer Aided Process Engineering*, Elsevier, 377–382, URL <http://www.sciencedirect.com/science/article/pii/S1570794607800861>, 2007.
- [113] Z.-W. Liao, J. WU, B. JIANG, J. WANG, Y. YANG, Design Energy Efficient Water Utilization Systems Allowing Operation Split*, *Chinese Journal of Chemical Engineering* 16 (1) (2008) 16–20, ISSN 1004-9541.
- [114] W. Xiao, R.-j. Zhou, H.-G. Dong, N. Meng, C.-Y. Lin, V. S. K. Adi, Simultaneous optimal integration of water utilization and heat exchange networks using holistic mathematical programming, *Korean Journal of Chemical Engineering* 26 (5) (2009) 1161–1174, ISSN 0256-1115, 1975-7220.

-
- [115] J. Kim, J. Kim, J. Kim, C. Yoo, I. Moon, A simultaneous optimization approach for the design of wastewater and heat exchange networks based on cost estimation, *Journal of Cleaner Production* 17 (2) (2009) 162–171, ISSN 0959-6526.
- [116] X. Feng, Y. Li, R. Shen, A new approach to design energy efficient water allocation networks, *Applied Thermal Engineering* 29 (11–12) (2009) 2302–2307, ISSN 1359-4311.
- [117] Z.-W. Liao, G. Rong, J. Wang, Y. Yang, Systematic Optimization of Heat-Integrated Water Allocation Networks, *Industrial & Engineering Chemistry Research* 50 (11) (2011) 6713–6727, ISSN 0888-5885.
- [118] S. Bandyopadhyay, G. C. Sahu, Energy targeting in heat integrated water networks with isothermal mixing, in: E. N. Pistikopoulos, M. C. Georgiadis, A. C. Kokossis (Eds.), *Computer Aided Chemical Engineering*, vol. 29 of 21 *European Symposium on Computer Aided Process Engineering*, Elsevier, 1989–1993, doi: \bibinfo{doi}{10.1016/B978-0-444-54298-4.50176-8}, URL <http://www.sciencedirect.com/science/article/pii/B9780444542984501768>, 2011.
- [119] R.-J. Zhou, L.-J. Li, H.-G. Dong, I. E. Grossmann, Synthesis of Interplant Water-Allocation and Heat-Exchange Networks. Part 2: Integrations between Fixed Flow Rate and Fixed Contaminant-Load Processes, *Industrial & Engineering Chemistry Research* 51 (45) (2012) 14793–14805, ISSN 0888-5885.
- [120] Y. L. Tan, D. K. S. Ng, M. M. El-Halwagi, Y. Samyudia, D. C. Y. Foo, Synthesis of Heat-Integrated Resource Conservation Networks, in: I. A. Karimi, R. Srinivasan (Eds.), *Computer Aided Chemical Engineering*, vol. 31 of 11 *International Symposium on Process Systems Engineering*, Elsevier, 985–989, doi: \bibinfo{doi}{10.1016/B978-0-444-59506-5.50028-6}, URL <http://www.sciencedirect.com/science/article/pii/B9780444595065500286>, 2012.
- [121] E. Ahmetović, Z. Kravanja, Solution strategies for the synthesis of heat-integrated process water networks, *Chemical Engineering Transactions* 29 (2012) 1015–1020, ISSN 1974-9791.
- [122] M. G. Rojas-Torres, J. M. Ponce-Ortega, M. Serna-González, F. Nápoles-Rivera, M. M. El-Halwagi, Synthesis of Water Networks Involving Temperature-Based Property Operators and Thermal Effects, *Industrial & Engineering Chemistry Research* 52 (1) (2013) 442–461, ISSN 0888-5885.
- [123] D. Li, Design of heat integrated water networks with multiple contaminants considering non-isothermal mixing, *Chemical Industry Eng. Process* .
- [124] N. Ibrić, E. Ahmetović, Z. Kravanja, A Two-Step Solution Strategy for the Synthesis of Pinched and Threshold Heat-Integrated Process Water Networks, *Chemical Engineering Transactions* 35 (2013) 43–48, ISSN 1974-9791.
- [125] I. M. L. Chew, D. C. Y. Foo, J.-C. Bonhivers, P. Stuart, A. Alva-Argaez, L. E. Savulescu, A model-based approach for simultaneous water and energy reduction in a pulp and paper mill, *Applied Thermal Engineering* 51 (1–2) (2013) 393–400, ISSN 1359-4311.
- [126] E. Ahmetović, Z. Kravanja, Simultaneous synthesis of process water and heat exchanger networks, *Energy* 57 (2013) 236–250, ISSN 0360-5442.
- [127] Y. L. Tan, D. K. S. Ng, D. C. Y. Foo, M. M. El-Halwagi, Y. Samyudia, Heat integrated resource conservation networks without mixing prior to heat exchanger networks, *Journal of Cleaner Production* 71 (2014) 128–138, ISSN 0959-6526.
- [128] A. Jiménez-Gutiérrez, J. Lona-Ramírez, J. M. Ponce-Ortega, M. El-Halwagi, An MINLP model for the simultaneous integration of energy, mass and properties in water networks, *Computers & Chemical Engineering* 71 (2014) 52–66, ISSN 0098-1354.
- [129] N. Ibrić, E. Ahmetović, Z. Kravanja, Two-step mathematical programming synthesis of pinched and threshold heat-integrated water networks, *Journal of Cleaner Production* 77 (2014) 116–139,

- ISSN 0959-6526.
- [130] N. Ibrić, E. Ahmetović, Z. Kravanja, Synthesis of Water, Wastewater Treatment, and Heat-Exchanger Networks, in: J. J. Klemeš, P. S. Varbanov, P. Y. Liew (Eds.), *Computer Aided Chemical Engineering*, vol. 33 of 24 *European Symposium on Computer Aided Process Engineering*, Elsevier, 1843–1848, doi: \bibinfo{doi}{10.1016/B978-0-444-63455-9.50142-2}, URL <http://www.sciencedirect.com/science/article/pii/B978044463455901422>, 2014.
 - [131] N. Ibrić, E. Ahmetović, Z. Kravanja, Simultaneous optimization of water and energy within integrated water networks, *Applied Thermal Engineering* 70 (2) (2014) 1097–1122, ISSN 1359-4311.
 - [132] Z. Chen, Y. Hou, X. Li, J. Wang, Simultaneous optimization of water and heat exchange networks, *Korean Journal of Chemical Engineering* 31 (4) (2014) 558–567, ISSN 0256-1115, 1975-7220.
 - [133] E. Ahmetović, Z. Kravanja, Simultaneous optimization of heat-integrated water networks involving process-to-process streams for heat integration, *Applied Thermal Engineering* 62 (1) (2014) 302–317, ISSN 1359-4311.
 - [134] E. Ahmetović, N. Ibrić, Z. Kravanja, Optimal design for heat-integrated water-using and wastewater treatment networks, *Applied Energy* 135 (2014) 791–808, ISSN 0306-2619.
 - [135] L. Zhou, Z. Liao, J. Wang, B. Jiang, Y. Yang, H. Yu, Simultaneous Optimization of Heat-Integrated Water Allocation Networks Using the Mathematical Model with Equilibrium Constraints Strategy, *Industrial & Engineering Chemistry Research* 54 (13) (2015) 3355–3366, ISSN 0888-5885.
 - [136] Z. Liu, Y. Luo, X. Yuan, Synthesis of heat-integrated water allocation network considering non-isothermal mixing, *Huagong Xuebao/CIESC Journal* 65 (2014) 285–291.
 - [137] Z. Liu, Y. Luo, X. Yuan, Simultaneous integration of water and energy in heat-integrated water allocation networks, *AIChE Journal* 61 (7) (2015) 2202–2214, ISSN 1547-5905.
 - [138] S. Ghazouani, A. Zoughaib, S. Pelloux-Prayer, Simultaneous heat integrated resource allocation network targeting for total annual cost considering non-isothermal mixing, *Chemical Engineering Science* 134 (2015) 385–398, ISSN 0009-2509.
 - [139] F. Yan, H. Wu, W. Li, J. Zhang, Simultaneous optimization of heat-integrated water networks by a nonlinear program, *Chemical Engineering Science* 140 (Supplement C) (2016) 76–89, ISSN 0009-2509.
 - [140] F. Torkfar, A. Avami, A simultaneous methodology for the optimal design of integrated water and energy networks considering pressure drops in process industries, *Process Safety and Environmental Protection* ISSN 0957-5820.
 - [141] A. Jagannath, A. Almansoori, Sequential synthesis of heat integrated water networks: A new approach and its application to small and medium sized examples, *Computers & Chemical Engineering* 90 (2016) 44–61, ISSN 0098-1354.
 - [142] N. Ibrić, E. Ahmetović, Z. Kravanja, Mathematical programming synthesis of non-isothermal water networks by using a compact/reduced superstructure and an MINLP model, *Clean Technologies and Environmental Policy* (2016) 1–35 ISSN 1618-954X, 1618-9558.
 - [143] X. Hong, Z. Liao, B. Jiang, J. Wang, Y. Yang, Simultaneous optimization of heat-integrated water allocation networks, *Applied Energy* 169 (2016) 395–407, ISSN 0306-2619.
 - [144] S. Ghazouani, A. Zoughaib, S. L. Bourdieu, An MILP model for simultaneous mass allocation and heat exchange networks design, *Chemical Engineering Science* 158 (Supplement C) (2017) 411–428, ISSN 0009-2509.
 - [145] X. Hong, Z. Liao, B. Jiang, J. Wang, Y. Yang, Targeting of heat integrated water allocation networks by one-step MILP formulation, *Applied Energy* 197 (Supplement C) (2017) 254–269,

ISSN 0306-2619.

- [146] X. Hong, Z. Liao, J. Sun, B. Jiang, J. Wang, Y. Yang, Energy and water management for industrial large-scale water networks: a systematic simultaneous optimization approach, *ACS Sustainable Chemistry & Engineering* .
- [147] L. Liu, H. Song, L. Zhang, J. Du, Heat-integrated water allocation network synthesis for industrial parks with sequential and simultaneous design, *Computers & Chemical Engineering* 108 (Supplement C) (2018) 408–424, ISSN 0098-1354.
- [148] A. M. Geoffrion, Generalized Benders decomposition, *Journal of Optimization Theory and Applications* 10 (4) (1972) 237–260, ISSN 0022-3239, 1573-2878.
- [149] I. E. Grossmann, J. Viswanathan, A. Vecchietti, R. Raman, E. Kalvelagen, Gams/dicopt: a discrete continuous optimization package .
- [150] N. V. Sahinidis, BARON 17.8.9: Global Optimization of Mixed-Integer Nonlinear Programs, User’s Manual, URL <http://www.minlp.com/downloads/docs/baron%20manual.pdf>, 2017.
- [151] M. Tawarmalani, N. V. Sahinidis, A polyhedral branch-and-cut approach to global optimization, *Mathematical Programming* 103 (2) (2005) 225–249, ISSN 0025-5610, 1436-4646.
- [152] Y. Lin, L. Schrage, The Global Solver in the LINDO API, *Optimization Methods Software* 24 (4-5) (2009) 657–668, ISSN 1055-6788.
- [153] M. A. Duran, I. E. Grossmann, An outer-approximation algorithm for a class of mixed-integer nonlinear programs, *Mathematical Programming* 36 (3) (1986) 307–339, ISSN 0025-5610, 1436-4646.
- [154] W. Xiao, H. Dong, X. Li, P. Yao, X. Luo, R. Wilfried, Synthesis of Large-scale Multistream Heat Exchanger Networks Based on Stream Pseudo Temperature, *Chinese Journal of Chemical Engineering* 14 (5) (2006) 574–583, ISSN 1004-9541.
- [155] B. T. Baumrucker, J. G. Renfro, L. T. Biegler, MPEC problem formulations and solution strategies with chemical engineering applications, *Computers & Chemical Engineering* 32 (12) (2008) 2903–2913, ISSN 0098-1354.
- [156] V. Pham, C. Laird, M. El-Halwagi, Convex Hull Discretization Approach to the Global Optimization of Pooling Problems, *Industrial & Engineering Chemistry Research* 48 (4) (2009) 1973–1979, ISSN 0888-5885.
- [157] K. Papalexandri, E. Pistikopoulos, A. Floudas, Mass exchange networks for waste minimization: A simultaneous approach, *Chemical Engineering Research and Design* 72 (A3) (1994) 279–294, ISSN 0263-8762.
- [158] Y. Luo, Z. Liu, S. Luo, X. Yuan, Thermodynamic analysis of non-isothermal mixing’s influence on the energy target of water-using networks, *Computers & Chemical Engineering* 61 (2014) 1–8, ISSN 0098-1354.
- [159] J. Martinez-Patiño, L. Serra, V. Verda, M. Picón-Núñez, C. Rubio-Maya, Thermodynamic Analysis of Simultaneous Heat and Mass Transfer Systems, *Journal of Energy Resources Technology* 138 (6) (2016) 062006–062006, ISSN 0195-0738.
- [160] P. H. Gleick, Water and Energy, *Annual Review of Energy and the Environment* 19 (1) (1994) 267–299.
- [161] D. J. Garcia, F. You, The water-energy-food nexus and process systems engineering: A new focus, *Computers & Chemical Engineering* 91 (2016) 49–67, ISSN 0098-1354.
- [162] E. Martinez-Hernandez, S. Samsatli, Biorefineries and the food, energy, water nexus—towards a whole systems approach to design and planning, *Current Opinion in Chemical Engineering* 18 (Supplement C) (2017) 16–22, ISSN 2211-3398.

- [163] M. Lee, A. A. Keller, P.-C. Chiang, W. Den, H. Wang, C.-H. Hou, J. Wu, X. Wang, J. Yan, Water-energy nexus for urban water systems: A comparative review on energy intensity and environmental impacts in relation to global water risks, *Applied Energy* 205 (2017) 589–601, ISSN 0306-2619.
- [164] T. R. Albrecht, A. Crootof, C. A. Scott, The Water-Energy-Food Nexus: A systematic review of methods for nexus assessment, *Environmental Research Letters* 13 (4) (2018) 043002, ISSN 1748-9326.
- [165] J. Dai, S. Wu, G. Han, J. Weinberg, X. Xie, X. Wu, X. Song, B. Jia, W. Xue, Q. Yang, Water-energy nexus: A review of methods and tools for macro-assessment, *Applied Energy* 210 (2018) 393–408, ISSN 0306-2619.
- [166] A. Inselberg, The plane with parallel coordinates, *The Visual Computer* 1 (2) (1985) 69–91, ISSN 0178-2789, 1432-2315.
- [167] T. Mao, Y. Luo, X. Yuan, Design method of heat integrated water networks considering non-isothermal mixing, *Huagong Xuebao/CIESC Journal* 61 (2) (2010) 369–377.
- [168] B. Linnhoff, S. Ahmad, Cost optimum heat exchanger networks—1. Minimum energy and capital using simple models for capital cost, *Computers & Chemical Engineering* 14 (7) (1990) 729–750, ISSN 0098-1354.
- [169] IBM ILOG CPLEX V12.2: User’s manual for CPLEX, Tech. Rep., IBM Corporation, 2010.
- [170] P. E. Gill, W. Murray, M. A. Saunders, User’s Guide for SNOPT Version 7: Software for Large-Scale Nonlinear Programming, Tech. Rep., 2008.
- [171] L. E. Savulescu, A. Alva-Argaez, Direct heat transfer considerations for improving energy efficiency in pulp and paper Kraft mills, *Energy* 33 (10) (2008) 1562–1571, ISSN 0360-5442.
- [172] J. J. J. Chen, Comments on improvements on a replacement for the logarithmic mean, *Chemical Engineering Science* 42 (10) (1987) 2488–2489, ISSN 0009-2509.
- [173] R. Fourer, D. M. Gay, B. W. Kernighan, *AMPL: A Modeling Language for Mathematical Programming*, Cengage Learning; 2 edition, ISBN 0-534-38809-4, 2003.

PART

II

MEDIUM-TEMPERATURE HEAT RECOVERY

Waste heat accounts for up to 70% of input energy in industrial processes which enunciates the importance of energy recovery measures to improve efficiency and reduce excessive energy consumption. A portion of this energy can be recovered within the process, while the rest is rejected to the environment as *unavoidable* [1] waste, thus, providing a large opportunity for ORCs capable of producing electricity from heat at medium to low temperatures. Although these cycles are often regarded as one of the best waste heat recovery measures, industrial applications are still limited due to the lack of comprehensive methodologies for their integration with existing processes. As such, a novel and comprehensive superstructure optimization methodology for ORC integration is proposed, including architectural features, such as turbine-bleeding, reheating, and transcritical cycles. Additional developments include a novel dynamic linearization technique for supercritical and near-critical streams and the calculation of heat transfer coefficients. The optimization problem is solved using a bi-level approach, including fluid selection, operating condition determination, and equipment sizing, and is applied to a literature case study. The results exhibit that interactions between these elements are complex and therefore underline the necessity of such methods to explore the optimal integration of ORCs with industrial processes.

The full content of this part is published in: *Kermani, M., Wallerand, A.S., Kantor, I.D., Maréchal, F., 2018. Generic superstructure synthesis of organic Rankine cycles for waste heat recovery in industrial processes. Applied Energy 212, 1203–1225. <https://doi.org/10.1016/j.apenergy.2017.12.094>*

Keywords: MILP, superstructure optimization, piece-wise linear envelope, process integration, combined heat and power, supercritical Rankine cycle, genetic algorithm, mathematical programming, linearization.

Acknowledgements: This research project is financially supported by the Swiss Innovation Agency Innosuisse and is part of the Swiss Competence Center for Energy Research SCCER EIP.

CHAPTER 4

Survey of methodologies in organic Rankine cycle modeling and optimization

Overview

This chapter provides a broad introduction into different ORC architectures and the effects of working fluids on the performance of the cycle (section 4.2). In addition a review of the literature with the focus on mathematical approaches in ORC integration in industrial processes is presented.

4.1 Introduction

Industrial processes often generate large amounts of waste heat which is evacuated by various media, such as air or cooling water. This evacuation of heat can reach 70% of the input energy in some industries [2], encouraging industries to evaluate heat recovery and process integration to mitigate associated cost and emissions [3]. Several researchers have focused on defining waste heat and developing methodologies to estimate the recovery potential from processes [1] and the combination of processes and excess heat of utility systems [4]. Guidance in this process commences with the definition and quantification of waste heat, followed by exploration of options for greater efficiency and system integration with a final step to identify appropriate technologies for waste heat recovery (WHR) technology. Bendig et al. [1] clearly dichotomized *avoidable* and *unavoidable* waste heat according to thermodynamic principles. The former can be avoided through better system design by improving energy efficiency, energy integration, and process integration; therefore, must not be used in WHR applications since this would create a dependency on inefficient processing. The latter is defined as the total exergy destruction after implementing all possible efficiency, integration and recovery measures. There are many technologies available for waste heat recovery and the choice is typically influenced by the temperature level of the waste heat. They include different types of heat exchangers for internal heat recovery, heat pumping, and organic Rankine cycles (ORCs). Several authors have proposed methodologies for optimal design and targeting of the combined integration of these technologies [5, 4, 6]. In particular, Holiastos and Manousiouthakis [5] presented a mathematical formulation for simultaneous integration of HENs with heat pumps and heat engines to minimize utility costs. Although they did not consider the investment cost of utilities, their methodology allows for calculation of utility targets without knowing the network design *a priori*. This can provide insights into the correct placement of these technologies before detailed network design. High temperature levels of waste heat (e.g., $> 650^{\circ}\text{C}$) [2] encourage application of steam cycles; however, at low temperatures (e.g., $< 370^{\circ}\text{C}$) [7] other options prevail. ORCs, in particular, can be utilized to produce electricity, reduce the cooling demands

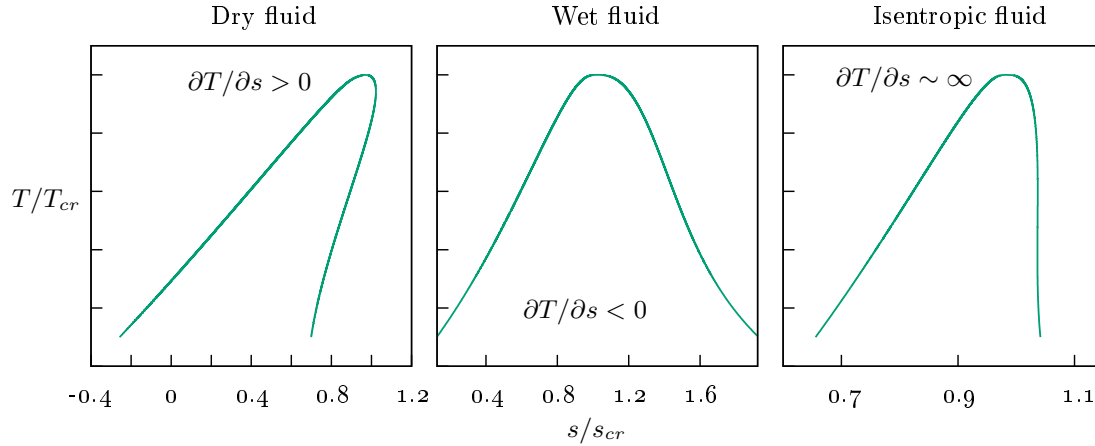


FIGURE 4.1— Different types of working fluids

and still provide heat for low temperature applications, such as district heating. ORCs are a type of Rankine cycle which use an organic fluid with high molecular weight instead of water as the working fluid. They have many advantages, such as long lifetimes, low operating cost and utilization of waste heat at a variety of temperatures [7]. ORCs are a mature technology in the domain of waste heat recovery, biorefineries and geothermal heat recovery with novel applications in other domains [8, 2] (Table 4.1). The main difference between water and other working fluids in Rankine cycles lies in their liquid-vapor characteristics. Steam cycles imply superheating of steam to high temperatures (e.g., 600°C) to avoid two fluid phases at the turbine outlet. Many organic fluids will become chemically unstable at these temperatures; thus, ORCs are typically applied below these temperatures. In addition, the difference between entropies of water in liquid and vapor states is large which results in higher irreversibility and hence higher exergy losses. Another major difference is that the steam cycle condenser normally operates at sub-atmospheric pressure to increase efficiency which necessitates use of a deaerator to remove the absorbed non-condensable gases. This can be avoided in ORCs by selecting a suitable working fluid with high pressure for low condensation temperature and hence reducing the maintenance and system costs [8]. Organic fluids can be categorized into three types depending on the slope of the saturated vapor curve on a temperature-entropy diagram as shown in Figure 4.1. For ORC applications, isentropic fluids are more favorable since they do not necessarily require superheating (required by wet fluids like water) and also have lower degree of superheating at the turbine outlet.

TABLE 4.1—ORC applications

Category	Applications (Related reviews)
Biomass	Combustion or gasification of biomass or biogas for combined heat and power (CHP) production [9]
Solar	Concentrated solar power, solar water desalination with reverse osmosis, hybrid solar/gas driven micro CHP, salt gradient solar pond. [9, 10]
Geothermal	Heat recovery from geothermal heat sources for power production and perhaps district heating. [10, 2]
Ocean thermal	Converting the captured solar radiation in the upper ocean water layers into electric power. [2, 11]
WHR	A wide category including recovery of any type of waste heat from any industrial processes. [9, 2]
Combined cycles	Bottoming with internal combustion engine, gas turbine/microturbine, combining ORC with vapor recompression or heat pumps for cooling, and cascaded applications, trigeneration plants with SOFC-ORC [2, 12, 13, 14]

Knowing the waste heat recovery potential, optimal integration of ORCs with industrial processes is still a challenging task. The major difficulties lay in the optimal selection of ORC architecture (e.g., transcritical, reheating cycles), its operating conditions (pressure and temperature levels), and its working fluid [15]. To this end, the main focus of this part is WHR in industrial processes using ORCs. Section 4.2 provides a broad introduction into different ORC architectures and the effects of working fluids on the performance of the cycle. In addition a review of the literature with the focus on mathematical approaches in ORC integration in industrial processes is presented.

4.2 State of the art

Numerous studies have been conducted on different aspects of ORCs and hence there exist many reviews in this field. Table 4.2 provides a summary of main topics covered by these reviews, while Table 4.3 gives a brief description on each published review.

TABLE 4.2—Main focus of the published reviews on ORC

Reviews	ORC applications	Working fluid selection	Expander selection	Pumps	Transcritical cycle	Exhaust heat recovery	ORC architectures	Internal combustion engine	Modeling	Optimization	Control [16]	WHR in processes	Market analysis
Quoilin and Lemort [9]	X	X	X										X
Schuster et al. [10]	X	X											
Chen et al. [17]		X			X								
Tchanche et al. [2]	X											X	
Wang et al. [12]		X	X			X							
Vélez et al. [13]	X	X										X	X
Bao and Zhao [18]		X	X										
Quoilin et al. [19]	X	X	X	X								X	
Sprouse III and Depcik [14]								X					
F. Tchanche et al. [11]	X		X		X		X					X	X
Ziviani et al. [20]		X	X						X				
Lecompte et al. [21]					X		X						
Linke et al. [22]		X							X	X	X	X	
Rahbar et al. [8]	X	X	X							X			
Chintala et al. [23]		X	X				X						
Tocci et al. [24]		X	X										X

Items in **bold** are the main focus of the corresponding review

It was observed that the main focus of the literature is on ORC applications, working fluid and expander selection with few reviews on transcritical cycles. Linke et al. [22] highlighted the importance of computer-aided tools in design and optimization of ORCs and stated that although recent efforts have contributed to this field, a gap remains for systematic methodologies in ORC applications compared to vast benefits they have in other domains. This section provides a brief literature review on ORC architecture, effects of working fluid on the performance of ORCs and optimization-based methodology with the focus on WHR in industrial processes. The readers are encouraged to refer to the references of Table 4.2 for other subjects related to ORC. A more detailed description on these reviews is also provided in supplementary materials.

TABLE 4.3—Available review papers on topics related to ORCs

Reviews	Remarks
Quoilin and Lemort [9]	An overview of different applications of small and middle-scale ORC technologies are provided together with a list of industrial manufacturers. Some general guidelines have been pointed out in selecting the best working fluid together with a literature survey of related studies. The most common fluids for current applications are considered to be R134a, R245fa, n-pentane and silicon oils (D4). Different types of expanders and their range of applications are also briefly discussed with the focus on positive displacement expanders in small-scale applications.
Schuster et al. [10]	Energetic and economic assessments of novel ORC applications, such as solar desalination with reverse osmosis, micro-CHP, and WHR from digestion plants are carried out.
Chen et al. [17]	An overview of research on two types of ORC, transcritical and subcritical, is presented.
Tchanche et al. [2]	Different applications of ORC have been described with their level of maturity. They have highlighted that research into waste heat recovery from thermal devices and industrial processes will continue to grow rapidly. Ocean thermal energy conversion with ORC is also among the interesting applications. They have proposed a classification of different working fluids for different temperature ranges based on the working fluid's critical temperature. Potential fluids for ORC applications are categorized into: Hydrocarbons, hydro-fluorocarbons, hydro-chloro-fluorocarbons, chloro-fluorocarbons, perfluorocarbons, siloxanes, alcohols, aldehydes, ethers, hydro-fluoro-ethers, amines, and fluids mixtures (zeotropic and azeotropic).
Wang et al. [12]	An overview of exhaust heat recovery by various technologies and in particular by ORC for on-road vehicles is presented. Different system configurations are analyzed and the effects of the choice of expander and working fluid are highlighted.
Vélez et al. [13]	Technical and economic features of ORCs are analyzed with a list of ORC manufacturers. Different applications of ORC and their market values are reported. Working fluid selection is discussed and highlighted as one of the main open research topics in the literature.
Bao and Zhao [18]	A review of research on selection of working fluids and expanders is provided. Effects of working fluid on the performance of ORCs together with their thermodynamic properties are investigated. A comprehensive list of pure and working fluids and mixtures are provided. Expanders can be categorized into turbines, scroll expander, screw expander, reciprocating piston expander, and rotary vane expander. Current gaps in ORC research are highlighted and several directions for future research are proposed: 1- methodologies for economic, environmental and efficient working fluid selection; 2- experimental research on expanders; and 3 - studies on high temperature applications (200–350°C).
Quoilin et al. [19]	They have provided a review of different applications of ORCs with experimental works on expanders and pumps. Technical challenges related to working fluid selection and expander selection are highlighted.
Sprouse III and Depcik [14]	They have provided a review on exhaust waste heat recovery in internal combustion engines using ORC with the focus on selection of expanders and working fluids as the two major influential factors on the performance of ORCs.
F. Tchanche et al. [11]	Several ORC architectures are discussed including basic, superheated, transcritical, regenerative, bleeding, and reheating ORCs. Different types of heat sources and their potentials for heat recovery are introduced.

TABLE 4.3—Available review papers on topics related to ORCs

Reviews	Remarks
Ziviani et al. [20]	They have provided a review of the advances and challenges in low-grade heat recovery using various technologies including ORCs. They outlined some issues on ORC modeling and proposed guidelines for developing modeling and simulation tools. Main issues in ORC system modeling are: thermodynamic property calculations, heat transfer rate in evaporator and condenser and modeling of expanders.
Lecompte et al. [21]	An overview of different ORC architectures and their challenges are discussed. In addition to F. Tchanche et al. [11] they considered multiple-evaporation ORCs, tri-lateral cycles, vapor injector, and cascaded cycles. They highlighted the fact that several of these novel architectures might be promising alternatives to the basic ORC when considering their thermodynamic effectiveness, however their economic feasibility is still an issue and that there are not many experimental works related to their performance evaluations.
Linke et al. [22]	They have presented a comprehensive overview of ORC cycles with the focus on computer-aided methods for working fluid (selection or design of novel fluid, i.e., computer aided molecular design methods) and design, optimization, control, and integration of ORC cycles. The scope is limited to subcritical cycles. Several areas have been distinguished as open research topics.
Rahbar et al. [8]	Thorough overview of ORC applications and criteria for working fluid selection. In addition, different types of expanders with related experimental works are presented.
Chintala et al. [23]	An overview of researches on waste heat recovery using ORC from compression ignition engines including fluid selection, types of expander, evaporator, and condensers.
Imran et al. [25]	A review on the overall contributions in the field of ORC from a bibliometric perspective is presented.

4.2.1 ORC architectures

Several architectures, i.e., configurations of ORC, have been analyzed in the literature. Since this work is proposing a new ORC superstructure encompassing several architectures, it is necessary to give a brief description of each type:

Basic cycles The simplest configuration (Figure 4.2-a) which consists of four parts, i.e., condenser, pump, evaporator, and expander.

Superheated cycles Superheating the vapor (Figure 4.2-b), which is mainly for wet fluids, ensures that the outlet of the expander does not end in the two-phase region to avoid corrosion of turbine blades. Dry fluids may also enter the two-phase region in specific cases where the curvature of the liquid-vapor envelope dictates and should be avoided [18]. Similarly, Hung et al. [26] argued that for wet and isentropic fluids, increasing the degree of superheating will increase the efficiency.

Regenerative cycles The heat at the outlet of the expander can be recovered by exchanging heat internally, heating the working fluid after pumping (Figure 4.2-c). This decreases the temperature difference in the evaporator which consequentially increases the heat recovery and reduces exergy losses; however, its effectiveness strongly depends on the type of working fluid [27].

Reheating cycles Like steam cycles, it is possible to extract part of the fluid from the expander at intermediate pressure for further reheat and re-injection into the expander (Figure

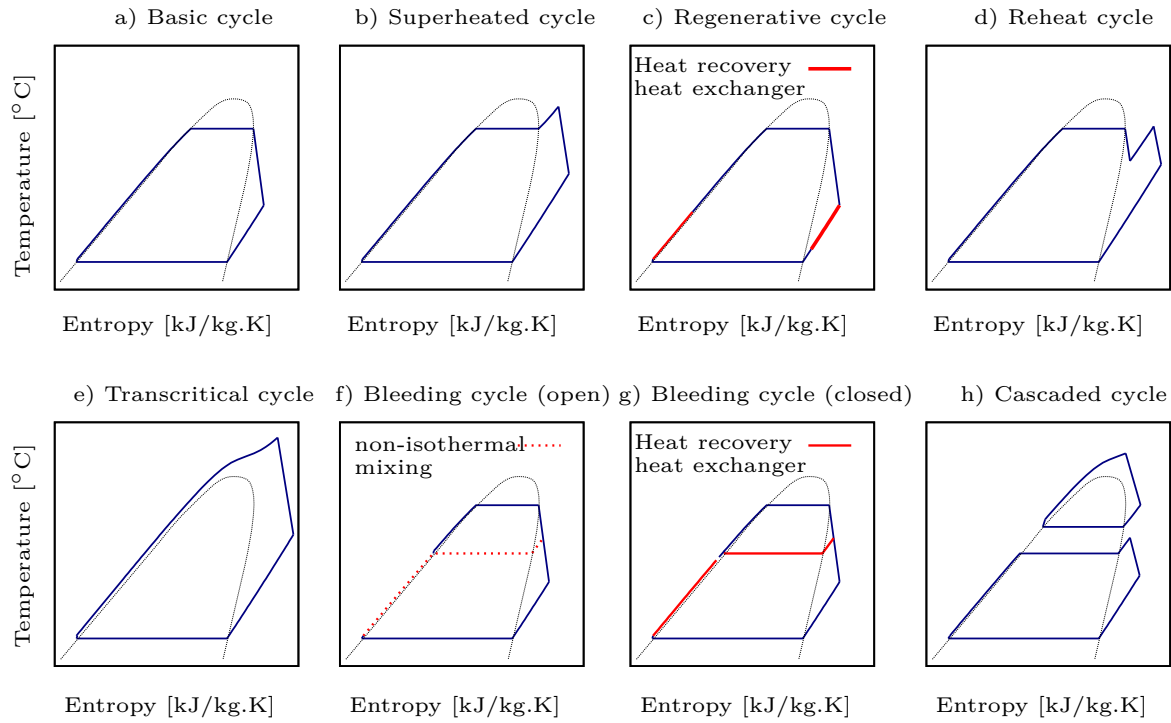


FIGURE 4.2— Different ORC architectures in temperature-entropy diagram

4.2-d). This practice is doubly beneficial, increasing the heat recovery and increasing superheated vapor after the second expansion that can be further used in a regenerator. However, a lower heat transfer coefficient in the vapor phase will require higher heat transfer area [28].

Supercritical/Transcritical cycles (Figure 4.2-e) Karellas and Schuster [29] demonstrated that supercritical conditions do not always result in better thermal efficiencies but better temperature matching between the fluid and the hot source is expected to improve heat recovery. Xu et al. [30] showed that the maximum net power output always occurs for transcritical configurations if the temperature of the waste heat is 25 to 50°C higher than the working fluid critical temperature.

Bleeding cycles Similar to steam cycles, the working fluid can be extracted from the expander at intermediate pressure for heating the condensate either directly (open feed liquid heater, Figure 4.2-f) or indirectly (closed feed liquid heater, Figure 4.2-g). Desai and Bandyopadhyay [7] showed that applications of turbine bleedings were promising when the temperature of the heat source stays high. Meinel et al. [31, 32] showed that turbine-bleeding ORCs exhibited higher thermodynamic and economic performances compared to basic and regenerative architectures and are hence promising alternatives in the ORC domain.

Multi-stage cycles Working fluid can be evaporated or condensed at more than one pressure. Multi-evaporation and condensation cycles are mainly suitable for better temperature matching with heat source(s) and heat sink(s), respectively. This is promising for industrial processes as there are opportunities for several waste heat streams to integrate with the same cycle for which using a single-stage ORC cannot recover the full potential.

Cascaded cycles consist of several ORCs in series (Figure 4.2-h). Li et al. [33] showed that the net power output, thermal efficiency and exergy efficiency of cascaded cycles (using R245a as the working fluid) was higher than basic cycles, though incurred more investment cost due to additional turbines.

It should be highlighted that ORC architectures resemble those of utility systems (i.e., steam cycle superstructure) [34, 35, 36, 37]. Several architectures including bleeding, reheating, and multi-stage cycles are directly inspired by their counterparts in steam cycle superstructures. To the best of authors' knowledge, only a paper by Romeo et al. [38] considers supercritical steam cycle design. Brayton cycles (i.e., gas turbines) have also been included in utility superstructures, which operate and are modeled similarly to ORCs. However, they operate at much higher temperatures and/or pressures than ORCs and are thus less flexible for design in such a way as is considered here for ORCs. Reviews on utility system synthesis (i.e., steam network) can be found in the work of Varbanov et al. [39], Chen and Grossmann [40], and Liew et al. [41].

4.2.2 Fluid selection

The two main factors influencing the performance of ORCs are architecture and choice of working fluid. An appropriate fluid must have suitable physical, chemical, thermodynamic, environmental, and safety properties while also satisfying case-specific and technical requirements. No single organic fluid can satisfy all requirements simultaneously for all applications. Toffolo et al. [42] showed that most optimal subcritical rankine cycles have working fluids with critical temperature slightly (10 to 40°C) below that of the heat source. Xu and Yu [43] similarly argued that critical temperature should be the sole criterion for working fluid selection and recommended a temperature range for the most efficient working fluids based on their critical temperatures $[T_{in}^{cu} - 30, T_{in}^{cu} + 100]$. Stijepovic et al. [44] highlighted that fluids with lower heat of vaporization compared to sensible heat have higher exergy efficiency. In addition, they stated that the heat transfer area of the evaporation depends on critical pressure and the molecular weight of the working fluid. Overall, it can be argued that working fluid selection is among the most heavily-investigated topics in ORC-related research. Two approaches are prominent in the existing literature:

- Set of predefined fluids is selected and ORC performance is optimized with respect to one or many performance indicators [45, 46]. The typical approach in this category is using a GA [47, 48, 49, 50, 51, 52, 53]. This approach, as stated by Linke et al. [22], limits the search space and hence excludes some potential candidates (mainly novel fluids).
- Computer-aided molecular design methodologies which provide tools for designing and determining molecules with appropriate set of physicochemical characteristics [54, 55, 56].

For more information, the reader is encouraged to read the review by Linke et al. [22] on computer-aided methods in fluid selection and other reviews listed in Table 4.2. The focus of this work is not on providing methodologies for fluid selection. As such, a preliminary set of working fluids is proposed for each case and their performances are evaluated using GA. The preliminary set is provided using heuristics based on thermodynamic, physical and environmental criteria. An interactive parallel coordinate visualization tool [57] was developed and used to easily filter the potential candidates. The link to this tool is provided in C.

4.2.3 ORC integration in industrial processes

The importance of integrating heat engines with industrial processes was first investigated by Townsend and Linnhoff [58, 59]. Their analysis showed that placing a heat engine's source and sink either above or below the pinch point yielded operational benefits while placing it across the pinch had no benefit compared to stand-alone operation of the heat engine. Similar conceptual methodologies like Pinch Analysis Technique, have been used by Desai and Bandyopadhyay [7] to investigate the effects of incorporating the combined regenerative-bleeding ORC as a bottoming cogeneration process in industrial processes. They highlighted the effects of integrating the condensation stream of the ORC with the process, showing that for processes with self-sufficient pockets below the pinch, raising the condensation temperature increased the power output.

Selection of the best ORC architecture and its operating conditions is as important as selecting the working fluid. Systematic methodologies are required that can find the best combinations of discrete (i.e., ORC architecture and working fluid) and continuous (i.e., operating conditions) decision variables for optimal ORC integration. The optimization-based approaches can be separated into two main categories: **parametric-based** approaches in which a predefined or a set of limited architectures will be evaluated for different operating conditions either by varying decision variables independently or through the use of GAs; and, **superstructure-based** approaches in which a superstructure of almost all possible architectures are defined *a priori* using mathematical programming techniques and optimization will be carried out to find the best configuration and operating conditions. The more complete superstructures become highly non-linear and non-convex with high computational costs for global optimality. As the result the research has focused at the same time on developing superstructures while proposing solution strategies to handle their complexity. Generally, the solution strategies applied to mathematical programming models can be categorized as *simultaneous vs sequential* and *deterministic vs stochastic* approaches [22]. Simultaneous deterministic approaches are computationally expensive and normally very good initialization procedure should be performed in order to guarantee their optimality. On the other hand, stochastic approaches (most notably GA) are robust to handle varieties of decision variables although to the expense of numerous function evaluations. In ORC optimization, overall, stochastic approaches are used for optimizing the operating conditions while deterministic approaches are needed to select the best architectures.

Colmenares and Seider [60] were the first to formulate an optimization problem for the placement of heat engines relative to the process by proposing an ORC superstructure using NLP which allowed mass exchange between adjacent heat engines (cascaded cycle). More complete superstructures become highly non-convex and require decomposition techniques. Maréchal and Kalitventzeff [15] proposed a three-stage solution strategy which identified the most promising temperature levels to minimize exergy losses followed by fluid selection and finally, minimization of total annualized cost for the system. Toffolo [61] proposed a hybrid evolutionary algorithm for optimal selection of ORC architecture formulated in two stages with a GA at the master level and a sequential quadratic programming model optimizing the maximum net power output as the slave. Several ORC architectures were generated using this method including multi-stage cycles, breeding, regenerative and reheat cycles. Similarly, Bendig et al. [48] developed a two-stage multi-objective optimization methodology using a master-level GA with exergy efficiency and cost as the two objective functions and acting on the decision variables of working fluid selection, cycle architecture (single-stage, double-cascaded,

or transcritical), and its operating conditions. The lower stage was based on the heat cascade formulation of Maréchal and Kalitventzeff [62] and was formulated as a MILP model. More recently, Stijepovic et al. [63] proposed a superstructure of cascaded ORCs using MINLP. The objective function was maximization of net power output by determining the number of cascades, HEN design, working fluid and operating conditions of each cascade. Yu et al. [64] proposed a two-stage methodology for integration of ORCs with industrial processes. The first step was formulated as an NLP model which optimized the ORC architecture (bleeding, regenerative, or superheated cycles) together with its operating conditions by maximizing net profit. The second step performed HEN synthesis by minimizing the number of heat exchangers using the extended transshipment MILP model [65]. Table 4.4 provides an overview of the proposed methodologies for ORC integration. Although the research of methodological approaches for integration of ORCs into industrial processes has received significant effort, several questions remain open. From recent publications, the following observations were made [22, 19]:

- a) Conceptual methods that only rely on graphical and insight-based rules cannot fully evaluate the vast search space for optimal selection of an ORC and its operating conditions. However, the insight from their application can be coupled with mathematical approaches.
- b) Several methods have focused on HEN design and synthesis by integrating ORCs. They, however, lack the optimization of operating conditions and are limited to regenerative single cycles.
- c) There are few superstructures proposed for ORC, and inside those, a limited number of architectures have been considered. There is a gap in superstructure-based approaches that can provide all possible interconnections and architectures. In particular, the transcritical cycle is only addressed by Bendig et al. [48]. As mentioned, the supercritical cold stream of the evaporator has the possibility of better temperature matching with the process waste heat.

The goal of this research is to address the aforementioned gaps by proposing a generic ORC superstructure using mathematical programming techniques and decomposition solution strategy to simultaneously find the optimal ORC architecture and its operating conditions (including the working fluid selection) for heat recovery in the context of waste heat recovery in industrial processes. ■

TABLE 4-4—Summary of proposed methodologies for waste heat recovery in industrial processes using ORC

Articles	Approach	Objective(s)	Superstructure	Formulation	Decision variables	Solution strategy	Features-ORC architectures
<i>Current article</i>	optimization	min. total cost max. net power output	X	MILP	Pressure levels Temperature levels Flow rates Working fluid	Decomposition (2): 1 - GA 2 - MILP solver	fluid selection, turbine bleeding multi-stage cycle, regeneration transcritical cycle
Colmenares and Seider [60] Colmenares and Seider [66]	optimization	min. total cost	X	NLP	Pressure levels Flow rates	1 - Finding T_{pinch} 2 - NLP solver 3 - HEN synthesis	multi-stage cycle, cascaded cycle fluid selection, turbine bleeding
Maréchal and Kalitventzeff [45]	optimization	min. exergy loss min. total cost	X	MILP	Temperature level Flow rates Working fluid	1 - min. exergy loss 2 - Fluid selection 3 - min. total cost	fluid selection, cascaded cycle
Desai and Bandyopadhyay [7]	optimization	max. thermal efficiency	-	-	Temperature levels	Simulation-based EES ¹	regeneration, turbine bleeding
Hipólito-Valencia et al. [67]	HEN synthesis	min. total cost		MINLP	HEN-related	MINLP solver	regeneration
Lira-Barragán et al. [68]	HEN synthesis	min. total cost min. GHG ¹ emissions max. number of jobs		MINLP	HEN-related	MOO ¹ (ϵ -constraint)	
Toffolo [61]	optimization	max. net power out	X	Mathematical	Temperature levels Flow rates	Hybrid: GA-SQP ¹	multi-stage cycle regeneration, turbine bleeding cascaded cycle
Chen et al. [69]	HEN synthesis	min. operating costs max. net power out	X	MINLP	HEN-related	Two stage MINLP: 1 - min. costs 2 - max. electricity	
Song et al. [70]	optimization	max. net power out			Temperature levels Working fluid	Simulation-based	fluid selection, cascaded cycle
Kwak et al. [47]	optimization	min. total cost		Mathematical	Temperature levels Working fluid	GA	fluid selection
Bendig et al. [48]	optimization	max. exergy efficiency min. total cost	X	MINLP	Pressure levels Temperature levels Working fluid	Decomposition (2): 1 - GA 2 - MILP solver	fluid selection, cascaded cycle transcritical cycle
Hipólito-Valencia et al. [71]	HEN synthesis	min. total cost	X	MINLP	HEN-related	MINLP solver	regeneration
Gutiérrez-Arriaga et al. [72]	hybrid	max. profit			Temperature levels Pressure levels Working fluid	Graphical-GA	Fluid selection
Oluleye and Smith [6]	optimization	max. economic potential	X	MILP		MILP solver	fluid selection, multi-stage cycle cascaded cycle
Yu et al. [73]	optimization	min. total cost	X	NLP		NLP solver	fluid selection
Stjepovic et al. [63]	optimization	max. net power out	X	MINLP		MINLP solver	fluid selection, multi-stage cycle cascaded cycle
Yu et al. [64]	optimization	max. net power out min. number of matches	X	NLP- λ -MINLP	Pressure levels Temperature levels Flow rates	MINLP solver	fluid selection, regeneration turbine bleeding

¹ - **EES** Engineering Equation Solver, **MOO** Multi-Objective Optimization, **GHG** Greenhouse Gases, **SQP** Sequential Quadratic Programming

CHAPTER 5

Optimal integration of organic Rankine cycles in industrial processes

Overview

Based on the literature and to address the current research gaps, a generic superstructure is proposed in this chapter which incorporates many ORC architectures and can address supercritical operating conditions via a novel linearization technique. A decomposition solution strategy is proposed in subsection 5.2.5 to find the optimal design and operating conditions of the ORC. The application of the methodology is illustrated using a literature test case in section 5.3. Section 5.4 presents the concluding remarks and provides some highlights for future research direction.

Nomenclature

Abbreviations

GA	genetic algorithm
GCC	grand composite curve
GWP	global warming potential
HEN	heat exchanger network
MILP	mixed integer linear programming
MINLP	mixed integer non-linear programming
NLP	nonlinear programming
ORC	organic Rankine cycle
SIC	specific investment cost
TAC	total annualized cost
WHR	waste heat recovery

Sets

$\mathbf{P}^H (\mathbf{P}^C)$	Set of all the hot (cold) process streams
$\mathbf{U}^H (\mathbf{U}^C)$	Set of all the available hot (cold) utility streams
\mathbf{T}_i^{liq}	Set of all the temperatures in the liquid layer at pressure stage i
\mathbf{T}_i^{vap}	Set of all the temperatures in the vapor layer at pressure stage i
\mathbf{U}^{all}	Set of all the units, i.e., turbines, pumps, evaporators, and condensers
\mathbf{TI}	Set of temperature intervals

Parameters

T_{in}, T_{out}	Inlet and outlet temperature of thermal stream (utility or process) [$^{\circ}\text{C}$]
\dot{Q}	Heat load of process stream [kW]
\dot{q}	Specific heat load of utility stream [kJ/kg]

N_p	Number of pressure stages
$F^{u,min}$	Minimum size of unit u [variable unit]
$F^{u,max}$	Maximum size of unit u [variable unit]
η	Isentropic efficiency of an equipment [-]
C^{hu}	Cost of hot utility hu [USD/kWh]
C^{cu}	Cost of cold utility cu [USD/kWh]
C^{el}	Cost of electricity el [USD/kWh]
$C^{ft(trh)}$	Fixed linearized cost of a main (reheat) turbine [USD]
$C^{pt(trh)}$	Proportional linearized cost of a main (reheat) turbine [USD/kW]
$C^{fp}_{i,j}$	Fixed linearized cost of a pump between pressure stages i and j [USD]
$C^{pp}_{i,j}$	Proportional linearized cost of a pump between pressure stages i and j [USD/kW]
C^{fHEN}	Fixed cost of a heat exchanger [USD]
C^{pHEN}	Proportional cost of a heat exchanger [USD/m ²]
α	Heat transfer coefficient [kW/(m ² K)]
irr	Interest rate [-]
t	Operating time [hr/y]
n_{year}	lifetime [y]
ΔT_{min}	Minimum approach temperature in heat recovery [°C]
ΔT_{LM}^k	Logarithmic mean temperature difference in interval k
T^{tol}	Maximum temperature difference defined for linearization [°C]
T_{boil}	Boiling temperature of working fluid (at 1 bar) [°C]
M_{molar}	Molar mass of working fluid [g/mol]

Independent Variables (outer GA)

κ	Variable in the range [0,1] for calculation of weighted TAC [-]
ζ_i	Variable in the range [0,1] for pressure calculation at stage i ($i < N_p$) [-]
P_{N_p}	Pressure at the lowest stage [bar]
ΔT_i^{sup}	Superheating temperature difference at stage i ($i < N_p$) [°C]
ΔT_i^{rh}	Reheating temperature difference at stage i ($2 < i < N_p$) [°C]
WF	Discrete set of working fluids

Dependent Variables (outer GA)

P_i	Pressure at the stage i ($i < N_p$) [bar]
$\dot{\omega}$	Specific electricity production (turbine) or consumption (pump) [kJ/kg]
T_i^{sat}	Saturation temperature at stage i [°C]
$T^{u,in}$	Inlet temperature of unit u [°C] ($u \in \{t, p, trh\}$)
$T^{u,out}$	Outlet temperature of unit u [°C] ($u \in \{t, p, trh\}$)
$h^{u,in}$	Inlet specific enthalpy of unit u [kJ/kg] ($u \in \{t, p, trh\}$)
$h^{u,out}$	Outlet specific enthalpy of unit u [kJ/kg] ($u \in \{t, p, trh\}$)
$s^{u,in}$	Inlet specific entropy of unit u [kJ/kg.K] ($u \in \{t, p, trh\}$)
$s^{u,out}$	Outlet specific entropy of unit u [kJ/kg.K] ($u \in \{t, p, trh\}$)
$\dot{\omega}$	Specific electricity production/consumption [kW/kg]
W_{net}	Net power output [kW]

Variables (inner MILP)

y	Binary variables denoting the existence of a unit
m	Continuous variables denoting the size of a unit

Superscripts

cap	capital cost
$cond$	condenser
cu	cold utility

<i>el</i>	electricity
<i>evap</i>	evaporator
<i>hu</i>	hot utility
<i>inv</i>	investment
<i>k</i>	temperature interval
<i>liq</i>	liquid state
<i>op</i>	operating
<i>p</i>	pump
<i>rh</i>	reheat state
<i>sat</i>	saturated state
<i>sup</i>	superheated state
<i>t</i>	main turbine
<i>tol</i>	tolerance
<i>trh</i>	reheat turbine
<i>vap</i>	vapor state
<i>u</i>	unit

Subscripts

<i>i,j,k</i>	pressure stages
<i>p</i>	pressure
<i>wf</i>	working fluid
<i>cr</i>	critical state
<i>pinch</i>	indicator of pinch temperature
<i>bleed</i>	indicator of bleeding state

5.1 Problem definition

Given are sets of hot and cold process thermal streams (\mathbf{P}^H and \mathbf{P}^C , respectively). Provided data on the thermal streams are inlet temperature T_{in} , outlet temperature T_{out} , and the heat load \dot{Q} . In addition, hot and cold utilities (\mathbf{U}^H and \mathbf{U}^C , respectively) are provided when process streams are not self-sufficient. The goals are first to determine the potentially recoverable waste heat, and second to find the best ORC architecture and its optimum operating conditions for recovering the waste heat with respect to objective(s), such as maximizing the system performance or minimizing losses subject to thermodynamic and technical constraints.

5.2 Methodology

5.2.1 Mathematical formulation

The superstructure is adapted from [74] by incorporating reheat turbines and detailed condensation recycling. Figure 5.1 illustrates the proposed ORC superstructure with five pressure levels. Turbines and pumps are added between any two pressure levels. In addition, different types of feed liquid heaters are modeled via implementation of the pumps and turbine extractions as shown in Figure 5.1. The overall superstructure embeds the basic cycle as well as superheated, regenerative, transcritical, reheating, bleeding, and multi-stage cycles which were described schematically in Figure 4.2.

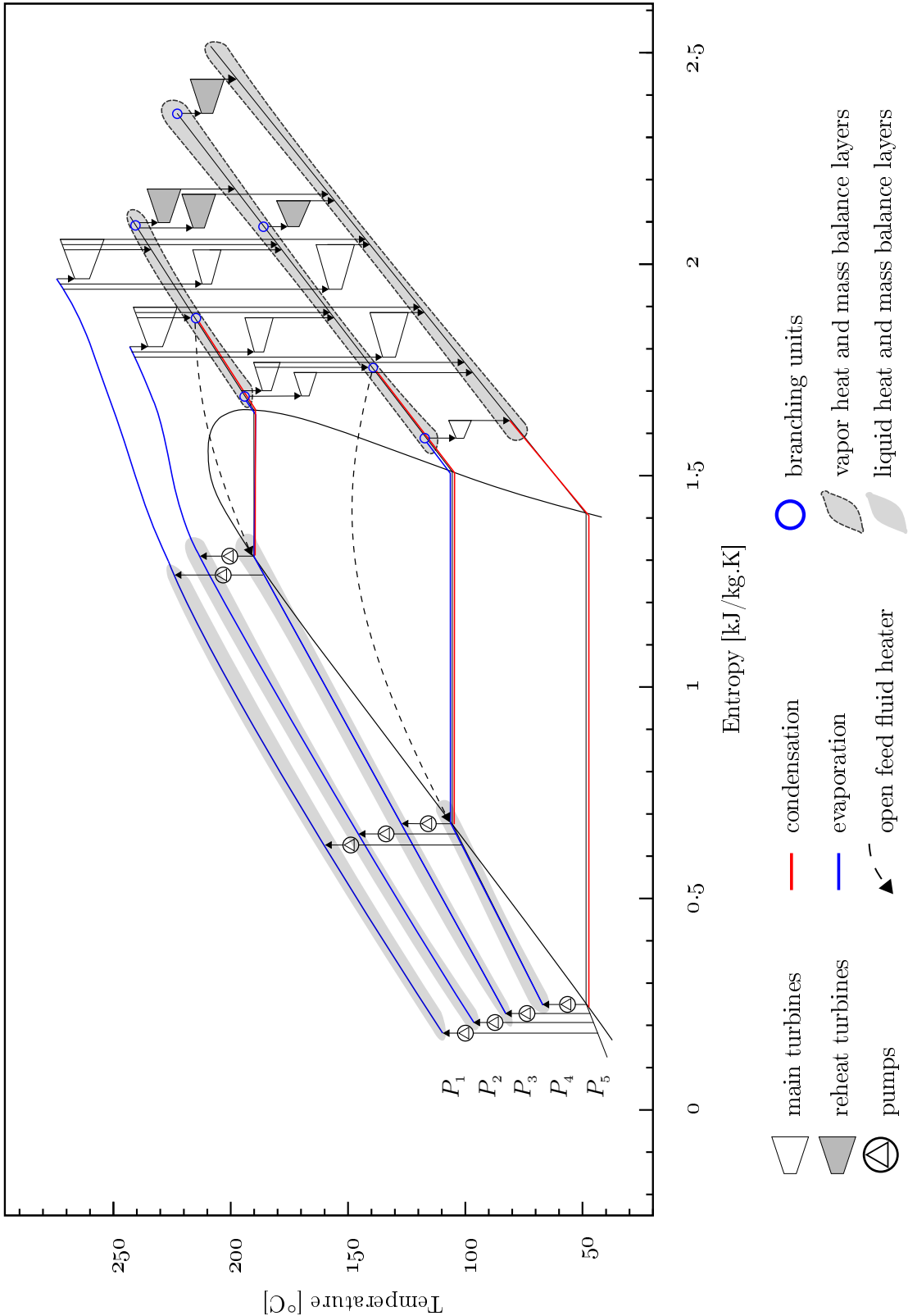


FIGURE 5.1— Schematic of the proposed ORC superstructure illustrated with five pressure levels on temperature-entropy (T-s) diagram

Table 5.2 provides the fundamental equations governing the main equipment in the superstructure, i.e., pumps, turbines (including the reheat turbines), condensers, and evaporators. For this formulation, $\dot{\omega}_{i,j}^p(\omega_{i,j}^t)$ is specific electricity consumption (production) [kJ/kg] of a pump (turbine) between pressure levels i and j with isentropic efficiency η^p (η^t). Similarly, $\dot{\omega}_{i,j,k}^{trh}$ is specific electricity production [kJ/kg] of a reheat turbine between pressure levels i and j starting from the outlet of a turbine between pressure levels k and i . The superscripts t , trh , p , $evap$ and $cond$ corresponds to turbine, reheat turbine, pump, evaporator and condenser, respectively. The superscripts in and out denote the thermodynamic properties at the inlet and outlet of equipment, respectively, i.e., temperature (T), specific enthalpy (h) and specific entropy (s). The inlet temperature of a turbine at level i ($T_i^{t,in}$) is defined as the saturation temperature at level i (T_i^{sat}) plus a degree of superheating (ΔT_i^{sup}). Similarly, the inlet temperature of a reheat turbine at level i ($T_{i,k}^{trh,in}$) is defined as temperature at level k (T_k) plus a degree of temperature difference (ΔT_i^{rh}). The thermodynamic property calculations are performed using CoolProp [75].

Choice of objective function Several objective functions can be considered in the optimization of ORCs [76], which is reinforced by the various applications presented in Table 4.4; though often, the choice depends mainly on the application of the ORC. Various authors have argued that the objective should be to maximize the total thermal efficiency as in solar-driven ORCs, while others suggest to maximize the net power output (like in WHR applications) [77, 78]. TAC of the system and specific investment cost (SIC) are also valid choices in process integration applications. In this work, a multi-objective optimization is performed by selecting two objectives, minimizing the investment cost (C^{inv}) and maximizing the net power output (W_{net}) (Table 5.3). Net power output is defined as the sum of all electricity production and consumption, where $\mathbf{m}_{i,j}^t$, $\mathbf{m}_{i,j,k}^{trh}$ and $\mathbf{m}_{i,j}^p$ denote mass flowrates [kg/s] of the working fluid in each turbine, reheat turbine and pump, respectively. Investment cost consists of capital cost associated to equipment sizing (C^{cap}) and the estimated HEN cost (C^{HEN}), where parameters Cf and Cp are the linearized coefficients of equipment cost functions and $\mathbf{y}_{i,j}^t$, $\mathbf{y}_{i,j,k}^{trh}$ and $\mathbf{y}_{i,j}^p$ are binary variables indicating the existence of a piece of equipment. In HEN cost estimation, area targeting is followed by the procedure proposed by Linnhoff and Ahmad [79], in which the process is divided into vertical temperature intervals (TI) and the area is calculated for each interval k knowing the logarithmic mean approach temperature (ΔT_{LM}^k), heat loads (q_i^k , q_j^k) and the heat transfer coefficients (α_i^k , α_j^k) of all hot (HS) and cold (CS) thermal streams involved in that interval.

It should be noted that in the case of reheat turbines, there exist as many at each pressure i as there are pressure levels above i . The reasoning for such implementation is to have independent reheat turbines in case a pressure level is not active in the optimization problem. Equation 5.10 enforces that reheat turbines are only active when the main turbine outlet enters that pressure level:

$$\mathbf{y}_{i,j,k}^{trh} \leq \mathbf{y}_{k,i}^t \quad \forall \quad i \in \{2, \dots, (N_p - 1)\}, \quad \forall \quad j \in \{i + 1, \dots, N_p\}, \quad \forall \quad k \in \{1, \dots, (i - 1)\} \quad (5.10)$$

$$\mathbf{m}_{i,j,k}^{trh} \leq \mathbf{y}_{k,i}^t \quad \forall \quad i \in \{2, \dots, (N_p - 1)\}, \quad \forall \quad j \in \{i + 1, \dots, N_p\}, \quad \forall \quad k \in \{1, \dots, (i - 1)\} \quad (5.11)$$

TABLE 5.2—Main equipment included in the superstructure and their governing equations/constraints

Equipment	Schematic representation	Equations/Constraints**
Pump		$\dot{\omega}_{i,j}^p = h_{i,j}^{p,out} - h_i^{p,in} = (h(s_i^{p,in}, P_j) - h_i^{p,in})/\eta^p$ $T_i^{p,in} = T_i^{sat}$ $\forall i \in \{2, \dots, N_p\} \quad \forall j \in \{1, \dots, (i-1)\}$
Turbine		$\dot{\omega}_{i,j}^t = h_{i,j}^{t,out} - h_i^{t,in} = \eta^t (h(s_i^{t,in}, P_j) - h_i^{t,in})$ $T_i^{t,in} = T_i^{sat} + \Delta T_i^{sup}$ $\forall i \in \{1, \dots, (N_p - 1)\} \quad \forall j \in \{i+1, \dots, N_p\}$
Reheat turbine		$\dot{\omega}_{i,j,k}^{trh} = h_{i,j,k}^{trh,out} - h_{i,k}^{trh,in} = \eta^{trh} (h(s_{i,k}^{trh,in}, P_j) - h_{i,k}^{trh,in})$ $T_{i,k}^{trh,in} = T_k + \Delta T_i^{rh}$ $\forall i \in \{2, \dots, (N_p - 1)\}$ $\forall j \in \{i+1, \dots, N_p\}$ $\forall k \in \{1, \dots, (i-1)\}$
Condenser*		$\dot{q}_i^{cond} = h_i^{cond,out} - h_i^{cond,in}$ $T_i^{cond,out} = T_i^{sat} \quad \forall i \in \{2, \dots, N_p\}$
Evaporator*		$\dot{q}_i^{evap} = h_i^{evap,out} - h_i^{evap,in}$ $T_i^{evap,in} = T_{i+1,i}^{p,out}$ $T_i^{evap,out} = T_i^{t,in} \quad \forall i \in \{1, \dots, (N_p - 1)\}$

Note: Pressure levels are in descending order, i.e., P_1 is the highest pressure level while P_{N_p} is the lowest pressure level.

* For condensers and evaporators, the piece-wise linearization are performed and for all the pieces, input and output temperatures and enthalpies are calculated.

** **Note:** Due to the number of parameters and variables for the technology definitions, the reader is referred to the nomenclature section of this chapter.

5.2 METHODOLOGY

TABLE 5.3—Selected objective functions and indicators in this work

List of objective functions*

Net power output	$W_{net} [\text{kW}]$	$= \sum_{i=1}^{N_p-1} \sum_{j=i+1}^{N_p} \underbrace{\mathbf{m}_{i,j}^t \dot{\omega}_{i,j}^t}_{W_{i,j}^t} + \sum_{i=2}^{N_p-1} \sum_{j=i+1}^{N_p} \sum_{k=1}^{i-1} \underbrace{\mathbf{m}_{i,j,k}^{trh} \dot{\omega}_{i,j,k}^{trh}}_{W_{i,j,k}^{trh}} + \sum_{i=2}^{N_p} \sum_{j=1}^{i-1} \underbrace{\mathbf{m}_{i,j}^p \dot{\omega}_{i,j}^p}_{W_{i,j}^p}$	(5.1)
Operating cost	$C^{op} [\text{USD/y}]$	$= \left[\sum_{hu=1}^{N_{UH}} \mathbf{m}^{hu} \dot{q}^{hu} C^{hu} + \sum_{cu=1}^{N_{UC}} \mathbf{m}^{cu} \dot{q}^{cu} C^{cu} + W_{net} C^{el} \right] t$	(5.2)
Capital cost ¹	$C^{cap} [\text{USD}]$	$= \sum_{i=1}^{N_p-1} \sum_{j=i+1}^{N_p} \left[C f^t \mathbf{y}_{i,j}^t + C p^t W_{i,j}^t \right]$ $+ \sum_{i=2}^{N_p-1} \sum_{j=i+1}^{N_p} \sum_{k=1}^{i-1} \left[C f^{trh} \mathbf{y}_{i,j,k}^{trh} + C p^{trh} W_{i,j,k}^{trh} \right]$ $+ \sum_{i=2}^{N_p} \sum_{j=1}^{i-1} \left[C f^p \mathbf{y}_{i,j}^p + C p^p W_{i,j}^p \right]$	(5.3)
HEN cost ²	$C^{HEN} [\text{USD}]$	$= N^{HE,min} \left[C f^{HEN} + C p^{HEN} \left(\frac{A_{total}}{N^{HE,min}} \right)^{\beta^{HEN}} \right]$	(5.4)
HEN area	$A_{total} [\text{m}^2]$	$= \sum_{k=1 \dots K} \frac{1}{\Delta T_{LM}^k} \left\{ \sum_{i=1 \dots I}^{HS} \frac{q_i^k}{\alpha_i^k} + \sum_{j=1 \dots J}^{CS} \frac{q_j^k}{\alpha_j^k} \right\}$	(5.5)
Investment Cost	$C^{inv} [\text{USD/y}]$	$= (C^{cap} + C^{HEN}) \frac{irr(1+irr)^{n_{year}}}{(1+irr)^{n_{year}-1}}$	(5.6)
TAC	$C^{tac} [\text{USD/y}]$	$= C^{op} + (C^{cap} + C^{HEN}) \frac{irr(1+irr)^{n_{year}}}{(1+irr)^{n_{year}-1}}$	(5.7)
Weighted TAC	$C^{wtac} [\text{USD/y}]$	$= (1-\kappa) \cdot C^{op} + \kappa \cdot C^{cap} \cdot \frac{irr(1+irr)^{n_{year}}}{(1+irr)^{n_{year}-1}} \quad 0 \leq \kappa \leq 1$	(5.8)
SIC ³	$SIC [\text{USD/kWh}]$	$= \frac{C^{inv}}{W_{net} t}$	(5.9)

* **Note:** The reader is referred to the nomenclature section of this chapter for full list of variables and parameters.

1 - Linearized for inner MILP problem. For equipments, bare module cost are used (Equation 5.15)

2 - $N^{HE,min}$ is calculated by applying heat load distribution (HLD) optimization [65].

3 - Grassroots cost correlations are used for equipments (Equation 5.17)

where $\mathbf{y}_{i,j,k}^{trh}$ and $\mathbf{m}_{i,j,k}^{trh}$ are the binary and continuous variables denoting the existence and the size of a reheat turbine from level i to j due to a main turbine outlet from level k entering level i ($\mathbf{y}_{k,i}^t, \mathbf{m}_{k,i}^t$), respectively. It should be noted here that the superstructure is constructed with fixed numbers of pressure levels, working fluids, and turbine inlet temperatures.

Automatic generation of interconnections in liquid and vapor layers As illustrated in Figure 5.1, two types of layers are defined for each pressure level, i.e., liquid and vapor layers. Mass and energy balance constraints are imposed for each layer separately; however, there are equipment which transfer heat and mass between layers and pressure levels. Condensers, evaporators, desuperheating liquids and open feed liquid heaters can transfer heat and mass between the layers at each pressure level, while turbines and pumps are the transfer units between pressure levels in vapor and liquid layers, respectively. Knowing the inlet and outlet thermodynamic properties of all equipment (Table 5.2), thermal and mass interconnections are generated by applying the method proposed by Kermani et al. [80]. The method proposes that “*branching*” units (in Figure 5.1 and Table 5.2 denoted by circles) are split to a set of predefined temperatures (Equation 5.12) at each pressure level. The enthalpy of these branched temperatures follows the thermodynamic property at each point. These “*branching*” units in the proposed ORC superstructure are inlets to turbines, condensers, and feed liquid heaters. Referring to Figure 5.1, this technique can be elaborated for an example of the condenser inlet at pressure P_4 : The set of all temperatures in the vapor layer at this level (\mathbf{T}_4^{vap}) includes all turbine outlets entering this pressure level. Several units will then be generated at this level with inlet conditions equal to the turbine outlets and the outlet conditions equal to the condenser inlet conditions. These units express all possible methods for superheating and desuperheating to the temperature at the condenser inlet. Enthalpy and mass balance constraints are enforced at the inlet of each branched unit as well as at the condenser inlet.

$$\begin{aligned} \mathbf{T}_i^{liq} &= \{T^{u,in} | \forall u \in \mathbf{U}^{all} : P^{u,in} = P_i, T^{u,in} \leq T_i^{sat}\} \cup \\ &\quad \{T^{u,out} | \forall u \in \mathbf{U}^{all} : P^{u,out} = P_i, T^{u,out} \leq T_i^{sat}\} \quad \forall i \in \{1, \dots, N_p\} \\ \mathbf{T}_i^{vap} &= \{T^{u,in} | \forall u \in \mathbf{U}^{all} : P^{u,in} = P_i, T^{u,in} \geq T_i^{sat}\} \cup \\ &\quad \{T^{u,out} | \forall u \in \mathbf{U}^{all} : P^{u,out} = P_i, T^{u,out} \geq T_i^{sat}\} \quad \forall i \in \{1, \dots, N_p\} \end{aligned} \quad (5.12)$$

Equipment sizing constraints Unit sizing in the superstructure uses a continuous variable (\mathbf{m}) while the existence of that unit is described by a binary variable (\mathbf{y}). Equation 5.13 links the size and existence of each unit while also enforcing the upper ($F^{u,max}$) and lower ($F^{u,min}$) capacity limits:

$$\mathbf{y}^u \cdot F^{u,min} \leq \mathbf{m}^u \leq \mathbf{y}^u \cdot F^{u,max} \quad \forall u \in \mathbf{U}^{all} \quad (5.13)$$

The overall problem is subjected to heat cascade constraints [62]. Mass balance constraints hold for each pressure level, each working fluid and each layer (liquid, vapor).

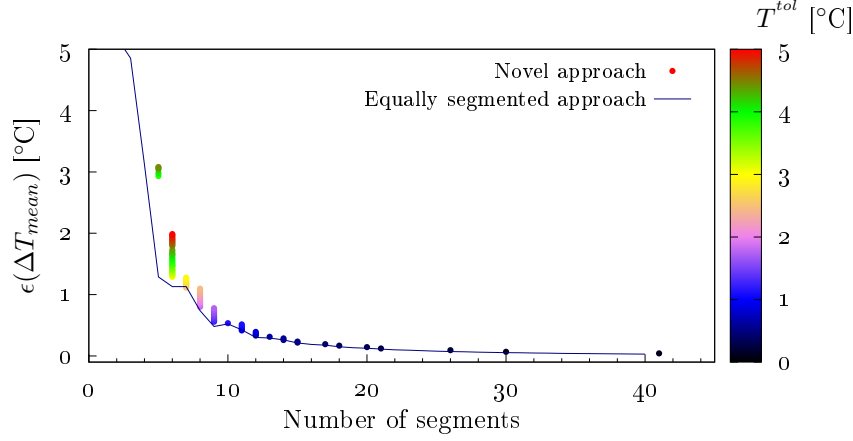
5.2.2 Piece-wise linear envelopes for thermal streams

The heat cascade constraints [62] require constant specific heat capacity (c_p) for each thermal stream which necessitates linear or piece-wise linear models. This is important in modeling the evaporators and condensers in WHR applications (Table 4.4), particularly for supercritical and near-critical streams. Near-critical isobaric T-h profiles can exhibit sharp curvatures for which

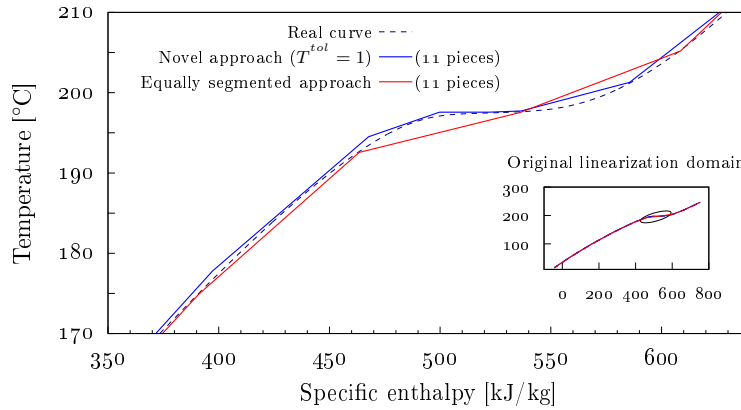
traditional three-piece linearization (subcooled, two-phase, and superheated regions) might exhibit large error. Throughout the entire literature, only two articles treat the problem by using piece-wise linearization of such streams. Bendig [81] used 20 segments for piece-wise linearization of supercritical cold streams and the conventional three-segment approach for sub-critical streams. More recently, Soffiato et al. [82] used 20 segments (enthalpy intervals) for both regions. These methods systematically underestimate the real T-h curve when $\partial^2 T / \partial h^2$ is negative (liquid phase for subcritical pressures and the first stage of supercritical pressures) and overestimate it when $\partial^2 T / \partial h^2$ is positive (vapor phase for subcritical pressures and second stage of supercritical pressures). Heat integration techniques dictate that cold (hot) streams should always be overestimated (underestimated). Conversely, linearization of the T-h profile is not strictly necessary for some situations (e.g., at ambient pressure) and thus a universal application of such techniques introduces an undue computational burden. These concerns motivated us to propose a dynamic method to calculate piece-wise linear envelopes for thermal streams. Several features are particularly relevant:

- a) The method always underestimates the hot streams and overestimates the cold streams (Figure 5.2b).
- b) The maximum temperature difference between the piece-wise linear envelope and the real curve (T^{tol}) is an input parameter. For the applications in this report, the tolerance is set at 1K.
- c) The number of segments is a function of working fluid, pressure, inlet/outlet temperatures and depends on profile curvature.

Figure 5.2a demonstrates the error for both approaches using pentane as the working fluid which is defined as the absolute temperature difference between the real curve and the piece-wise models. The pressure used for this illustration was selected as 0.5 bar above critical since this region is often the most problematic due to the curvature near the critical point and therefore requires the largest number of pieces. It can be observed that at this pressure, 11 pieces results in a linearization error below the tolerance of 1K. The full algorithm is provided in the supplementary material. It should be pointed out that tolerance represents the deviation of the linearized envelope from the real curve and hence any inaccuracies in the real curve cannot be corrected by this method, relying on the equations of state to provide a true profile. Nevertheless, as the technique always overestimates (underestimates) a cold (hot) stream, the result will always penalize these inaccuracies and hence results in a ‘worst case’ scenario. Furthermore, the error resulting from the thermodynamic property model is impossible to quantify without comparing results of the property package with experimental data. Considering that the proposed method will be used as a screening method to identify the promising options, the risk of inaccurate thermodynamic properties from equations of state is acceptable at this stage. Once the selected configuration will be implemented, it will be necessary to check the properties in the vicinity of the pinch point, knowing that pressure will be adapted in the case of pinch point activation. Figure 5.2b demonstrates the application of this technique ($T^{tol} = 1\text{K}$) for a cold stream together with the equally-segmented approach using 11 segments. It can be seen that the traditional segmented approach fails to correctly estimate the temperature-enthalpy profile of the cold stream. Additionally, it fails to predict the curvature, particularly near the pseudo-critical point. This emphasizes the importance of using such a dynamic linearization algorithm which can address the trade-offs between number of segments and curvature matching.



(a) Linearization comparison (pentane at 34.2 bar)



(b) Example of linearization for pentane at 34.2 bar between 15–246°C (cold stream)

FIGURE 5.2—(a) Comparison of linearization techniques (proposed approach *vs* segmented approach) for Pentane, (b) Example of linearization for pentane at 34.2 bar between 15–246°C (cold stream)

5.2.3 Economic model

Purchased cost (C_p) of equipments (turbines and pumps) is based on cost correlation of [83]. The following nonlinear cost functions have been used to evaluate the solution of inner MILP level for the outer GA level. A linearization of these cost functions are performed and added to the MILP formulation. The general purchased cost function is:

$$\log_{10} C_p = K_1 + K_2 \log_{10}(W) + K_3 [\log_{10}(W)]^2 \quad (5.14)$$

Where W is the mechanical power. The bare module cost is considered to be the cost of equipment which takes into account the material and the operating pressure of the equipment

as follows:

$$C_{BM} = C_p \left(\underbrace{B_1 + B_2}_{\text{bare module constants (Table 5.4)}} \underbrace{F_M}_{\text{material factor}} \underbrace{F_P}_{\text{pressure factor}} \right) \quad (5.15)$$

$$\log_{10} F_P = C_1 + C_2 \log_{10}(P) + C_3 [\log(P)]^2 \quad (5.16)$$

The constants of the above equations are provided in Table 5.4. Operating costs for the case study are provided in Table 5.5. The grassroots cost which takes into account the complete cost of construction of new facilities can be calculated as follows [83]:

$$C_{GR} = \underbrace{1.18 C_{BM}}_{\text{Total module cost [83]}} + 0.5 C_{BM} \quad (5.17)$$

TABLE 5.4—Constants of cost functions [83] (Reference year 2001, reference index CEPCI)

Equipment type [83]	K_1	K_2	K_3	B_1	B_2	F_M (CS)	C_1	C_2	C_3	Pressure range [bar]
Turbine (radial expander)	2.2476	1.4965	-0.1618	0	1	3.5	0	0	0	-
Pump (centrifugal)	3.3892	0.0536	0.1538	1.89	1.35	1.6	0	0	0	$P < 10$
							-0.3935	0.3957	-0.00226	$10 < P < 100$

TABLE 5.5—Cost data for the case study

Parameter	Unit	Value	Description	Reference
C^{hu}	USD/kWh	192.096	Cost of hot utility	[67]
C^{cu}	USD/kWh	10.1952	Cost of cold utility	[67]
Cf^{HEN}	USD	7,000	Fixed cost of heat exchanger	[84]
Cp^{HEN}	USD	360	Proportional cost of heat exchanger	[84]
β^{HEN}	-	0.8	exponential parameter	[84]
i	-	0.08	Internal rate of return	
n_{year}	-	25	Plant lifetime	
η^p	-	0.65	Pump isentropic efficiency	[7]
$\eta^{t(trh)}$	-	0.80	Turbine isentropic efficiency	[7]

1 - Reference year is assumed to be 2003.

5.2.4 Thermodynamic model (heat transfer calculation)

Shell-and-tube heat exchangers are the most common type of heat exchangers in process industries which can handle a wide range of operating conditions and materials [85]. Following this convention, their correlations are selected for calculating the heat transfer coefficients. The thermal flows are divided into four categories of single-phase, two-phase condensing, two-phase evaporating, and supercritical flows. The single-phase (including the supercritical flows) and two-phase evaporating flows are modeled on the tube side while the two-phase condensing flows are modeled on the shell side. In all following correlations, the default tube diameter, D , is selected as 25 mm [85]. Due to practical limits on flow velocity in and over tubes, diameter can vary between 15 and 30 mm. The velocity of the flow is bounded between 0.9 and 2.4 m/s for liquids and between 15 and 30 m/s for vapors [86] on the tube side and between 0.6

and 1.5 m/s on the shell side [85]. These bounds are applied to find the flowrate in tubes and hence the number of tubes.

Single-phase flows For single-phase flows (subcritical conditions), the Gnielinski correlation [87] has been used. This type of flow includes superheating, desuperheating, preheating, and sub-cooling stages:

$$Nu_D = \frac{\alpha D}{k} = \frac{(f/8)(Re_D - 1000)Pr}{1 + 12.7(f/8)^{1/2}(Pr^{2/3} - 1)} \quad 3000 \leq Re_D \leq 5 \times 10^6 \quad 0.5 \leq Pr \leq 2000 \quad (5.18)$$

$$f = (0.790 \ln Re_D - 1.64)^{-2} \quad 3000 \leq Re_D \leq 5 \times 10^6 \quad (\text{Moody friction factor}) \quad (5.19)$$

Where Nu_D is the Nusselt number, $Re_D = \rho u_m D / \mu$ is the Reynolds number, $u_m = (4\dot{m})/(\pi \rho D^2)$ is the mean velocity in the tube, \dot{m} is the mass flow of the working fluid passing through each tube and ρ , μ , Pr , and k are mass density [kg/m³], dynamic viscosity [Pa.s], Prandtl number [dimensionless], and thermal conductivity [kW/(mK)] of the fluid, respectively.

Supercritical flows Available correlations for heat transfer coefficient calculations at supercritical conditions are based on water and CO₂. Cayer et al. [88], Shengjun et al. [89], Song et al. [90], Baik et al. [91] use Krasnoshchekov-Protopov correlation for this reason. Yu et al. [92] performed an analysis and found that the Bishop correlation [93] performs better in predicting the heat transfer coefficient:

$$Nu_D = \frac{\alpha D}{k} = 0.0069 Re_D^{0.9} Pr^{0.66} \left(\frac{\bar{c}_p}{c_p} \right)^{0.66} \left(\frac{\rho_w}{\rho_b} \right)^{0.43} \underbrace{\left(1 + 2.4 \frac{D}{x} \right)}_{\simeq 1 \quad (\text{assuming } \frac{D}{x} \ll 1, \text{ i.e., neglecting entrance region})} \quad (5.20)$$

where \bar{c}_p is the average specific heat capacity of the stream at the inlet and outlet conditions. c_p and ρ_b (bulk specific heat capacity and density, respectively) are calculated at the mean (bulk) temperature, i.e., $T_b = (T_{in} + T_{out})/2$. ρ_w is the density of the flow calculated at the wall temperature that is assumed to be ΔT_{min} above T_b .

Two-phase condensing flows The correlation for film condensation over radial systems is used to evaluate the average heat transfer coefficient ($\bar{\alpha}$) during condensation [94] :

$$\overline{Nu}_D = \frac{\bar{\alpha} D}{k_l} = 0.729 \left[\frac{\rho_l g (\rho_l - \rho_v) h'_{lv} D^3}{\mu_l k_l (T_{sat} - T_s)} \right]^{1/4} \quad (5.21)$$

where $h'_{lv} = h_{lv} + 0.68 c_{p,l} (T_{sat} - T_s)$. All liquid properties are evaluated at the film temperature $T_f = (T_{sat} + T_s)/2$. The vapor density (ρ_v) and latent heat of vaporization (h_{lv}) are evaluated at T_{sat} . T_s is the tube surface temperature and is assumed to be ΔT_{min} below T_{sat} .

Two-phase evaporating flows Heat transfer coefficient for evaporation in cylindrical tubes have been estimated using Gungor-Winterton simplified correlation [95]:

$$Nu_D = \frac{\alpha D}{k_l} = \underbrace{0.023 Re_{D,l}^{0.8} Pr_l^{0.4}}_{\text{DittusBoelter correlation}} \left[1 + 3000 Bo^{0.86} + 1.12 \left\{ \frac{\chi}{1-\chi} \right\}^{0.75} \left\{ \frac{\rho_l}{\rho_v} \right\}^{0.41} \right] \quad (5.22)$$

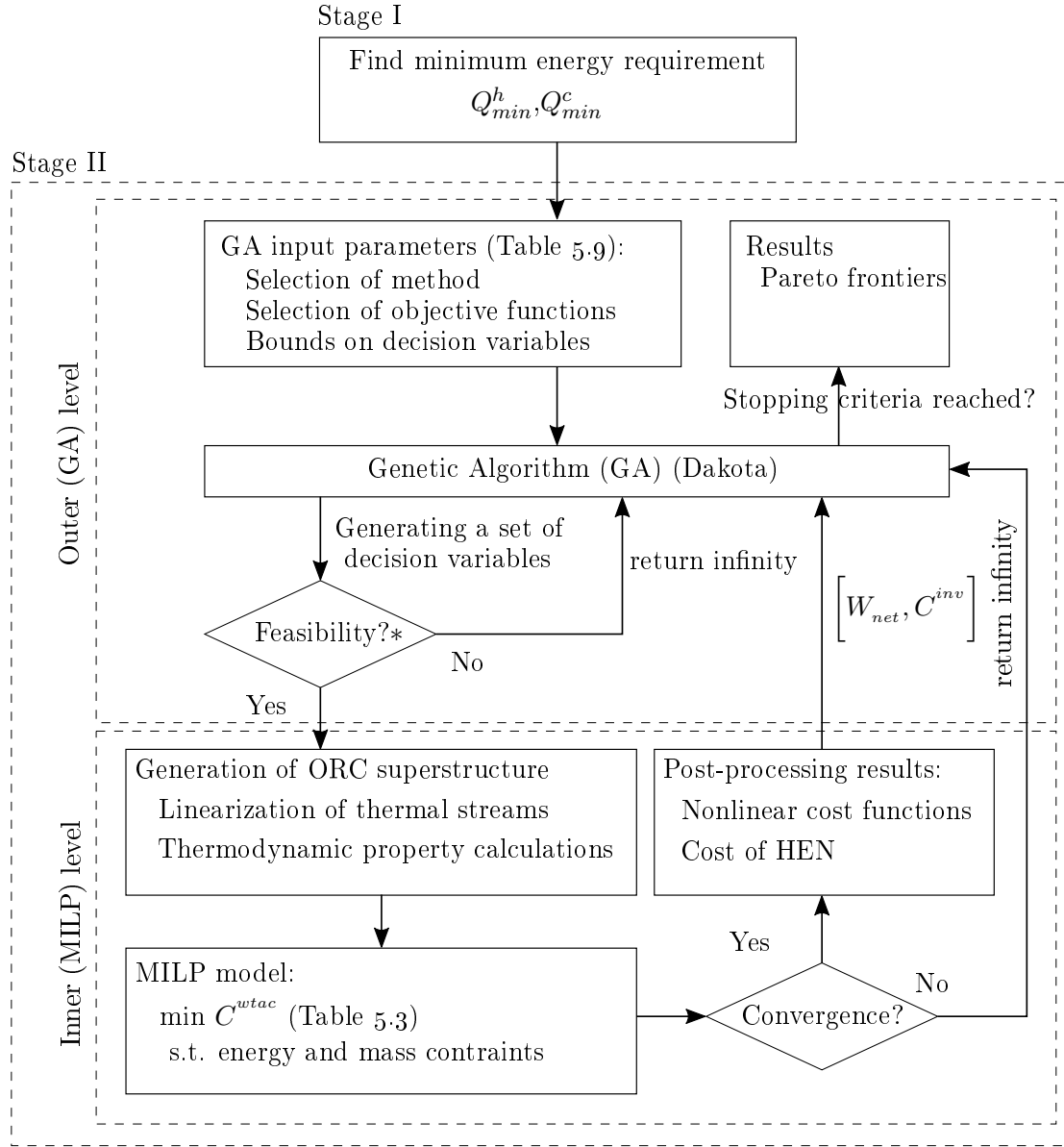
Where $Bo = \dot{q}/(\dot{m}h_{lv})$ is the boiling number and χ is the vapor quality. Reynolds and Prandtl Numbers are calculated at saturated liquid state. For finding the mean heat transfer coefficient over the entire evaporation, α is calculated for 10 different χ values and the average is considered to be reflective of the phase transition.

Due to lack of data on the process streams from the literature, the heat transfer coefficient is assumed to be 1 kW/m²K for all process streams. For those fluids which CoolProp does not have the required information following values have been assumed: Liquid phase (including supercritical) 1 kW/m²K, gas phase 0.06 kW/m²K, evaporation 3.6 kW/m²K, and condensation 1.6 kW/m²K.

5.2.5 Solution strategy

The ORC design and integration problem is solved in two stages. The first stage is finding the maximum energy recovery of the system which can be formulated as an MILP model. The result of this stage (i.e., \dot{Q}_{min}) sets the upper boundaries on utility consumption in the second stage. The proposed superstructure in this work is principally non-convex due to the presence of unknown continuous (pressure and temperature levels) as well as binary variables (selection of pumps, turbines, condensation and evaporation levels, and working fluid). A decomposition technique using two levels is pursued in this work for optimal integration of ORCs. The first level (outer level) uses GA as differentiation is not required and is most suitable for optimizing the operating conditions of the cycle. The decision variables in the first level consist of pressures, temperatures, reheating temperature rises, and working fluid. Setting these variables to the values provided by GA, the second level (inner level) becomes an MILP model. The decision variables in the inner level are the size and the selection of the ORC architecture, i.e., active pressure levels, turbines, pumps, condensers, evaporators, and mass flowrate of the working fluid in each. For the outer level, Dakota's JEGA library [96, 97] has been used, while the commercial solver CPLEX [98] within AMPL [99] is used for the inner MILP level. Figure 5.3 illustrates the proposed strategy.

Bounds on non-discrete decision variables The set of continuous decision variables consists of pressure stages, amount of superheating, and reheating temperatures. The superheating temperature differences (ΔT_i^{sup}) are bounded by the range [0:20K] while the reheating temperature differences (ΔT_i^{rh}) are bounded by the range [-10:0K]. At each level, knowing the pressure ($P_{i,wf}$) and the amount of superheating (ΔT_i^{sup} in subcritical pressures), the full thermodynamic properties of that point ($T_{i,wf} = T_{i,wf}^{sat} + \Delta T_i^{sup}$) can be calculated. Including supercritical pressure levels in the superstructure without a valid reference point from which the superheating decision variable can be evaluated, and requiring consistency in defining the decision variables for both conditions, a novel reference point is defined for supercritical



* Checking minimum pressure difference between successive levels and from critical pressure

FIGURE 5.3—Proposed methodology for ORC integration in industrial processes

pressure levels (Equation 5.23):

$$\forall \quad i \mid P_{i,wf} > P_{wf,cr} \quad T_{i,wf}^{sat} = T(P_{i,wf}, wf) \Big|_{\frac{\partial^2 T}{\partial h^2} = 0} \quad (5.23)$$

This point is referred to in thermodynamics as the pseudo-critical point and is where the specific heat at constant pressure takes its maximum value. Instead of having all the pressure levels as decision variables, the r-formulation [100] is adapted to generate the pressure levels in descending order. For each level i , ζ_i is defined in the range $[0:1]$ as the decision variable.

Accordingly, pressure at each level is defined (Equation 5.24):

$$P_{i,wf} = P_{wf}^{max} \left[\prod_{j=1}^i (1 - \zeta_j) \right] \quad \forall \quad i \in \{1..(N_P - 1)\} \quad (5.24)$$

Where P_{wf}^{max} is the maximum allowed pressure for working fluid wf . In this chapter $P_{wf}^{max} = P_{wf,cr} + 20$ bar. The bounds of the lowest pressure level is set as (Equation 5.25):

$$P_{N_P,wf} \in \left[\min_{wf \in WF} P_{wf}^{cond,min} : \max_{wf \in WF} P_{wf}^{cond,max} \right] [bar] \quad (5.25)$$

where $P_{wf}^{cond,min}$ ($P_{wf}^{cond,max}$) are the minimum (maximum) condensation pressure of the working fluid wf which corresponds to the cooling water inlet (outlet) temperatures T_{in}^{cu} (T_{out}^{cu}) including the minimum heat recovery approach temperature. Several optimization results demonstrated that the lowest pressure level is always active in the optimal solution and its value lies in the vicinity of the cooling water temperature.

5.3 Results and discussion

The proposed methodology combined with the novel linearization technique has been applied to a case study “*Illustrative Example 2*” originally presented by Desai and Bandyopadhyay [7] (Table 5.6). Several assumptions have been considered in this case study:

- Minimum approach temperature (ΔT_{min}) of ORC thermal streams and the processes are fixed *a priori* at 20°C. The optimal value of this parameter varies for different thermal streams and is a trade-off between operating cost and the investment cost of heat exchanger area and thus this assumption is immediately questionable but is used here to be consistent with the case study. Ahmad et al. [101] argued that the optimal value is proportional to the heat transfer coefficient ($\Delta T_{min}^i \cdot \alpha_i^{\beta/(\beta+1)} = K$) where K is a constant based on a reference state and β is the exponential of the HEN investment cost.
- Steady state conditions; Pressure drops are neglected in the equipment.

TABLE 5.6—Operating data of the case study [7]

Stream	T_{in} [°C]	T_{out} [°C]	Heat capacity [kW/K]	Heat [kW]
H_1	353	313	9.802	392.1
H_2	347	246	2.931	296.0
H_3	255	80	6.161	1,078.2
C_1	224	340	7.179	832.8
C_2	116	303	0.641	119.8
C_3	53	113	7.627	457.6
C_4	40	293	1.690	427.6

Minimum hot and cold utility requirements can then be calculated as $Q_{min}^h = 244.1$ and $Q_{min}^c = 172.6$ kW, respectively. Figure 5.4a demonstrates the grand composite curve of the test case with pinch point at 234°C. It is assumed that the hot utility cannot exchange heat

with the ORC and hence the upper bound of the hot utility consumption is set to the minimum requirement. The goal is to find the optimal integrated ORC below the pinch for maximum electricity production. Section 5.3.1 provides a benchmarking analysis for validating the proposed superstructure while several optimization cases are considered using GA in section 5.3.2.

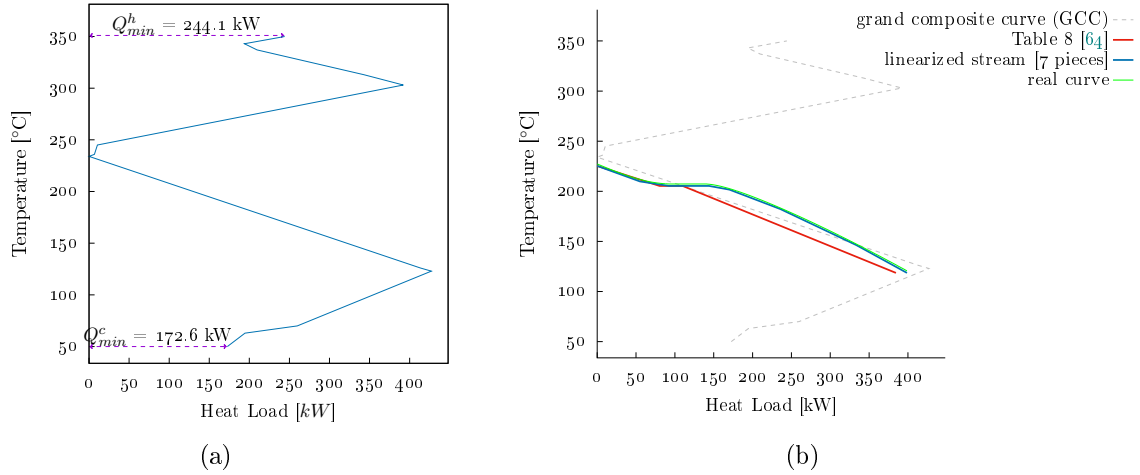


FIGURE 5.4—(a) GCC of the case study ($T_{pinch} = 234^{\circ}\text{C}$), (b) Integration of evaporation stream with GCC for pentane at 33.06 bar

5.3.1 Comparative analysis

The performance of the proposed superstructure is evaluated using the reported operating conditions of the optimally integrated ORCs for this test case from the literature. Table 5.7 provides the basic comparison with respect to net power output. It is observed that the proposed superstructure provides similar results to those of Desai and Bandyopadhyay [7]. Applying the operating conditions proposed by Yu et al. [64], large differences are observed. In these cases (13-15 from Table 5.7), the differences can be explained by the thermodynamic property calculation methods. Additional differences in case 15 originate from the shape of the evaporation stream as depicted in Figure 5.4b. The working fluid, in this case pentane, is operating at $T_{sat} = 195.3^{\circ}\text{C}$ which corresponds to 33.06 bar. Since pentane's critical pressure is 33.7 bar, an intense curvature of the isobaric T-h profile is expected (Figure 5.4b blue curve). Estimating this curve by a typical three-piece profile (preheating, evaporation, superheating) grossly underestimates the temperature glide of the stream and therefore an infeasible solution is generated since the minimum approach temperature is fixed at 20°C . Correct linearization of the thermal streams is therefore justified as being of great importance in providing realistic solutions. Additionally, further analysis of the solution provided by Yu et al. [64] highlights that the mass balance for the ORC is not closed. It should be mentioned that this test case was also used by Hipólito-Valencia et al. [67]. They applied the operating parameters of *case 1* and claimed to reach net power output of 98 kW by better integration of ORC with background processes. Upon inspection, it was observed that the latent heat of the evaporation was neglected which resulted in eliminating the pinch point of the evaporation stream and thus invalidating the results.

TABLE 5.7—Results of benchmarking using the test case

Case	Fluid	T^{evap} [°C]	ΔT^{sup} [°C]	T^{cond} [°C]	T_{bleed}^{sat} [°C]	\dot{W}_{net} [kW]	
						literature	current chapter
Desai and Bandyopadhyay [7]							
1	Hexane	207.5	0	50	-	37.6	37.08
2	Hexane	196.5	0	50	123.25	41.1	41.33
3	Hexane	186.5	0	80	-	42.7	42.21
4	Benzene	200.5	0	50	-	36.9	36.84
5	Benzene	179.3	0	80	-	40.5	40.50
6	Benzene	192.1	0	50	121.05	39.3	39.72
7	Benzene	166.9	0	80	123.45	39.8	39.89
8	Toluene	199.1	0	50	-	38.0	37.89
9	Toluene	177.2	0	80	-	41.0	41.03
10	Toluene	190.5	0	50	120.25	40.3	40.58
11	Toluene	165.0	0	80	122.5	40.2	40.17
12[69]	Hexane	180	0	77	-	48.3	37.26
Yu et al. [64]							
13	Hexane	178.7	20	50	85.4	54.8	49.89
14	Benzene	174.7	20	50	85.4	57.4	49.00
15	Pentane	195.3	20	80	108.4	62.1	42.52

5.3.2 Optimization

The proposed methodology for optimal ORC integration is applied to several test cases and the results are discussed. Three cases are considered which include single and multi-objective optimizations. It should be noted that the final active pressure levels are the results of the inner MILP model. Table 5.8 provides the objective functions and the bounds on the decision variables (Table 5.9 provides the input parameters of the GA). In the first two cases, the heat transfer coefficients (α) of all thermal streams are set at $1 \text{ kW}/(m^2K)$. This fixed value for heat transfer coefficient might invoke the criticism of not being a realistic value, especially considering different working fluids and operating conditions that are being evaluated. Since the goal is to compare the performance of the proposed superstructure with the literature results using criteria apart from the HEN cost, this assumption is inconsequential. Case III, however, considers the calculation of heat transfer coefficients. In cases II and III, the objective functions are selected to be maximizing the net power output (Equation 5.1) and minimizing the investment cost (Equation 5.6). These objectives are independent of the market value of energy and hence provide a better comparison basis for optimization.

5.3.2.1 Case I: single-objective optimization

As the first case, single-objective optimization of the ORC integration is considered for hexane as the working fluid. The ORC superstructure is considered to have six pressure levels. Objective functions in both the outer GA and the inner MILP stages are set to maximizing the net power output (Equation 5.1). The optimal operating conditions are presented in Table 5.8. The optimal integration of ORC with the waste streams can be demonstrated using the integrated composite curve as shown in Figure 5.5. The net electricity production reaches 57.7 kW which is higher than the reported values in the literature for hexane; however, the network is more complex due to the existence of several turbines, evaporations, and pumps. The TAC of the overall system is calculated to be 103,137 USD/yr using cost functions which can be

TABLE 5.8—Decision variables and their optimal values for different cases

Cases	I	II	III
Method	SOGA ¹	MOGA ¹	MOGA ¹
Objective function			
Outer GA	$\max W_{net}$ (Equation 5.1)	$\max W_{net}$ (Equation 5.1) , $\min C^{inv}$ (Equation 5.6)	
Inner MILP	$\min C^{op}$ (Equation 5.2)	$\min C^{wtac}$ (Equation 5.8)	
Heat transfer coefficient	1 [kW/m ² K]	1 [kW/m ² K]	subsection 5.2.4
Pressure levels N_p	6	6	4
Decision variables ^{2,3}			
κ (Equation 5.8)			[0:1]
ζ_i ($i \leq N_p$)	[0:1]		[0:1]
P_{N_p}	[0.3:1.4]		Equation 5.25
ΔT_i^{sup} ($i < N_p$)	[0:20]		[0:20]
ΔT_i^{rh} ($2 \leq i < N_p$)	[-10:0]		[-10:0]
Working fluid	Hexane	5 organic fluids (Figure 5.6)	14 organic fluids (Figure 5.10)
Results			
\dot{W}_{net} [kW]	57.69		
C^{op} [USD/yr]	12,691		
C^{cap} [USD/yr]	17,678	Figure 5.7	Figure 5.11
C^{HEN} [USD/yr]	72,769	Figure 5.8	
C^{tac} [USD/yr]	103,137		

1 - **SOGA** Single-Objective GA, **MOGA** Multi-Objective GA

2 - Further bounds on decision variables:

- $P_{wf}^{max} = P_{wf,cr} + 20$ and $\forall i \in \{1..N_p\}, |P_{i,wf} - P_{wf,cr}| > 0.5$
- For Case III: $P_4 \geq 1$

3 - Optimal operating conditions in Case I (SOGA). For ζ_i the corresponding pressure values are reported.

TABLE 5.9—Input parameters of JEGA [96, 97]

Parameter	Value	Description
Population size	250	Number of initial population
Initialization type	unique_random	Creating random initial solutions but enforce uniqueness
Crossover type	multi_point_binary	Performing crossover by bit switching
Crossover rate	0.9	Probability of the crossover event
Mutation type	bit_random	Performing mutation by flipping a random bit of a randomly chosen design variable
Mutation rate	0.2	Probability of the mutation event
Convergence type	metric_tracker*	Tracking changes in the non-dominated frontier (Pareto frontier)
Fitness type	domination_count*	Ranking based on number of dominations
Max. number of evaluations	[15,000:30,000]	-
Max. number of generations	[40:100]	-

* - In case of Multi-objective GA

found in the appendix. These results underline the utility of multi-objective optimization to better capture the trade-off between electricity production and total cost of the system.

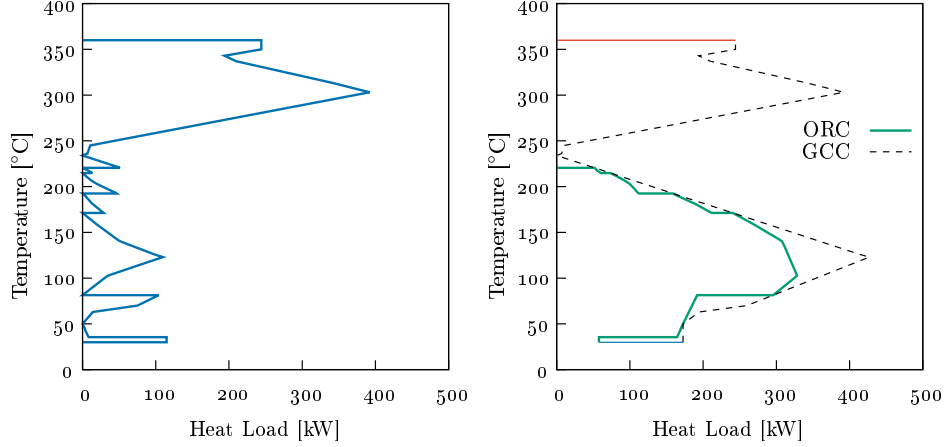


FIGURE 5.5— GCC (left) and integrated composite curve (right) of the optimal ORC integration for case I)

5.3.2.2 Case II: multi-objective optimization

Multi-objective optimization is carried out using the five working fluids which were reported in the literature for the selected case study. The optimization was performed for each working fluid separately to illustrate their individual results in terms of investment cost and electricity production. The main properties of these fluids and their corresponding T-s diagrams are shown in Figure 5.6. The ORC superstructure was constructed with a limit of six pressure levels. As considered by Desai and Bandyopadhyay [7], no constraint is imposed on the minimum allowed pressure in the lowest pressure level. Before presenting the results of optimization it should be highlighted that any conclusion being made is restricted to this case study, although some general remarks and trends can be observed. In addition, this case study has a gliding waste heat profile which logically favors gliding evaporation profiles, i.e., supercritical and near-critical evaporations.

The overall results are illustrated in Figure 5.7 and Figure 5.7f. For each fluid, adding additional stages increases the electricity production while consequently requiring increased investment for additional turbines, pumps, evaporators and condensers. As the cycle becomes highly integrated with the waste heat profile, the HEN cost also increases with increased electricity production. The number of pressure levels included in the optimal solution also explains the discontinuities observed in the Pareto frontiers shown in Figure 5.7. For pentane (Figure 5.7b) and butane (Figure 5.7d), transcritical cycles are observed among the optimal solutions. Transcritical cycles exhibit better temperature matching with the heat source (Figure 5.8a); however, also lead to increased heat exchanger investment cost due to lower approach temperatures. From Figure 5.7f, it is observed that butane is not a good fluid for this case study as its Pareto frontier is dominated by other fluids meaning that at least one other fluid produces more electricity for the same investment cost, requires lower investment cost for the same electricity production, or is better in both cost and production. Examining all fluids (Figure 5.7f) and considering their critical temperatures, it is observed that for low electricity production, fluids with critical temperature slightly higher than the pinch point (i.e., benzene) perform

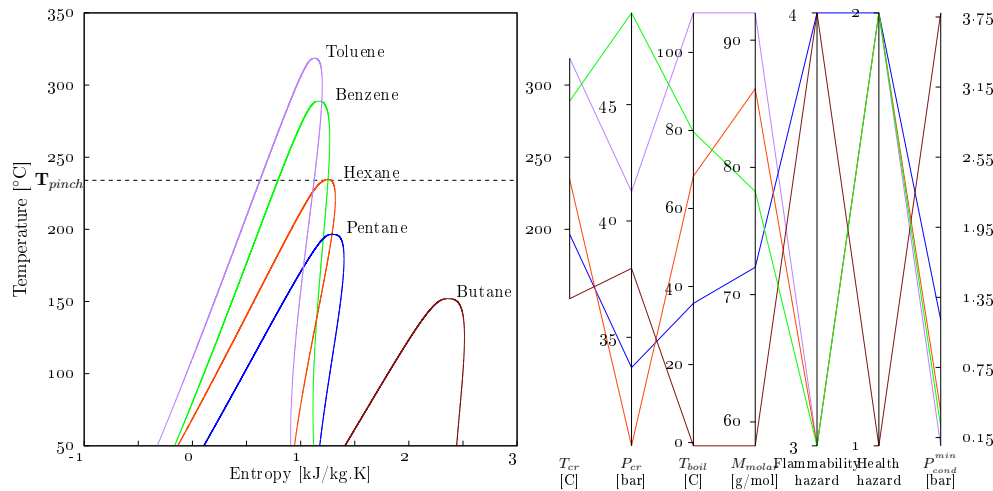


FIGURE 5.6— Selected working fluids for the case study (case II), T-s diagram (left), main properties (right)

better. Moreover, for high electricity production, fluids with critical temperature slightly lower than the pinch point (i.e., pentane) exhibit lower investment cost for the same level of electricity production among the considered fluids. Hexane is a special case for this example as its critical temperature coincides with the pinch point, which explains its high performance over the entire range of electricity production.

Point “A” on Figure 5.7b for pentane is selected for further explanation of the results. This solution lies on the global non-dominated frontier (Figure 5.7f). The temperature-entropy diagram of this solution is demonstrated in Figure 5.8b and exhibits a combination of four ORC features, i.e., multi-stage, transcritical, reheating, and bleeding. The integration of ORC for this solution with the process waste heat is illustrated using the integrated composite curve [102] (Figure 5.8a). It is observed that combination of transcritical evaporation, reheating and multiple condensation steps provides better matching with the process profile. Nevertheless, this figure does not show how the heat flows between different thermal streams. To this end, Figure 5.8c illustrates the heat load distribution among the thermal streams below the pinch point (HEN does not change above the pinch point) with, and without, ORC integration. It is observed that in this case, stream H_3 is providing the required heat both for reheating and supercritical evaporation in the ORC which allows for better use of this high temperature heat since the cold utility placement is now at lower temperature (pentane condensation at 1.17 bar). The detailed HEN design is also performed for this case (Figure 5.9, only shown for below the pinch) using the NLP formulation [103, 104] based on the results of heat load distribution. The cost associated with the HEN shown in Figure 5.9 is 26,700 USD/yr, which compares well with the 28,800 USD/yr estimation obtained from the targeting method used in this chapter (Equation 5.4).

This work enunciates that it is imperative to consider all possible architectures to discover the optimal ORC integration with a source of waste heat. Combinations of different cycles and features exhibit performances and trade-offs which are often non-intuitive and intractable to solve manually. Additionally, at least for this popular case study, fluids with critical points close to the process pinch point demonstrate better economic and energetic objectives which should be considered in other applications.

5.3 RESULTS AND DISCUSSION

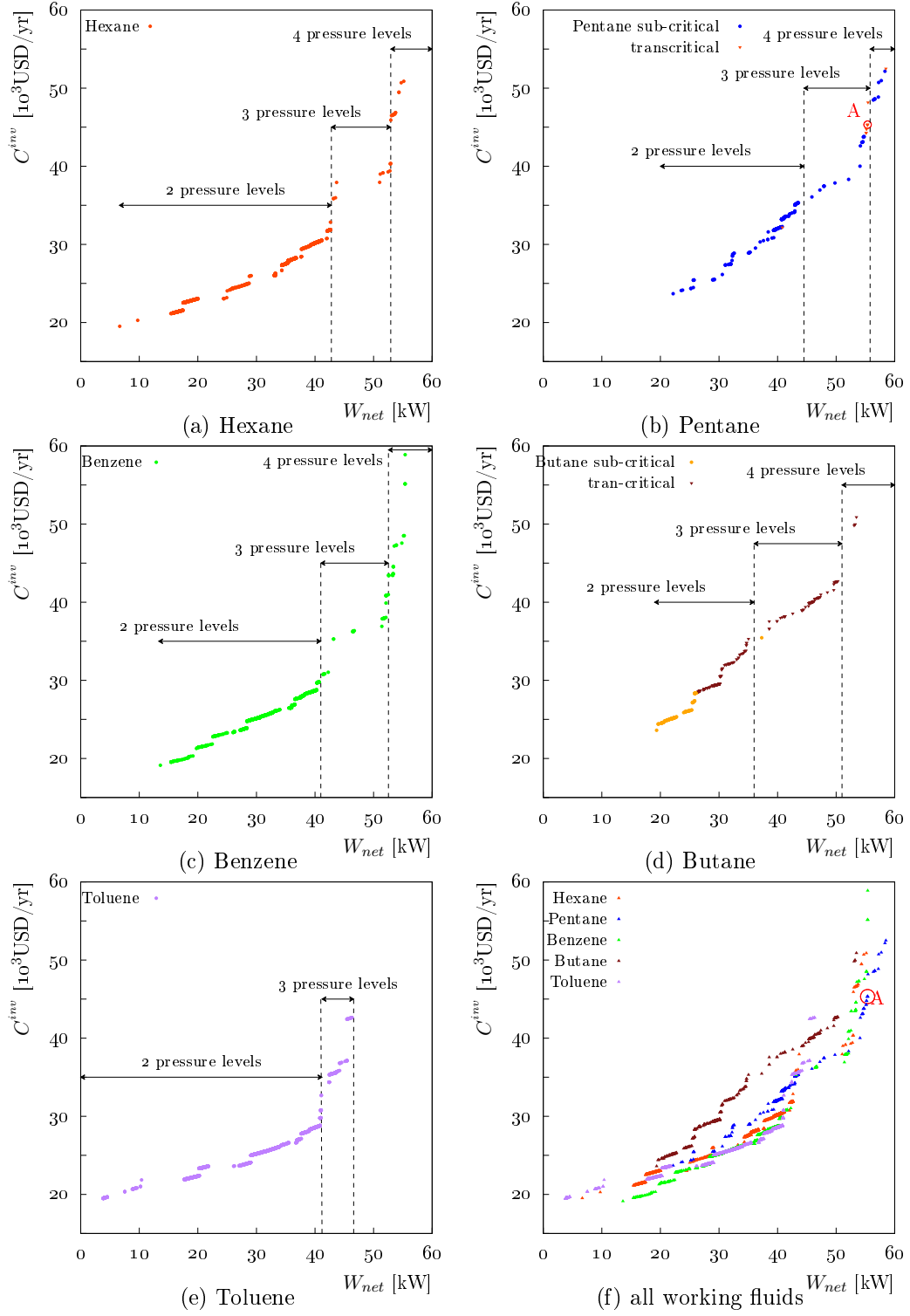
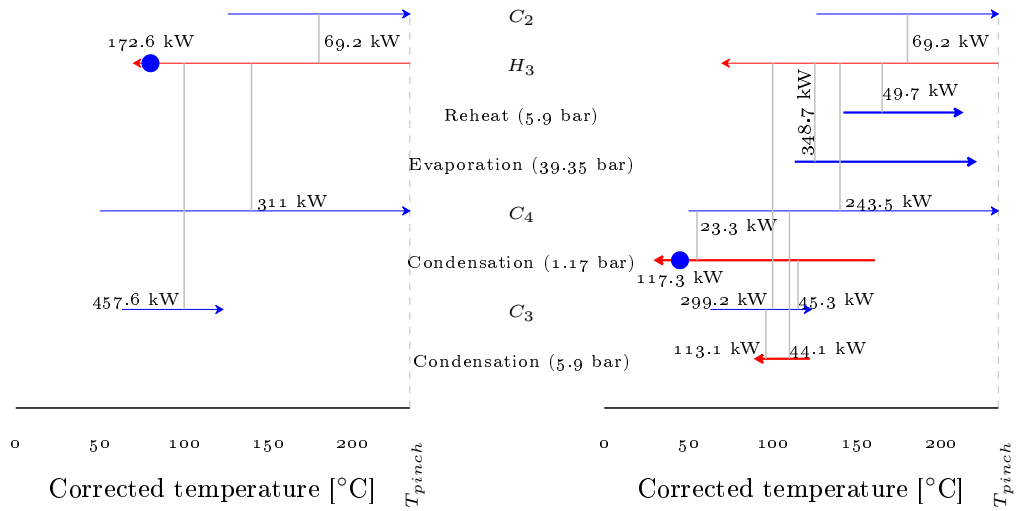
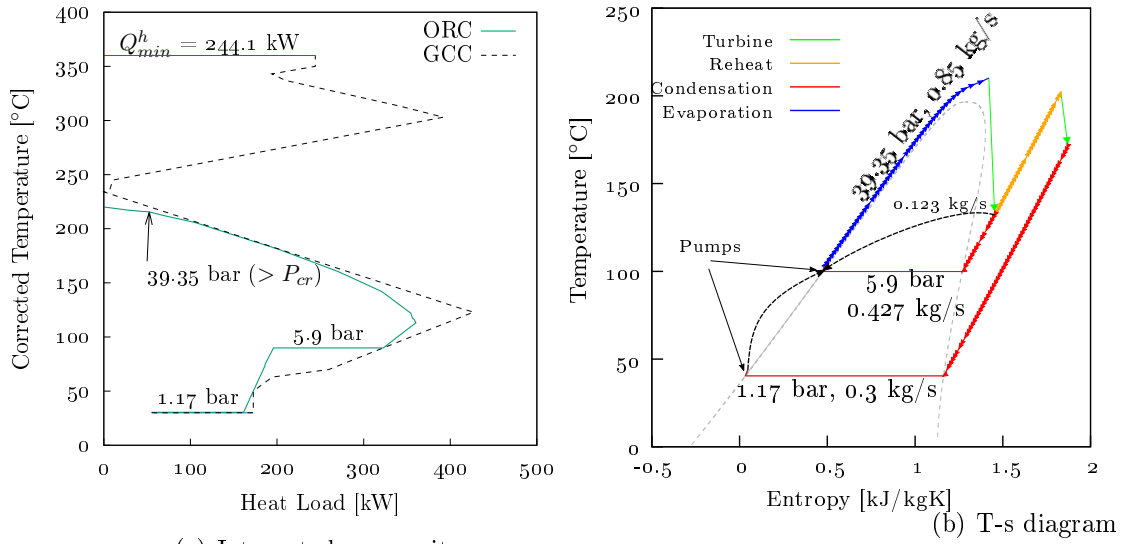


FIGURE 5.7—Case II Pareto frontiers for Hexane (a), Pentane (b), Benzene (c), Butane (d), Toluene (e)



(c) Heat load distribution before (left) and after (right) ORC integration

FIGURE 5.8—Results of solution point “A” (Figure 5.7b): Two-stage transcritical cycle with reheat and open feed liquid heater

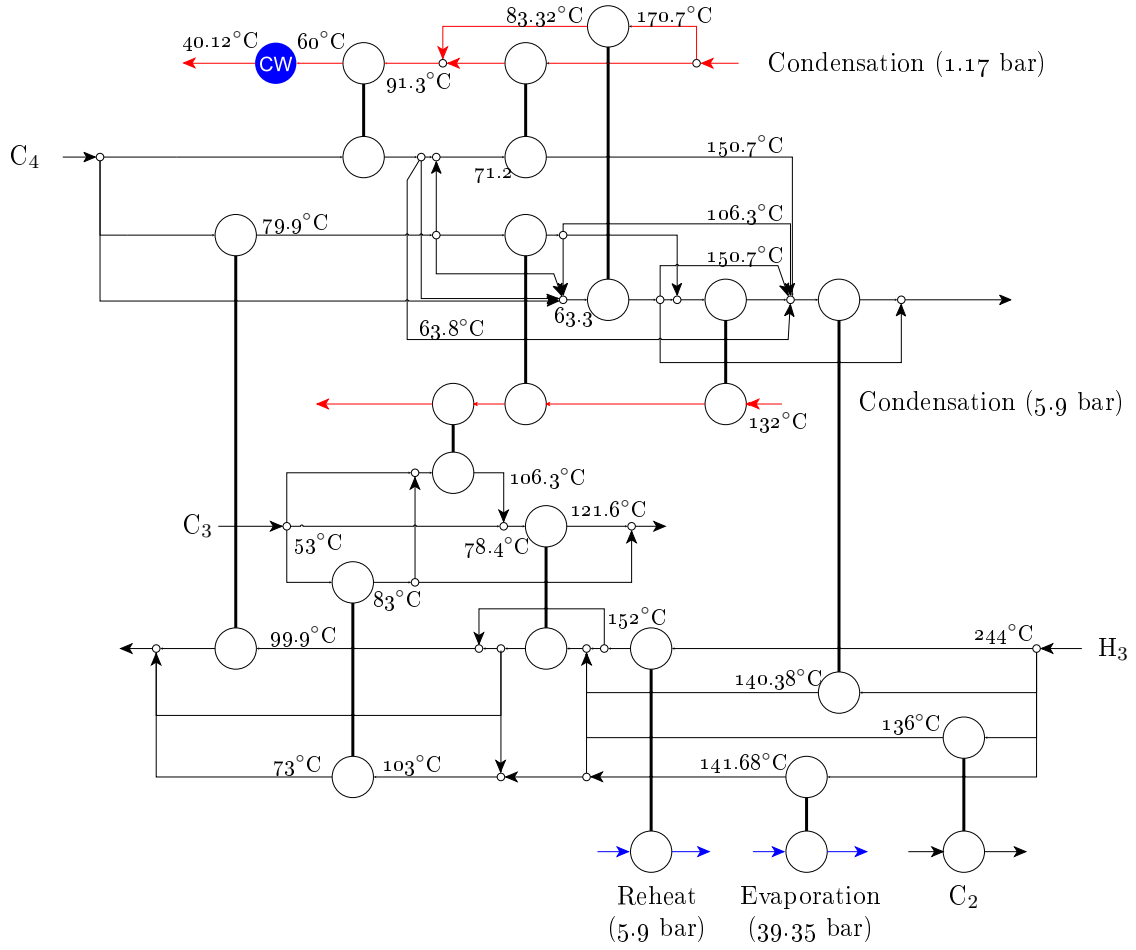


FIGURE 5.9—Results of solution point “A” (Figure 5.7b): HEN for below the pinch point

5.3.2.3 Case III: multi-objective optimization including heat transfer coefficients

Optimization approaches for waste heat recovery using ORCs often assume heat transfer coefficients to calculate the heat exchanger network area. Since fluid selection is an important component of the optimization framework, it was decided that this comprehensive work should also include calculation of the heat transfer coefficients to better estimate the heat exchanger costs for the proposed systems. The approach, assumptions and equations for including heat transfer coefficient calculations in the optimization are included in 5.2.4. From a comprehensive set of working fluids, an initial heuristic screening was used to reduce the problem size by quickly eliminating candidate fluids based on critical temperature, boiling point, global warming potential (GWP), and dryness which deviated from the range where the best fluids would be found, based on the literature and the results of Case II. Main properties of the 14 selected fluids and their corresponding T-s diagrams are shown in Figure 5.10. The “slope” in Figure 5.10a is defined as the slope of the vapor saturated curve at 100°C and is directly proportional to fluid dryness. An interactive parallel coordinate visualization tool is developed for facilitating the working fluid selection (Appendix C).

The choice of working fluids was defined as an integer decision variable at the outer GA level. To avoid identification of a local optimum as the global optimum, several types of cross-over and mutation procedures were tested. Additionally, the results from Case II (Figure 5.7) pointed to a reduction of the superstructure to consider only four pressure levels since solutions with five and six did not appear on the global Pareto frontier with any of the five common fluids. The lower bound of the lowest pressure level was set at 1 bar. The GA settings are presented in Table 5.9.

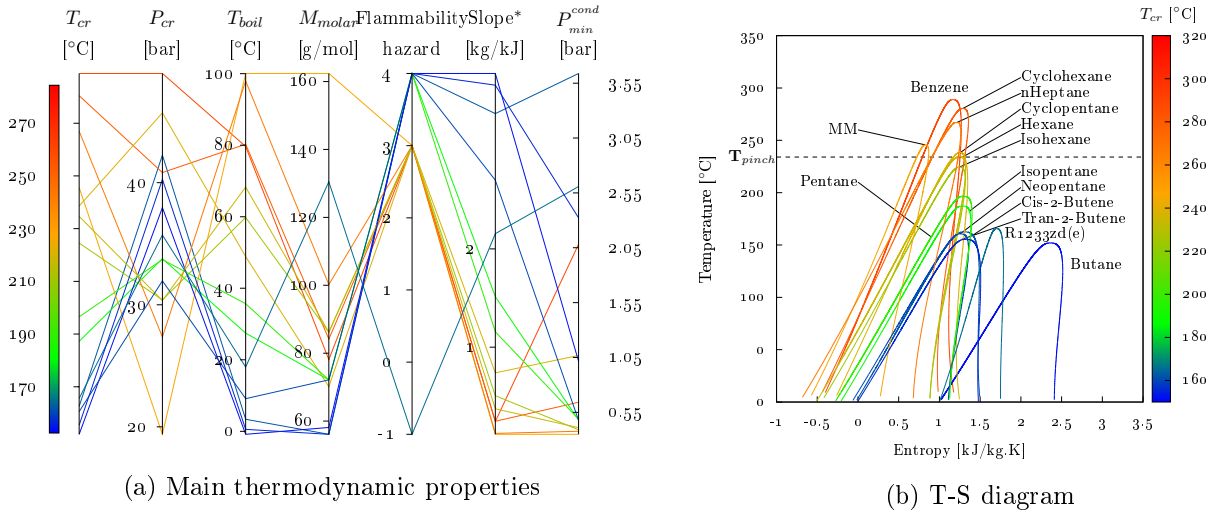


FIGURE 5.10—Selected working fluids for the case study (case III)

Figure 5.11a shows the non-dominated frontier where it is clearly visible that four groups of working fluids dominate for this case, namely: hexane isomers (n-hexane and isohexane), pentane, cyclopentane, and benzene. The optimal working fluid for the high electricity production range is pentane with three to four active pressure levels. The majority of solutions based on pentane are transcritical cycles. It should be noted that the results of Case III are not comparable with the previous case due to the pressure constraint and heat transfer calculations; however, it is observed that fluids with critical temperature below the pinch point can achieve higher electricity production.

The SIC (Equation 5.9) of the solutions of the Pareto frontier are also plotted in Figure 5.11b. The minimum SIC was found to be 0.136 USD/kWh (1,200 USD/kW_{el}) for a 43 kW_{el} ORC (grassroots cost, Equation 5.17) using hexane as the working fluid. The specific cost of the solutions (represented on the right axis in Figure 5.11b) lies between 1,200–1,500 USD/kW_{el} in the power range 25–60 kW. Based on a recent study by Tocci et al. [24] on competitiveness of small-scale ORCs, the specific cost should not exceed 2,000 USD/kW_{el} to ensure that ORCs are cost-competitive with other technologies, particularly internal combustion engines, solar photovoltaics and gas turbines. As discussed by Tocci et al. [24], the aforementioned technologies have weaknesses including cost of fuel, CO₂ emissions and production intermittency in the case of solar photovoltaic. The number of turbines and pumps and their contributions to the total capital cost are plotted in Figure 5.11c. This figure exhibits that the HEN cost accounts for more than 60 % of the total investment cost which provides further motivation for rigorous heat transfer coefficient calculations as were performed here. By producing more electricity, the cycle becomes more integrated with the process and hence the share of C^{HEN} increases.

5.3 RESULTS AND DISCUSSION

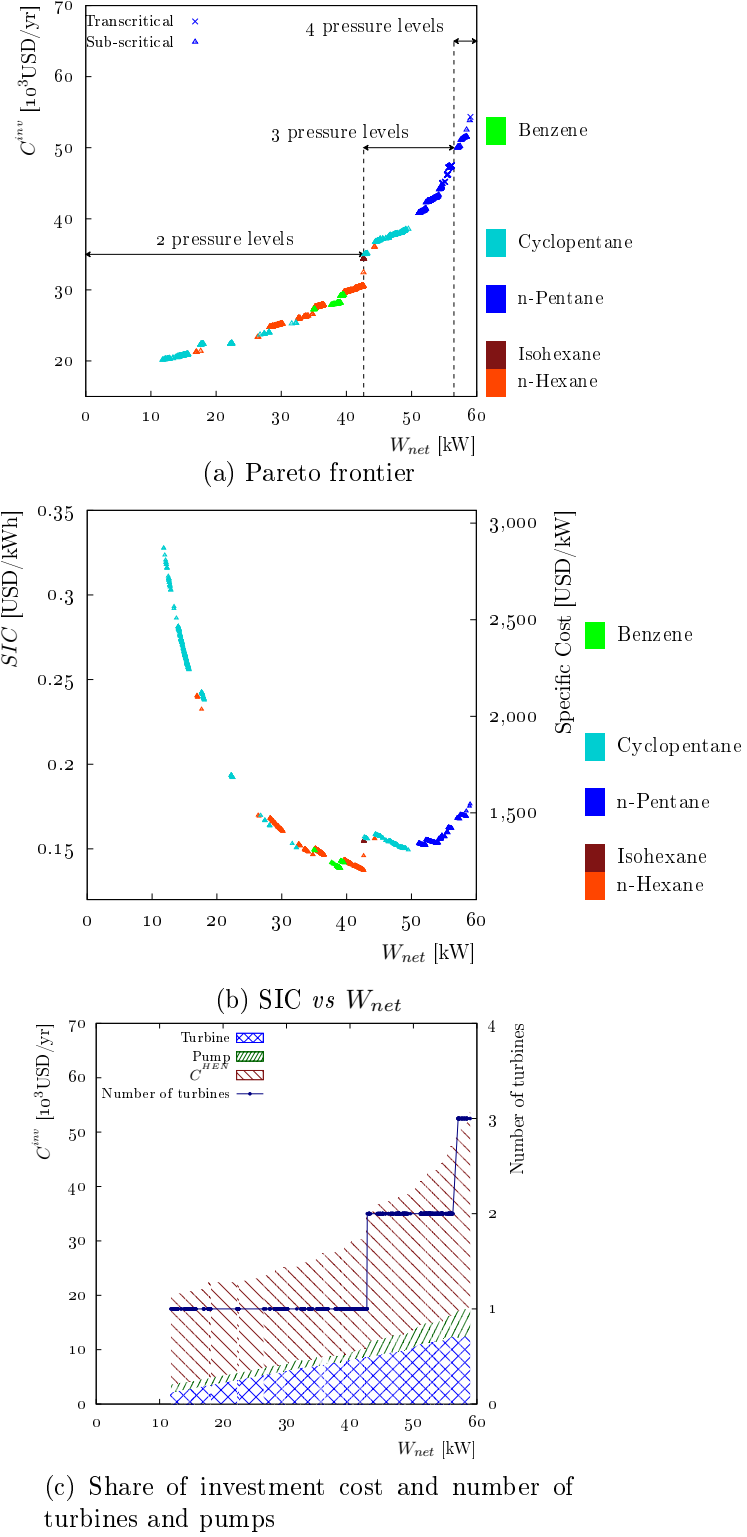


FIGURE 5.11—Case III: (a) Pareto frontier, (b) Specific investment cost SIC, (c) investment cost partitioning

5.4 Conclusion

This work presented a systematic methodology for optimal integration of ORCs for waste heat recovery in industrial processes. It consists of a novel ORC superstructure which is solved using a two-stage solution strategy. The superstructure includes several ORC architectures including regenerative, superheating, reheating, turbine-bleeding (open/closed feed liquid heater), transcritical, and multi-stage cycles. Depending on the case specificities and the industrial processes requirements, several of these cycles can be combined or forbidden in the superstructure. Maintaining linearity in the heat cascade formulation also prompted development of a novel dynamic linearization technique for the hot and cold streams of the superstructure.

The first level in the solution strategy is handled by GA in which the working fluid and its operating conditions are optimized while the second level, a deterministic MILP model, solves the optimal ORC architecture and equipment sizes. The second level could be extended to heat exchanger network synthesis but was simplified in this approach to consider only the heat exchanger area and minimum number of connections. The overall methodology considers a variety of objective functions and potential working fluids and is extensible in both aspects to include alternative objectives or working fluids, such as water (steam) or supercritical CO₂. The multi-objective optimization generates a set of competing solutions to be analyzed by the engineers who will choose the most appropriate solution.

Applications of the methodology on a literature case study showed that combining several ORC architectures yields economic and energetic benefits as illustrated in Figure 5.8. The methodology provides a promising set of solutions which is essential for industrial decision-making processes. Benchmarking the method against the published literature revealed several issues with previous studies including inadequate treatment of fluid thermodynamics, *a priori* selection of working fluid, mass imbalances and dubious assumptions regarding heat transfer coefficients; each of these shortcomings were addressed by the comprehensive methodology presented herein.

Future work will focus on adaptation of the proposed methodology for large-scale industrial applications by incorporating practical constraints and HEN design. This includes addressing multi-period operation with seasonal variability of operating conditions and interplant operations, where the ORC can be combined with storage to provide a flexible heat transfer medium to compete with conventional ones. To this end, pursuing a holistic approach will require improved solution strategies to alleviate the computational burden of large-scale cases. The methodology presented should be applied to industrial cases where significant sources of waste heat remain after recovering the maximum amount of energy within the processes. Nonetheless, the varying price of electricity production can directly affect the economic viability of ORC integration in such cases which requires further analysis of major market forces and their associated uncertainties. ORCs are therefore an important technology for recovering waste heat and must be implemented according to such a systematic method. Industrial applications will drive equipment manufacturers and researchers to explore and provide solutions for major industrial sectors. ■

References

- [1] M. Bendig, F. Maréchal, D. Favrat, Defining “Waste Heat” for industrial processes, *Applied Thermal Engineering* 61 (1) (2013) 134–142, ISSN 1359-4311.
- [2] B. F. Tchanche, G. Lambrinos, A. Frangoudakis, G. Papadakis, Low-grade heat conversion into power using organic Rankine cycles – A review of various applications, *Renewable and Sustainable Energy Reviews* 15 (8) (2011) 3963–3979, ISSN 1364-0321.
- [3] M. Z. Stijepovic, P. Linke, Optimal waste heat recovery and reuse in industrial zones, *Energy* 36 (7) (2011) 4019–4031, ISSN 0360-5442.
- [4] G. Oluleye, M. Jobson, R. Smith, S. J. Perry, Evaluating the potential of process sites for waste heat recovery, *Applied Energy* 161 (2016) 627–646, ISSN 0306-2619.
- [5] K. Holiasos, V. Manousiouthakis, Minimum hot/cold/electric utility cost for heat exchange networks, *Computers & Chemical Engineering* 26 (1) (2002) 3–16, ISSN 0098-1354.
- [6] G. Oluleye, R. Smith, A mixed integer linear programming model for integrating thermodynamic cycles for waste heat exploitation in process sites, *Applied Energy* 178 (2016) 434–453, ISSN 0306-2619.
- [7] N. B. Desai, S. Bandyopadhyay, Process integration of organic Rankine cycle, *Energy* 34 (10) (2009) 1674–1686, ISSN 0360-5442.
- [8] K. Rahbar, S. Mahmoud, R. K. Al-Dadah, N. Moazami, S. A. Mirhadizadeh, Review of organic Rankine cycle for small-scale applications, *Energy Conversion and Management* 134 (2017) 135–155, ISSN 0196-8904.
- [9] S. Quoilin, V. Lemort, Technological and economical survey of organic Rankine cycle systems, in: 5th European Conference Economic and Management of Energy in Industry, Portugal, 1–12, URL https://www.researchgate.net/publication/228540064_Technological_and_economical_survey_of_organic_Rankine_cycle_systems, 2009.
- [10] A. Schuster, S. Karellas, E. Kakaras, H. Spliethoff, Energetic and economic investigation of Organic Rankine Cycle applications, *Applied Thermal Engineering* 29 (8–9) (2009) 1809–1817, ISSN 1359-4311.
- [11] B. F. Tchanche, M. Pétrissans, G. Papadakis, Heat resources and organic Rankine cycle machines, *Renewable and Sustainable Energy Reviews* 39 (2014) 1185–1199, ISSN 1364-0321.
- [12] T. Wang, Y. Zhang, Z. Peng, G. Shu, A review of researches on thermal exhaust heat recovery with Rankine cycle, *Renewable and Sustainable Energy Reviews* 15 (6) (2011) 2862–2871, ISSN 1364-0321.
- [13] F. Vélez, J. J. Segovia, M. C. Martín, G. Antolín, F. Chejne, A. Quijano, A technical, economical and market review of organic Rankine cycles for the conversion of low-grade heat for power generation, *Renewable and Sustainable Energy Reviews* 16 (6) (2012) 4175–4189, ISSN 1364-0321.
- [14] C. Sprouse III, C. Depcik, Review of organic Rankine cycles for internal combustion engine exhaust waste heat recovery, *Applied Thermal Engineering* 51 (1–2) (2013) 711–722, ISSN

1359-4311.

- [15] F. Maréchal, B. Kalitventzeff, A Methodology for the Optimal Insertion of Organic Rankine Cycles in Industrial Processes, 2nd International Symposium of Process Integration .
- [16] S. Quoilin, R. Aumann, A. Grill, A. Schuster, V. Lemort, H. Spliethoff, Dynamic modeling and optimal control strategy of waste heat recovery Organic Rankine Cycles, *Applied Energy* 88 (6) (2011) 2183–2190, ISSN 0306-2619.
- [17] H. Chen, D. Y. Goswami, E. K. Stefanakos, A review of thermodynamic cycles and working fluids for the conversion of low-grade heat, *Renewable and Sustainable Energy Reviews* 14 (9) (2010) 3059–3067, ISSN 1364-0321.
- [18] J. Bao, L. Zhao, A review of working fluid and expander selections for organic Rankine cycle, *Renewable and Sustainable Energy Reviews* 24 (2013) 325–342, ISSN 1364-0321.
- [19] S. Quoilin, M. V. D. Broek, S. Declaye, P. Dewallef, V. Lemort, Techno-economic survey of Organic Rankine Cycle (ORC) systems, *Renewable and Sustainable Energy Reviews* 22 (2013) 168–186, ISSN 1364-0321.
- [20] D. Ziviani, A. Beyene, M. Venturini, Advances and challenges in ORC systems modeling for low grade thermal energy recovery, *Applied Energy* 121 (2014) 79–95, ISSN 0306-2619.
- [21] S. Lecompte, H. Huisseune, M. van den Broek, B. Vanslambrouck, M. De Paepe, Review of organic Rankine cycle (ORC) architectures for waste heat recovery, *Renewable and Sustainable Energy Reviews* 47 (2015) 448–461, ISSN 1364-0321.
- [22] P. Linke, A. I. Papadopoulos, P. Seferlis, Systematic Methods for Working Fluid Selection and the Design, Integration and Control of Organic Rankine Cycles—A Review, *Energies* 8 (6) (2015) 4755–4801.
- [23] V. Chintala, S. Kumar, J. K. Pandey, A technical review on waste heat recovery from compression ignition engines using organic Rankine cycle, *Renewable and Sustainable Energy Reviews* 81, Part 1 (2018) 493–509, ISSN 1364-0321.
- [24] L. Tocchi, T. Pal, I. Pesmazoglou, B. Franchetti, Small Scale Organic Rankine Cycle (ORC): A Techno-Economic Review, *Energies* 10 (4) (2017) 413.
- [25] M. Imran, F. Haglind, M. Asim, J. Zeb Alvi, Recent research trends in organic Rankine cycle technology: A bibliometric approach, *Renewable and Sustainable Energy Reviews* 81, Part 1 (2018) 552–562, ISSN 1364-0321.
- [26] T. C. Hung, T. Y. Shai, S. K. Wang, A review of organic rankine cycles (ORCs) for the recovery of low-grade waste heat, *Energy* 22 (7) (1997) 661–667, ISSN 0360-5442.
- [27] R. Rayegan, Y. X. Tao, A procedure to select working fluids for Solar Organic Rankine Cycles (ORCs), *Renewable Energy* 36 (2) (2011) 659–670, ISSN 0960-1481.
- [28] K. J. DiGenova, B. B. Botros, J. G. Brisson, Method for customizing an organic Rankine cycle to a complex heat source for efficient energy conversion, demonstrated on a Fischer Tropsch plant, *Applied Energy* 102 (2013) 746–754, ISSN 0306-2619.
- [29] S. Karellas, A. Schuster, Supercritical fluid parameters in organic rankine cycle applications, *International Journal of Thermodynamics* 11 (3) (2008) 101–108, ISSN 1301-9724.
- [30] H. Xu, N. Gao, T. Zhu, Investigation on the fluid selection and evaporation parametric optimization for sub- and supercritical organic Rankine cycle, *Energy* 96 (2016) 59–68, ISSN 0360-5442.
- [31] D. Meinel, C. Wieland, H. Spliethoff, Economic comparison of ORC (Organic Rankine cycle) processes at different scales, *Energy* 74 (2014) 694–706, ISSN 0360-5442.
- [32] D. Meinel, C. Wieland, H. Spliethoff, Effect and comparison of different working fluids on a two-stage organic rankine cycle (ORC) concept, *Applied Thermal Engineering* 63 (1) (2014)

-
- 246–253, ISSN 1359-4311.
- [33] X. Li, X. Li, Q. Zhang, The first and second law analysis on an organic Rankine cycle with ejector, *Solar Energy* 93 (2013) 100–108, ISSN 0038-092X.
 - [34] X. Luo, J. Hu, J. Zhao, B. Zhang, Y. Chen, S. Mo, Multi-objective optimization for the design and synthesis of utility systems with emission abatement technology concerns, *Applied Energy* 136 (2014) 1110–1131, ISSN 0306-2619.
 - [35] B. J. Zhang, K. Liu, X. L. Luo, Q. L. Chen, W. K. Li, A multi-period mathematical model for simultaneous optimization of materials and energy on the refining site scale, *Applied Energy* 143 (2015) 238–250, ISSN 0306-2619.
 - [36] J. C. Bruno, F. Fernandez, F. Castells, I. E. Grossmann, A Rigorous MINLP Model for the Optimal Synthesis and Operation of Utility Plants, *Chemical Engineering Research and Design* 76 (3) (1998) 246–258, ISSN 0263-8762.
 - [37] J. A. Caballero, M. A. Navarro, R. Ruiz-Femenia, I. E. Grossmann, Integration of different models in the design of chemical processes: Application to the design of a power plant, *Applied Energy* 124 (2014) 256–273, ISSN 0306-2619.
 - [38] L. M. Romeo, S. Espatolero, I. Bolea, Designing a supercritical steam cycle to integrate the energy requirements of CO₂ amine scrubbing, *International Journal of Greenhouse Gas Control* 2 (4) (2008) 563–570, ISSN 1750-5836.
 - [39] P. S. Varbanov, S. Doyle, R. Smith, Modelling and Optimization of Utility Systems, *Chemical Engineering Research and Design* 82 (5) (2004) 561–578, ISSN 0263-8762.
 - [40] Chen, I. E. Grossmann, Recent Developments and Challenges in Optimization-Based Process Synthesis, *Annual Review of Chemical and Biomolecular Engineering* 8 (1) (2017) null.
 - [41] P. Y. Liew, W. L. Theo, S. R. Wan Alwi, J. S. Lim, Z. Abdul Manan, J. J. Klemeš, P. S. Varbanov, Total Site Heat Integration planning and design for industrial, urban and renewable systems, *Renewable and Sustainable Energy Reviews* 68, Part 2 (2017) 964–985, ISSN 1364-0321.
 - [42] A. Toffolo, A. Lazzaretto, G. Manente, M. Paci, A multi-criteria approach for the optimal selection of working fluid and design parameters in Organic Rankine Cycle systems, *Applied Energy* 121 (2014) 219–232, ISSN 0306-2619.
 - [43] J. Xu, C. Yu, Critical temperature criterion for selection of working fluids for subcritical pressure Organic Rankine cycles, *Energy* 74 (2014) 719–733, ISSN 0360-5442.
 - [44] M. Z. Stijepovic, P. Linke, A. I. Papadopoulos, A. S. Grujic, On the role of working fluid properties in Organic Rankine Cycle performance, *Applied Thermal Engineering* 36 (2012) 406–413, ISSN 1359-4311.
 - [45] O. Badr, P. W. O’Callaghan, S. D. Probert, Rankine-cycle systems for harnessing power from low-grade energy sources, *Applied Energy* 36 (4) (1990) 263–292, ISSN 0306-2619.
 - [46] H. Chen, D. Yogi Goswami, M. M. Rahman, E. K. Stefanakos, Energetic and exergetic analysis of CO₂- and R₃₂-based transcritical Rankine cycles for low-grade heat conversion, *Applied Energy* 88 (8) (2011) 2802–2808, ISSN 0306-2619.
 - [47] D.-H. Kwak, M. Binns, J.-K. Kim, Integrated design and optimization of technologies for utilizing low grade heat in process industries, *Applied Energy* 131 (2014) 307–322, ISSN 0306-2619.
 - [48] M. Bendig, D. Favrat, F. Marechal, Methodology for Identification of Suitable ORC-Cycle and Working-Fluid using Integration with Multiple Objectives, *Pres 2014, 17Th Conference On Process Integration, Modelling And Optimisation For Energy Saving And Pollution Reduction*, Pts 1-3 39 (2014) 1141–1146.
 - [49] L. Pierobon, T.-V. Nguyen, U. Larsen, F. Haglind, B. Elmegaard, Multi-objective optimization

- of organic Rankine cycles for waste heat recovery: Application in an offshore platform, *Energy* 58 (2013) 538–549, ISSN 0360-5442.
- [50] S. Lecompte, S. Lemmens, A. Verbruggen, M. van den Broek, M. De Paepe, Thermo-economic Comparison of Advanced Organic Rankine Cycles, *Energy Procedia* 61 (2014) 71–74, ISSN 1876-6102.
- [51] F. A. Boyaghchi, P. Heidarnajad, Thermoeconomic assessment and multi objective optimization of a solar micro CCHP based on Organic Rankine Cycle for domestic application, *Energy Conversion and Management* 97 (2015) 224–234, ISSN 0196-8904.
- [52] F. Yang, H. Zhang, S. Song, C. Bei, H. Wang, E. Wang, Thermoeconomic multi-objective optimization of an organic Rankine cycle for exhaust waste heat recovery of a diesel engine, *Energy* 93, Part 2 (2015) 2208–2228, ISSN 0360-5442.
- [53] S. Lee, Multi-parameter optimization of cold energy recovery in cascade Rankine cycle for LNG regasification using genetic algorithm, *Energy* 118 (2017) 776–782, ISSN 0360-5442.
- [54] A. I. Papadopoulos, M. Stijepovic, P. Linke, P. Seferlis, S. Voutetakis, Toward Optimum Working Fluid Mixtures for Organic Rankine Cycles using Molecular Design and Sensitivity Analysis, *Industrial & Engineering Chemistry Research* 52 (34) (2013) 12116–12133, ISSN 0888-5885.
- [55] P. M. Harper, R. Gani, P. Kolar, T. Ishikawa, Computer-aided molecular design with combined molecular modeling and group contribution, *Fluid Phase Equilibria* 158 (1999) 337–347, ISSN 0378-3812.
- [56] W. Su, L. Zhao, S. Deng, Simultaneous working fluids design and cycle optimization for Organic Rankine cycle using group contribution model, *Applied Energy* 202 (2017) 618–627, ISSN 0306-2619.
- [57] A. Inselberg, The plane with parallel coordinates, *The Visual Computer* 1 (2) (1985) 69–91, ISSN 0178-2789, 1432-2315.
- [58] D. W. Townsend, B. Linnhoff, Heat and power networks in process design. Part I: Criteria for placement of heat engines and heat pumps in process networks, *AIChE Journal* 29 (5) (1983) 742–748, ISSN 1547-5905.
- [59] D. W. Townsend, B. Linnhoff, Heat and power networks in process design. Part II: Design procedure for equipment selection and process matching, *AIChE Journal* 29 (5) (1983) 748–771, ISSN 1547-5905.
- [60] T. R. Colmenares, W. D. Seider, Heat and power integration of chemical processes, *AIChE Journal* 33 (6) (1987) 898–915, ISSN 1547-5905.
- [61] A. Toffolo, A synthesis/design optimization algorithm for Rankine cycle based energy systems, *Energy* 66 (2014) 115–127, ISSN 0360-5442.
- [62] F. Maréchal, B. Kalitventzeff, Process integration: Selection of the optimal utility system, *Computers & Chemical Engineering* 22, Supplement 1 (1998) S149–S156, ISSN 0098-1354.
- [63] M. Z. Stijepovic, A. I. Papadopoulos, P. Linke, V. Stijepovic, A. S. Grujic, M. Kijevčanin, P. Seferlis, Organic Rankine Cycle system performance targeting and design for multiple heat sources with simultaneous working fluid selection, *Journal of Cleaner Production* 142, Part 4 (2017) 1950–1970, ISSN 0959-6526.
- [64] H. Yu, J. Eason, L. T. Biegler, X. Feng, Process Integration and Superstructure Optimization of Organic Rankine Cycles (ORCs) with Heat Exchanger Network Synthesis, *Computers & Chemical Engineering* ISSN 0098-1354.
- [65] S. A. Papoulias, I. E. Grossmann, A structural optimization approach in process synthesis—II: Heat recovery networks, *Computers & Chemical Engineering* 7 (6) (1983) 707–721, ISSN 0098-1354.

-
- [66] T. R. Colmenares, W. D. Seider, Synthesis of utility systems integrated with chemical processes, *Industrial & Engineering Chemistry Research* 28 (1) (1989) 84–93.
- [67] B. J. Hipólito-Valencia, E. Rubio-Castro, J. M. Ponce-Ortega, M. Serna-González, F. Nápoles-Rivera, M. M. El-Halwagi, Optimal integration of organic Rankine cycles with industrial processes, *Energy Conversion and Management* 73 (2013) 285–302, ISSN 0196-8904.
- [68] L. F. Lira-Barragán, J. M. Ponce-Ortega, M. Serna-González, M. M. El-Halwagi, Sustainable Integration of Trigeneration Systems with Heat Exchanger Networks, *Industrial & Engineering Chemistry Research* 53 (7) (2014) 2732–2750, ISSN 0888-5885.
- [69] C.-L. Chen, F.-Y. Chang, T.-H. Chao, H.-C. Chen, J.-Y. Lee, Heat-Exchanger Network Synthesis Involving Organic Rankine Cycle for Waste Heat Recovery, *Industrial & Engineering Chemistry Research* 53 (44) (2014) 16924–16936, ISSN 0888-5885.
- [70] J. Song, Y. Li, C.-w. Gu, L. Zhang, Thermodynamic analysis and performance optimization of an ORC (Organic Rankine Cycle) system for multi-strand waste heat sources in petroleum refining industry, *Energy* 71 (2014) 673–680, ISSN 0360-5442.
- [71] B. J. Hipólito-Valencia, E. Rubio-Castro, J. M. Ponce-Ortega, M. Serna-González, F. Nápoles-Rivera, M. M. El-Halwagi, Optimal design of inter-plant waste energy integration, *Applied Thermal Engineering* 62 (2) (2014) 633–652, ISSN 1359-4311.
- [72] C. G. Gutiérrez-Arriaga, F. Abdelhady, H. S. Bamufleh, M. Serna-González, M. M. El-Halwagi, J. M. Ponce-Ortega, Industrial waste heat recovery and cogeneration involving organic Rankine cycles, *Clean Technologies and Environmental Policy* 17 (3) (2015) 767–779, ISSN 1618-954X, 1618-9558.
- [73] H. Yu, J. Eason, L. T. Biegler, X. Feng, Simultaneous heat integration and techno-economic optimization of Organic Rankine Cycle (ORC) for multiple waste heat stream recovery, *Energy* 119 (2017) 322–333, ISSN 0360-5442.
- [74] F. Maréchal, B. Kalitventzeff, Targeting the optimal integration of steam networks: Mathematical tools and methodology, *Computers & Chemical Engineering* 23, Supplement (1999) S133–S136, ISSN 0098-1354.
- [75] I. H. Bell, J. Wronski, S. Quoilin, V. Lemort, Pure and Pseudo-pure Fluid Thermophysical Property Evaluation and the Open-Source Thermophysical Property Library CoolProp, *Industrial & Engineering Chemistry Research* 53 (6) (2014) 2498–2508.
- [76] E. Cayer, N. Galanis, H. Nesreddine, Parametric study and optimization of a transcritical power cycle using a low temperature source, *Applied Energy* 87 (4) (2010) 1349–1357, ISSN 0306-2619.
- [77] S. Quoilin, S. Declaye, B. F. Tchanche, V. Lemort, Thermo-economic optimization of waste heat recovery Organic Rankine Cycles, *Applied Thermal Engineering* 31 (14–15) (2011) 2885–2893, ISSN 1359-4311.
- [78] S. Lecompte, S. Lemmens, H. Huisseune, M. van den Broek, M. De Paepe, Multi-Objective Thermo-Economic Optimization Strategy for ORCs Applied to Subcritical and Transcritical Cycles for Waste Heat Recovery, *Energies* 8 (4) (2015) 2714–2741.
- [79] B. Linnhoff, S. Ahmad, Cost optimum heat exchanger networks—1. Minimum energy and capital using simple models for capital cost, *Computers & Chemical Engineering* 14 (7) (1990) 729–750, ISSN 0098-1354.
- [80] M. Kermani, Z. Périn-Levasseur, M. Benali, L. Savulescu, F. Maréchal, A novel MILP approach for simultaneous optimization of water and energy: Application to a Canadian softwood Kraft pulping mill, *Computers & Chemical Engineering* ISSN 0098-1354.
- [81] M. Bendig, Integration of Organic Rankine Cycles for Waste Heat Recovery in Industrial Processes, Ph.D. thesis, STI, Lausanne, doi: `\bibinfo{doi}{10.5075/epfl-thesis-6536}`, 2015.

-
- [82] M. Soffiato, C. A. Frangopoulos, G. Manente, S. Rech, A. Lazzaretto, Design optimization of ORC systems for waste heat recovery on board a LNG carrier, *Energy Conversion and Management* 92 (2015) 523–534, ISSN 0196-8904.
- [83] R. C. Bailie, J. A. Shaeiwitz, R. Turton, W. B. Whiting, *Analysis, Synthesis, and Design of Chemical Processes*, Third Edition, Prentice Hall, 3 edn., ISBN 978-0-13-507291-2, URL <http://proquest.safaribooksonline.com/9780135072912>, 2012.
- [84] M. Taal, I. Bulatov, J. Klemeš, P. Stehlik, Cost estimation and energy price forecasts for economic evaluation of retrofit projects, *Applied Thermal Engineering* 23 (14) (2003) 1819–1835, ISSN 1359-4311.
- [85] R. K. Shah, D. P. Sekulić, Heat Exchanger Design Procedures, in: *Fundamentals of Heat Exchanger Design*, John Wiley & Sons, Inc., ISBN 978-0-470-17260-5, 601–672, doi: \bibinfo{doi}{10.1002/9780470172605.ch9}, URL <http://dx.doi.org/10.1002/9780470172605.ch9>, 2007.
- [86] J. E. Edwards, Design and Rating of Shell and Tube Heat Exchangers, Tech. Rep., P & I Design Ltd, Teesside, UK, URL http://www.chemstations.com/content/documents/Technical_Articles/shell.pdf, 2009.
- [87] V. Gnielinski, New equations for heat and mass transfer in turbulent pipe and channel flows, *International Journal of Chemical Engineering* 16 (1976) 359–68.
- [88] E. Cayer, N. Galanis, M. Desilets, H. Nesreddine, P. Roy, Analysis of a carbon dioxide transcritical power cycle using a low temperature source, *Applied Energy* 86 (7–8) (2009) 1055–1063, ISSN 0306-2619.
- [89] Z. Shengjun, W. Huaixin, G. Tao, Performance comparison and parametric optimization of subcritical Organic Rankine Cycle (ORC) and transcritical power cycle system for low-temperature geothermal power generation, *Applied Energy* 88 (8) (2011) 2740–2754, ISSN 0306-2619.
- [90] Y. Song, J. Wang, Y. Dai, E. Zhou, Thermodynamic analysis of a transcritical CO₂ power cycle driven by solar energy with liquified natural gas as its heat sink, *Applied Energy* 92 (2012) 194–203, ISSN 0306-2619.
- [91] Y.-J. Baik, M. Kim, K. C. Chang, S. J. Kim, Power-based performance comparison between carbon dioxide and R125 transcritical cycles for a low-grade heat source, *Applied Energy* 88 (3) (2011) 892–898, ISSN 0306-2619.
- [92] J. Yu, B. Jia, D. Wu, D. Wang, Optimization of heat transfer coefficient correlation at supercritical pressure using genetic algorithms, *Heat and Mass Transfer* 45 (6) (2009) 757–766, ISSN 0947-7411, 1432–1181.
- [93] A. A. Bishop, R. O. Sandberg, L. S. Tong, Forced-Convection Heat Transfer to Water at Near-Critical Temperatures and Supercritical Pressures, Tech. Rep. WCAP-5449; CONF-650603-1, Westinghouse Electric Corp., Pittsburgh, Pa. Atomic Power Div., URL <https://www.osti.gov/scitech/biblio/4595384>, 1964.
- [94] T. L. Bergman, A. S. Lavine, F. P. Incropera, D. P. Dewitt, *Fundamentals of Heat and Mass Transfer*, John Wiley & Sons, 7th edn., ISBN 978-0-470-50197-9, 2011.
- [95] A. A. Lakew, O. Bolland, Y. Ladam, Theoretical thermodynamic analysis of Rankine power cycle with thermal driven pump, *Applied Energy* 88 (9) (2011) 3005–3011, ISSN 0306-2619.
- [96] B. Adams, L. Bauman, W. Bohnhoff, K. Dalbey, M. Ebeida, J. Eddy, M. Eldred, P. Hough, K. Hu, J. Jakeman, J. Stephens, L. Swiler, D. Vigil, T. Wildey, Dakota, A Multilevel Parallel Object-Oriented Framework for Design Optimization, Parameter Estimation, Uncertainty Quantification, and Sensitivity Analysis: Version 6.0 User’s Manual, Sandia Technical Report SAND2014-4253,, 2015.

- [97] J. Eddy, K. Lewis, Effective Generation of Pareto Sets Using Genetic Programming, in: ASME Design Engineering Technical Conference, 2001, URL http://does.eng.buffalo.edu/index.php?option=com_jresearch&view=publication&task=show&id=59, 2001.
- [98] IBM ILOG CPLEX V12.2: User's manual for CPLEX, Tech. Rep., IBM Corporation, 2010.
- [99] R. Fourer, D. M. Gay, B. W. Kernighan, AMPL: A Modeling Language for Mathematical Programming, Cengage Learning; 2 edition, ISBN 0-534-38809-4, 2003.
- [100] Y. C. Ong, S. Sharma, G. P. Rangaiah, Evaluation of Simulated Annealing, Differential Evolution and Particle Swarm Optimization for Solving Pooling Problems, in: A. Gujrathi, B. Babu (Eds.), Evolutionary Computation: Theory and Applications, Apple Academic Press Inc, 513–543, 2016.
- [101] S. Ahmad, B. Linnhoff, R. Smith, Cost optimum heat exchanger networks—2. targets and design for detailed capital cost models, Computers & Chemical Engineering 14 (7) (1990) 751–767, ISSN 0098-1354.
- [102] F. Maréchal, B. Kalitventzeff, Targeting the minimum cost of energy requirements: A new graphical technique for evaluating the integration of utility systems, Computers & Chemical Engineering 20, Supplement 1 (1996) S225–S230, ISSN 0098-1354.
- [103] C. A. Floudas, I. E. Grossmann, Automatic generation of multiperiod heat exchanger network configurations, Computers & Chemical Engineering 11 (2) (1987) 123–142, ISSN 0098-1354.
- [104] A. Mian, E. Martelli, F. Maréchal, Framework for the Multiperiod Sequential Synthesis of Heat Exchanger Networks with Selection, Design, and Scheduling of Multiple Utilities, Industrial & Engineering Chemistry Research 55 (1) (2016) 168–186, ISSN 0888-5885.

PART

III

TOWARDS THE GRAND DESIGN

In Part I of this report, a novel iterative sequential solution strategy was proposed for the design of HIWAnS. A simplified kraft pulp mill case study highlighted the benefit of simultaneously considering process thermal streams and water unit operations. It was observed that in several industries, e.g., pulp and paper, process water streams cannot be distinguished from cooling water streams, emphasizing the fact that they should be considered simultaneously and even treated the same. Furthermore, water streams can be regarded as heat transfer media between various sections of an industrial plant through continuous loops of heating and cooling. In Part II, a mathematical superstructure of ORC was proposed for heat recovery in industrial processes. It was shown that integration of ORC should not be limited to available waste heat and that there is a great potential in exploiting self-sufficient pockets of the process to further produce electricity and reduce the specific cost of electricity production. This reiterates that all energy recovery measures should be considered simultaneously. This part of the report aims at bringing together the two methodologies developed in Part I and Part II in the prospect of emphasizing holistic designs by proposing a methodology for simultaneous consideration of heat, mass, and power in industrial processes. Within chapter 6, a generic superstructure is constructed. Furthermore, a simple case study is presented comparing sequential and simultaneous approaches. By applying simultaneous approaches, the specific cost of electricity production could be reduced by 9%, while the electricity production was more than tripled. In chapter 7, a kraft pulp mill case study, based on a real pulp mill in Canada producing 1000 adt of pulp/day, is analyzed. Several techniques are incorporated in the modeling stage to better address realistic scenarios.

Keywords: holistic approach, mathematical programming, industrial application, industrial symbiosis, superstructure optimization, process integration, pinch analysis

Acknowledgements: This research project is financially supported by the Swiss Innovation Agency Innosuisse and is part of the Swiss Competence Center for Energy Research SCCER EIP.

CHAPTER 6

Holistic approaches: background and motivation

Overview

This chapter aims at bringing together the two methodologies developed in Part I and Part II in the prospect of emphasizing holistic designs by proposing a methodology for simultaneous consideration of heat, mass, and power in industrial processes. Sequential and simultaneous approaches are compared on the basis of a motivating example. Results exhibit a large potential for synergies within and among industrial sites and emphasize the importance of a generic approach.

6.1 Background

The growing desire to improve resource efficiency and environmental impact of industrial processes is directly linked to optimal management of heat, mass and power flows. This requires development of holistic approaches addressing all these elements together. Such approaches must consider energy and water recovery within a comprehensive process integration framework which includes other options such as ORCs, which are capable of generating electricity from medium to low temperature heat and cascading the remainder for low temperature processes or other uses. Water, in its liquid and vapor phases, is a ubiquitous energy carrier and acts as an intermediate heat transfer medium at different temperature levels. Steam can also be used in a Rankine cycle to produce electricity. Moreover, at medium to low temperature levels, ORCs can be utilized to produce electricity, reduce cooling duties, and if integrated with process streams can serve as a heat transfer medium at different temperature levels. These complex interactions accentuate the necessity of their combined consideration to improve efficiency and environmental impact of industrial processes. These interactions exhibit even stronger significance in interplant operations in which waste heat/resources of one plant can be recycled or reused in others [1].

Although HIWANS have been extensively studied in recent years (Part I), few authors have proposed interplant methodologies [2, 3, 4] and those that do are limited to water recovery in interplant operations without heat recovery since they do not consider process non-water thermal streams. Interplant heat recovery has also been extensively addressed in the literature as part of "total site heat integration" (TSHI) methodologies [5]. Liew et al. [6] provided a comprehensive overview of these methodologies with emphasis on inter-process (interplant) direct and indirect heat integration. In summary of the aforementioned research directions, Liew et al. [6] proposed the current gaps in this domain:

- 1) Development of methodologies for total site heat and power integration,
- 2) Incorporation of sustainability and environmental criteria,
- 3) Optimal design of hot water and hot oil loops,
- 4) Development of multi-period, multi-objective methodologies,
- 5) Prioritizing hybrid methodologies to overcome the main weakness of mathematical approaches by incorporating industrial insights.

The combined heat and power superstructure developed in Part II of this thesis can address gap 1, while the HIWAN hyperstructure developed in Part I of this thesis can address gap 2 by integrating cold utility within the water network. The aim of this part of the thesis is to address several gaps (1,3,5) by proposing a hybrid MILP superstructure for simultaneous optimization of heat, water, and power. The superstructure is constructed by combining the targeting superstructure of HIWAN (chapter 2) and the combined heat and power superstructure (chapter 5) for both ORC and steam cycle modeling and optimization.

6.2 Problem definition and proposed approach

The proposed methodology is formulated as an MILP superstructure. Figure 6.1 encapsulates the major elements of the proposed generic superstructure. Given is a set \mathbf{P} of industrial sites (or clusters within each plant). Each site i has a set of water unit operations (demands: $\mathbf{WAN}_{i,in}$, sources: $\mathbf{WAN}_{i,out}$) and a set of process thermal streams (hot: \mathbf{HS}_i , cold: \mathbf{CS}_i). No direct heat or mass exchanges are allowed between sites. Mass exchange is managed through the water network by incorporating several tanks. Heat exchange is managed through addition of several heat transfer vectors, such as steam cycle, ORC, heat pump, and water network. ORC and steam cycle can both be used to transfer heat by evaporating and condensing in between sites while producing electricity where a pressure difference exists. The cooling utility is modeled as part of the water network. Inter-site and inter-plant operations are essentially the same in terms of the modeling (i.e., restricted exchanges of heat and resources except via a (de)centralized utility hub) which can both be addressed by the proposed superstructure.

The objective function is defined as minimizing the total annualized cost of the system including operating cost (i.e., resources consumption including freshwater and thermal utility consumptions) and annualized investment cost of equipment (i.e, pumps, turbines, compressors, furnace, HEN, etc.) subject to heat, mass, power balances, and sizing constraints. To this end, combined heat and power superstructure constraints introduced in Part II can be added to problem $\mathbf{P1}$ (Part I) to address the entire set of constraints.

6.3 Motivating example

A motivating example (simplified kraft mill case study, section 2.5) is analyzed using sequential and simultaneous approaches. The temperatures of process thermal streams are corrected with data from a real kraft mill. Among the modifications, the turpentine condenser is modeled as steam condensation with sub-cooling at 2.2 bar. Table 6.1 provides the data with corrected parameters presented in bold. The example is limited to a single plant for the sake of simplicity. Furthermore, the cold utility is modeled separately from the water network. The focus of the

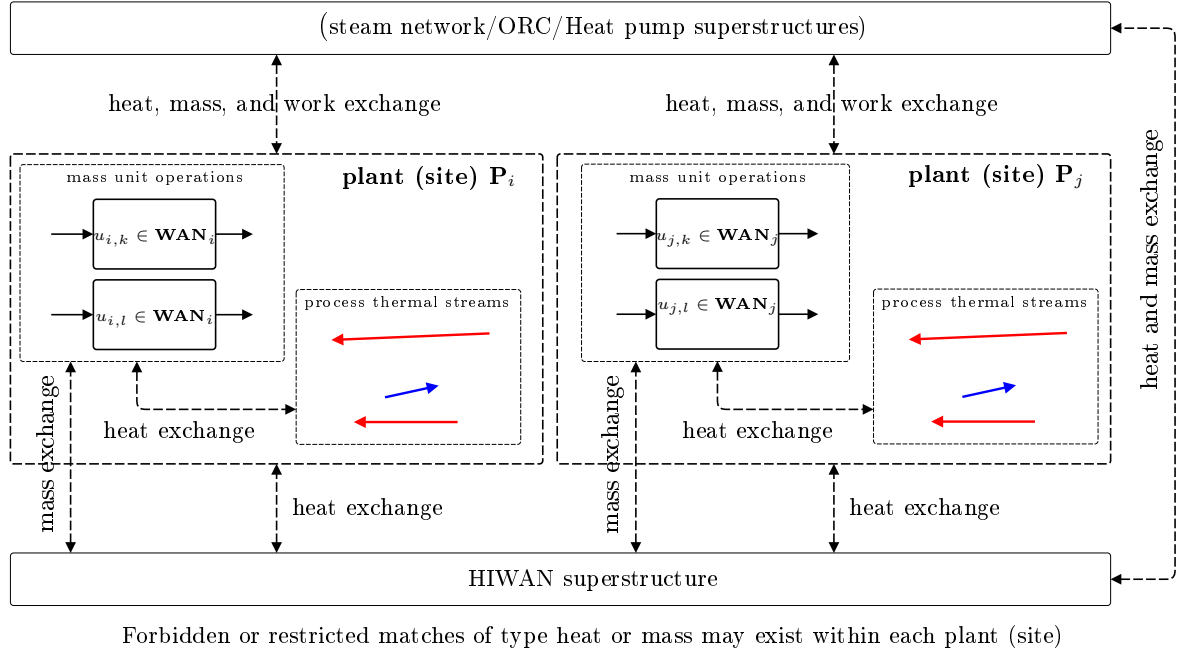


FIGURE 6.1—Schematic of the proposed mathematical superstructure for combined heat, mass, and power integration in industrial processes

example is to illustrate the importance of holistic (simultaneous) approaches for integration of combined heat and power production technologies within the process.

TABLE 6.1—Operating data for the motivating kraft pulp case study

	T_{in} [°C]	T_{out} [°C]	\dot{m} [kg/s]		T_{in} [°C]	T_{out} [°C]	Heat load [kW]
Water unit operations				Process thermal streams*			
Pulp machine (1)	50	50	10	Surface condenser (1)	78	78	-7,560
Bleaching (2)	70	70	20	Turpentine condenser** (2)	123.25	60	-10,920
Washing (3)	65	65	35	Effluent (3)	75	40	-2,205
Stock preparation (4)	62	62	25	Dryer exhaust (4)	68	35	-1,050
Recausticization (5)	35	35	20	Contaminated condensate (5)	80	65	-630
Water utilities				Thermal utilities			
Fresh water	-	10	-	Hot utility (Steam)	120	120	-
Waste water	30	-	-	Cold utility	10	35	-
Water tanks							
Warm water tank	35	35	-	Hot water tank	62	62	-

* HRAT is set at 5°C;

** Turpentine condenser is modeled as 4.44 kg/s of steam at 2.2 bar.

Cost parameters were presented in Table 2.1. Figure 6.2 illustrates the grand composite curve of process thermal streams. Overall, 22.36 MW of cooling utility is required. In addition, water unit operations are shown in Figure 6.2. Their location on the y-axis specifies their temperature level, while the x-coordinate is proportional to the amount of heating required for freshwater to meet the demand, e.g., to satisfy the demand of bleaching at 70°C using

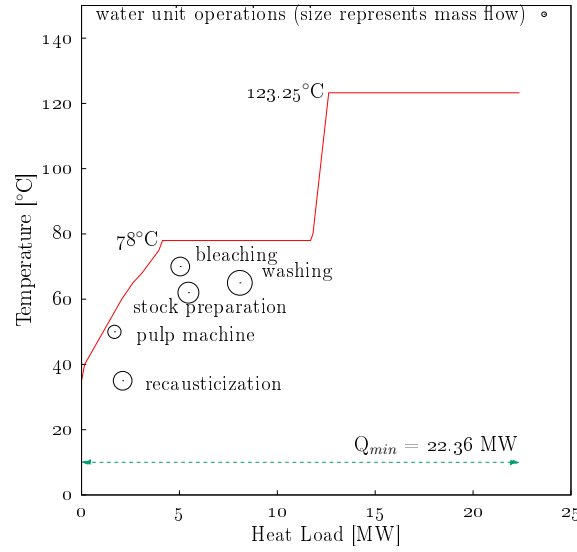


FIGURE 6.2—Cumulative heat load of all the thermal streams of the motivating example and water unit operations (size of points represents water flowrates)

freshwater, 5,040 kW heat is required. Figure 6.2 further shows that heat recovery from several processes outlets, i.e., bleaching, washing, and stock preparation can significantly reduce the thermal demand of the process. Moreover, it can be seen that all processes temperatures lay below the one of surface condenser and hence a high opportunity for ORC to exploit the condensation level of turpentine at 123.25°C.

6.3.1 Case I - sequential approach

Sequential approach comprises two steps: in the first step, HIWAN is designed for the minimum total annualized cost following the methodology presented in section 3.3. In the optimal network, streams connected to cooling utilities are extracted as waste thermal streams. In the second step, ORC integration is carried out for waste heat recovery following the methodology presented in subsection 5.2.5. For the sake of motivating example, only one potential solution is presented here.

Step 1 - Heat-integrated water allocation network Following the solution strategy proposed in section 3.3, number of integer cut constraints are set at 10 for both problems **P1** and **P2**, ($N_{icc}^{P1} = 10$, $N_{icc}^{P2} = 10$), while HRAT is set at 8°C. The solution with the lowest total annualized cost (exhibiting the lowest HEN cost of 278.5 kUSD/yr) was reached at $n_{icc}^{P1} = 5$ and $n_{icc}^{P2} = 4$. 80 kg/s freshwater is consumed, while 15,645 kW of cold utility is required to exhaust the excess heat. H_1 (surface condenser) and H_5 (contaminate condenser) are fully cooled down by heating up freshwater. H_2 (turpentine condenser) is partly used to heat up freshwater. Cooling utility is used for part of H_2 and the entirety of H_3 (effluent) and H_4 (dryer exhaust). Moreover, wastewater streams (outlet of stock preparation, washing and bleaching) are mixed and then cooled using cold utility. HEN consists of nine heat exchangers with four of them cooling down the waste thermal streams. Total annualized cost of the system amount to 920.4 kUSD/yr. Figure 6.3 illustrates the cumulative heat load of extracted hot waste thermal streams (in red) with the original set of thermal streams (in dashed line).

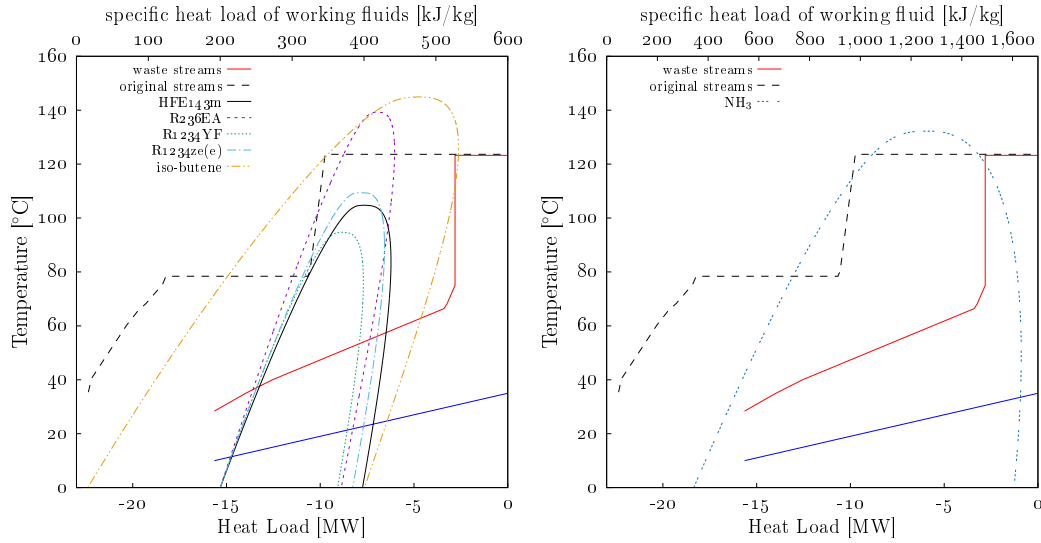


FIGURE 6.3—GCC of the motivating kraft mill illustrating the waste hot streams with potential working fluids

Step 2 - ORC integration Selection of a working fluid is, in itself, an optimization problem as no single fluid can satisfy all requirements. Pre-screening potential candidates can be performed by applying several criteria as follows:

- It is widely reported (Part II) that the critical temperature of the best working fluid is close to that of the thermal stream, in this case, 123°C and 78°C (Figure 6.2);
- Working fluids are limited to dry fluids with the exception of ammonia (due to its wide use).

Figure 6.3 illustrates the many possibilities for potential working fluids and their temperature-enthalpy diagrams (ammonia is shown separately on the right figure due to its high latent heat) relative to the process profile. Compared with the original set of thermal streams (dashed black curve), it can be seen how a sub-cooled region of a working fluid in evaporation mode such as R236ea can match the middle near-vertical temperature interval, while working fluids such as ammonia and iso-butene can match the low near-vertical temperature interval and hence further exploiting the waste stream. Comparing the grand composite curve of waste streams with that of the original set of thermal streams (Figure 6.3), it can be observed that more than 60% of turpentine condenser is integrated within the water network (reducing the HEN cost through increased approach temperature). This has a dramatic influence on the potential of ORC integration as it is shown in Figure 6.4.

Two cases of ORC integration with the waste thermal streams using ammonia and R236ea are shown in Figure 6.4. An ORC superstructure with four pressure levels was modeled. Pressure levels, degree of superheating (if necessary), and reheating temperature (if necessary) were manually adapted for this example. Due to the gliding medium-temperature waste stream and temperature levels of cooling utility, R236ea does not exhibit the potential for further exploiting the medium-temperature waste heat. The overall electricity production using only one turbine with R236ea was found to be 480.1 kW. The HEN cost is increased by more than 65% compared with the case without any electricity generation. Conversely, optimal ORC

integration for ammonia required two turbines with different inlet conditions. The amount of electricity production is increased by more than 17% to 564.9 kW. However, higher integration of ORC with the thermal streams further increased the HEN cost by 36%. Considering the electricity price of 0.13 USD/kWh, the payback time for this investment is around 8.2 years which is 60% higher than that of R236ea-based ORC. The results of the sequential approach is summarized in Table 6.2. HEN design is carried out using problem $\mathbf{P3}^{\text{init}}$ (NLP formulation of Floudas and Ciric [7]).

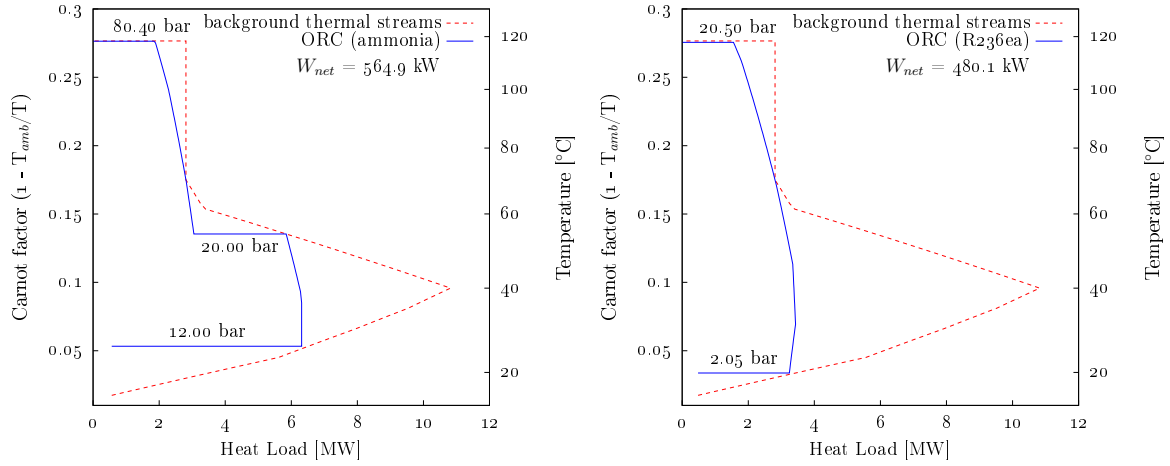


FIGURE 6.4—Integration of ORC with waste thermal streams using ammonia (left) and R236ea (right) as working fluids

6.3.2 Case II - simultaneous approach

In the simultaneous approach, HIWAN synthesis and ORC integration are considered at the same time. Figure 6.5 presents the results with ammonia and R236ea. It can be observed that the medium-temperature stream (at 78°C) is now exploited by the ORC. With ammonia, the optimum solution exhibits three turbines (one reheating turbine from 31 bar to 17 bar). The ORC is highly integrated with the thermal streams and produces 1,914.1 kW of electricity (3.4 times higher than the sequential solution with ammonia), while maintaining the same fresh-water consumption. Similar results were observed using R236ea where electricity production increased by 1.5% to 1,943.4 kW.

Table 6.2 summarizes the key results of the motivating example. Payback time (PBT) and cost of electricity production (COE) are calculated as two financial indicators for comparing different scenarios. To calculate the operating cost and PBT, electricity price is set at 0.13 USD/kWh (Switzerland). COE is defined as the annual extra cost that is imposed due to the production of electricity per annual production of electricity and is given by Equation 6.1:

$$\text{COE [USD/kWh]} = \frac{\overbrace{(C'^{\text{inv}} + C'^{\text{HEN}} - C^{\text{HEN}})}^{\text{additional investment cost [USD]}} \cdot \underbrace{f_a}_{\text{annualization factor}} + \overbrace{(C'^{\text{op}} - C^{\text{op}})}^{\text{additional/savings in operating cost [USD/yr]}}}{\mathbf{W}_{\text{net}}[\text{kW}] \cdot t_{\text{op}}[\text{hr/yr}]} \quad (6.1)$$

Where C' denotes the costs after ORC integration and C^{op} includes the cost of thermal utility and freshwater consumption (note that the C^{op} in Table 6.2 includes as well the profit

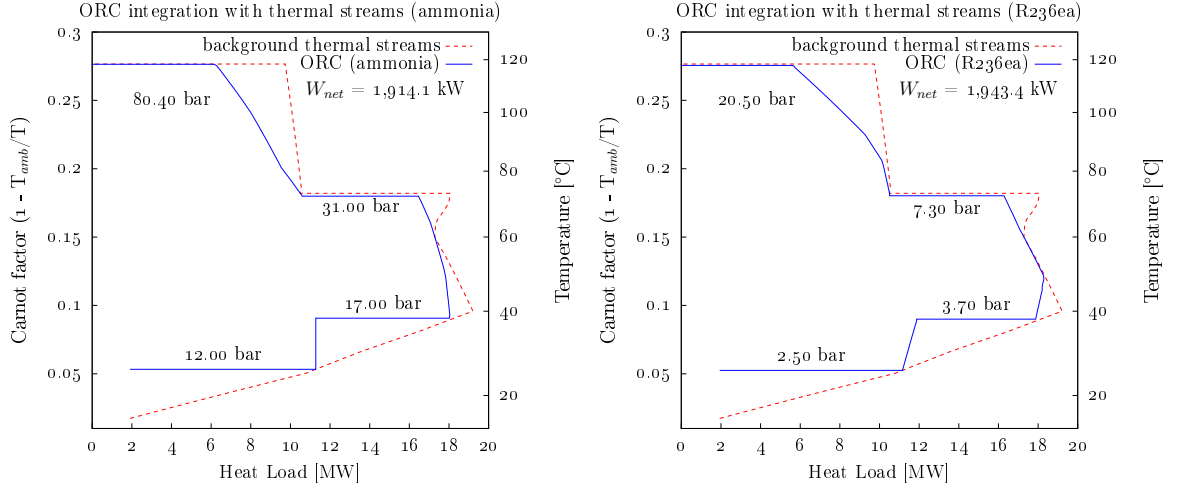


FIGURE 6.5—Integration of ORC with thermal streams and water unit operations using ammonia (left) and R236ea (right) as working fluids

from selling the produced electricity). For the motivating example, as shown previously, hot utility consumption is zero and freshwater consumption remains the same in all cases. Hence, Equation 6.1 can be further simplified as Equation 6.2 (note that the difference between cold utility consumptions is, by definition, the amount of electricity production):

$$\begin{aligned} \text{COE} &= \frac{(C'^{\text{inv}} + C'^{\text{HEN}} - C^{\text{HEN}}) \cdot f_a - \mathbf{W}_{\text{net}} \cdot C_{\text{cu}} \cdot t_{\text{op}}}{\mathbf{W}_{\text{net}} \cdot t_{\text{op}}} \\ &= \frac{(C'^{\text{inv}} + C'^{\text{HEN}} - C^{\text{HEN}}) \cdot f_a}{\mathbf{W}_{\text{net}} \cdot t_{\text{op}}} - C_{\text{cu}} \end{aligned} \quad (6.2)$$

Furthermore, payback time (PBT) is defined as the amount of time (normally in years) required for an investment to be returned given the foreseen savings in operating cost:

$$\text{PBT [yr]} = \frac{(C'^{\text{inv}} + C'^{\text{HEN}} - C^{\text{HEN}})}{|C'^{\text{op}} - C^{\text{op}} - \mathbf{W}_{\text{net}} \cdot C_{\text{el}} \cdot t_{\text{op}}|} \quad (6.3)$$

Substituting Equation 6.2 in Equation 6.3 and respecting the sign of the denominator (i.e., operating cost after integration of ORC reduces, hence the term $C'^{\text{op}} - C^{\text{op}}$ is negative and so savings - a positive value - is calculated as $-C'^{\text{op}} + C^{\text{op}} + \mathbf{W}_{\text{net}} \cdot C_{\text{el}} \cdot t_{\text{op}}$), payback time can be formulated as Equation 6.4:

$$\text{PBT [yr]} = \frac{1}{f_a} \cdot \frac{C_{\text{cu}} + \text{COE}}{C_{\text{cu}} + C_{\text{el}}} \quad (6.4)$$

Equation 6.4 implies that selling electricity at the cost of production (COE) results in a payback time equal to the inverse of annualization factor (in this case 10.6 years). For the current cost parameters, i.e., interest rate 8%, lifetime 25 yr, price of electricity 0.13 USD/kWh, and cost of cold utility 18.568 USD/kWy, the cost of producing electricity would have to reach 0.035 USD/kWh in order to have payback time of 3 years. For the case of R236ea-based ORC an investment subsidy of around 49% can make this possible. PBT and COE are shown for all cases and working fluids of the motivating example in Table 6.2. It can be observed that

TABLE 6.2—Results of sequential and simultaneous approaches for the motivating example

Indicators	Unit	No ORC	Sequential approach		Simultaneous approach	
			R236ea	NH ₃	R236ea	NH ₃
\dot{m}_{fw}	kg/s	80	80	80	80	80
\dot{Q}_u^C	kW	15,645.0	15,165.2	15,080.6	13,703.1	13,731.9
\dot{Q}_u^H	kW	0	0	0	0	0
W_{net}	kW	0	480.1	564.9	1,943.4	1,914.1
η_{el}	%	-	14.08%	9.00%	10.62%	10.61%
N_s^{th}	-	11	13	15	23	25
N_{HE}	-	9	15	23	51	55
A_{HEN}^{total}	m ²	1,598	2,739	3,584	8,637	9,229
C_{HEN}^{HEN}	kUSD/yr	278.5	461.8	629.8	1,477.2	1,557.6
C^{inv}	kUSD/yr	0	60.5	98.4	216.0	228.0
$C^{op}(\star)$	kUSD/yr	641.9	133.6	43.8	-1,415.3	-1,384.3
C^{TAC}	kUSD/yr	920.4	655.9	772.0	277.8	401.2
PBT	yr	-	5.1	8.0	7.3	7.9
COE	USD/kWh	-	0.0612	0.0972	0.0887	0.0961
Solve time	s	1.450	1.621	1.637	5.600	7.816

(\star) C^{op} considers the electricity production with the selling price of 0.13 USD/kWh.

- PBT = payback time; COE = cost of electricity production
- $C^{TAC} = C^{op} + C^{inv} + C^{HEN}$

PBT is decreased by 0.7 yrs for the case of R236ea (simultaneous approach) as compared to NH₃ (sequential approach) for the current electricity price of 0.13 USD/kWh.

Despite higher investment cost for solutions from the simultaneous approach (which is natural due to higher production of electricity), it can be observed that COE and PBT can be lowered by properly optimizing the system. It should be emphasized that all the input parameters are subject to uncertainties, but nevertheless, simultaneous approaches provide lower operating costs, in this case manifested as higher electricity production and decreased cooling demand.

6.4 Conclusion

This chapter aimed at highlighting the benefits of simultaneous approaches in optimizing energy systems by proposing a linear superstructure for combined consideration of heat, mass (water) and power. The superstructure addresses HIWAN synthesis problem as well as combined heat and power production systems. A motivating example demonstrated the benefits of simultaneous approaches compared with sequential approaches by showing large potential for synergies among various systems within an industrial site and emphasized the importance of a generic approach. It can be said that sequential approaches fail to consider the entire synergies among various elements; nevertheless, the computational time of such approaches tend to be lower than simultaneous approaches as they deal with smaller problem sizes at different steps (Table 6.2). Chapter 7 studies the application of the proposed methodology on a real kraft mill via a multi-objective GA. ■

CHAPTER 7

Industrial application: kraft pulp mill

Overview

The methodologies developed in previous parts were applied to an industrial case study. This chapter first introduces the selected case study, a kraft pulp mill, and its main processes. Next, the algorithm proposed in chapter 2 was applied to extract the required data and formulate the problem. Finally, the combined approaches were applied and the results are presented. The results indicate promising opportunities for the industrial application of the proposed methodologies while highlighting the necessity of applying holistic approaches in the optimization of industrial processes.

The pulp and paper industry is energy-intensive and involves transferring large quantities of energy to complex freshwater and contaminated water networks, including several hot thermal streams at medium to low temperatures that need to be cooled down. This makes it an ideal candidate to validate the performance and robustness of the proposed methodologies. A large-scale kraft pulp mill, producing up to 1,000 air-dried tonnes (adt) of kraft pulp per day, was selected as an industrial application.

7.1 Kraft process

The kraft process is a manufacturing process converting wood chips to pulp (Figure 7.1). The process starts with the steaming and screening of wood chips to be prepared for cooking. Steaming is used to preheat the chips, recover heat from the flashed cooking liquor, and remove the entrained air to facilitate impregnation during the cooking stage. Screening is also carried out to remove knots or any other non-wood elements. The steamed chips are sent to a high-pressure and high-temperature ($\sim 160\text{--}170^\circ\text{C}$) cooker (i.e., digester), where cellulosic fibers are separated from the chips by use of a chemical blend known as liquor. Liquor consists of white liquor and spent black liquor from the previous cooking batch. White liquor is a mixture of NaOH and Na_2S that is used for the delignification of wood chips. Heating is provided either via direct steam injection/blowing or through indirect heating in steam/liquor heat exchangers. The outlet of the digester is washed to separate the spent liquor (i.e., black liquor) from the fibers and goes through a recovery process for reuse. Any incomplete cooked fibers, knots, or debris are separated using screening devices and are recycled to the digester. The pulp is then bleached using a sequence of bleaching agents, such as ClO_2 , O_2 , and H_2O_2 . It is dried before being sold to the market from the pulp machine. At the wet-end section of the pulp machine, pulp is pressed to drive out water. Thereafter, it is sent to the dry-end where any additional water is removed by evaporation via blowing hot air. The final moisture content is approximately 10%. The black liquor (around 15% dry solid content), from the

washing section, is sent to multi-effect evaporators and subsequent concentrators to yield highly-concentrated dry solid (75% dried solid content). The resulting heavy black liquor is then burned in a recovery boiler. The recovery boiler has four functionalities [8]:

- burning of organic materials to produce water and CO_2 which are more environmentally benign;
- recovering the energy content of the burnt organic materials in the hot flue gases to run turbo-generators or to satisfy the steam demands of the mill;
- restoration of inorganic chemicals in black liquor as chemical pulping agents; and
- recovery of by-products, e.g., tall oil and turpentine.

The inorganic residues form a smelt that consists of Na_2CO_3 and Na_2S . The smelt is used to produce green liquor, which goes through causticizing process to produce NaOH that, together with Na_2S , form the white liquor.

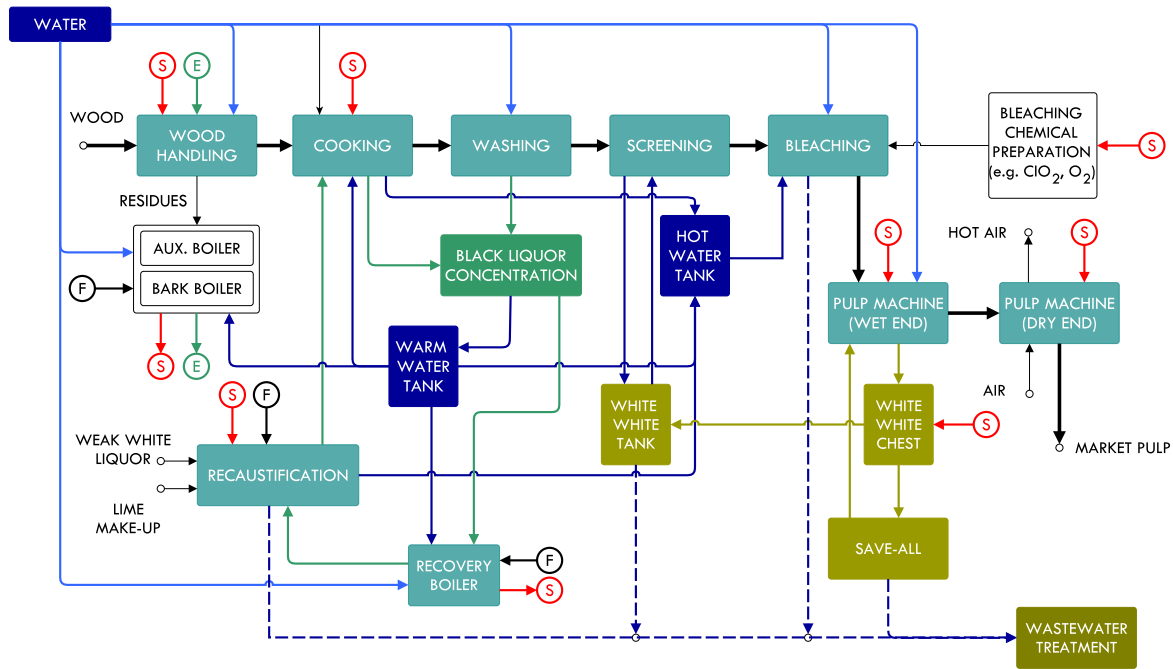


FIGURE 7.1—General schematic of water and energy flows in a kraft mill

Each section of a pulp mill can have water, heating, and/or cooling demands. The clean cold water is used in all mill departments for cooling or dilution purposes. The cooling water is then stocked in water tanks at several temperature levels and is distributed to the processes. Water, as a process stream, is used in several sections including the washing, bleaching, recovery boiler, lime burning, and steam production sections. Moreover, water can be recovered from some sections, such as washing and bleaching for reuse and recycling. In a pulp mill, water is a contaminant and an energy carrier [9]. In a typical bleached kraft mill 20–90 t/adt of freshwater and 10–14 GJ/adt of heat is consumed and the electricity generation from the recovery boiler is between 600–800 kWh/adt [8]. The energy efficiency of the kraft mill is strongly interconnected with the correct management of water and energy in the mill [10].

Process integration techniques, including heat integration, water network optimization, and steam cycle operation optimization, can significantly reduce the water and energy consumption in the mill. Main researches in water–energy optimization in the pulp and paper industry are insight-based approaches limited to specific sections of the kraft mill as they lack a global vision of the process. This results in the absence of a systematic approach that is able to address all interconnections among heat, water, and power in the pulp and paper industry. This chapter proposes a methodology to address all of these elements in a systematic manner through its application on a bleached kraft pulp mill case study.

7.2 Data extraction and problem formulation

Gathering process data consists of characterizing an industrial site and its specificities. This step is crucial, as subsequent steps rely on a deep understanding of the processes and their operation modes. Project objectives should be defined and discussed at this step as it directly influences the amount and level of detail in data extraction. Furthermore, this must be performed in such a way to facilitate future projects [11]. Three main approaches are considered to facilitate data extraction and building the related mathematical model:

- Only the temperature and maximum allowed inlet and outlet contaminations must be extracted from water unit operations, such as bleaching or washing. The proposed MILP superstructure will automatically generate all thermal streams within the water network and add them to the optimization problem.
- Streams passing in heat exchangers (in series) are combined into a single grassroots stream (i.e., hot streams that pass through three heat exchangers for the desuperheating, condensation, and sub-cooling stages are modeled as one stream). Phase changes are still modeled with the corresponding heat load.
- Several process hot thermal streams in the current mill are cooled in the water network. Those with unknown (i.e., unmeasured) temperatures are replaced by their corresponding cooling water stream. This adds two water unit operations of type demand and supply to the problem.

Before application of the methodology, i.e., in the current state of the mill, cold process streams were heated with steam, whereas hot process streams were cooled with water, hence exhibiting no heat integration among them. Water process operations were satisfied in the water network, while any additional heating required in the water network was satisfied by steam, either directly or indirectly.

7.2.1 Data classification

Appendix D provides the operating data of the case study. This list was gathered through communication with mill personnel and expert insight to provide an accurate representation of a typical kraft pulp mill:

- **Cold process streams:** 19 cold process streams exist in the mill (Table D.2). Among these, the heat loads of the air preheater and black liquor heater are proportional to the size of the recovery boiler and hence were modeled as part of the black liquor furnace (section 7.2.2.1).

- **Hot process streams:** 20 hot process streams are cooled in the mill (Table D.3). After combining heat exchangers in series, fifteen (15) hot streams should be considered. As an example, the primary, secondary and inlet/outlet condensers in the evaporation section are modeled as 9.9 kg/s of saturated steam at 1.9 bar. Among the hot streams, five represent several equipment cooling duties where temperatures of the hot sides are unknown (or uncertain), such as the bearing cooler, pulp machine cooler, and fan cooler. These heat exchangers were each modeled as two water unit operations, i.e., source and sink.
- **Waste thermal streams:** There are four waste hot streams that can be recovered for heating purposes (Table D.5).
- **Hot utility:** Highly-concentrated black liquor is burnt in a recovery boiler to produce steam at high pressure (60 bar). The steam is passed through steam turbines to generate electricity. The process steam demands are satisfied using three pressure levels: high (10–12 bar), medium (5 bar), and low (1 bar) pressures (see section 7.2.2.1).
- **Water unit operations:** 14 water unit operations were extracted for this case study (Table D.4, 13 demands and six sources of water at various temperatures). One major issue in developing a mathematical model of water recycling is the availability of quantitative data on the contamination levels of water streams. To overcome this issue, several restrictions are discussed and imposed. In addition to the method described in section 2.4 (step 2), which is used to forbid or restrict specific mass exchanges, a level of quality is defined for each water unit operation (source/sink) using binary parameters. To address this, following constraint was added to the model:

$$\sum_{i \in \mathbf{WAN}_{out}} \dot{\mathbf{m}}_{i,j} \cdot q_i \geq \dot{\mathbf{m}}_j \cdot q_j \quad \forall j \in \mathbf{WAN}_{in} \quad (7.1)$$

where q_i and q_j are quality parameters assigned to units i and j , respectively. This constraint implies that a source unit of quality o cannot be recycled in any other sink unit except those of quality o . Moreover, the demand of a sink unit with a quality of o can be satisfied by any source unit. The quality of all water tanks and all water units acting as cooling utility (i.e., indirect heat exchange) was set to 1. The quality of wastewater disposal units was set to 0. Contaminated water unit operations were modeled with a quality of 0: the demands of bleaching, washing, pulp machine, pressure disc filter, and smelt spout, and the sources of pulp machine, condensates in recausticization section, and smelt spout. This approach facilitates the implementation of specific restrictions. Additional mill-specific restrictions and/or recycling–reusing opportunities were incorporated into the model:

- Direct recycling within each tank is forbidden.
 - The outlet of the pulp machine cannot be directly reused. For this reason, the white water tank was modeled to recycle white water back to the pulp machine.
 - The outlet of the vacuum pump cannot be recycled in the bleaching section.
 - The outlet of the cooling water cooler cannot be sent to wastewater disposal.
 - Freshwater cannot be used to dilute or (directly) cool wastewater.
- **Water network:** Freshwater is available at 20°C. Wastewater disposal is at 30°C. The water pathways through the plant are managed by three tanks, namely, treated

warm water (28°C), raw warm water (52°C), and treated hot water (60°C) tanks. Their temperatures are due to the current operating conditions of the mill and are defined as variables in the optimization.

7.2.2 Problem formulation

To represent the current distribution of different departments in the kraft mill and to impose certain restrictions on heat and mass exchange, the mill was divided into three “industrial clusters” (similar to the schematic representation in Figure 6.1):

- **DG** cluster: Digester cluster, which encircles the digester, washing, and recausticization departments and represents the process of breaking down wood chips for pulp production.
- **PM** cluster: Pulp machine cluster, which encompasses the pulp machine, bleaching, and ClO₂ departments and represents the industrial site for producing market-value pulp.
- **RB** cluster: Recovery boiler cluster, which encompasses evaporation, concentration, and recovery boiler departments. It represents the steam production section and the process of regenerating chemicals for green liquor production.

No direct heat or mass exchanges are allowed between clusters: mass exchange can only take place via water tanks, whereas heat exchange can take place either through hot water loops (part of the water network) or via evaporation and condensation of water (i.e., steam cycle) or another working fluid (i.e., ORC).

7.2.2.1 Recovery boiler

The steam and electricity demand in kraft mills is satisfied through burning concentrated black liquor. Data from Vakkilainen [12] was used to model the furnace in the recovery boiler (Table 7.1). The furnace is assumed to be existing and thus does not have an investment cost. Given the lower heating value of black liquor, air to fuel ratio, and the furnace’s temperature level, the radiative (constant temperature, 1000°C) and convective heat loads of furnace mount to 4,065 and 7,154 kJ/kg of black liquor, respectively.

TABLE 7.1—Parameters for recovery boiler [12]

Parameters	Unit	Value
Solid content of black liquor	%	75
Adiabatic combustion temperature	°C	1,500
Flue gas outlet temperature	°C	120
Boiler thermal efficiency	-	0.888
Air to fuel ratio		4.196
Lower heating value of black liquor	kJ/kg	12,250
The highest temperature that furnace can reach (radiation temperature)*	°C	1,000
Temperature of preheated air at the furnace inlet	°C	110
Available heat for steam production (removing air preheating)	kJ/kg	10,880.2

* The furnace temperature is about a third below the adiabatic temperature [12]

7.2.2.2 Steam cycle

Steam is currently produced at 58.7 bar and 473°C. Process steam consumption is at 3 levels: 12, 5.2, and 1 bar. The ORC superstructure (Part II) is used to model the steam cycle by changing the working fluid to water and introducing four (4) pressure levels. Several architectures, including regenerative, superheating, and open and closed feedwater heaters, are considered. Moreover, to meet the specificities of combined heat and power production in typical industrial plants, the following adaptations are imposed:

- Steam production can only happen at the highest pressure level.
- Turbines are placed between the highest pressure and subsequent lower pressures.

7.2.2.3 Cooling water system

The cooling water system has the task of cooling the process streams, equipment, and waste streams. The heated cooling water can be recirculated (recirculating system) in the mill or discharged (once-through system). The latter requires a great amount of water usage and is most suitable for mills located near an appropriate water source. Moreover, the temperature of the discharged water should comply with environmental regulations. Recirculating cooling systems significantly reduce water consumption in the mill by reusing the cooled cooling water for cooling or as part of the process and are mainly classified as closed or open cycles. In an open cycle, the heated water is cooled by directly blowing air and evaporating part of the cooling water. The lowest temperature to which the water can be cooled down is theoretically limited to the wet bulb temperature. This requires the addition of clean makeup water to compensate for the loss. A closed cycle uses refrigeration and heat exchangers to cool the water; the lowest possible outlet temperature of the cooled cooling water is limited by ΔT_{min} [8]. Open recirculating cooling systems were modeled using data presented in Table 7.2 [13]. The outlet temperature of cooled cooling water is assumed to be 26°C.

TABLE 7.2—Parameters for wet open recirculating cooling systems [13]

Parameters	Unit	Value
Wet bulb temperature	°C	18
Approach temperature	°C	8
Make-up water	m ³ /hr/MW _{th}	2
Specific electricity consumption	kW/MW _{th}	30

Figure 7.2 illustrates the overall layout of the kraft mill together with the considered clustering. All water unit operations are also shown in this figure. The units with filled arrows follow the approach in section 2.2 for which a splitter/mixer is placed at their outlets/inlets.

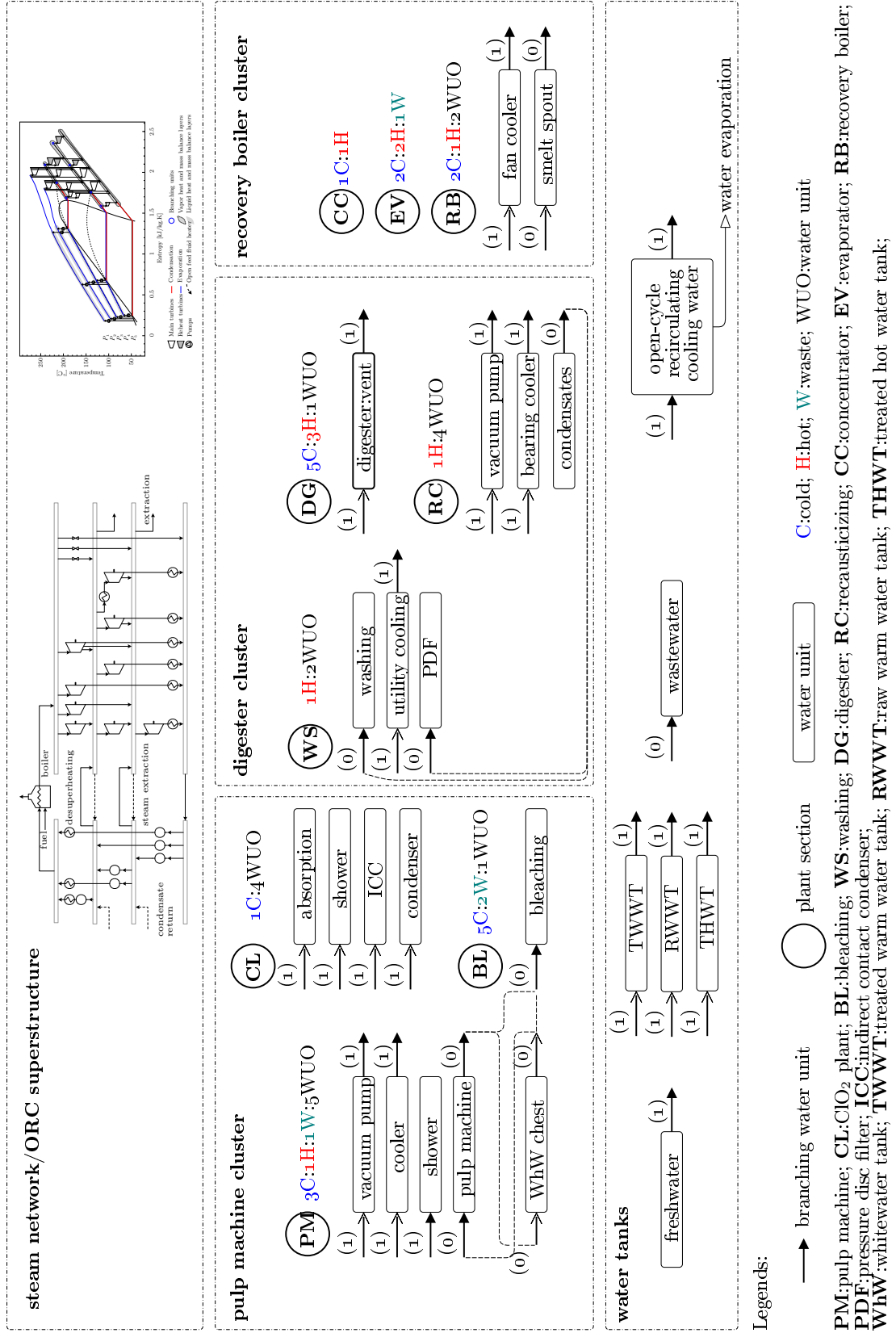


FIGURE 7.2—Layout of the industrial case study including thermal streams and water unit operations

7.2.3 Solution strategy

Within the previous two parts, two solution strategies were proposed:

- In Part I, an iterative three-step sequential solution strategy was proposed for targeting and designing HIWANs where problems **P1** and **P2** were formulated as MILP models to target utility consumptions and provide potential thermal matches. Problem **P3** was proposed and formulated as NLP to optimize the operating conditions, i.e., temperatures and flows, in the HIWAN subject to thermal matches of problem **P2** and utility targets of problem **P1**. In addition, HRAT in the water network was optimized by iteratively changing its value and selecting the best solution among all. Temperatures of water tanks could also be optimized as part of problem **P3**.
- In Part II, a decomposition solution strategy and a novel superstructure were proposed for the optimal integration of ORCs into industrial processes addressing fluid selection, operating condition determination, and equipment sizing. The solution strategy uses a decomposition approach where the upper level handled by GA in which the working fluid and its operating conditions are optimized. The lower level optimization applies a sequential solution strategy to solve the optimal ORC architecture and equipment sizes using a deterministic MILP model (similar formulation to problem **P1** in Part I) and to provide a set of potential thermal matches using problem **P2** (Part I).

To solve the problem of combined heat, water, and power optimization, a solution strategy should be considered that can address the specificities of the two problems, i.e., HIWAN and combined heat and power, in a systematic manner. Accordingly, problem **P1** can include ORC and steam cycle superstructures with fixed operating conditions to maintain linearity. Problem **P2** is, in fact, the HLD model and remains unchanged. In order to optimize the operating conditions of the ORC and steam cycle, GA is implemented similarly to the solution strategy in Part II. However, in addition to decision variables of ORC and steam cycle superstructures, HIWAN variables can be addressed, including temperatures of water tanks and HRAT. As the aim of the proposed methodology is not to provide a detailed design of HEN, problems **P3^{init}** and **P3** can be eliminated at this stage. Estimating HEN cost is carried out similar to the approach used in Part II (Equation 5.3). The objectives of the solution strategy are considered to be: maximizing electricity production, minimizing freshwater consumption, and minimizing TAC.

7.3 Preliminary analysis

7.3.1 Current operating conditions

In the current operating conditions of the mill, hot and cold process thermal streams are not integrated with each other; hence, to estimate utility consumptions, i.e., hot utility (steam consumption, black liquor flowrate), grand composite curves of thermal streams were considered separately, as presented in Figure 7.3. Overall, 131.4 MW (10.36 GJ/adt, assuming operating time of 8000 hr/yr) of steam are required. Taking into account the operating conditions of the steam cycle and the characteristics of black liquor furnace, this corresponds to 14.89 kg/s of black liquor (75% solid content) combustion in the recovery boiler and producing 28.3 MW of electricity. Assuming a demand of 550 kWh/adt of electricity [13], this corresponds to 3.2

MW of net electricity output. It should be noted that the steam and electricity production of a black liquor recovery boiler is more than enough to satisfy the demands of a typical kraft pulp mill [13], hence a bark boiler was not added to the model.

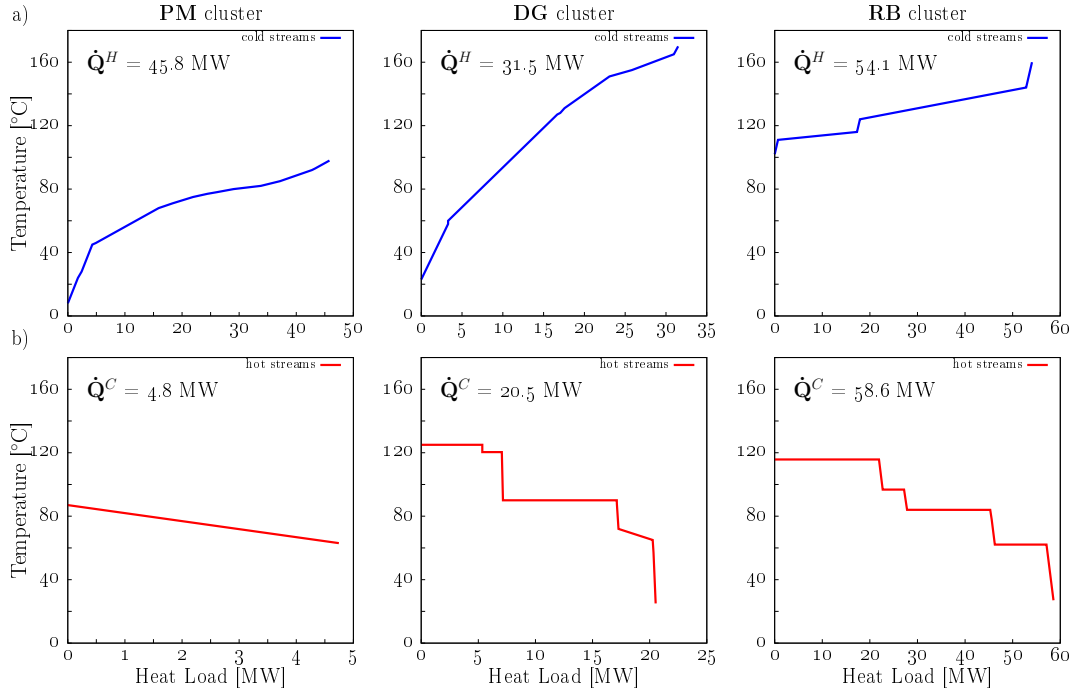


FIGURE 7.3—Hot and cold grand composite curves of considered clusters for kraft case study

Figure 7.3-b illustrates the hot grand composite curves of the three clusters (83.8 MW in total) that are cooled using the water network. Among the hot thermal streams and water unit operations in the case study, several consume freshwater at 20°C (under the current operating conditions) as provided in Table 7.3:

TABLE 7.3—Freshwater (20°C) consumers in the kraft mill (under the current operating conditions)

Section	Unit	Value [kg/s]
ClO ₂ plant	all water unit operations	86.3
Recausticization	bearing cooler and vacuum pump	25.0
	green liquor cooler	6.6
Pulp machine	cooler and vacuum pump	71.9
	cooler and shower	9.8
Washing	miscellaneous cooling	183.2
Digester	chip bin vent and turpentine condenser	15.1
Evaporation	reflux and last effect condensers	277.8
Concentrator	non-condensable gas and FHD coolers	59.3
Recovery boiler	surface condenser	86.1
Total		821.1

Other streams/units are cooled via the water management system in which three water tanks manage and distribute water. Hence, it can be assumed that total water consumption is the summation of freshwater directly used in the above-mentioned processes, i.e., 821.1 kg/s.

7.3.2 Thermal heat integration

Considering all hot and cold thermal streams in the system (Figure 7.4-a), the minimum hot and cold energy requirements was estimated as 49.6 and 2.1, respectively, which shows an 81.8 MW heat recovery potential between thermal streams. This presents the ideal case where all thermal streams can exchange heat; however, this is unrealistic for a number of reasons, particularly related to plant layout.

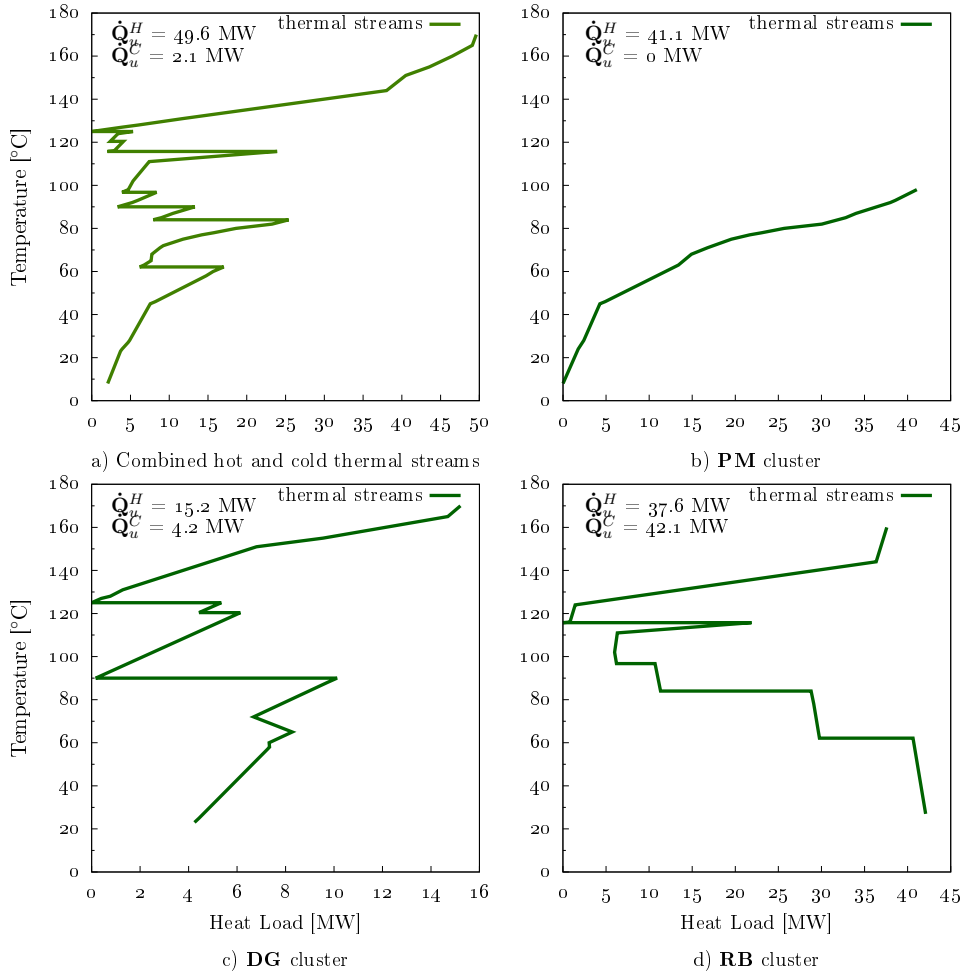


FIGURE 7.4—Grand composite curves of considered clusters for kraft case study

Figure 7.4-b-d illustrate heat integration potentials within each industrial cluster. In total, 93.9 MW of hot utility and 46.3 MW of cold utility are required, exhibiting an increase of 44.2 MW compared to the total site minimum energy requirement (MER), due to cluster distribution and forbidden matches. Heat recycling among clusters can alleviate this increase in utility consumption. Notably, the pulp machine cluster requires heat at low temperatures (below 100°C), which can be partially satisfied by available medium temperature waste heat from the other two clusters. Heat recovery between clusters can be achieved via the water network or through an ORC. An ORC can be integrated such that thermal streams in the pulp machine cluster act as a condenser while heat is transferred and electricity is produced.

7.3.3 ORC and potential working fluids

It can be observed from Figure 7.4-b-d that there is a large potential for integrating ORC with the kraft process which can act as heat transfer medium while producing electricity from medium to low temperature heat (90–125°C, as shown in Figure 7.4). An ORC superstructure with four pressure levels was modeled for this purpose. The two highest pressure levels are in evaporators and can feed turbines. The superstructure encompasses turbine-bleeding, reheating, regeneration, and multi-stage cycles. Several criteria are considered in selecting potential working fluids:

- the critical temperature of working fluids is limited between 100–240°C;
- the GWP of working fluids is limited to 200;
- working fluids with a flammability hazard [14] higher than 2 are excluded;
- fluids, such as R21 and R123 that are being phased out are excluded.

7.4 Results and discussion

The optimization was run on a Windows machine with an Intel(R) Xeon(R) E5-2680 v4 2.40GHz CPU and 32 GB RAM. Due to the large size of the case study, function evaluation was computationally expensive with time required in solving the combined problems **P1** and **P2** ranging between 3–130 seconds. On average, 2,000 evaluations could be performed in a 24-hour time horizon.

Table 7.4 presents the set of decision variables for the current case study. It comprises the decision variables of steam cycle (i.e., pressures and level of superheating at the highest pressure level), ORC (i.e., pressures, levels of superheating, reheating, and the working fluid), and water network (i.e., tank temperatures and HRAT of water thermal streams). Solver options used in the outer and inner optimization levels are also provided in Table A.4. Similar to the approach in Part II, Dakota's JEGA library [15, 16] was used for the outer level, while the commercial solver CPLEX [17] within AMPL [18] was used for the inner MILP problems **P1** and **P2**. Each instance of problem **P1** had 1,129–1,359 binary variables and 7,588–9,053 constraints. In contrast, problem **P2** consisted of 101–361 binary variables (i.e., potential thermal matches) and 1,021–3,012 constraints. The number of solutions in each generation of GA was fixed at 400 to reduce the number of mutations and crossovers while maintaining a diversity within the Pareto frontier. In what follows, the last two generations (after 80,000 function evaluations) are combined and presented.

7.4.1 Pareto frontiers

Overall results of the optimization are shown in Figure 7.5. Freshwater consumption of the optimal solutions ranged between 230–295 kg/s, (less than 35% of the current consumption), while net power output increased from 3.2 MW in the current conditions to 10–25.4 MW. The main reasons of the large increase in the electricity production can be attributed to many factors:

- increased heat recovery among hot and cold process streams which reduced the steam demand of the processes resulting in higher amount of steam available for the turbines; in addition, the condensation temperature at the outlet of turbines (consequently the pressure) was lower in these cases;

TABLE 7.4—Set of decision variables of the optimization

Variables	Range	Unit	Type	Description/remarks
κ	[0:0.5]	-	continuous	Total annualized cost weight factor; the range is limited to 0.5 to emphasize reduction in operating cost (Equation 5.8);
P_1^{st}	[50:160]	bar	step of 0.1	Boiler pressure; the upper bound is limited to reported values for a typical steam power plant;
P_2^{st}	[9:14]	bar	step of 0.1	High pressure steam header
P_3^{st}	[3:8]	bar	step of 0.1	Medium pressure steam header
P_4^{st}	[0.5:2]	bar	step of 0.1	Low pressure steam header
ΔT_1^{sup}	[150:300]	°C	continuous	Degree of superheating in the highest pressure level
$\zeta_{1,fw}^{ORC}$	[0.25:1]	-	continuous	Pressure level 1 in ORC, $P_{1,fw}^{ORC} = P_{wf}^{max} (1 - \zeta_{1,fw}^{ORC})$, where $P_{wf}^{max} = P_{wf,cr}$, (Equation 5.24)
$\zeta_{2,fw}^{ORC}$	[0:1]	-	continuous	Pressure level 2 in ORC, $P_{2,fw}^{ORC} = P_{1,fw}^{ORC} (1 - \zeta_{2,fw}^{ORC})$
$\zeta_{3,fw}^{ORC}$	[0:1]	-	continuous	Pressure level 3 in ORC, $P_{3,fw}^{ORC} = P_{2,fw}^{ORC} (1 - \zeta_{3,fw}^{ORC})$
$P_{4,fw}^{ORC}$	[1:16]	bar	continuous	Lowest pressure level in ORC; the range is derived following Equation 5.25 for selected fluids and given water temperature 20–30°C
$T_{2,1}^{trh,in,ORC}$	[-10:1]	°C	integer	Degree of reheating relative to the temperature of pressure level 1; it is assumed that only first and second pressure levels are turbines inlets.
$\Delta T_1^{sup,ORC}$	[0:20]	°C	integer	Amount of superheating at highest pressure level p1
$\Delta T_2^{sup,ORC}$	[0:20]	°C	integer	Amount of superheating at pressure level p2
wf	[1:3]	-	integer	Working fluids for the case study; Ammonia, R1234ze(Z), IsoButene
HRAT ^{water}	[1:10]	°C	integer	HRAT for water streams; the contribution of water thermal stream to the overall HRAT is half of this value.
T_{tw}^{water}	[25:39]	°C	step of 0.1	Temperature of treated warm water tank
T_{th}^{water}	[55:65]	°C	step of 0.1	Temperature of treated hot water tank
T_{rw}^{water}	[40:55]	°C	step of 0.1	Temperature of raw warm water tank

- higher pressure and temperature of the produced steam in the recovery boiler;
- better water management among clusters that resulted in reduced cooling duties and hence less heat sent to the environment which is valorized via ORC or the process itself; and,
- use of ORC to further increase the net electricity production.

Figure 7.5-a presents the Pareto frontier of the investment cost *vs* the net power output with colors representing the freshwater consumption and the point size representing the HRAT of water thermal streams. Higher HRAT values exhibit lower investment cost (HEN cost was the dominant element in the total investment cost of the solutions) while less electricity was produced. Investment cost *vs* freshwater consumption also exhibits Pareto frontiers at each level of power production (Figure 7.5-b), i.e., for a specific net power, decreasing the freshwater consumption results in an increase in the investment cost. TAC of the system is also shown in Figure 7.5-c. The price of freshwater was set at 375 USD/t (as given in Table 2.1) while the price of electricity was set at 10 USD/MWh (average in Europe).

From the economic perspective, it should be noted that although economic parameters might change, minimum freshwater and maximum electricity production potential will remain the same as long as the cost correlations remain relevant. As previously discussed in Part I, in the current global environmental conditions reducing resource consumption and increasing resource efficiency should be of utmost priority. Moreover, TAC of a project must not be

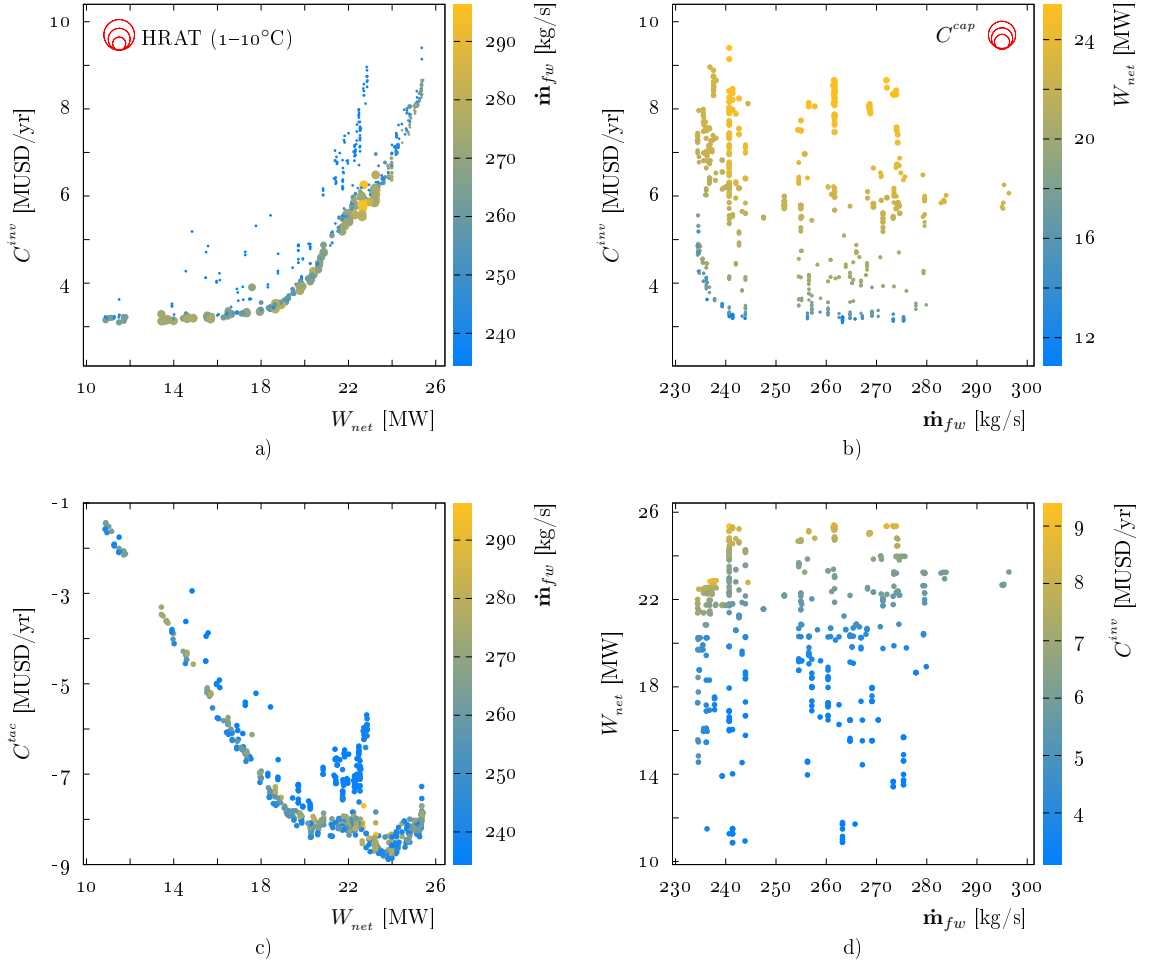


FIGURE 7.5—Pareto frontiers of the kraft case study

the sole criterion for decision makers to choose from. The solution strategy in this chapter puts emphasis on increasing the resource efficiency while providing a set of good solutions (Figure 7.5) which exhibit different performance indicators. The project manager and the mill experts are then able to analyze these solutions and decide which roadmap to select.

7.4.2 Analysis

It should be noted here that the cooling utility has variable make-up and power consumptions proportional to its cooling duty (Table 7.2). For this reason, reducing the cooling duty by, e.g., 1 MW_{th} , potentially increases the electricity production by 1.03 MW_{el} (electricity demand of the cooling utility reduces by $30 \text{ kW}_{el}/\text{MW}_{th}$), while more water remains in the system due to less make-up water demand in the cooling utility. These interactions manifest intertwined relations among these elements. The aim of this subsection is to analyze these relations to some extent by studying several selected scenarios. For each scenario, the integrated grand composite curve of each cluster is provided. This type of figure illustrates how steam and ORCs are thermally integrated with the process. Furthermore, for few selected scenarios, example heat load distributions are also shown. Analysis of the results of HLD provides insight into

possible heat recovery opportunities that should be further analyzed by mill experts to evaluate their feasibilities.

7.4.2.1 Visualization of all the solutions by several indicators

Figure 7.7 presents several indicators for all solutions in the Pareto frontiers (color spectrum is based on net power output). Several observations were made:

- The treated warm water tank temperature was mainly influenced by the return temperature of the cooling tower, i.e., fluctuated around 26°C.
- For solutions with lower electricity production, the temperature of the treated hot water tank was in higher ranges (62–64°C). This was due to the heat recovery using hot water loops among clusters. Furthermore the freshwater flow was higher for these solutions which was due to higher cooling loads in the cooling tower and hence higher demand of make-up water.
- The steam production in the recovery boiler occurred at very high pressure levels (150–160 bar) for high power output while for lower power outputs the pressure was lower while no ORC was integrated within the process (Figure 7.6).
- Higher electricity production required more stream matches and higher heat exchange areas indicating a highly integrated system.
- For high cooling loads, the temperature of cooling water was lower (around 35–40°C). The reason can be attributed to lower cost of heat exchangers in these cases due to higher approach temperatures.

The visualization of other indicators illustrates how different from or similar to each other these solution can become, necessitating the application of multi-criteria decision making tools in evaluating different solutions.

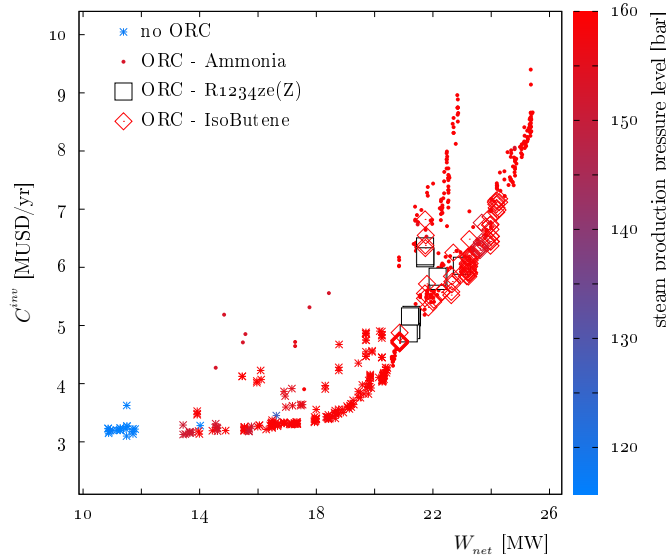


FIGURE 7.6—Pressure level of the recovery boiler and ORC working fluids of the Pareto frontiers

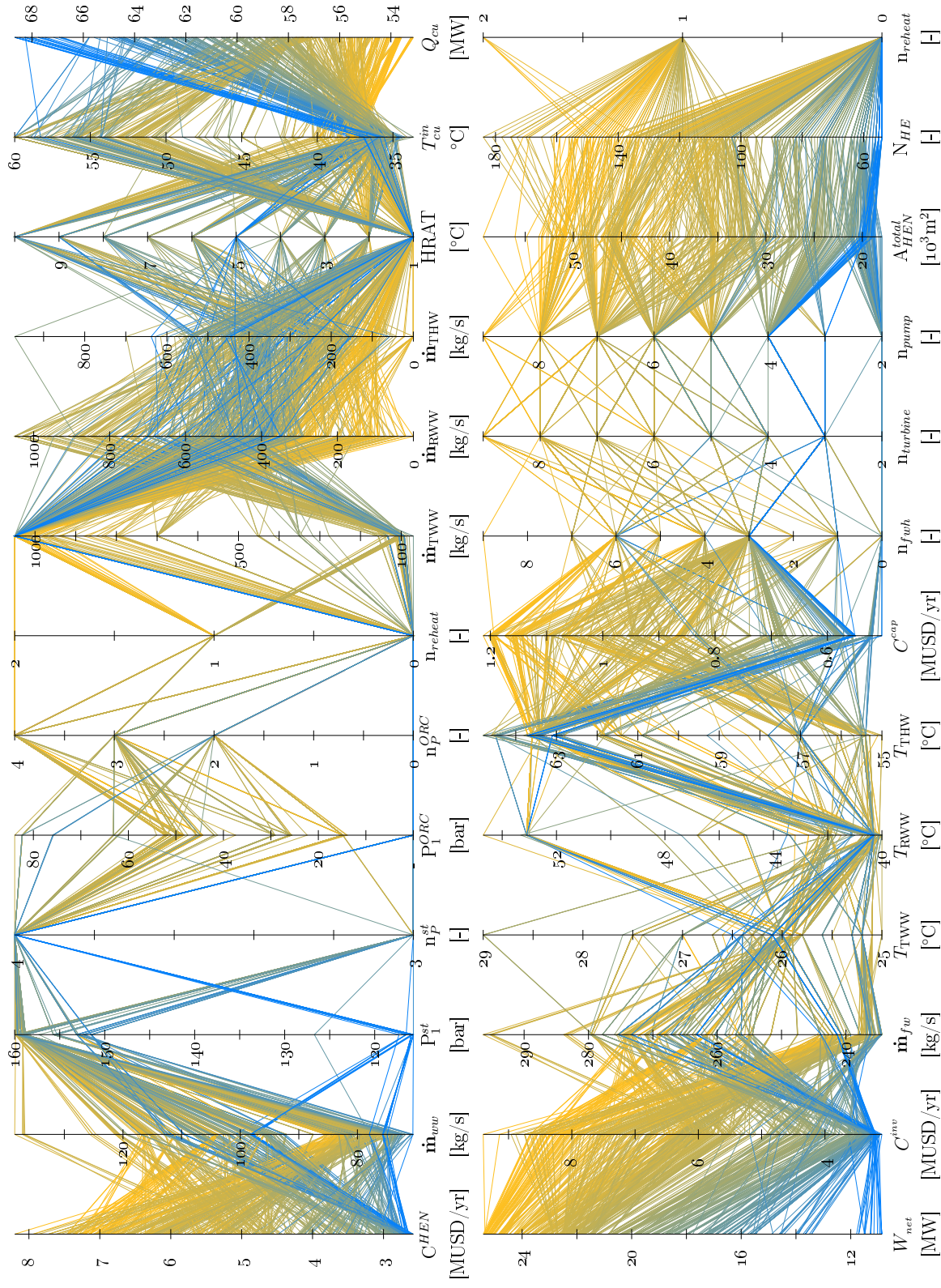


FIGURE 7.7—Visualization of key indicators of the Pareto frontiers (color spectrum is based on electricity production column)

7.4.2.2 Extreme points

Figure 7.8-a illustrates the Pareto frontier by highlighting the solutions with minimum and maximum values of the objective functions. Three solutions reached the minimum freshwater consumption of 234 kg/s with electricity production ranging between 17–25 MW_{el}. Figure 7.8-b presents some of the main indicators of these solution on a parallel coordinates. It can be observed that higher number of feed liquid heaters increased for higher values of electricity production. Furthermore, the cooling water inlet temperature to the cooling tower is indirectly proportional to freshwater consumption.

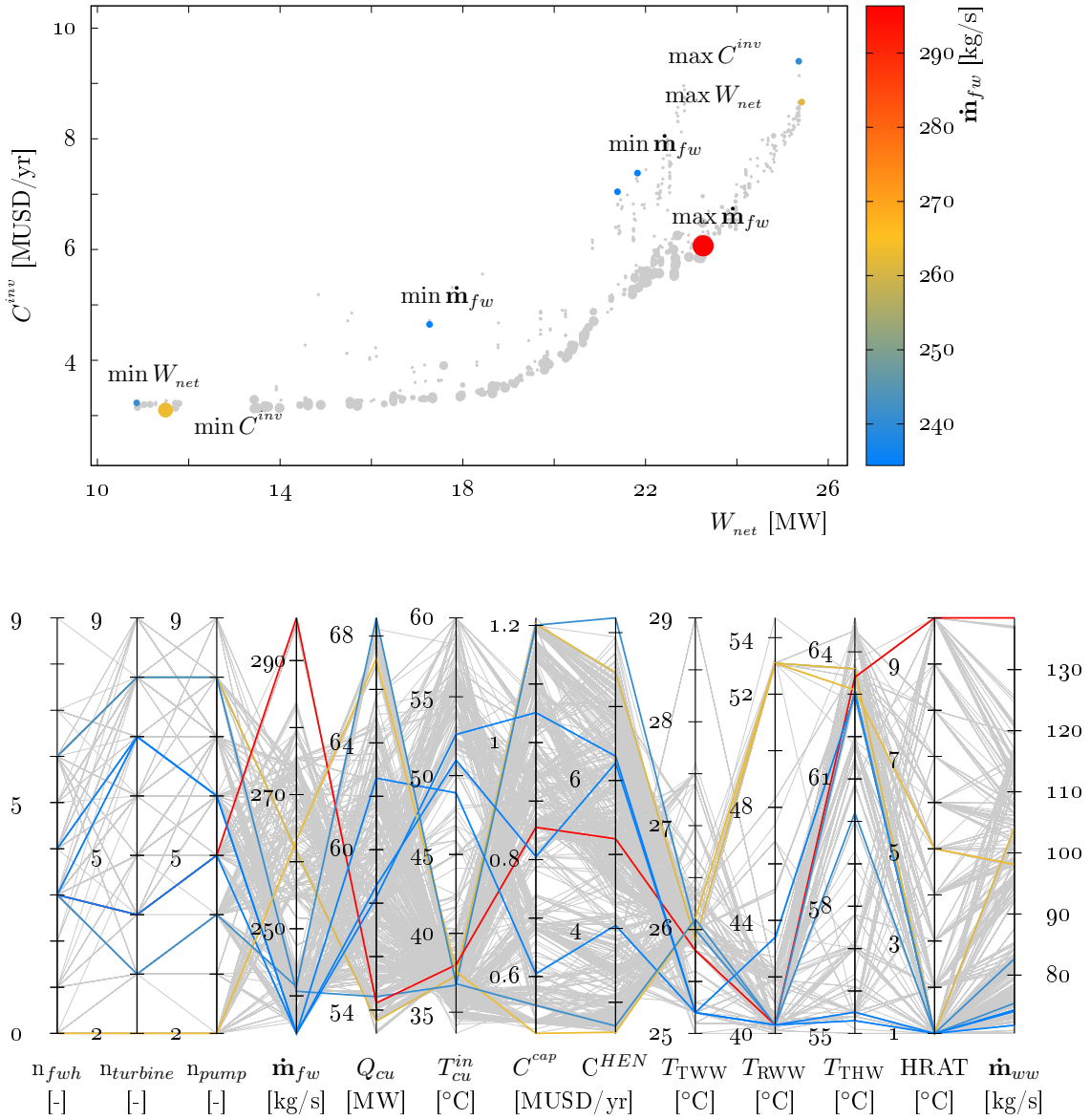


FIGURE 7.8—Solutions with minimum and maximum value of the three objectives

7.4.2.3 Cooling utility, freshwater consumption, and net power output

Figure 7.9 presents a simple schematic of the energy balance of the case study. Every dashed line represents a potential combination of energy conversion technologies and heat exchangers; for instance, available heat in terms of cooling demands of the clusters, $\sum_{clusters} Q_{cl}^C$, can be converted into electricity, W_{kraft} or W_{net} , by using ORC, while it can satisfy the heating demands of the clusters, $\sum_{clusters} Q_{cl}^H$, by heat recovery among clusters via hot water loops or ORC (i.e., condensation and evaporation at two different pressure levels). By rearranging the elements of the energy balance (Equation 7.2), a simple correlation can be derived among cooling duty, electricity consumption and freshwater consumption (proportional to the amount of heat in the water network) which is shown in Equation 7.3, where Q denotes a constant heat value:

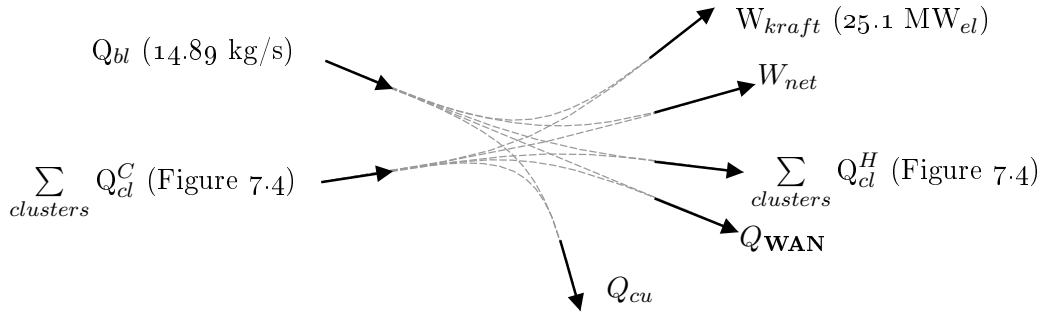


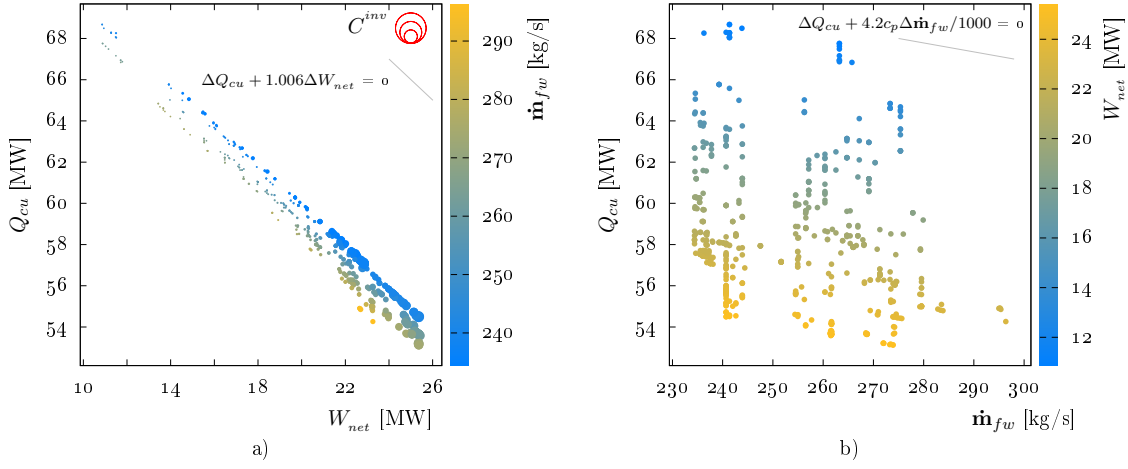
FIGURE 7.9—Schematic of energy balance in the kraft mill case study

$$Q_{bl} + \sum_{clusters} Q_{cl}^C = W_{kraft} + W_{net} + Q_{cu} + Q_{WAN} \quad (7.2)$$

$$Q = W_{net} + Q_{cu} + f(\dot{m}_{fw}) \quad (7.3)$$

Equation 7.3 states that for a given value of any of these three elements, a negative correlation exists among the other two. This was observed in the solutions of the optimization and are shown in Figure 7.10. For a given freshwater consumption, reducing the cooling utility by 1 MW_{th} increases the net power output by 1.03 MW_{el} . However, this also reduces the demand of make-up water by 0.556 kg/s which, for a given amount of freshwater consumption, means an increase in the flowrate of wastewater and evacuating 23.33 kW_{th} ¹ heat to the wastewater sink, resulting in overall 1.006 MW_{el} of power production. This is visible in Figure 7.10-a by the near-45-degree lines of constant freshwater consumption. The same reasoning can be applied for constant net power output production as shown in Figure 7.10-b where every line is formulated as $c_p \cdot (T_{ww} - T_{fw}) \cdot \Delta \dot{m}_{fw} + 1.03 \Delta Q_{cu} = 0$. Thus, for a specific net power output, the reduction in cooling duty (i.e., potential increase in power production) should be compensated by increasing the freshwater consumption and hence increasing the wastewater flow. If the increase in the freshwater flow is less than $\Delta \dot{m}_{fw}$, this amount of thermal energy should be converted to electricity, hence increasing the electricity production while increasing freshwater consumption.

¹ 0.556 [kg/s] × 4.2 [kJ/kgK] × (T_{ww}(30) - T_{fw}(20))

FIGURE 7.10—Cooling load *vs* freshwater consumption *vs* net power production

7.4.3 Heat integration and heat load distribution

In this section, several solutions were selected and analyzed from the Pareto frontiers by applying several criteria. Similar to the tool developed in Part II for fluid selection, parallel coordinates [19] were used to facilitate the procedure. For each selected solution, four graphs were plotted:

- Pareto frontier of the investment cost *vs* the net power output: to position the selected solution with respect to all the solutions on the basis of the values of the three objectives;
- parallel coordinates: similar to Figure 7.8, to highlight the value of other indicators of the selected solution with respect to all the solutions;
- integrated grand composite curve: to illustrate how a steam cycle and/or ORC are integrated with other processes, and how heat is transferred among the three clusters;
- Heat load distribution: to find potential thermal matches prior to the HEN design. As stated before, several HLD results are available for one solution of problem **P1**. For every solution of problem **P2** (HLD), large heat exchanges can be targeted to identify opportunities that should be evaluated for economic, physical, and thermodynamic feasibilities. This requires deep knowledge of the process and hence should be performed in collaboration with mill personnel. In this section, only the first solution of problem **P2** is presented. Furthermore, several heat recovery opportunities are extracted, however, the likelihood of their implementations are not discussed here.

7.4.3.1 Case I - no ORC integration

The first case was selected with the following criteria: the solution with maximum net power output which did not require an ORC and had minimum freshwater consumption and minimum investment cost. The selected solution is shown in Figure 7.11. The net power output was 18.7 MW_{el} with freshwater consumption of 234.7 kg/s (0.4 kg/s higher than the minimum freshwater consumption). The optimal steam network comprised four pressure levels (three

of which acted as condensers for the process as shown in Figure 7.11-c). Highest and lowest pressure levels, P_{st}^1 and P_{st}^4 , were at 159.5 and 1 bar, respectively. Sub-ambient pressure levels could have been selected, however, as the lowest pressure level creates a pinch point in the **PM** cluster, this necessitates increased use of steam at higher pressure and consequently lower electricity production. For each cluster, the heat load distribution shows the connections between streams and the related heat loads of these connections (Figure 7.12). All of these connections serve to reach the energy and water targets of the solution. Several types of heat exchanges can be observed by looking at the HLD results including new heat recovery opportunities by the use of black liquor flash tank (hot stream) in the steaming vessel (**DG** - 5.48 MW_{th}) and preheating water at the inlet of washing (**DG** - 4.48 MW_{th}). Furthermore, low temperature heating demands such as the ClO_2 heater in the bleaching section can be satisfied using hot water loops instead of consuming steam by transferring excess heat from **RB** cluster via water tanks.

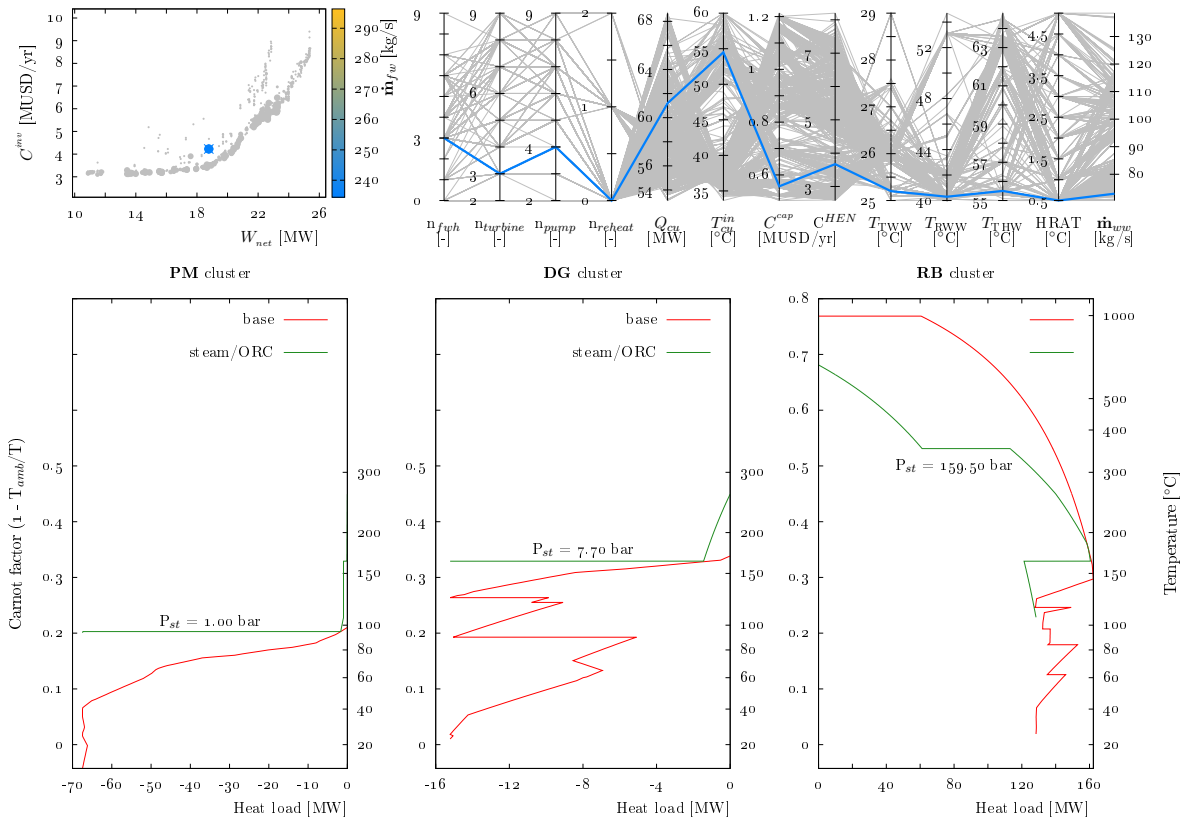


FIGURE 7.11—Integrated grand composite curves of case I



100%

7.4.3.2 Case II - maximum electricity production

The second case was selected with the following criteria: the solution with maximum net power which had minimum freshwater consumption and minimum investment cost. The selected solution is shown in Figure 7.13. The net power output was 25.1 MW_{el} (34.2% higher than case I) with freshwater consumption of 240.7 kg/s (2.4% higher than case I). As shown in Figure 7.13-c) this solution exhibits a highly integrated system with both a steam cycle and ORC (using ammonia as working fluid) functioning over four pressure levels. Increased value of the lowest pressure level in the steam cycle, P_{st}^4 , from 1 bar (case I) to 1.1 bar eliminated the use of medium pressure steam in **PM** cluster, while three condensation levels of the ORC supplied the heating requirement in this cluster. For each cluster, the heat load distribution

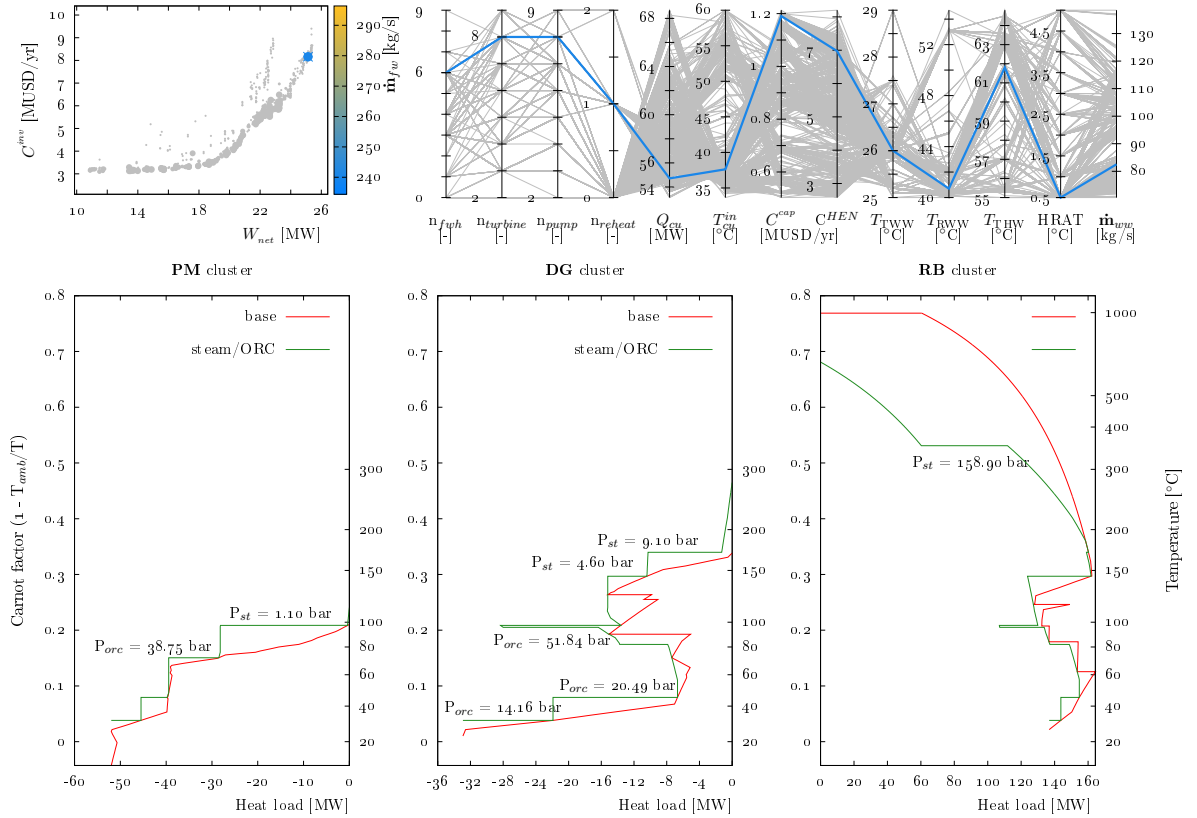
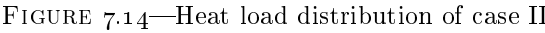


FIGURE 7.13—Integrated grand composite curve of case II

results are shown in (Figure 7.14). All of these connections serve to reach the energy and water targets of the solution. Several types of heat exchanges can be observed by looking at the HLD results including new and sometimes unusual heat recovery opportunities such as using dryer exhaust in the pulp machine section to preheat air (**PM** - 2.94 MW_{th}). Furthermore, in the **RB** cluster, opportunities exist in heat recovery between the condenser of the multi-effect evaporation and preheating the inlet of the concentration section (15.43 MW_{th} out of 16.22 MW_{th} demand) that must be evaluated by mill experts. It should be noted that in the current state of the mill, preheating is conducted by using steam while cooling is carried out using freshwater at 20°C. This heat recovery opportunity, alone, brings 11.7% reduction in steam



7.4.3.3 Case III - ORC with Isobutene

The optimal working fluid for the solution of case II was ammonia. Case III studies the potential of other working fluids. The following criteria were considered: A solution with a single-stage ORC working with isobutene that exhibits the lowest capital cost of the equipment. The selected solution is shown in Figure 7.15. The net power output was 21.8 MW_{el} with freshwater consumption of 279.6 kg/s. The electricity production has decreased by only 13% compared with case II, while the capital cost has reduced by more than 42% and freshwater consumption increased by 16%. This solution exhibits a simpler network structure while still achieving acceptable performance. Case III highlights the importance of providing multiple solutions to an optimization problem. This solution exhibits a relatively simpler network design compared with previous two cases which can be better-suited for real applications.

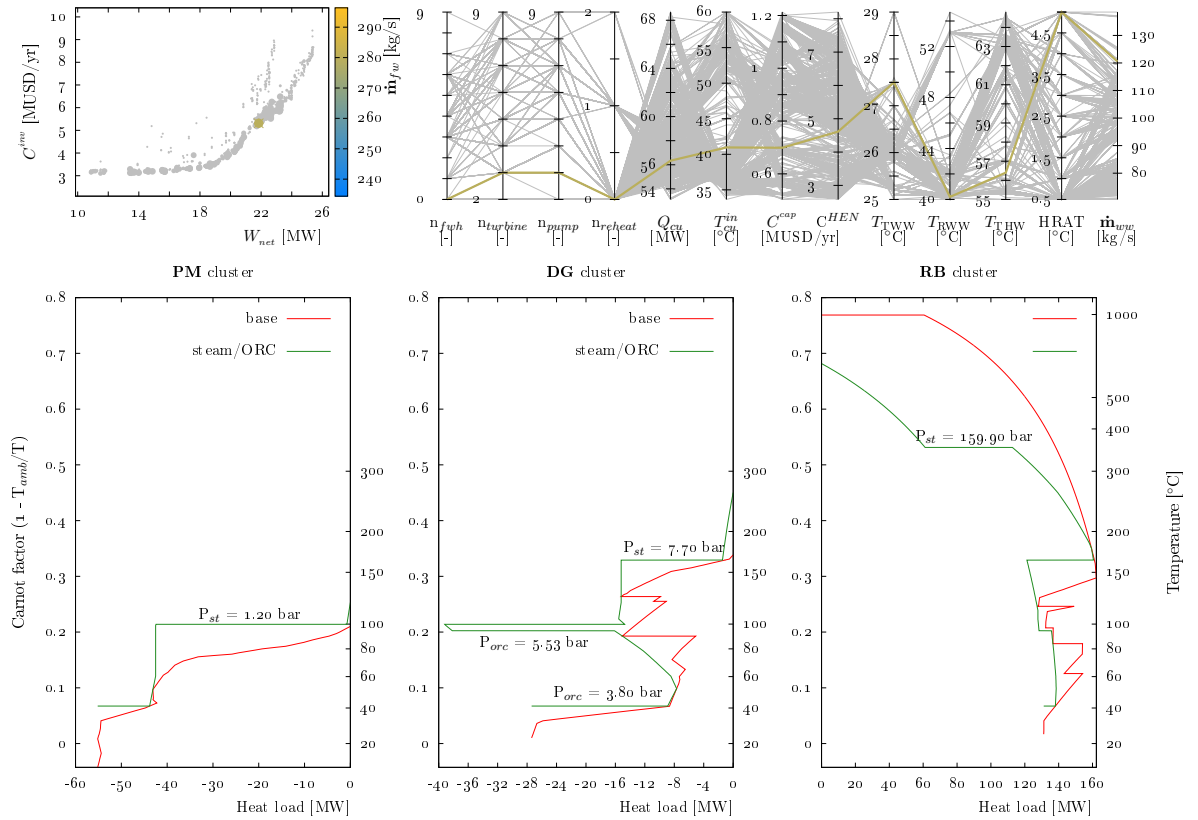


FIGURE 7.15—Integrated grand composite curve of case III

7.5 Conclusion

This chapter proposed and applied a holistic approach for the simultaneous consideration of heat, water, and power in industrial processes combining the proposed methodologies in Part I and Part II in several stages and making use of stochastic programming and deterministic techniques to optimize the water and energy consumption. The approach is able to generate a large set of optimal solutions where no single solution is better than others in all objectives. Par-

evaluations. Although the solution time was long, many promising solutions could be used directly in problem **P3** to further optimize the temperature and flowrates of the HIWAN or in a comprehensive MINLP model as very good initialization points. A complex system such as industrial mill cannot be fully designed by use of strict mathematical programming tools and requires human intervention at various stages to check, analyze, prevent, and improve the process. On improving the solution strategy, one interesting future work can be on development of hybrid genetic algorithms which can account for human insight at various levels of the evolution towards improving the generation of solutions and accelerating the solution strategy. Implementing any of the solutions will affect the implementation of any future energy efficiency measures or considerations and thus it is important to perform a holistic study which also includes potential changes or extensions to the system boundary by addressing network flexibility before making detailed designs.

In the kraft pulp mill case study, several emerging technologies and concepts have not been addressed in this chapter and will be the focus of future work. One promising concept requiring further research is the integration of biorefineries in the kraft pulp mill via thermochemical pathways, such as gasification or pyrolysis, and synthesizing their products into value-added bio-products such as ethanol and methanol. Syngas produced via a gasification can also be used in a gas turbine to produce electricity; consequently, the flue gases can be used to produce steam and, via a steam turbine, additional electricity. Furthermore, syngas can also be used in solid oxide fuel cells to further increase the electricity production. Storing excess electricity can be performed by producing hydrogen via water electrolysis for seasonal storage. Investigation and optimization of the integration of these technologies will require the generation and validation of rigorous models followed by reapplication of the techniques discussed throughout this thesis to provide highly-efficient, integrated bioprocessing systems. ■

References

- [1] M. Kermani, A. S. Wallerand, I. D. Kantor, F. Maréchal, A Hybrid Methodology for Combined Interplant Heat, Water, and Power Integration, in: A. Espuña, M. Graells, L. Puigjaner (Eds.), *Computer Aided Chemical Engineering*, vol. 40 of *27 European Symposium on Computer Aided Process Engineering*, Elsevier, 1969–1974, doi: \bibinfo{doi}{10.1016/B978-0-444-63965-3.50330-5}, URL <http://www.sciencedirect.com/science/article/pii/B9780444639653503305>, 2017.
- [2] R.-J. Zhou, L.-J. Li, H.-G. Dong, I. E. Grossmann, Synthesis of Interplant Water-Allocation and Heat-Exchange Networks. Part 2: Integrations between Fixed Flow Rate and Fixed Contaminant-Load Processes, *Industrial & Engineering Chemistry Research* 51 (45) (2012) 14793–14805, ISSN 0888-5885.
- [3] R.-J. Zhou, L.-J. Li, H.-G. Dong, I. E. Grossmann, Synthesis of Interplant Water-Allocation and Heat-Exchange Networks. Part 1: Fixed Flow Rate Processes, *Industrial & Engineering Chemistry Research* 51 (11) (2012) 4299–4312, ISSN 0888-5885.
- [4] N. Ibrić, E. Ahmetović, Z. Kravanja, F. Maréchal, M. Kermani, Synthesis of single and interplant non-isothermal water networks, *Journal of Environmental Management* 203 (Part 3) (2017) 1095–1117, ISSN 0301-4797.
- [5] V. R. Dhole, B. Linnhoff, Total site targets for fuel, co-generation, emissions, and cooling, *Computers & Chemical Engineering* 17 (1993) S101–S109, ISSN 0098-1354.
- [6] P. Y. Liew, W. L. Theo, S. R. Wan Alwi, J. S. Lim, Z. Abdul Manan, J. J. Klemes, P. S. Varbanov, Total Site Heat Integration planning and design for industrial, urban and renewable systems, *Renewable and Sustainable Energy Reviews* 68, Part 2 (2017) 964–985, ISSN 1364-0321.
- [7] C. A. Floudas, A. R. Ciric, Strategies for overcoming uncertainties in heat exchanger network synthesis, *Computers & Chemical Engineering* 13 (10) (1989) 1133–1152, ISSN 0098-1354.
- [8] M. Suhr, G. Klein, I. Kourti, M. R. Gonzalo, G. G. Santonja, S. Roudier, L. D. Sancho, Best available techniques (BAT) reference document for the production of pulp, paper and board, JRC science and policy reports, Industrial Emissions Directive 2010/75/EU Integrated Pollution Prevention and control -, URL <http://eippcb.jrc.ec.europa.eu/reference/pp.html>, 2015.
- [9] Z.-W. Liao, G. Rong, J. Wang, Y. Yang, Systematic Optimization of Heat-Integrated Water Allocation Networks, *Industrial & Engineering Chemistry Research* 50 (11) (2011) 6713–6727, ISSN 0888-5885.
- [10] E. Mateos-Espejel, L. Savulescu, F. Maréchal, J. Paris, Unified methodology for thermal energy efficiency improvement: Application to Kraft process, *Chemical Engineering Science* 66 (2) (2011) 135–151, ISSN 0009-2509.
- [11] M. Kermani, Z. Périn-Levasseur, M. Benali, L. Savulescu, F. Maréchal, A novel MILP approach for simultaneous optimization of water and energy: Application to a Canadian softwood Kraft pulping mill, *Computers & Chemical Engineering* ISSN 0098-1354.
- [12] E. Vakkilainen, Kraft recovery boilers – Principles and practice, Suomen Soodakattilayhdistys r.y., ISBN 952-91-8603-7, URL <http://www.doria.fi/handle/10024/111915>, 2005.

- [13] IPPC, Best available techniques (BAT) reference document for the production of pulp, paper and board, JRC science and policy reports, Industrial Emissions Directive 2010/75/EU Integrated Pollution Prevention and control -, URL <http://eippcb.jrc.ec.europa.eu/reference/cv.html>, 2001.
- [14] I. H. Bell, J. Wronski, S. Quoilin, V. Lemort, Pure and Pseudo-pure Fluid Thermophysical Property Evaluation and the Open-Source Thermophysical Property Library CoolProp, *Industrial & Engineering Chemistry Research* 53 (6) (2014) 2498–2508.
- [15] B. Adams, L. Bauman, W. Bohnhoff, K. Dalbey, M. Ebeida, J. Eddy, M. Eldred, P. Hough, K. Hu, J. Jakeman, J. Stephens, L. Swiler, D. Vigil, T. Wildey, Dakota, A Multilevel Parallel Object-Oriented Framework for Design Optimization, Parameter Estimation, Uncertainty Quantification, and Sensitivity Analysis: Version 6.0 User’s Manual, Sandia Technical Report SAND2014-4253, 2015.
- [16] J. Eddy, K. Lewis, Effective Generation of Pareto Sets Using Genetic Programming, in: ASME Design Engineering Technical Conference, 2001, URL http://does.eng.buffalo.edu/index.php?option=com_jresearch&view=publication&task=show&id=59, 2001.
- [17] IBM ILOG CPLEX V12.2: User’s manual for CPLEX, Tech. Rep., IBM Corporation, 2010.
- [18] R. Fourer, D. M. Gay, B. W. Kernighan, AMPL: A Modeling Language for Mathematical Programming, Cengage Learning; 2 edition, ISBN 0-534-38809-4, 2003.
- [19] A. Inselberg, The plane with parallel coordinates, *The Visual Computer* 1 (2) (1985) 69–91, ISSN 0178-2789, 1432-2315.

Concluding remarks

“In theory, theory and practice are the same. In practice, they are not.”
-Anonymous

This chapter provides a thesis summary by highlighting the main contributions, outcomes, and limitations. Furthermore, it postulates several guidelines as future research directions. This is carried out for each of the research topics presented in the introduction.

How can heat and water exchanges be systematically managed within industrial processes? How can industrial specificities be addressed in the solution strategy? What are the main criteria in optimizing such systems? What approach can be used to generate a set of energy and water saving opportunities? ([Part I](#))

A comprehensive literature review was conducted throughout chapter 1, focusing on mathematical approaches rather than conceptual approaches, because they are capable of encompassing many water–energy reduction opportunities. However, a lack of industrial insight and solution complexity illustrated the necessity of prioritizing hybrid approaches. Two main difficulties arise when generating a superstructure for HIWANs: the state of water streams and their interactions with HEN, i.e., what types of water streams (freshwater, wastewater, recycle, reuse) are subject to heat exchanges and whether they are labeled hot or cold. This can be addressed by considering all water streams participating in heat exchange and by introducing binary variables to represent their states; however, this brings a combinatorial complexity to the overall MINLP formulation. These issues were addressed throughout chapter 2 and chapter 3 by proposing an iterative sequential solution strategy and a novel NLP hyperstructure for the design of HIWANs. The overall MINLP formulation was broken down into three models: the first model (problem **P1**, section 2.2) is a targeting model formulated as MILP with the objective of minimizing the total cost of the system while considering penalty costs for water thermal streams. Non-isothermal mixing was addressed by discretizing the temperature intervals. The solution of problem **P1** provides minimum targets as well as a set of potential water thermal streams that can participate in heat exchange. Furthermore, a feasible water allocation network is designed. The second model (problem **P2**, subsection 2.2.4) is the well-known HLD model that minimizes the number of thermal matches for a given set of thermal streams. The third model (problem **P3**, section 3.2) is a novel HIWAN hyperstructure that is formulated as NLP by considering heat exchanger and water network constraints. Problem **P3** optimizes the temperatures and flowrates of the water network subject to the given thermal matches and their states. The water allocation network of problem **P1** can be changed at this stage. As the choice of integers in problems **P1** and **P2** may not result in an overall HIWAN with the minimum total cost, an integer cut constraint is implemented in the first two models to generate and rank many solutions. To address the trade-off between the operating

cost and the investment cost of the heat exchangers, the overall problem can be solved for different values of HRAT (problems **P1** and **P2**) while ΔT_{min} (problem **P3**) is set equal to HRAT. Following the validation procedure, it was observed that the proposed methodology was able to reach the minimum total cost (given the only objective function in the literature) and generated a set of good solutions exhibiting different key performance indicators. The formulated water allocation network addresses the lack of quantitative contamination data by incorporating restricted/forbidden matches. Furthermore, water tanks were modeled that can be regarded as interceptors in interplant operations. Their temperatures can be optimized by solving problem **P3**. These two features can address a variety of industrial applications, particularly in the pulp and paper industry. Although the main objective of the overall solution strategy is the minimization of total cost, several key performance indicators were proposed that can help decision-makers find the most appropriate solution among the generated set of options. Industrial constraints and expert insight can easily be incorporated in the modeling framework using a variety of constraints in problems **P1** and **P2** before going into the detailed HEN design.

Limitations, future directions, and possible solutions Due to the sequential nature of the solution strategy in which the overall model is solved over three loops, i.e., integer cut on problems **P1** and **P2** and value of HRAT, **resolution time** may increase dramatically; however, the generation of many solutions is potentially useful in decision-making process for industrial applications in which no one solution exists that satisfies all criteria. As discussed in chapter 1, use of **live steam** (i.e., direct steam injection) can be beneficial in reducing the investment cost even with the expense of adding additional boiler make-up water [1]. This feature has not been investigated in this work; however, the implementation can be straightforward: assuming a constant heat capacity (c_p) for liquid-state water streams, a *pseudo-temperature* can be defined for vapor-state water streams, $T_{live\ steam}$, given by $h_{p,T}/c_p$, where $h_{p,T}$ is the enthalpy of steam at pressure p and temperature T .

Wastewater treatment has not been addressed in this work. One possible approach is to include the choice of the treatment technology using binary variables in problem **P1** while optimizing their operating conditions in problem **P3**. Contamination concentration of the treatment technology can be discretized following the same approach of temperature levels. Furthermore, the targeting approach proposed by Yang and Grossmann [2] can be implemented in order to provide good initialization points. The proposed superstructure is intended for the grassroot design of HIWAN and cannot be applied to **retrofit** problems; however, as shown for problem **P3**, for a given set of thermal matches, the operating conditions of a water allocation network can be optimized, i.e., temperatures, flowrates, and heat exchange areas. Thus, for retrofit cases in which additional heat exchangers are not envisaged, the proposed superstructure can be applied at the current level. For investigating the addition of new heat exchangers, problem **P2** can be reformulated by adding new constraints.

In addition to these limitations of the current work, and following the literature survey in chapter 1, further developments can be envisaged (a more complete list is provided in section 1.6): **multi-period operation** of HIWANs is still not addressed in the literature. Considering the daily to seasonal variations of operating conditions of processes, temperatures of freshwater, etc., multi-period problem formulation plays a vital role in the design of a system. **Uncertainty analysis** of HIWAN should also be addressed to find the most resilient networks given system uncertainties, including costs and operating conditions. Furthermore,

with a large set of alternative solutions several scenarios can be created by sampling the domain of influential parameters within feasible and practical ranges via different sampling techniques. These parameters are not fixed, but some examples are cost data, interest rate, expected lifetime, and environmental performance. The generated set of solutions could then be evaluated for every scenario and ranked based on the probability of their appearance in the best set with regard to several key performance indicators. The solution with the highest appearance can be regarded as the most resilient design given the uncertainties in the parameters. **Flexible design** of HIWAN should be addressed as it facilitates the implementation of future possible (retrofit) projects. The proposed NLP hyperstructure combined with the targeting and HLD models are proven to encompass large water–energy reduction possibilities; nevertheless, the NLP model faces many convergence challenges, which necessitates research in **improved optimization techniques** to be developed for non-convex problems.

Given the ORC as a promising technology to produce electricity from low to medium temperature heat, how can it be optimally integrated within a process for maximizing electricity production? What are the influential elements and how can they be addressed in the modeling and optimization stages? ([Part II](#))

A comprehensive literature review was carried out in section 4.2 by investigating the main elements of an ORC and current approaches in ORC integration with industrial processes. Conceptual methods relying only on graphical and insight-based rules cannot fully evaluate the vast search space for the optimal selection of an ORC and its operating conditions. However, the insight from their application can be coupled with mathematical approaches. The main elements of an ORC, i.e., architecture and working fluid, are directly linked to the type of processes in which the ORC is integrated. Few superstructures have been proposed for ORC usage, and inside those, a limited number of architectures have been considered. There is a gap in superstructure-based approaches that can provide all possible interconnections and architectures, in particular, bleeding cycles and transcritical cycle (only addressed by Bendig et al. [3]). At the level of industrial integration, the majority of research in the literature focused on waste heat recovery by neglecting the potential of simultaneous optimization and ORC integration. ORC architectures resemble those of utility systems (i.e., steam cycle superstructure) and hence many more architectural possibilities can be addressed. To this end, a systematic methodology for optimal integration of ORCs in industrial processes was proposed in chapter 5. This methodology consists of a novel ORC superstructure solved using a two-stage decomposition solution strategy. The superstructure includes several ORC architectures including regenerative, superheating, reheating, turbine-bleeding (open/closed feed liquid heater), transcritical, and multi-stage cycles. Depending on the case specificities and the industrial process requirements, several of these cycles can be combined or forbidden in the superstructure. Maintaining linearity in the heat cascade formulation prompted the development of a novel dynamic linearization technique for hot and cold streams of the superstructure. Near-critical and transcritical isobaric temperature-enthalpy profiles of all working fluids can exhibit sharp curvatures for which traditional three-piece linearization (subcooled, two-phase, and superheated regions) might exhibit large error, particularly in the superheated region of hot streams and subcooled region of cold streams. Dynamic linearization techniques provide inner (outer) approximations for hot (cold) streams in the ORC superstructure, as shown in subsection 5.2.2. The two-stage decomposition technique was carried out using a genetic algorithm by optimizing the complicating variables (i.e., working fluid and its operating con-

ditions) in the upper level while selecting the ORC architecture and equipment sizing in the resulting MILP inner level. The overall methodology considers a variety of objective functions and potential working fluids and is extensible in both aspects to include alternative objectives or working fluids, such as supercritical CO₂. The multi-objective optimization generates a set of competing solutions to be analyzed by the engineers who ultimately select the most appropriate solution. Applications of the methodology on a literature case study showed that combining several ORC architectures yielded economic and energetic benefits, as illustrated in Figure 5.8. The methodology provides a promising set of solutions, which is essential for industrial decision-making processes.

Limitations, future directions, and possible solutions The calculation of thermodynamic properties in the proposed methodology relies on packages such as CoolProp [4] or RefProp [5]. For this reason, **investigating novel fluids** is not possible at this stage. Incorporating techniques such as the group contribution method to allow designing and determining molecules with the appropriate set of physicochemical characteristics [6, 7, 8] can alleviate this limitation. Furthermore, the working fluids are limited to pure fluids and hence **mixtures (zeotropic and azeotropic)** cannot be addressed. The efficiency of turbines and pumps are assumed constant in the proposed superstructure; it is hence required to implement **efficiency curves** for more detailed analysis, particularly in **part-load operations**. **Pressure drops** are neglected in the approach and should also be considered. Additional research is needed for **improving the accuracy of correlations for heat transfer coefficients**, particularly for **supercritical correlations**. As was shown, supercritical correlations are mainly derived from water and CO₂. **HEN design** is not addressed as part of the optimization but rather as a post-processing step. Due to the sequential approach taken at the inner level of the solution strategy (similar to the strategy in Part I), the NLP formulation of Floudas and Ciric [9] can be incorporated; however, this would require additional modifications by incorporating condensation and evaporation streams and modeling of piece-wise thermal streams.

Future work should focus on the adaptation of the proposed methodology to **large-scale industrial applications** by incorporating practical constraints. This includes addressing **multi-period operation** with seasonal variability of operating conditions and interplant operations, where the ORC can be combined with storage to provide a flexible heat transfer medium to compete with conventional ones. To this end, pursuing a holistic approach will require improved solution strategies to alleviate the computational burden of large-scale cases. Many other developments can be envisaged, such as the **controllability** and **part-time operation** of ORCs, and addressing the **technological constraints** in the design and operations stages.

How can heat, mass (water), and power flows be simultaneously considered in planning an industrial site? What type of approach and what steps should be taken in tackling such problems? (Part III)

The growing desire to improve the resource efficiency and environmental impact of industrial processes is directly linked to the optimal management of heat, mass, and power flows. This requires the development of holistic approaches to address all of these elements together. Interactions among heat and mass have been extensively studied in the literature regarding heat-integrated mass allocation network (chapter 1) where thermal utilities were excluded.

Thermal utility integration in industrial processes or in broader perspective studies on combined heat and power production and integration have been also addressed in the literature regarding steam and ORC optimization (section 4.2). In both cases, any interactions with mass streams were neglected. These excluded interactions are significant in interplant operations in which heat/resources of one plant (site) can be recycled or reused in others. Total site analysis studies interplant operations by only considering heat recovery via steam production and condensation while neglecting power production and other heat transfer media. A gap was observed in the literature for approaches that can address these elements in a systematic manner, particularly by combining heat, mass, and power optimization in inter-process (interplant) operations.

A motivating case study in chapter 6 showed the potential in the simultaneous consideration of these elements. It further illustrated the complexity of optimizing the whole system by highlighting the high number of decision variables and modeling features that must be considered. Chapter 7 aimed to solve the overall problem by introducing an industrial case study of a kraft pulp mill and providing the necessary steps towards the final design. HIWAN, ORC, a steam cycle, interplant operations, forbidden matches, and cooling utilities were combined to illustrate the synergies and the necessity of applying a holistic approach. The methodologies developed in Parts I and II of this report were combined at various levels. Due to the high number of decision variables, the use of stochastic optimization techniques (GA) combined with decomposition approaches was favored in solving the problem. The set of decision variables comprised operating conditions of the steam cycle and ORC, and temperatures of water tanks. Furthermore, due to the existence of many indicators, multi-objective optimization of the overall system was performed by optimizing the three conflicting objectives of minimizing freshwater consumption, maximizing electricity generation, and minimizing the total investment cost. In general, GA requires many function evaluations to solve the problem within a reasonable convergence threshold. As detailed design of the system is not considered at this level, and to further reduce the computational time, problem **P3** was excluded from the overall solution strategy, while HEN cost was estimated by Equations 2.43–2.45. The solution strategy proposed in Part I could be applied on each solution of the Pareto frontier to further optimize the overall network. Several solutions of the Pareto frontier were selected and presented using integrated grand Carnot composite curves by plotting the processes against the steam cycle and ORC. They illustrated the interactions and the synergies among the elements and that they must be treated simultaneously, as neglecting one element would result in a tendentious approach.

Limitations and future directions The proposed solution strategy in chapter 7 did not aim at providing an exhaustive approach to address the grand design of an industrial process but rather to highlight the necessity of applying holistic approaches in optimizing industrial processes. To this end, the work is limited in many aspects and requires further research. In addition to the limitations already discussed, **resolution time** is a critical issue; for the investigated case study, every function evaluation took between 3–130 seconds, or 2,000 function evaluations per 24 hours, on a machine with 16 CPU cores and 32 GB of RAM. **Systematic size reduction** of the overall superstructure and **novel solution strategies** must be addressed in future work. The work in this part was limited to thermal and mass streams of an industrial plant, neglecting the main processes and how the quality of a thermal or mass stream might affect the overall production efficiency of a plant. This requires **rigorous**

modeling of all the processes for **simultaneous process design and integration**.

The potential implications of this work are broad, extending from total site integration to industrial symbiosis. ■

References

- [1] L. E. Savulescu, R. Smith, Simultaneous energy and water minimisation, in: 1998 AIChE Annual Meeting, Miami Beach, Florida, 13–22, unpublished work, 1998.
- [2] L. Yang, I. E. Grossmann, Water Targeting Models for Simultaneous Flowsheet Optimization, *Industrial & Engineering Chemistry Research* 52 (9) (2013) 3209–3224, ISSN 0888-5885.
- [3] M. Bendig, D. Favrat, F. Marechal, Methodology for Identification of Suitable ORC-Cycle and Working-Fluid using Integration with Multiple Objectives, *Pres 2014, 17Th Conference On Process Integration, Modelling And Optimisation For Energy Saving And Pollution Reduction, Pts 1-3* 39 (2014) 1141–1146.
- [4] I. H. Bell, J. Wronski, S. Quoilin, V. Lemort, Pure and Pseudo-pure Fluid Thermophysical Property Evaluation and the Open-Source Thermophysical Property Library CoolProp, *Industrial & Engineering Chemistry Research* 53 (6) (2014) 2498–2508.
- [5] E. W. Lemmon, M. L. Huber, M. O. McLinden, NIST Standard Reference Database 23: Reference Fluid Thermodynamic and Transport Properties-REFPROP, Version 9.1, Natl Std. Ref. Data Series (NIST NSRDS) - .
- [6] P. M. Harper, R. Gani, P. Kolar, T. Ishikawa, Computer-aided molecular design with combined molecular modeling and group contribution, *Fluid Phase Equilibria* 158 (1999) 337–347, ISSN 0378-3812.
- [7] A. I. Papadopoulos, M. Stijepovic, P. Linke, P. Seferlis, S. Voutetakis, Toward Optimum Working Fluid Mixtures for Organic Rankine Cycles using Molecular Design and Sensitivity Analysis, *Industrial & Engineering Chemistry Research* 52 (34) (2013) 12116–12133, ISSN 0888-5885.
- [8] W. Su, L. Zhao, S. Deng, Simultaneous working fluids design and cycle optimization for Organic Rankine cycle using group contribution model, *Applied Energy* 202 (2017) 618–627, ISSN 0306-2619.
- [9] C. A. Floudas, A. R. Ciric, Strategies for overcoming uncertainties in heat exchanger network synthesis, *Computers & Chemical Engineering* 13 (10) (1989) 1133–1152, ISSN 0098-1354.

APPENDIX

APPENDIX A

Assumptions and solver options for test cases

All test cases are run on a Windows machine with Intel(R) Core(TM) i7-4600U CPU 2.10GHz 2.7 GHz and 8.00 GB RAM. Industrial kraft pulp case study of chapter 7 is run on a Windows machine with Intel(R) Xeon(R) CPU E5-2680 v4 2.40GHz 2.4 GHz and 32 GB RAM. The models are written in AMPL programming language ¹

General assumptions for all test cases

- ▶ Numbers of integer cuts for problem **P1** and **P2** are $N_{icc}^{P1} = 50$ and $N_{icc}^{P2} = 50$.
- ▶ To apply integer cuts, minimum size of water units (problem **P1**) is set at 0.05 kg/s and minimum heat exchange between thermal streams ($Q_{i,j,l}^{min}$ in problem **P2**) is set at 0.1 kW.
- ▶ $HRAT = \Delta T_{min}$ for each iteration.
- ▶ For problem **P1**, sum of mass exchanges is added to the objective function (Equation 2.7) to reduce the number of mass exchanges while minimizing the total cost.
- ▶ In mathematical formulation of HIWAN hyperstructure, the optimality gap of constraints of heat balance at mixing points is set at 0.01%.
- ▶ The value of ΔT_{min} for hot and cold utilities is set at 10°C.
- ▶ Enthalpy values of thermal stream are rounded for HEN design to 10^{-6} (test case I and the simplified industrial case study) and 10^{-2} (test case II and III)

¹R. Fourer, D. M. Gay, B. W. Kernighan, AMPL: A Modeling Language for Mathematical Programming, Cengage Learning; 2 edition, ISBN 0-534-38809-4, 2003

TABLE A.1—Assumption and solver options for test case I (subsection 3.5.1)

Solver Option	Value	Description (mainly from respective solver's manual)
AMPL		
reset_initial_guesses	1	Reset variables to their initial values between different calls to solve command (all steps)
presolve_eps	variable	Maximum difference between lower and upper bounds in constraint violations (10^{-6} (P1) and 10^{-5} for the rest)
presolve	1	Simplifying problem prior to the solver by fixing variables and dropping redundant constraints (all steps)
P1 (CPLEX)		
mipgap	10^{-4}	Relative tolerance for optimizing integer variables: stop if $\text{abs}((\text{best bound}) - (\text{best integer})) < \text{mipgap} * (1 + \text{abs}(\text{best bound}))$.
integrality	10^{-10}	Amount by which an integer variable can differ from the nearest integer and still be considered feasible.
P2 (CPLEX)		
mipgap	10^{-7}	See above
integrality	10^{-10}	See above
P3 (initialization) (SNOPT)		
▷ Problem P3 is solved by minimizing the sum of flows between heat exchangers		
meminc	1	Increment to minimum memory allocation
iterations	10^6	Minor iteration limit
feas_tol	10^{-6}	Minor feasibility tolerance, Feasibility tolerance for all variables and linear constraints
P3 (SNOPT)		
meminc = 1 iterations = 10^6 feas_tol = 10^{-4} (see above)		
P3 HIWAN hyperstructure (SNOPT)		
meminc = 1 iterations = 10^6 feas_tol = 10^{-4} (see above)		

TABLE A.2—Assumption and solver options for test cases II and III (subsection 3.5.2 and 3.5.3)

Solver Option	Value	Description (mainly from respective solver's manual)
AMPL		
reset_initial_guesses	1	All steps (see Table A.1 for description)
presolve_eps	variable	10^{-6} (P1) and 10^{-5} for the rest (see Table A.1 for description)
presolve	1	All steps (see Table A.1 for description)
P1 (CPLEX)		
mipgap	10^{-4}	(see Table A.1 for description)
integrality	10^{-10}	(see Table A.1 for description)
P2 (CPLEX)		
mipgap	variable	10^{-4} (test case II), 10^{-5} (test case III) (see Table A.1 for description)
integrality	10^{-8}	(see Table A.1 for description)
P3 (initialization) (SNOPT)		
▷ Problem P3 is solved by minimizing the sum of flows between heat exchangers		
meminc	1	(see Table A.1 for description)
iterations	10^6	(see Table A.1 for description)
feas_tol	10^{-4}	(see Table A.1 for description)
P3 (SNOPT)		
meminc = 1 iterations = 10^6 feas_tol = 10^{-4} (see Table A.1 for description)		
P3 HIWAN hyperstructure (SNOPT)		
meminc = 1 iterations = 10^6 feas_tol = 10^{-4} (see Table A.1 for description)		

TABLE A.3—Assumption and solver options for simplified industrial case study (subsection 3.5.4)

Solver Option	Value	Description (mainly from respective solver's manual)
AMPL		
reset_initial_guesses	1	All steps (see Table A.1 for description)
presolve_eps	variable	10^{-4} (P1) and 10^{-5} for the rest (see Table A.1 for description)
presolve	1	All steps (see Table A.1 for description)
P1 (CPLEX)		
mipgap	10^{-5}	(see Table A.1 for description)
integrality	10^{-4}	(see Table A.1 for description)
P2 (CPLEX)		
mipgap	10^{-5}	(see Table A.1 for description)
integrality	10^{-8}	(see Table A.1 for description)
P3 (initialization) (SNOPT)		
▷ Problem P3 is solved by minimizing the sum of flows between heat exchangers		
meminc	1	(see Table A.1 for description)
iterations	10^6	(see Table A.1 for description)
feas_tol	10^{-4}	(see Table A.1 for description)
P3 (SNOPT)		
meminc = 1 iterations = 10^6 feas_tol = 10^{-4} (see Table A.1 for description)		
P3 HIWAN hyperstructure (SNOPT)		
meminc = 1 iterations = 10^6 feas_tol = 10^{-4} (see Table A.1 for description)		

Assumptions

- Constraints fixing the heat load of heat exchangers for non-water process thermal streams are dropped. The total sum of these heat loads (for a given thermal stream) is fixed at the heat load of that thermal stream.

TABLE A.4—Assumption and solver options for industrial kraft pulp mill (chapter 7)

Solver Option	Value	Description (mainly from respective solver's manual)
GA (see Table 5.9 for descriptions)		
Population size	400	—
Initialization type	unique_random	—
Crossover type (rate)	multi_point_real 1	performing a variable switching crossover routing at 1 crossover point in the real valued genome of two designs
Crossover rate	0.8	—
Mutation type	bit_random	—
Mutation rate	0.2	—
Convergence type	metric_tracker	Converge if metric is below “percent_change” (0.01) for a given consecutive generations (10)
Fitness type	domination_count	below_limit = 1
Niching type	max_designs = 0.02	encourage differentiation along the Pareto frontier. Minimum distance between any two points is set at 2%
Number of evaluations	num_designs = 400	Limit the number of solutions that remain in each generation to 400
Number of generations	60,000	Maximum number of evaluations (a convergence criterion)
	100	Maximum number of generations (a convergence criterion)
AMPL		
reset_initial_guesses	1	All steps (see Table A.1 for description)
presolve_eps	variable	10^{-4} (P1) and 10^{-6} (P2)
presolve	1	All steps (see Table A.1 for description)
P1 (CPLEX)		
mipgap	$5 \cdot 10^{-3}$	(see Table A.1 for description)
integrality	10^{-9}	(see Table A.1 for description)
timelimit	120	Time limit in seconds
P2 (CPLEX)		
mipgap	10^{-2}	(see Table A.1 for description)
integrality	10^{-8}	(see Table A.1 for description)
flowcuts	1	Aggressive use of flow cuts in solving MIP
mircuts	1	Moderate generation of MIP rounding cuts
dgradient	2	Pricing algorithm for dual simplex (2 = steepest-edge pricing)
timelimit	60	
Assumptions		

► Values of “flowcuts”, “mircuts”, and “dgradient” are selected by running CPLEX’s automatic tuning tool.

APPENDIX B

Algorithm for outer and inner approximation of thermal streams

B.1 Bounds of linearization

Table B.1 provides the algorithm for finding upper and lower bounds in the linearization procedure.

TABLE B.1—Algorithm for finding the boundaries of the linearization

Steps	Procedure
1	Input $T_{i,in}, T_{i,out}, wf(\text{working fluid}), P_i, T^{tol}$
3	Calculate $P_{wf,cr}, T_{wf,cr}$, and $T_{i,wf}^{sat}$
2	Calculate the upper and lower bounds of temperature and enthalpy: $T_{min} = \min(T_{i,in}, T_{i,out})$ $T_{max} = \max(T_{i,in}, T_{i,out})$
	$h_{min} = \begin{cases} h_{i,wf}^{vap} & P_i < P_{wf,cr} \quad , \quad T_{i,wf}^{sat} < T_{min} < T_{i,wf}^{sat} + 0.01 \\ h_{i,wf}^{liq} & P_i < P_{wf,cr} \quad , \quad T_{i,wf}^{sat} - 0.01 < T_{min} < T_{i,wf}^{sat} \\ h(P_i, T_{min}) & \text{other cases} \end{cases}$
	$h_{max} = \begin{cases} h_{i,wf}^{vap} & P_i < P_{wf,cr} \quad , \quad T_{i,wf}^{sat} < T_{max} < T_{i,wf}^{sat} + 0.01 \\ h_{i,wf}^{liq} & P_i < P_{wf,cr} \quad , \quad T_{i,wf}^{sat} - 0.01 < T_{max} < T_{i,wf}^{sat} \\ h(P_i, T_{max}) & \text{other cases} \end{cases}$
4	If $P < P_{wf,cr}$ then calculate $h_{i,wf}^{liq}, h_{i,wf}^{vap}$ else calculate $h_i^{dev2} = h_i _{\frac{\partial^2 T}{\partial h^2}=0}$
5	Defining h_{left} and h_{right} for two intervals $[h_{min}, h_{left}], [h_{right}, h_{max}]$: The linearization will be carried out in two intervals, i.e., 'left' interval and 'right' interval. For subcritical pressures the 'left' interval is the sub-cooled region while in supercritical pressures it is defined as the region with $\frac{\partial^2 T}{\partial h^2} < 0$. The 'right' interval similarly is the superheated region for subcritical pressures and the region with $\frac{\partial^2 T}{\partial h^2} > 0$ for supercritical pressures. The linearization then will be performed in these two intervals. Depending on the initial temperatures one of these interval might be inactive: $h_{left} = \begin{cases} h_{max} & P_i > P_{wf,cr} \quad , \quad h_{min} < h_i^{dev2} \quad , \quad h_{max} < h_i^{dev2} \\ h_i^{dev2} & P_i > P_{wf,cr} \quad , \quad h_{min} < h_i^{dev2} \quad , \quad h_{max} \geq h_i^{dev2} \\ h_{max} & P_i < P_{wf,cr} \quad , \quad h_{max} < h_{i,wf}^{liq} \\ h_{i,wf}^{liq} & P_i < P_{wf,cr} \quad , \quad h_{max} \geq h_{i,wf}^{liq} \\ h_{min} - 1 & \text{other cases (the left loop will not be active)} \end{cases}$ $h_{right} = \begin{cases} h_{min} & P_i > P_{wf,cr} \quad , \quad h_{max} > h_i^{dev2} \quad , \quad h_{min} > h_i^{dev2} \\ h_i^{dev2} & P_i > P_{wf,cr} \quad , \quad h_{max} > h_i^{dev2} \quad , \quad h_{min} \leq h_i^{dev2} \\ h_{min} & P_i < P_{wf,cr} \quad , \quad h_{min} > h_{i,wf}^{vap} \\ h_{i,wf}^{vap} & P_i < P_{wf,cr} \quad , \quad h_{min} \leq h_{i,wf}^{vap} \\ h_{max} + 1 & \text{other cases (the right loop will not be active)} \end{cases}$
6	Perform linearization based on the code provided in Listing B.1

B.2 Lua code for linearization

Listing B.1 provides the code for the piecewise linear envelope generation implemented in Lua programming language.

LISTING B.1—Linearization algorithm implemented in Lua programming language.

```

1 local Ttan,init , Ttan , hinit , htan , ∂T/∂hinit , ∂T/∂htan
2 local found_tangent = false
3 local dh = 0.5kW — the increment of specific enthalpy
4 local List = {} — the list of all the points by linearisation
5 local isHot if Tin > Tout then isHot = true else return isHot = false end
6 local εsmall = 0.001 — very small number for convergence
7
8 — [hmax, hright] in descending order
9
10 if |hmax - hright| < εsmall then
11   table.insert(List, {h = hmax, t = T(P, hmax)})
12 else
13   local number_steps = |hmax - hright|/dh
14   for i=0, number_steps, 1 do
15     local h = hmax - i × dh
16     if i = 0 then
17       — take hmax and start from Ttol
18
19       hinit = h
20       Ttan,init = T(P, h) - Ttol
21
22       —if stream is hot then go lower, if cold use exactly the max point
23
24       if isHot and Tsat,Pfluid and (T(P, h) - Tsat,P) > 0.01 and Ttan,init < Tsat,Pfluid then
25         table.insert(List, {h = hv,Pfluid, t = Tsat,Pfluid})
26         table.insert(List, {h = h, t = (h - hv,Pfluid) * ∂T/∂h|P,q=1 + Tsat,Pfluid})
27         break
28       elseif isHot then
29         table.insert(List, {h = h, t = Ttan,init})
30       else
31         table.insert(List, {h = h, t = T(P, h)})
32       end
33     end
34   else
35     if not(found_tangent) then
36       local tprime = T(P, hmax)
37       if |h - hv,Pfluid| > dh then
38         if |∂T/∂h|P,tprime - (tprime - Ttan,init)/(h - hinit)| ≤ 0.01 then
39           found_tangent = true
40           htan = h
41           ∂T/∂htan = ∂T/∂h|P,tprime
42           ttan = tprime
43         elseif h < hright + dh or |h - dh| - hright < 0.1 then
44           table.insert(List, {h = hright, t = T(P, hright)})
45           break
46         end
47       else
48         table.insert(List, {h = hright, t = T(P, hright)})
49       end
50     else
51       if |T(P, h) - (ttan - ∂T/∂htan × (htan - h)) - Ttol| ≤ 0.03 then
52         if isHot then
53           if h - dh < hright then
54             table.insert(List, {h = hright, t = T(P, hright)})
55           else
56             if (ttan - ∂T/∂htan × (htan - h)) < T(P, hright) then
57               table.insert(List, {h = h, t = T(P, hright)})

```

```

59         else
60             table.insert(List, {h = h, t =  $t_{tan} - \partial T / \partial h_{tan} \times (h_{tan} - h)$ })
61         end
62     end
63     else
64         table.insert(List, {h = h, t =  $\mathbf{T}(P, h)$ })
65     end
66     found_tangent = false
67      $h_{init} = h$ 
68      $T_{tan,init} = t_{tan} - \partial T / \partial h_{tan} \times (h_{tan} - h)$ 
69     elseif h <=  $h_{right} + dh$  then
70         table.insert(List, {h =  $h_{right}$ , t =  $\mathbf{T}(P, h_{right})$ })
71     end
72 end
73 end
74 end
75
76 — [ $h_{min}, h_{left}$ ] in ascending order
77
78 local  $t_{init}$ ,  $h_{init,tan}$ ,  $t_{init,tan}$ 
79 local found_intersect = false
80 if  $|h_{min} - h_{left}| < \epsilon_{small}$  then
81     table.insert(List, {h =  $h_{min}$ , t =  $\mathbf{T}(P, h_{min})$ })
82 else
83     local number_steps =  $|h_{left} - h_{min}| / dh$ 
84     for i = 0, number_steps, 1 do
85         local h =  $h_{min} + i \times dh$ 
86         if i = 0 then
87             table.insert(List, {h = h, t =  $\mathbf{T}(P, h)$ })
88              $h_{init} = h$ 
89              $t_{init} = \mathbf{T}(P, h)$ 
90              $\partial T / \partial h_{init} = \partial T / \partial h|_{P, T=t_{init}}$ 
91         else
92             if not(found_intersect) then
93                 local  $\tan\_t = t_{init} + \partial T / \partial h_{init} \times (h - h_{init})$ 
94                 if  $|( \tan\_t - \mathbf{T}(P, h) ) - T^{tol}| \leq 0.03$  then
95                     if  $\tan\_t > \mathbf{T}(P, h_{left})$  then
96                         table.insert(List, {h =  $h_{left}$ , t =  $\mathbf{T}(P, h_{left})$ })
97                     if isHot then
98                         table.insert(List, {h = h, t =  $\mathbf{T}(P, h)$ })
99                     else
100                         table.insert(List, {h =  $h_{init} + \partial T / \partial h_{init} \times (\mathbf{T}(P, h_{left}) - t_{init})$ , t =  $\mathbf{T}(P, h_{left})$ })
101                     end
102                     found_intersect = true
103                      $h_{init,tan} = h$ 
104                      $t_{init,tan} = \mathbf{T}(P, h_{left})$ 
105                     break
106                 else
107                     if isHot then
108                         table.insert(List, {h = h, t =  $\mathbf{T}(P, h)$ })
109                     else
110                         table.insert(List, {h = h, t =  $\tan\_t$ })
111                     end
112                     found_intersect = true
113                      $h_{init,tan} = h$ 
114                      $t_{init,tan} = \tan\_t$ 
115                 end
116             end
117             elseif h >=  $h_{left} - dh$  then
118                 table.insert(list, {h =  $h_{left}$ , t =  $\mathbf{T}(P, h_{left})$ })
119                 table.insert(List, {h =  $h_{init} + \partial T / \partial h_{init} \times (\mathbf{T}(P, h_{left}) - t_{init})$ , t =  $\mathbf{T}(P, h_{left})$ })
120             end
121         else
122             if  $|h - h_{l,P}^{fluid}| > dh$  then
123                 local  $t_{prime} = \mathbf{T}(P, h)$ 

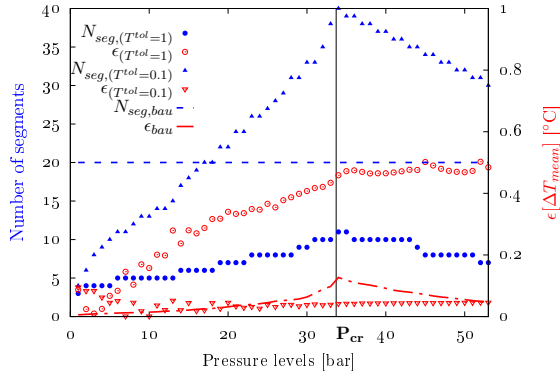
```

```

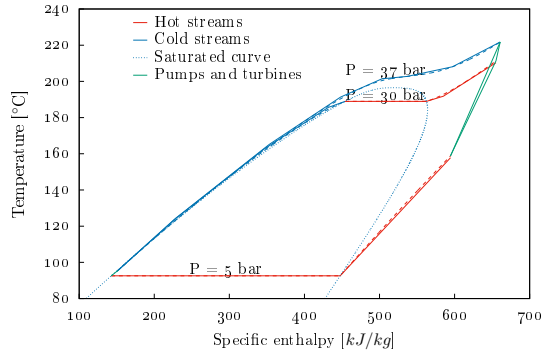
123 | if  $|\partial T / \partial h|_{P, t_{prime}} - (t_{prime} - t_{init, tan}) / (h - h_{init, tan})| \leq 0.01$  then
125 |     found_intersect = false
125 |      $h_{init} = h$ 
127 |      $\partial T / \partial h_{init} = \partial T / \partial h|_{P, t_{prime}}$ 
127 |     t_init =  $t_{prime}$ 
129 |     if  $h + dh > h_{left}$  then
129 |         table.insert(List, {h =  $h_{left}$ , t =  $t_{prime}$ })
131 |     end
131 |     elseif  $h \geq h_{left} - dh$  then
133 |         table.insert(List, {h =  $h_{left}$ , t =  $T(P, h_{left})$ })
133 |     end
135 |     else
135 |         table.insert(List, {h =  $h_{left}$ , t =  $T(P, h_{left})$ })
137 |     end
137 | end
139 | end
141 | end
141 | --[[
143 | ## TABLE 'List' has all the points for the piece-wise linear envelope.
143 | --]]
    
```

B.3 Error of linearization

Figure B.1 illustrates the number of pieces and their associated errors for piece-wise linearization of an evaporation stream using Pentane for different pressure levels.



(a) Comparison of the proposed linearization algorithm ($T^{tol} = 0.1$ and 1) with 20-piece linearization approach



(b) Illustration using Pentane ($T^{tol} = 1$)

FIGURE B.1—a) Error of linearization and b) Example of linearization for Pentane

APPENDIX C

Interactive parallel coordinate visualization tool for fluid selection

As part of the work conducted on ORC optimization, an interactive parallel coordinate visualization tool is developed in this work to filter out potential working fluids for optimization. The tool can be accessed [here](https://infoscience.epfl.ch/record/230303/files/interatctive_fluid_selection_orc_1.html) or by going to the following url: https://infoscience.epfl.ch/record/230303/files/interatctive_fluid_selection_orc_1.html. Thermodynamic property calculations and values of flammability and health hazards are based on CoolProp database¹.

TABLE C.1—Included fluid properties in parallel coordinate tool

Property	Unit	Description
T_{cr}	[°C]	Critical temperature
P_{cr}	[bar]	Critical pressure
T_{boil}	[°C]	Boiling temperature at 1 bar
T_{triple}	[°C]	Temperature at triple point
Acentric factor	-	A measure of non-sphericity (centricity) of molecules
M_{molar}	[g/mol]	Molar mass of fluid
GWP ₁₀₀	-	GWP
Flammability Hazard		(From CoolProp database)
Health Hazard		(From CoolProp database)
T_{min}	[°C]	Lowest temperature of feasibility for property method (CoolProp)
T_{max}	[°C]	Highest temperature of feasibility for property method (CoolProp)
$\partial s / \partial T$	[kJ/kgK ²]	The inverse of the slope of the saturated vapor curve. Negative values represent wet fluids while positive values denote dry fluids. The closer the value is to zero, the more the fluid is isentropic. The slope is calculated at $(T_{cr} + T_{triple})/2$

¹I. H. Bell, J. Wronski, S. Quoilin, V. Lemort, Pure and Pseudo-pure Fluid Thermophysical Property Evaluation and the Open-Source Thermophysical Property Library CoolProp, Industrial & Engineering Chemistry Research 53 (6) (2014) 2498-2508

APPENDIX D

Kraft pulp mill data

The data in this chapter is reproduced from our previous work ¹ by adding several remarks on the state of thermal streams. The value of $\Delta T_{min}/2$ of thermal streams are assumed to be 5°C, unless otherwise stated. Moreover, some thermal streams are removed due to their low thermal duties.

Water tanks There are five (5) water tanks which have the task of managing water flows among processes for process water use and cooling purposes (Table D.1). Freshwater can be fed to any of these tanks. In the current state of the mill, there is no water recycling between water unit operations.

TABLE D.1—Kraft pulp mill industrial case study: water tanks

Water tank	Abbreviation	Current temperature (°C)
Fresh water	FW	20
Treated warm water	TWW	28
Raw warm water	RWW	52
Treated hot water	THW	60
Waste water	WW	30

Cold process streams Overall, there are nineteen (19) cold process streams (Table D.2). In the current state of the mill, they are all being heated with steam.

Hot process streams Overall, fifteen (15) hot process streams are being cooled in the water network (Table D.3, combining heat exchangers in series into one hot stream). Several of these streams are cooling duties of machineries.

Water unit operations The main water unit operations are presented in Table D.4. The only required data to be extracted are the demand (supply) of each unit together with their operating temperatures. The level of contamination is not measured for any water stream in this kraft pulp mill. To this end, any recycling and reuse opportunity must be added to the superstructure while any infeasible and impractical one must be forbidden. This requires direct communication with experts in kraft process who know quantitatively the levels of contamination and can propose new ones to be investigated. In the pulp machine department, white water chest collects the removed water from the pulp. This water can be used in the pulp machine via save-all tank.

¹M. Kermani, Z. Périn-Levasseur, M. Benali, L. Savulescu, F. Maréchal, A novel MILP approach for simultaneous optimization of water and energy: Application to a Canadian softwood kraft pulping mill, Computers & Chemical Engineering ISSN 0098-1354.

TABLE D.2—Kraft pulp mill industrial case study: thermal streams

Section/Stream ID	Type*	T _{in} [°C]	T _{out} [°C]	Heat Load [kW]	Remarks
Digester					
Chip bin heater	C	20	55	3,290	$\Delta T_{min}/2 = 3$
Steaming vessel	C	55	123	13,583	
Upper liquor heater	C	122	150	4,810	
Lower liquor heater	C	146	160	5,750	
Washer liquor heater	C	126	165	4,060	
Black liquor flash tank 1	H	128	128	5,350	$\Delta T_{min}/2 = 3$
Black liquor flash tank 2	H	93	93	9,960	$\Delta T_{min}/2 = 3$
Turpentine condenser	H	123.25	60	1,916	$\Delta T_{min}/2 = 3$, at 2.2 bar
Bleaching					
Steam mixer 1	C	70	75	1,860	$\Delta T_{min}/2 = 3$
Pulp heater	C	75	77	2,520	
Steam mixer 2	C	72	80	2,630	
Steam mixer 3	C	73	87	3,100	
ClO ₂ heater	C	5	43	4,183	
Pulp machine					
Wash water heater	C	66	88	1,640	$\Delta T_{min}/2 = 3$
Dryer	C	42	95	26,510	
Room air pre-heater	C	21	25	210	
Dryer exhaust - chimney	H	92	68	4,745	
Evaporators, concentrators, and recovery boiler					
Evaporator heater (1st)	C	119	139	33,390	$\Delta T_{min}/2 = 3$
Concentrator heater	C	106	111	16,220	
Boiler air pre-heater	C	32	110	6,240.6	
Black liquor heater	C	111	129	1,300	
Stripping and ClO₂					
Stripping column heater	C	97	155	4,457	$\Delta T_{min}/2 = 3$
ClO ₂ heater before reactor	C	65	75	3,170	

* C: cold stream, H: hot stream

Waste thermal streams Four waste hot streams are available on site.

Thermal utilities Steam is being produced at high pressure (~ 60 bar) on site in recovery boiler, auxiliary boilers and also using the waste heat of the on-site gas turbines. This steam is expanded within several steam turbines to meet the electrical and thermal demands of the mill. Nonetheless, only two pressure levels are being used for process use as shown in Table D.6.

TABLE D.3—Kraft pulp mill industrial case study: thermal streams in water network (see Table D.1 and footnote of Table D.2 for abbreviations)

Section	From	To	Type	T _{in} [°C]	T _{out} [°C]	Heat Load [kW]
Evaporators (modeled as steam at 1.9 bar, 9.932 kg/s, ΔT _{min} /2 = 3)						
Primary condenser	FWT	FHD	W	20	50	22,650
			H	119	55	
Secondary condenser	FWT	FHD	W	20	30	2,360
			H	119	30	
Inter/after condenser	FWT	FWT	W	20	30	600
			H			
Flash Heat Double (FHD) (modeled as steam at 0.25 bar, 4.628 kg/s, ΔT _{min} /2 = 3)						
Flash heat double cooler	-	RWWT	W	46	54	9,045
			H	65	65	
Non-condensable gas cooler	FWT	FWT	W	21	25	460
			H	81	81	
Inter/After condenser	FWT	FWT	W			1,340
			H	30	30	
Recausticizing						
Green liquor cooler	FWT	FWT	W	20	33	364
			H	93	30	
Bearing cooler	FWT	THWT	W	20	31	385
			H	80	40	
Pulp Machine						
Water cooler	FWT	Press shower	W	20	25	70
			H	120	105	
Cooler	FWT	Economizer	W	20	36	1,605
			H	46	30	
Stripping (modeled as steam at 1 bar, 1.983 kg/s, ΔT _{min} /2 = 3)						
Reflux condenser	FWT	RWWT	W	20	60	4,634
			H	101	81	
Recovery Boiler						
Main surface condenser	TWWT	THWT	W	28	78	13,672
			H	89	88	
Auxiliary surface condenser	TWWT	THWT	W	28	70	3,700
			H	89	88	
Fan cooler	TWWT	THWT	W	28	38	1,346
			H	48	38	
Washing						
Cold blow cooler	FWT	FWT	W	20	34	2,930
			H	77	70	
Miscellaneous cooling	FWT	FWT	W	20	26	3,360
			H	-	-	

KRAFT PULP MILL DATA

TABLE D.4—Kraft pulp mill industrial case study: water unit processes

Inlet conditions			Unit	Outlet conditions	
Flow [kg/s]	T _{in} [°C]			T _{out} [°C]	Flow [kg/s]
3.7	20	— ►	digester - chip bin vent	— ► 60	3.7
69	60	— ►	bleaching		
29.8	20	— ►	ClO ₂ - absorption		
6.7	20	— ►	ClO ₂ - shower		
33.3	20	— ►	ClO ₂ - indirect contact cooler (ICC)		
16.5	20	— ►	ClO ₂ - barometric condenser		
16.7	20	— ►	recausticizing - vacuum pump	— ► 36	16.7
6.7	60	— ►	recausticizing - pressure disc filter		
48	20	— ►	pulp machine - vacuum pump	— ► 36	48
6.5	45	— ►	pulp machine - shower		
57.8	71	— ►	pulp machine - recycled white water	— ► 66	666
69	60	— ►	washing		
16	28	— ►	smelt spout	— ► 45	16
			contaminated condensate	— ► 85	22

TABLE D.5—Kraft pulp mill industrial case study: waste thermal streams

Section/Stream ID	T _{in} (°C)	T _{out} [°C]	Heat Load [kW]
Bleaching			
Alkaline bleach effluent	82	35	14,852
Acid bleach effluent	71	35	11,492
Pulp machine			
Dryer exhaust	68	35	9,643
Evaporators			
Combined condensate	89	35	4,608

TABLE D.6—Kraft pulp mill industrial case study: thermal and mass utilities

Utility	Pressure (bar)	Temperature (°C)
Steam #60	5.13	198
Steam #160	12	228
Freshwater	-	20

Curriculum vitae

Personal details

Name	Maziar KERMANI
Date of birth	16.06.1987
Citizenship	Iran
Address	Rue due Nord 12, 1800 Vevey
Contact	maziar.kermani@epfl.ch , kermani.maziar@gmail.com
Web address	https://people.epfl.ch/maziar.kermani https://www.researchgate.net/profile/Maziar_Kermani
Languages	Persian (mother tongue), English (fluent), French (B2), German (elementary)

Scientific and work experience

2014	–	2018	PhD student, industrial process and energy systems engineering (IPESE) group, Ecole Polytechnique Fédérale de Lausanne (EPFL), Switzerland.
2013	–	2014	Internship/master's thesis, Natural Resources Canada (CanmetENERGY), Varennes, Montreal, Canada.
2011	–	2013	Student assistant, industrial energy systems laboratory (LENI), EPFL.

Education

2011	–	2013	M.Sc. in mechanical engineering, minor in “management of technology and entrepreneurship”, EPFL, Switzerland.
2005	–	2010	B.Sc. in mechanical engineering, Sharif university of technology, Iran.

Honors and awards

2008	Ranked 18 th among 120 undergraduate students, school of mechanical engineering, Sharif university of technology.
2007	Selected as one of the top students of the mechanical engineering department of Sharif university of technology and obtained permission to study two disciplines simultaneously, mechanical and civil engineering.
2005	Ranked 90 th among some five hundred thousand participants in national matriculation board entry exam for B.Sc. degree hence admitted to do mechanical engineering at Sharif university of technology.

Journal publications

- **Kermani, M.**, Kantor, I.D., Maréchal, F., 2018. Synthesis of heat-integrated eater allocation networks: a meta-analysis of solution strategies and network features. *Energies* 11, 1158. <https://doi.org/10.3390/en11051158>
- Wallerand, A.S., **Kermani, M.**, Kantor, I., Maréchal, F., 2018. Optimal heat pump integration in industrial processes. *Applied Energy* 219, 68–92. <https://doi.org/10.1016/j.apenergy.2018.02.114>

- **Kermani, M.**, Wallerand, A.S., Kantor, I.D., Maréchal, F., 2018. Generic superstructure synthesis of organic Rankine cycles for waste heat recovery in industrial processes. *Applied Energy* 212, 1203–1225. <https://doi.org/10.1016/j.apenergy.2017.12.094>
- Ahmetović, E., Ibrić, N., Kravanja, Z., Grossmann, I.E., Maréchal, F., Čuček, L., **Kermani, M.**, 2018. Simultaneous optimisation and heat integration of evaporation systems including mechanical vapour recompression and background process. *Energy*. <https://doi.org/10.1016/j.energy.2018.06.046>
- Wallerand, A.S., **Kermani, M.**, Voillat, R., Kantor, I., Maréchal, F., 2017. Optimal design of solar-assisted industrial processes considering heat pumping: Case study of a dairy. *Renewable Energy*. <https://doi.org/10.1016/j.renene.2017.07.027>
- Ibrić, N., Ahmetović, E., Kravanja, Z., Maréchal, F., **Kermani, M.**, 2017a. Synthesis of single and interplant non-isothermal water networks. *Journal of Environmental Management, Environmental management as a pillar for sustainable development* 203, 1095–1117. <https://doi.org/10.1016/j.jenvman.2017.05.001>
- Ibrić, N., Ahmetović, E., Kravanja, Z., Maréchal, F., **Kermani, M.**, 2017b. Simultaneous synthesis of non-isothermal water networks integrated with process streams. *Energy*. <https://doi.org/10.1016/j.energy.2017.07.018>
- **Kermani, M.**, Périn-Levasseur, Z., Benali, M., Savulescu, L., Maréchal, F., 2017. A novel MILP approach for simultaneous optimization of water and energy: application to a Canadian softwood kraft pulping mill. *Computers & Chemical Engineering*. <https://doi.org/10.1016/j.compchemeng.2016.11.043>

Conference papers

- **Kermani, M.**, Wallerand, A.S., Kantor, I.D., Maréchal, F., 2017b. A hybrid methodology for combined interplant heat, water, and power integration, in: Espuña, A., Graells, M., Puigjaner, L. (Eds.), *Computer Aided Chemical Engineering*, 27th European Symposium on Computer Aided Process Engineering. Elsevier, pp. 1969–1974. <https://doi.org/10.1016/B978-0-444-63965-3.50330-5>
- **Kermani, M.**, Celebi, A.D., Wallerand, A.S., Ensinas, A.V., Kantor, I.D., Maréchal, F., 2017a. Techno-economic and environmental optimization of palm-based biorefineries in the Brazilian context, in: Espuña, A., Graells, M., Puigjaner, L. (Eds.), *Computer Aided Chemical Engineering*, 27th European Symposium on Computer Aided Process Engineering. Elsevier, pp. 2611–2616. <https://doi.org/10.1016/B978-0-444-63965-3.50437-2>
- Wallerand, A.S., **Kermani, M.**, Kantor, I.D., Maréchal, F., 2017. General superstructure synthesis and bi-level solution strategy for industrial heat pumping, in: Espuña, A., Graells, M., Puigjaner, L. (Eds.), *Computer Aided Chemical Engineering*, 27th European Symposium on Computer Aided Process Engineering. Elsevier, pp. 1159–1164. <https://doi.org/10.1016/B978-0-444-63965-3.50195-1>
- Yoo, M.-J., Lessard, L., **Kermani, M.**, Maréchal, F., 2015. OsmoseLua – An integrated approach to energy systems integration with LCIA and GIS, in: Krist V. Gernaey, J.K.H. and R.G. (Ed.), *Computer Aided Chemical Engineering*, 12th International Symposium on Process Systems Engineering and 25th European Symposium on Computer Aided Process Engineering. Elsevier, pp. 587–592. <https://doi.org/10.1016/B978-0-444-63578-5.50093-1>
- **Kermani, M.**, Périn-Levasseur, Z., Benali, M., Savulescu, L., Maréchal, F., 2014. An improved linear programming approach for simultaneous optimization of water and energy, in: Jiří Jaromír Kleměš, P.S.V. and P.Y.L. (Ed.), *Computer Aided Chemical Engineering*, 24th European Symposium on Computer Aided Process Engineering. Elsevier, pp. 1561–1566. <https://doi.org/10.1016/B978-0-444-63455-9.50095-7>

Programming skills Lua, Matlab, AMPL

Notes

